Dissertation zur Erlangung des Doktorgrades
der Fakultät für Chemie und Pharmazie
der Ludwig-Maximilians-Universität München

The role of Kindlin-1 in skin homeostasis and tumor development

Emanuel Goffredo Rognoni

aus Berlin

Juni 2014

Erklärung

Diese Dissertation wurde im Sinne von § 7 der Promotionsordnung vom 28. November 2011 von Herrn Prof. Dr. Reinhard Fässler betreut.

Eidesstattliche Versicherung

Diese Dissertation wurde eigenständig und ohne unerlaubte Hilfe erarbeitet.

München, ……

(Emanuel Rognoni)

Dissertation eingereicht am	05.06.2014
1. Gutachterin / 1. Gutachter:	Prof. Dr. Reinhard Fässler
2. Gutachterin / 2. Gutachter:	Prof. Dr. Ralf Huss
Mündliche Prüfung am	01.07.2014

Für meine Eltern

Table of content

Summary 7
Abbreviations 11
List of publications 14
1 Introduction 15
1.1 The skin and its appendages 15
1.1.1 Hair follicle morphogenesis 17
1.1.2 Skin stem cells 19
1.1.3 The postnatal hair cycle 21
1.1.4 Hair pigmentation 24
1.2 Integrin receptor family and adhesion structures 25
1.2.1 Integrins in the skin 26
1.2.2 Integrin structure and activation 28
1.2.3 Integrin clustering and catch-bond mechanisms 31
1.2.4 Integrin activation is mediated by Talin and Kindlin 32
1.2.4.1 Talin 33
1.2.3.2 Kindlin 34
1.2.4.3 Kindlin and Talin at the integrin tail 35
1.2.5 From integrin activation to mature integrin adhesions 37
1.3 TGFβ signaling 39
1.3.1 TGFβ superfamily members 39
1.3.2 TGFβ receptors and ligands 40
1.3.3 Canonical Smad TGFβ signaling 41
1.3.4 Non-canonical Smad TGFβ signaling 43
1.3.5 TGFβ synthesis and storage 44
1.3.6 TGFβ release mechanisms 45
1.3.6.1 Integrin independent TGFβ release mechanisms 45
1.3.6.2 Integrin mediated TGFβ release 46
1.4 Wnt signaling pathways 48
1.4.1 Wnt ligands 49
1.4.2 Wnt ligand receptors 51

1.4.3 β-catenin and Plakoglobin 51
1.4.4 Cell-cell adhesion in the context of β-catenin signaling 53
1.4.5 Canonical Wnt signaling pathway 54
1.4.6 Non-canonical Wnt signaling pathways 56
1.4.7 Soluble Wnt agonists and antagonists: 57
1.4.8 Wnt and TGFβ signaling cross talk 58
1.4.9 Wnt and Notch signaling are highly interconnected in skin 59
1.5 The Kindlin family 63
1.5.1 Subcellular Kindlin localizations and specificities 64
1.5.2 Post-transcriptional modifications of Kindlins 65
1.5.3 Kindlin pathogenesis and molecular function and signaling 66
1.5.3.1 Kindlin-1 and Kindler syndrome 66
1.5.3.2 Kindlin-2 69
1.5.3.3 Kindlin-3 71
1.6 Skin cancer 73
1.6.1 Comparison of wound healing and cancer in the skin 73
1.6.2 Skin tumor entities 75
1.6.3 Integrins and cancer 76
1.6.4 αvβ6 integrin and cancer 78
1.6.5 The paradoxical role of TGFβ signaling in cancer 80
1.6.6 Wnt signaling in cancer 83
2 Aim of the thesis 84
3 Short summary of manuscripts 86
3.1 Kindlin-1 controls Wnt and TGF-β availability to regulate cutaneous stem cell proliferation 86
3.2 Loss of Kindlin-1 causes skin atrophy and lethal neonatal intestinal epithelial dysfunction 87
3.3 Kindlin-3 mediated integrin adhesion is dispensable for quiescent hematopoietic stem cells but required to maintain activated hematopoietic stem and precursor cells 88
3.4 Integrins synergistically induce the MAL/SRF target gene ISG15 to ISGylate cytoskeletal and focal adhesion proteins necessary for cancer cell invasion 89
3.5 Integrin-linked kinase at a glance 91
4 References 92
5 Acknowledgements 117

6 Curriculum vitae 119
7 Appendix 121
7.1 Paper I 121
7.2 Paper II 135
7.3 Paper III 149
7.4 Paper IV 188
7.5 Paper V 221

Summary

Kindlin-1 belongs to a family of evolutionarily conserved focal adhesion proteins (Kindlin-1, 2 and 3), which bind β-integrin tails and increase integrin affinity for ligand (also called integrin activation). Integrins are a large αβ-heterodimeric cell surface receptor family essential for cell adhesion, spreading and migration, but also involved in assembly of the extracellular matrix and cell survival. Epidermal keratinocytes express several integrins, most notably β1 integrin subfamily members, and Kindlin family members 1 and 2. Kindlin-3 is only expressed in hematopoietic cells. Despite their high sequence similarity, Kindlin-1 and -2 cannot compensate for each other. Hence, mutations in the Kindlin-1 (*KINDLIN-1*) gene cause Kindler syndrome (KS) in man. In KS, the skin is the main affected organ, displaying blisters, pigmentation defects, atrophy, photosensitivity and increased tumor susceptibility. Of note, the increased tumor risk is unexpected, as hyperactive integrins are associated with high skin tumor risk and dysfunctional integrins prevent skin tumor formation. This discrepancy suggests that the absence of Kindlin-1 triggers novel, integrin-independent oncogenic function(s) that are sufficient to induce skin tumors early in the life of KS patients.

To analyze the molecular mechanisms of the KS disease, we first constitutively deleted the *Kindlin-1* gene in mice (**Paper II**). Besides the expected KS disease symptoms in skin, the constitutive Kindlin-1 loss also caused an early lethal ulcerative colitis-like phenotype, which prevented investigations on the role of Kindlin-1 in tumor development.

Thus, in **Paper I**, I deleted Kindlin-1 conditionally in the skin with a mouse line driving Cre recombinase under the control of the keratin5-promoter, enabling for the first time to fully recapitulate the human KS skin disease in mice. In addition to the classic KS symptoms - blistering, pigmentation defects, skin atrophy and impaired β1 integrin activation - loss of Kindlin-1 led to skin area dependent keratinocyte hyperproliferation and a severe and unexpected hair follicle phenotype comprising dense packaging of hair follicles and multiple hair shafts growing out from a single hair canal.

To dissect which KS symptoms are caused by impaired β1 integrin function, I compared the Kindlin-1 deletion phenotype with a mouse model in which a Kindlin-binding deficient β1 integrin is expressed in the epidermis. The mutated β1 integrin tail prevents Kindlin induced β1 integrin activation, while β1-integrin-independent Kindlin functions remain unaffected.

Interestingly, while blistering and associated inflammation were present in both models, the aberrant hair coat was absent, indicating that this defect is caused by a Kindlin-1-specific and β1 integrin-independent mechanism.

I decided to analyze the hair follicle defect in order to unravel novel Kindlin-1 functions. A detailed hair follicle and hair cycle analysis revealed that Kindlin-1 loss led to premature anagen (hair follicle growth phase) induction after the first hair cycle and to ectopic hair follicle development from the interfollicular epidermis as well as from pre-existing hair follicles. These findings strongly suggested a severe perturbation in epithelial stem cell homeostasis. I established several flow cytometry and immunohistochemistry based techniques that allowed analyzing the skin stem cell populations during mouse development. The experiments revealed that Kindlin-1 deficiency increased epithelial stem cell proliferation, numbers, mobility and compartment size.

To find an explanation for the disrupted stem cell homeostasis, I started analyzing the integrin profile of Kindlin-1 deleted keratinocytes. While the surface levels of most β integrin isotypes were only slightly changed, I observed an upregulation of αvβ6 integrin. Besides its role in cell adhesion, αvβ6 integrin is essential for transforming growth factor-β (TGFβ) release from the latency associated protein (LAP), which in turn suppresses keratinocyte proliferation. I performed several adhesion and spreading assays on αvβ6-specific surfaces and TGFβ release assays. Although αvβ6 integrin was highly expressed on the cell surface, Kindlin-1 deleted keratinocytes were neither able to spread on αvβ6-integrin specific surfaces nor to release TGFβ from a matrix. Intriguingly, integrin tail pull-down experiments revealed that while Kindlin-1 and -2 were able to bind and activate β1 integrin, only Kindlin-1 but not Kindlin-2 could perform this task for αvβ6-integrin. *In vivo*, the lack of αvβ6 integrin function led to impaired TGFβ signaling, especially in the bulge, and thus to a loss of stem cell quiescence. Most importantly, I could confirm impaired TGFβ signaling in KS patient biopsies.

Premature anagen induction, ectopic hair follicle development and expansion of stem cell compartments have also been observed in transgenic mice with elevated wingless-type (Wnt)/β-catenin signaling. In line with this, I observed increased nuclear localization of lymphoid enhancer-binding factor 1 (Lef1) and β-catenin as well as increased TOPGal mouse Wnt reporter activity in the hair follicle and interfollicular epidermis of Kindlin-1 deleted mice. In collaboration with Prof. John McGrath, King's College London, I confirmed increased Wnt signaling in KS patients and identified aberrant Wnt ligand expression as a cause of the elevated Wnt signaling

in mouse and humans. Indeed, I could prevent premature hair follicle induction and elevated Wnt signaling in Kindlin-1 deleted mice and keratinocytes by treating them with the Wnt inhibitor IWP-2, which inhibits Wnt ligand secretion, or with IWR-1, which stabilizes the β-catenin destruction complex. Together with further *in vitro* experiments these findings demonstrated that Kindlin-1 inhibits Wnt/β-catenin signaling in keratinocytes by regulating the transcription of Wnt ligands and receptors in a cell autonomous and integrin-independent manner.

I hypothesized that decreased TGFβ and augmented Wnt signaling in KS patients and Kindlin-1 deleted mice could be responsible for the elevated risk of skin tumors. To test this, I performed a two-stage carcinogenesis model with 7,12-Dimethylbenz(a)anthracene (DMBA) and 12-O-Tetradecanoylphorbol-13-acetate (TPA). Kindlin-1 deleted mice developed tumors earlier and obtained more tumors than littermate control mice. Histological analysis revealed that Kindlin-1 deficient mice developed a higher percentage of tumors associated with deregulated Wnt signaling including sebaceous papillomas, trichofolliculoma- and basal cell carcinoma-like lesions. Remarkably, I could induce tumors with a single DMBA treatment, indicating that the hyperproliferative state of Kindlin-1 deleted keratinocytes is sufficient to promote tumors.

In summary, my findings assigned Kindlin-1 a novel function for epithelial stem cell homeostasis by fine tuning the TGFβ and Wnt signaling pathways. As a result KS is no longer considered exclusively a β1 integrin mediated adhesion disease, but rather a disease of skin stem cells involving multiple signaling pathways that result in an increased risk for skin tumor development.

In parallel, I started studying the photosensitivity in KS. Therefore, I crossed Kindlin-1 mouse model into SKH-hr1 hairless mouse strain, suitable for UV experiments. After detailed phenotype characterization, I performed short- and long-term UV experiments in collaboration with Dr. Norbert Wikonkál from the University of Budapest. The short-term UV experiment revealed that photosensitivity observed in KS patients is reproducible in mice, which displayed increased numbers of sun burned cells as compared to wild type littermates at different UV dosages. The long-term UV treatment for 48 weeks with a low UV dosage promoted significantly more tumors, which developed earlier and progressed to a more malignant phenotype in Kindlin-1 deleted mice. The cause for increased photosensitivity is still unclear, and will be further investigated by a new PhD student who I am supervising.

In addition, I was involved in two other projects (**Paper III** and **IV**) during my PhD: In **Paper III** we addressed the role of Kindlin-3 in the regulation and maintenance of hematopoietic stem and precursor cells in the bone marrow. Besides helping with sophisticated stem cell experiments, I translated epidermal stem cell Kindlin-1 findings to Kindlin-3 and the hematopoietic system. We could show that Kindlin-3 deficient hematopoietic stem and precursor cells critically rely on Kindlin-3 mediated integrin activation for homing, whereas Kindlin-3 is dispensable for hematopoietic stem cell quiescence during homeostasis. Conversely, upon hematopoietic stress, impaired retention of activated hematopoietic stem and precursor cells leads to a premature exhaustion of Kindlin-3 deficient hematopoietic stem cells, emphasizing the importance of Kindlin-3 for maintaining actively proliferating hematopoietic stem and precursor cells in the bone marrow.

For **Paper IV**, I assisted in the exploration of how the two major fibronectin binding integrin classes αv and β1 cooperate in megakaryocyte acute leukemia protein (MAL) / serum response factor (SRF) signaling and how newly identified MAL/SRF-target genes control the turnover of actin regulatory proteins, adhesome proteins and integrins. Briefly, we found that through modulation of the cellular globular (g) / filamentous (f)-Actin composition both integrin classes synergize to regulate the expression of MAL/SRF target genes. Furthermore, we identified the small ubiquitin-like modifier interferon-specific gene 15 (ISG15) as a novel MAL/SRF target gene. Similar to ubiquitin, ISG15 can be conjugated covalently to specific lysine residues of multiple MAL/SRF target proteins including Vinculin, Talin and Eplin and thereby preventing their ubiquitination and degradation. Thus, we show that these two integrin classes trigger a feed-forward loop through modulation of free g-Actin which controls SRF/MAL activity, leading to increased transcription of focal adhesion and cytoskeletal genes, which at the same time are post-translationally modified and thereby potentially stabilized via ISGylation. Such an autoregulatory circuit allows precise and robust activation of the cellular adhesion and motility machinery to promote cell migration during cancer metastasis.

Finally, one of the most prominent interaction partners of Kindlins that links the integrins to the actin cytoskeleton is the focal adhesion scaffolding protein integrin-linked-kinase (ILK). In **Paper V** we reviewed the ILK functions, subcellular localizations and structural properties of this interesting molecule.

Abbreviations

Å	Angstrom
ActR-II	Activin type II receptor
ADP	Adenosine diphosphate
ADAM	A disintegrin and metalloproteinase
ADMIDAS	Adjacent to metal ion-dependent adhesion site
αI	α-inserted
ALK	Activin receptor-like kinase
AMHR-II	Anti-Müllerian hormone receptor type II
APC	Adenomatous polyposis coli gene
APM	Arrector pili muscle
ARM	Armadillo
BCC	Basal cell carcinoma
BCL	B-cell chronic lymphocytic leukemia/lymphoma
βI	β-inserted
β-TrCP	β-transducin repeat containing E3 ubiquitin protein ligase
BM	Basement membrane
uPA	Urokinase-type plasminogen activator
BDNF	Brain-derived neurotrophic factor
bHLH	Basic helix-loop-helix
BMP	Bone morphogenetic protein
BMPR2	BMP type II receptor
BrdU	5-bromo-2'-deoxyuridine
Ca^{2+}	Calcium ions
CAMkII	Ca^{2+}/calmodulin-dependent protein kinase II
CAS	Crk-associated substrate
CBP	Calcium-binding protein
CD	Cluster of differentiation
Cdc	Cell division cycle
CDKN2B	Cyclin-dependent kinase inhibitor 2B
CK1α	Casein kinase 1α
COOH	Carboxyl group
Co-Smad	Common mediator Smad
CpG	Cytosine-phosphate- guanine nucleotide sequence
CtBP	C-terminal binding protein
CTS	Connective tissue sheath
CXCR4	Chemokine (C-X-C motif) receptor 4, cytein (C), any (X)
DAAM1	Dishevelled-associated activator of morphogenesis 1
DAG	Diacyl-glycerol
DAP	Death-associated protein
Dct	Dopachrome tautomerase
Dkk	Dickkopf
DMBA	7,12-Dimethylbenz (a)anthracene
DNA	Deoxyribonucleic acid
Dvl	Dishevelled
E-Cadherin	Epithelial cadherin
e.g.	“Exempli gratia” (for example)
ECM	Extracellular matrix
EGF	Epidermal growth factor
ERK	Extracellular signal-regulated kinase
EMT	Epithelial-mesenchymal transition
ER	Endoplasmatic reticulum
FACS	Flow cytometry
f-Actin	Filamentous Actin
FAK	Focal adhesion kinase
FAP	Familial Adenomatous Polyposis
FERM	Four point one protein, ezrin, radixin, moesin domain
FGF	Fibroblast growth factor
FoxO	Forkhead box protein O
Fzd	Frizzled receptor
g-Actin	Globular (monomeric) actin
Gadd45b	Growth arrest and DNA-damage inducible, beta
GDF	Growth/differentiation factors
GDP	Guanosine diphosphate
GFFKR	Peptide motif glycine (G), phenylalanine (F), lysine (K), arginine (R)
GFOGER	Glycine (G), phenylalanine (F), hydroxyproline (O), glutamic acid (E), arginine(R) motif
Gli1	Glioblastoma 1
Glu	Glutamine
GS	Glycine (G), serine (S) rich domain
GSK3	Glycogen synthase kinase 3

GTP	Guanosine triphosphate
HDR(R/K)E	Peptide motif histidine (H), aspartic acid (D), arginine (R), lysine (K), glutamic acid (E)
HAX1	HS1-associated protein X-1
H&E	Hematoxylin and eosin
HF	Hair follicle
h-G-h	Carboxylate binding motif with a glycine (G) flanked by two hydrophobic residues (h)
HS	Hair shaft
HSPG	Heparan sulfate proteoglycan
ICAM-1	Intercellular adhesion molecule-1
Id	Inhibitor of differentiation
i.e.	"Id est" (that is)
I-EGF	Rich integrin epidermal growth factor–like
IFE	Interfollicular epidermis
IGF	Insulin growth factor
IKK	IκB kinase
IL	Interleukin
ILK	Integrin linked kinase
IMD	Integrin mediated death
IPP	ILK-Pinch-Parvin complex
IP_3	Inositol trisphosphate
IRS	Inner root sheath
I-Smad	Inhibitory Smad
ISG15	Interferon-induced 15 kDa protein
JNK	Jun N-terminal kinase
K5-Cre	Keratin5 promoter driven Cre line
kDa	Kilodalton
Krt15	Keratin 15
Krt19	Keratin 19
KGF	Keratinocyte growth factor
KS	Kindler syndrome
LAD I, II, III	Leukocyte adhesion deficiency type I, II or III
LAP	Latency-associated protein
LacZ	β-galactosidase gene
Lef1	Lymphoid enhancer-binding factor 1
LIMBS	Ligand-induced metal ion–binding site
LIMK1	LIM kinase 1
LDV	Leucine (L), aspartic acid (D), valine (V) peptide motif
Lgr	Leucine-rich repeat containing G protein-coupled receptor
LLC	Large latent TGFβ complex
LRG1	Leucine-rich alpha-2-glycoprotein 1
Lrp5/6	Lipoprotein receptor-related protein 5 or 6
LTBP	Latent TGFβ binding protein
MD	Membrane distal
MET	Mesenchymal to epithelial transition
MF	Microfilaments
MIDAS	Metal ion dependent adhesion site
miR200	MicroRNA200
MAL	Megakaryocyte acute leukemia
MAPK	Mitogen-activated protein kinase
Mg^{2+}	Magnesium ions
MH1	Mad homology domain 1
MMP	Matrix metallopeptidase
Mn^{2+}	Manganese ion
MP	Membrane proximal
MRTFA	Myocardin related transcription factor A
mTORC	Mammalian target of rapamycin
MTS24	Thymic epithelial progenitor cell marker
NEXT	Notch extracellular truncation
NFAT	Nuclear factor of activated T-cells
NF-κB	Nuclear factor kappa-light-chain enhancer of activated B cells
NICD	Notch intracellular domain
NMR	Nuclear magnetic resonance
NPxY	Peptide motif asparagine (N), proline (P), any (x), tyrosine (Y)
NT-3/4	Neurotrophins 3 or 4
NxxY	Peptide motif asparagine (N), proline (P), any (x)
ORS	Outer root sheath
p130Cas	p130 Crk-associated substrate
Par6	Partitioning defective 6
PAT	Paralyzed, arrested elongation at twofold

PCP	Planar cell polarity
PDGF	Platelet derived growth factor
PEST	Rich in proline (P), glutamic acid (E), serine (S) and threonine (T)
$PI(4,5)P_2$	Phosphatidylinositol 4,5-bisphosphate
$PI(3,4,5)P_3$	Phosphatidylinositol 3,4,5-trisphosphate
PI3K	Phosphoinositide 3-kinase
Pinch	Particularly interesting Cys-His-rich protein
PIPKIγ	Phosphatidylinositol 4-phosphate-5-kinase type I γ
PH	Pleckstrin homology
PkC or PkA	Protein kinase C or A
PLC	Phospholipase C
PLET1	Placenta-expressed transcript-1
PLK1	Polo-like kinase 1
PPM1A	Protein phosphatase, Mg^{2+} / Mn^{2+} dependent, 1A
PRDM1	PR domain zinc finger protein 1, (previously BLIMP1)
PSI	Plexin/semaphorin/integrin
PTB	Phosphotyrosine binding site
Pyro	Pygopus family PHD finger
qPCR	Quantitative polymerase chain reaction
Rab	Ras-related in brain
Rac1	Ras-related C3 botulinum toxin substrate 1
Raf	Rapidly accelerated fibrosarcoma
RAM	Rbp-associated molecule
Rap1	Ras-related protein 1
Ras	Rat sarcoma
RIAM	Rap1 interacting adaptor molecule
RGD/E	Tripeptide motif arginine (R), glycine (G), aspartate (D) or glutamic acid (E)
RhoA	Ras homolog family member A
RNA	Ribonucleic acid
Rnf43	Ring finger protein 43
ROCK	Rho-associated kinase
ROS	Reactive oxygen species
Ror2	Receptor tyrosine kinase-like orphan receptor 2
R-Smad	Receptor-activated Smad
Ryk	Receptor-like tyrosine kinase
SARA	Smad anchor for receptor activation
S	Sedimentation coefficient
SC	Stem cell
SCC	Squamous-cell carcinoma
SDL	Specificity determining loop
sFRP	Secreted frizzled-related protein
SG	Sebaceous gland
SGSGSG	Serine (S) and glycine (G) rich peptide motif
SH2	Src homology 2
Shc	Src homology containing protein
Shh	Sonic hedgehog
SHIP	SH2 domain-containing 5' inositol phosphatase
SKH-hr1	Hair less mouse strain
SLC	Small latent TGFβ complex
Smurf	Smad specific E3 ubiquitin protein ligase
Sos1	Son of sevenless homolog 1
SPR	Surface plasmon resonance
Src	Proto-oncogene tyrosine-protein kinase Sarcoma
SRE	Smad responsive elements
TAK1	TGFβ-activated kinase 1
TβRI/II	TGFβ receptor type I or II
TCF	Transcription factor
TGFα	Transforming growth factor-α
TGFβ	Transforming growth factor-β
THATCH	Talin/HIP1R/Sla2p actin tethering C-terminal homology
TIF	Tubular intestinal fibrosis
TMD	Transmembrane domain
TNF	Tumor necrosis factor
TPA	12-O-Tetradecanoylphorbol-13-acetate
TRAF6	Tumor necrosis factor receptor-associated factor 6
Unc112	Uncoordinated protein 112
UV	Ultra violet
VCAM	Vascular cell adhesion molecule
VEGF	Vascular endothelial growth factor
Wif1	Wnt inhibitory factor 1
Wnt	Wingless-type

List of publications

This thesis is based on the following publications, which are referred in the text by **roman numerals letters (I-V):**

Paper I: **Rognoni E**, Widmaier M, Jakobson M, Ruppert R, Ussar S, Katsougkri D, Böttcher RT, Lai-Cheong JE, Rifkin DB, McGrath JA, Fässler R. Kindlin-1 controls Wnt and TGF-β availability to regulate cutaneous stem cell proliferation. *Nat Med.* 2014, 20(4), 350-9.

Paper II: Ussar S, Moser M, Widmaier M, **Rognoni E**, Harrer C, Genzel-Boroviczeny O, Fässler R. Loss of Kindlin-1 causes skin atrophy and lethal neonatal intestinal epithelial dysfunction *PLoS Genet.* 2008, 4(12), e1000289.

Paper III: Ruppert R, Moser M, Sperandio M, **Rognoni E**, Orban M, Liu WH, Schulz A, Oostendorp RA, Massberg S, Fässler R. Kindlin-3 mediated integrin adhesion is dispensable for quiescent hematopoietic stem cells but required to maintain activated hematopoietic stem and precursor cells. *Immunity* (under revision).

Paper IV: Hermann MR, **Rognoni E**, Jakobson M, Widmaier W, Yeroslaviz A, Zent R, Posern G, Hofstädter F, Fässler R. Integrins synergistically induce the MAL/SRF target gene ISG15 to ISGylate cytoskeletal and focal adhesion proteins necessary for cancer cell invasion. (Manuscript in preparation).

Paper V: Widmaier M, **Rognoni E**, Radovanac K, Azimifar SB, Fässler R. Integrin-linked kinase at a glance. *J Cell Sci.* 2012, 125(Pt 8), 1839-1843.

Nature Medicine Cover Image
(Issue April 2014 Volume 20 No 4)
Kindler syndrome (KS) is a skin blister disease associated with an increased risk for skin cancer. In this issue, Reinhard Fässler and his colleagues have developed a new mouse model of KS, which allowed them to uncover new insight into the mechanisms of the disease. The cover image by Emanuel Rognoni illustrates ectopic hair follicles with enlarged hair follicle bulges (red) and small hair germs (green) in the tail skin of a mouse lacking Kindlin-1 (nuclei in blue).

1 Introduction

1.1 The skin and its appendages

The skin is the largest organ of the human body that protects from environmental stresses such as dehydration, irradiation, mechanical trauma and pathogenic infection (Fuchs, 2008). It has the remarkable ability to regenerate in a controlled fashion, including its appendages, hair follicles (HF) and sebaceous glands. These regulate body temperature and influence social and reproductive behavior.

Adult skin is composed by approximately 20 different cells types, which are organized in three layers arising from different embryonic cell lineages. The outer most layer (epidermis) is derived from neuroectodermal cells that form during embryo development a single layer of undifferentiated progenitors, which develop into the multilayered (stratified) epidermis, HFs and sebaceous glands, which are separated through a basement membrane from the underlying dermis (second layer). The dermis is composed by cells of multiple developmental origins: mesoderm-derived cells giving rise to the extracellular matrix (ECM) secreting fibroblasts and arrector pili muscle cells, which attach to each HF regulating HF movement; endothelial cells forming the dermovascular system essential for skin nutrition; immune cells, which infiltrate and reside in the skin (epidermis and dermis). The last skin layer, referred as the sub cutis, comprises subcutaneous adipocytes (fat cells) originating from differentiated fibroblasts (Driskell et al., 2013).

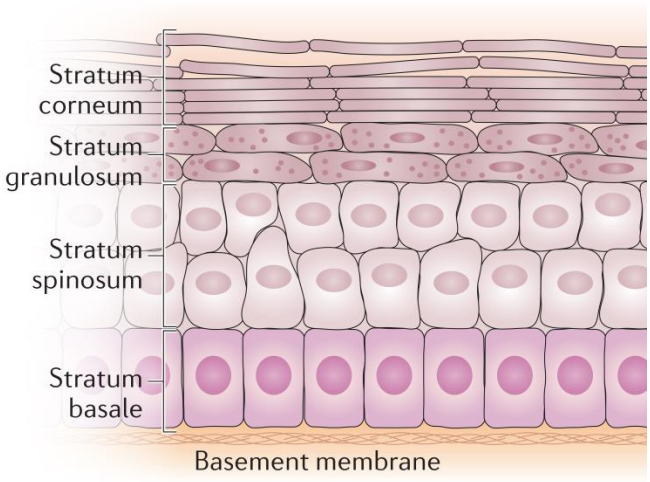

Figure1: The structure of the epidermal skin layer

Proliferative keratinocytes are in contact with basement membrane forming the stratum basale. The overlying stratum spinosum, granulosum and corneum are built by the delamination and progressive differentiation of basal keratinocytes, referred as epidermal stratification (modified from (Winograd-Katz et al., 2014)).

The main cell type of the epidermis are the keratinocytes, which are organized into multiple layers ("strata") thereby establishing together with the basement membrane a physical barrier to the outer environment (Figure1). This barrier is frequently renewed. The basal keratinocytes contact the basement membrane and harbor the proliferative cell pool of the epidermis as well as multiple slow cycling stem cell (SC) populations (discussed in 1.1.2). The turnover rate of basal keratinocytes (i.e. the time they are renewed) in mice is estimated to one week, whereas in humans it is about 60 days (Ghazizadeh and Taichman, 2001). The process of epidermal layer formation (stratification) is characterized by change of keratin expression, downregulation of surface adhesion receptor integrin and laminin expression of basal cells undergoing differentiation. Consequently, these cells leave the basal layer moving upwards to the stratum spinosum and granulosum, withdraw from the cell cycle and denucleate at the end of the differentiation program giving rise to a cornified layer (stratum corneum), which eventually sheds off the skin surface (Blanpain and Fuchs, 2006). At present, the molecular signals that orchestrate cell proliferation, differentiation and patterning in skin, remain incompletely understood.

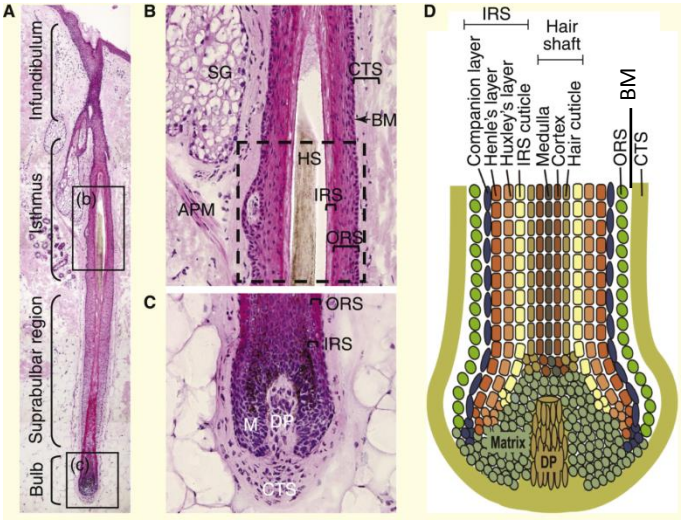

Figure2: The HF structure and layers
(**A**-**C**) HF in anagen stained by H&E. (**A**) The permanent (infundibulum and isthmus) and the cycling (suprabulbar region and hair bulb) components of the HF are shown. (**B**,**C**) High magnification of the isthmus region with the HF bulge indicated by the dashed square (**B**) and the hair bulb (**C**). (**D**) Schematic illustration of the concentric HF layers of the outer root sheath (ORS), inner root sheath (IRS) and hair shaft which are enclosed by the basement membrane (BM) and a connective tissue sheath (CTS). APM, arrector pili muscle; DP, dermal papilla; M, matrix; HS, hair shaft; SG, sebaceous gland (modified from (Schneider et al., 2009)).

In the skin each HF is considered a distinct mini organ composed by up to eight layers organized in a concentric manner around the hair shaft (Figure2). The layers from outside to the center are the outer root sheath, the inner root sheath, composed of Companion layer, Henle's layer, Huxley's layer and the inner root sheath cuticle, and finally the hair shaft composed of hair cuticle, medulla and cortex. A connective tissue sheath of dermal cells and collagen surround the HF epithelium (Figure2D). The HFs are formed during embryonic development (day 14.5 in mice) and

subsequently the lower part of the HF undergoes repeated cycles of growth, regression and self-renewal, referred as hair cycle, while the upper part maintains a constant morphology (see section 1.1.1 and 1.1.3 for details). This cycling of the HF depends on three compartments located in the lower area of the HF: the hair bulb, the suprabulbar region and the hair bulge. The upper non-cycling part consists of the infundibulum and the isthmus (Figure2A-C). The infundibulum forms the hair canal opening where the interfollicular epidermis surrounds the hair shaft and ends at the duct of the sebaceous gland. Below lies the isthmus region which is connected to the arrector pili muscle. At the lower isthmus region follows the HF bulge, required for the maintenance of the whole HF, as it forms the main reservoir of epithelial HF and melanocyte SC (see section 1.1.2 for details). The hair bulb is composed by the dermal papilla, a densely packed cluster of fibroblasts that is enwrapped by matrix keratinocytes (matrix), and harbors the pigmentary unit (see also section 1.1.4). The sebaceous gland comprise specialized skin cells, the sebocytes, that produce and accumulate lipids (sebum), which can be released to the skin surface and contribute to the skin barrier function.

Interestingly, a recent study has revealed that not only the epidermal keratinocytes but also dermal fibroblasts form distinct cell lineages in the skin (Driskell et al., 2013). Transplantation and lineage tracing experiments identified two distinct lineages with specialized functions: while the upper dermal fibroblast lineage is involved in HF formation giving rise to dermal papilla and arrector pili muscle cells, the lower dermal fibroblasts are mainly responsible for ECM synthesis and are able to differentiate into preadipocytes and adipocytes of the sub cutis.

1.1.1 Hair follicle morphogenesis

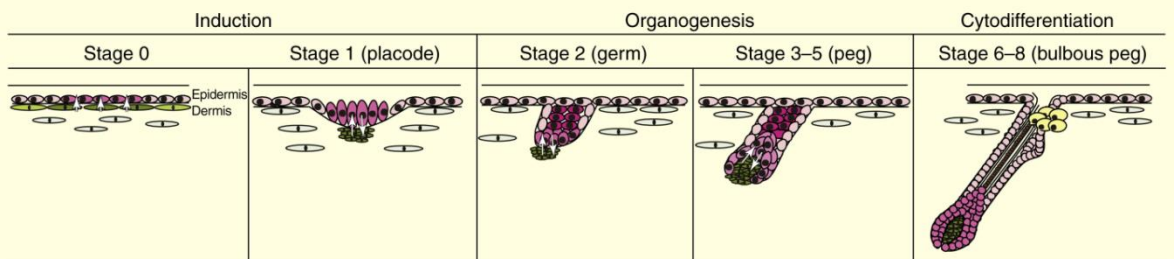

Figure3: HF morphogenesis in mice
The murine HF development is induced by dermal signals (stage 0), which leads to the hair placode (stage 1) in the induction phase. During organogenesis (stage 2-5) extensive dermal-epidermal cross talk promotes the hair germ maturation. In the following cytodifferentiation phase (stage 6-8) the distinct HF layers, sebaceous gland and HF SC compartments are formed (modified from (Schneider et al., 2009)).

During embryonic development HF morphogenesis is initiated by a priming dermal signal (stage 0), leading to the condensation of epidermal cells in a regular pattern (discussed below) to form epidermal placodes (stage 1), referred as induction phase (Figure 3). Although there are a lot of strong evidences that this first initiating dermal signal is based on the release of small glycolipoproteins, termed wntless type (Wnt) ligands, the precise source and identity of these Wnt ligands remain unknown (Andl et al., 2002). The epidermal placodes then start to signal involving Wnt/β-catenin, sonic hedgehog (Shh) and transforming growth factor β (TGFβ) pathway, which results in the aggregation of underlying mesenchymal cells to dermal condensates that develop into a hair germ (stage 1-2). In response to a second dermal signal, now originating from the further developed dermal condensate, epidermal placode cells proliferate, invade the dermis and form the dermal papilla by embracing the dermal condensate (stage 2-5) during the organogenesis phase. At later stages (stage 6-8) extensive cross talk between epithelial cells of the developing hair maintains high proliferation levels and leads to differentiation of the inner root sheath and hair shaft of the mature HF (cytodifferentation phase). The dominant role of the Wnt/β-catenin pathway for hair morphogenesis is underlined by the fact that deletion of β-catenin or its co-factor Lef1 in skin abolishes HF development (Huelsken et al., 2001; van Genderen et al., 1994). Conversely, increased Wnt signaling through stabilized β-catenin or overexpressed Wnt ligands is sufficient to direct epidermal cells to an appendage fate, leading to *de novo* HF formation (Gat et al., 1998; Widelitz et al., 1999).

In mouse back skin, HFs emerge at an angle of approximately 40 degree to the epidermis aligned from anterior to posterior direction (Paus et al., 1999). It has been speculated that this polarity is regulated by the Wnt target gene Shh since it is asymmetrically expressed in the HF bulb in a small patch of cells at the side of the matrix closest to the skin surface (Bitgood and McMahon, 1995; Gat et al., 1998).

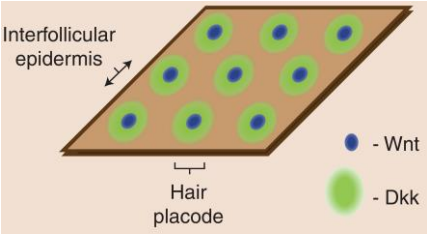

Figure4: Turing reaction diffusion model for HF patterning
In the HF morphogenesis induction phase simultaneous secretion of low distance diffusing inductive Wnt ligands and faster diffusing Wnt inhibitor Dickkopf (Dkk) establish a regular array of elevated Wnt signaling nodes which eventually develop into HFs (modified from (Lim and Nusse, 2013)).

During morphogenesis the HF spacing is established by the patterning of the placode array which is suggested to be governed by the “turing reaction diffusion model” (Sick et al., 2006), which was previously described for feather development (Jiang et al., 1999). In this model Wnt signaling

activators (Wnt ligands) and inhibitors (e.g. Dickkopf (Dkk)4) are secreted by the placodes and diffuse into the extracellular space (Figure4). The large, hydrophobic Wnt ligands diffuse only for a short range in the aqueous extracellular environment, while the Wnt inhibitors such as Dkks travel a longer range due to smaller size and better solubility. Through this mechanism, placodes can only persist in discrete interdistances: placodes at too close interdistances will cancel out Wnt ligand induced induction through high Dkk levels, whereas empty spaces with low Dkk levels promotes placode induction. At the end of HF morphogenesis (stage 6-8) the sebaceous gland and the multiple HF SC compartments start to form, which will be discussed below.

1.1.2 Skin stem cells

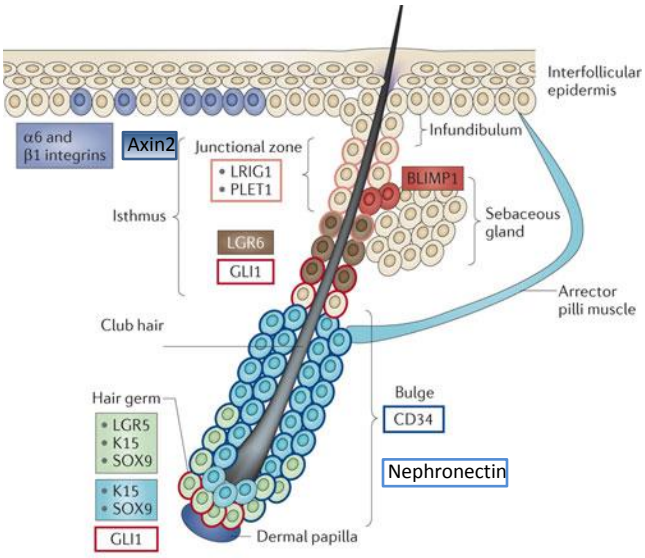

Figure5: The epithelial SC populations in the murine skin

The HF bulge can give rise to all epidermal lineages and harbors different HF SC subpopulations enwrapped by nephronectin characterized by the partially differing expression pattern of CD34, Sox9, Krt15 and Lgr5. Gli1 positive HF SCs can be found in the bulge and isthmus region, whereas Lgr6 and Lrig1 / PLET1 expressing cells are restricted to the isthmus and junctional zone. The unipotent Blimp1 positive SCs are located close to the sebaceous gland. SC in the interfollicular epidermis seems to express high level of integrins and Axin2, but their organization is still unclear (modified from (Arwert et al., 2012)).

Throughout life skin homeostasis relies on epidermal SCs, which are able to self-renew or differentiate into all epidermal lineages (Fuchs, 2008). The adult skin is maintained by multiple SC populations which develop during HF morphogenesis and reside in different locations within the tissue (Figure5). Under normal homeostatic conditions, SCs in these distinct locations maintain associated cell lineages: HF SCs maintain HF linages, sebaceous gland SCs produce differentiated sebocytes and SCs in the interfollicular epidermis renew epidermal cells. But upon injury, genetic manipulations or transplantation different SC populations are able to reprogram and to give rise to multiple lineages (Ito et al., 2005; Taylor et al., 2000). One key pathway for SC fate determination is the Wnt/β-catenin pathway. In mice, Wnt signaling disruption inhibits embryonic HF formation, whereas ectopic epidermal activation results in *de novo* formation of sebaceous

gland and HF from existing HF and interfollicular epidermis in a dose dependent manner (Gat et al., 1998; Huelsken et al., 2001; Silva-Vargas et al., 2005).

In murine skin the main SC compartment is the bulge, first identified by the long-term retention of a DNA label, such as 5-bromodeoxyuridine (BrdU) (Cotsarelis et al., 1990; Lyle et al., 1998). The first molecular marker of the bulge to be identified was keratin-15 (Krt15), followed by CD34, Sox9 and leucine-rich repeat-containing G protein-coupled receptor 5 (Lgr5) (Jaks et al., 2008; Lyle et al., 1998; Trempus et al., 2003; Vidal et al., 2005). In contrast to cells from other regions of the HF and the epidermis, bulge cells display the greatest *in vitro* growth capacity and clonogenicity and can fully reconstitute skin in transplantation experiments, indicating that these cells are multipotent (Taylor et al., 2000). *In vivo* lineage tracing experiments revealed that under homeostatic conditions bulge cells give rise to the lower HF, including the outer root sheath, matrix and hair shaft, and upon injury migrate upwards to differentiate into epidermal keratinocytes (Ito et al., 2005; Taylor et al., 2000). Bulge SCs crucially rely on quiescence for long-term maintenance and perturbations in the quiescent regulation result in premature SC loss (Arai and Suda, 2008).

Whereas in the past the bulge was believed to be the primary residence of HF SCs, in recent years it has become clear that SCs also reside in the isthmus (these cells are positive for Lgr6 and/or MTS24) (Nijhof et al., 2006; Snippert et al., 2010) as well as in the junctional zone adjacent to the sebaceous glands and infundibulum (these cells are positive for leucine-rich repeats and immunoglobulin-like domains 1 (Lrig1)) (Jensen et al., 2009). Lgr6, MTS24, and Lrig1 positive SC constitute partially overlapping SCs niches, which can be separated by flow cytometry (Jensen et al., 2010). In the upper part, Lrg6 expressing cells partly overlap with unipotent B lymphocyte-induced maturation protein 1 (Blimp1) expressing cells that are confined to fueling cells to the sebaceous gland (Horsley et al., 2006). Of note, when Blimp1 positive cells are lost they are replaced by multipotent bulge SC, underlining the SC hierarchy in the HF.

Although the presence of SC in the interfollicular epidermis has been indicated by linage tracing experiments (Clayton et al., 2007), for a long time their molecular identity has remained obscure due to lack of specific markers (Watt and Jensen, 2009). Intriguingly, a recent study proposes that interfollicular epidermal SC express high levels of Wnt target gene Axin2. These cells require Wnt/β-catenin signals to proliferate and do not rely on quiescence for maintenance (Lim et al., 2013). For HF SCs the niche environment is highly important. One major niche component in the HF bulge is the extracellular matrix protein nephronectin which is secreted by bulge SCs (Fujiwara

et al., 2011). Within the HF the niche environment of specialized SC compartments influences the identity "stemness" and dictates the development of phenotypically and molecularly distinct populations of HF SCs. Indeed, in the bulge two subpopulations have been identified with distinct transcriptional profiles imposed by the localization within the bulge niche: a basal bulge SC subpopulation, which maintain basement membrane contact, and a suprabasal SC subpopulation, which arise only after the first hair cycle (Blanpain et al., 2004). Further sensory neurons in contact with the HF cultivate a perineural niche microenvironment in the bulge and isthmus. The induced secretion of Shh results in a specialized subset of bulge cells characterized by high Glioblastoma 1 (Gli1) expression and activated Hedgehog pathway, which are able to become epidermal SCs (Brownell et al., 2011). For interfollicular epidermal SCs, however, it remains unclear if they also rely on dermal and basement membrane niche factors forming interfollicular epidermal SC niches. It is conceivable that many more specialized SC subpopulations, maintained and defined by a complex array of niche factors, will be discovered in the near future. In human HF, specific hair SC markers remain to be identified. So far human bulge SC could be best described by high KRT15, keratin-19 (KRT19) and CD200 expression and absence of CD34 (which is high in mouse SCs), nestin and connexin 43 (Kloepper et al., 2008). Interestingly, comparative transcriptional profiling of human and mouse bulge cells have revealed similarities in upregulation of Wnt signaling inhibitors, TGFβ signaling components and CD200 expression, but also discrepancies such as the CD34 expression pattern (Ohyama et al., 2006). This indicates that besides the divergences in SC compartments between mouse and humans, also phenotypic and molecular differences in similar SC populations exist, which will be a challenge to characterize in the future.

1.1.3 The postnatal hair cycle

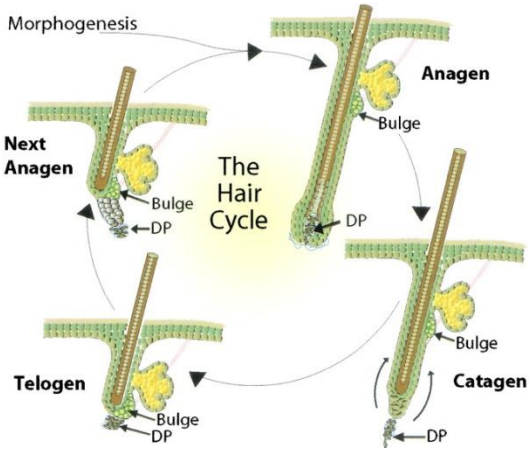

Figure6: The hair cycle
HF periodically cycle from anagen (growth phase), through catagen (regression phase) and into telogen (resting phase) (modified from (Alonso and Fuchs, 2003)).

The postnatal hair cycle is initiated with a phase of regression and controlled cell death (catagen), followed by a resting phase (telogen) and ends in a phase of HF growth (anagen), which then is followed by further rounds of catagen, telogen and anagen (Figure6). The HF is governed by an autonomous, intrafollicular oscillator system, referred as "hair cycle clock" (Paus and Foitzik, 2004). During each hair cycle a new hair shaft is formed during anagen and the old club hair is shed off after catagen. In mice, the first hair cycle is synchronized for all HFs and occurs in a wave from the venter dorsally and posteriorly (Plikus and Chuong, 2008). The postnatal hair cycle starts at 17 days after birth after completion of HF morphogenesis with the first catagen, which has been shown to be induced by a plethora of growth factor signals such as fibroblast growth factor (FGF)5, TGFβ1, the neurotrophins (NT)-3 and NT-4, brain-derived neurotrophic factor (BDNF), bone morphogenetic protein (BMP)2/4 and tumor necrosis factor (TNF)α (Stenn and Paus, 2001). During catagen the HF matrix, inner root sheath and outer root sheath keratinocytes of the cycling HF part undergo a controlled apoptosis, while bulge HF SCs are protected and remain quiescent. Consequently, the cycling part of the HF regresses in the shape of a thin epithelial strand towards the epidermis, which brings the dermal papilla in close proximity to the bulge (Muller-Rover et al., 2001; Stenn and Paus, 2001).

The following telogen phase lasts only several days during the first HC and usually more than three weeks during the second telogen. Although the telogen phase is considered as a stage of low proliferation, it coincides with major changes in gene activity (Lin et al., 2004). During this resting phase the bulge and the dermal papilla in very close proximity, providing proliferation inhibitory signals to the bulge leading to their quiescence. It is generally believed that during telogen little or no Wnt/β-catenin signaling occurs. Indeed, during telogen the bulge expresses multiple Wnt inhibitors, such as secreted frizzled-related protein (sFRP)1, Wnt inhibitory factor 1 (Wif1) and Dkk3 (discussed in section 1.4.7) (Morris et al., 2004; Tumbar et al., 2004) as well as the transcription factor (Tcf)3, which is believed to repress Wnt/β-catenin signaling in the absence of nuclear β-catenin (discussed in section 1.4.3) (Lien et al., 2014; Wu et al., 2012). This refractory phase of the telogen is further supported by high expression of BMP2/4 and TGFβ from the dermal papilla and bulge cells (Plikus et al., 2008; Woo and Oro, 2011). At the end of the telogen, bulge SCs become highly sensitive for anagen inducing factors which promotes hair regeneration. This induction appears to result from the antagonistic interplay between BMP, TGFβ, FGF and Wnt/β-catenin signaling in follicular SCs (Greco et al., 2009; Plikus et al., 2008). However, the molecular details how Wnt signaling is switched on at anagen onset remain poorly understood. A

recent study using live cell imaging demonstrates that constitutive activation of Wnt/β-catenin in a small pool of HF SCs is sufficient to induce hair growth independent of dermal papilla niche cell signals (Deschene et al., 2014). These Wnt signaling high SCs are able to activate Wnt signaling in neighboring cells via Wnt ligand secretion resulting in a coordinated tissue growth. Interestingly, during this phase most bulge SCs remain quiescent and only a small number of cells becomes fully activated, starts proliferating and migrate out of the bulge forming a new (secondary) hair germ. In these cells, Lef1 is upregulated, binds to β-catenin forming an active transcription factor complex, which replaces the inhibitory Tcf3 from the promoters regions of Wnt target genes (Lien et al., 2014). Because Lef1 is a β-catenin target gene itself, Wnt signaling is amplified in a positive feedback loop (Wu et al., 2012). Indeed, studies with Wnt signaling reporter mice showed that in the secondary hair germ and hair matrix the high Lef1 expression correlates with the strongest Wnt signaling activation (DasGupta and Fuchs, 1999).

Interestingly, expression of constitutively stable β-catenin in basal epidermal keratinocytes leads to hyperactive Wnt/β-catenin signaling and is sufficient to induce anagen onset (Silva-Vargas et al., 2005; Van Mater et al., 2003), whereas β-catenin loss-of-function blocks entry into anagen when induced postnatally (Huelsken et al., 2001), placing Wnt/β-catenin upstream of hair cycle regulation.

During full anagen, the upper matrix cells stop proliferating and differentiate into the various cell linages of the hair shaft and inner root sheath. Conversely, the relatively undifferentiated outer root sheath originates from epithelial progenitor cells derived from a small and distinct bulge population. Linage tracing experiments has revealed that these cells form a very narrow proliferative zone between the lower bulge and the hair bulb (Rompolas et al., 2013). At the end of the anagen, dermal BMP signaling and TGFβ2 in the hair bulb have been suggested to mediate catagen induction (Plikus et al., 2008; Soma et al., 2002). Subsequently the HF enters the telogen phase. Nevertheless, although many key players have been identified, the molecular mechanism driving hair cycling remains obscure.

1.1.4 Hair pigmentation

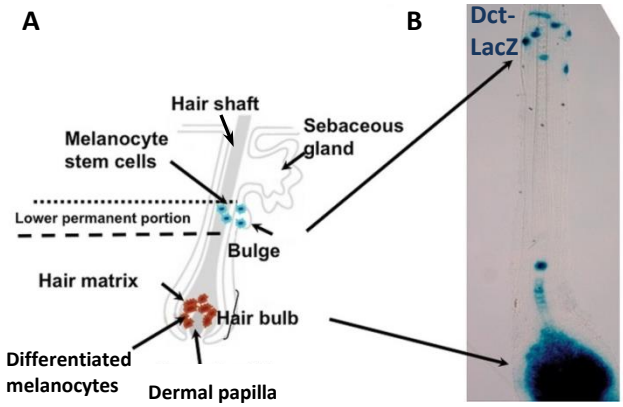

Figure7: Localization of melanocyte stem and precursor cells in the HF

(**A**) Melanocyte SCs reside in the bulge in close contact with HF bulge SCs, whereas differentiated melanocytes are located in the hair matrix forming the pigmentary unit. (**B**) Melanocytes can be easily visualized with a LacZ reporter gene under control of the tyrosinase dopachrome tautomerase (Dct-LacZ) promoter (modified from (Osawa, 2008)).

Skin pigmentation plays an important physiological and evolutionary role by protecting animals against mutagenic ultra violet (UV) irradiation as well as allowing camouflage, mimicry, and social communication. Pigmentation of the HF is important for skin UV protection, thermoregulation, camouflage and sexual signals. Hair pigment melanin is produced by melanocytes arising from neural crest-derived melanoblasts (Rawles, 1947), which reside in the hair matrix and along the outer root sheath of anagen HFs (Figure7A,B). In adult mouse back skin, melanocytes are located exclusively in HFs, while in human skin melanocytes are maintained in the interfollicular epidermis as well. In contrast to the continuous epidermis melanogenesis, in HF the melanin production by melanocytes is strictly coupled to the hair cycle where it exclusively occurs during anagen (Slominski et al., 2005). During catagen most melanocytes in the HF undergo apoptosis and will be replenished during the next anagen by melanocyte SCs residing in the bulge and secondary hair germ (Sharov et al., 2005) (Figure7A,B). Intriguingly, their homeostasis and activation is synchronized with and directly dependent on the keratinocytes of the bulge, involving Wnt, TGFβ and Notch signaling from the bulge SCs (Moriyama et al., 2006; Nishimura et al., 2010; Rabbani et al., 2011). Hair pigment production occurs only in the HF pigmentary unit located in the hair bulb. There, melanocytes synthesize melanin in melanosomes (lysosome related organelles), which are actively exported and transferred to receiving HF keratinocytes leading to the formation of a pigmented hair shaft (Nishimura et al., 2002; Slominski et al., 2005). The melanocytes and melanoblasts in the outer root sheath normally do not engage in pigment production but can replace lost epidermal melanocytes. Graying of hair cavities in mice as well as humans is the direct consequence of a loss of active melanocytes in the HF pigmentary unit, which results from a depletion of the melanocyte SC reservoir in the bulge. Why HF melanocytes seem to age faster compared to the epidermal counterparts, is still a mystery.

1.2 Integrin receptor family and adhesion structures

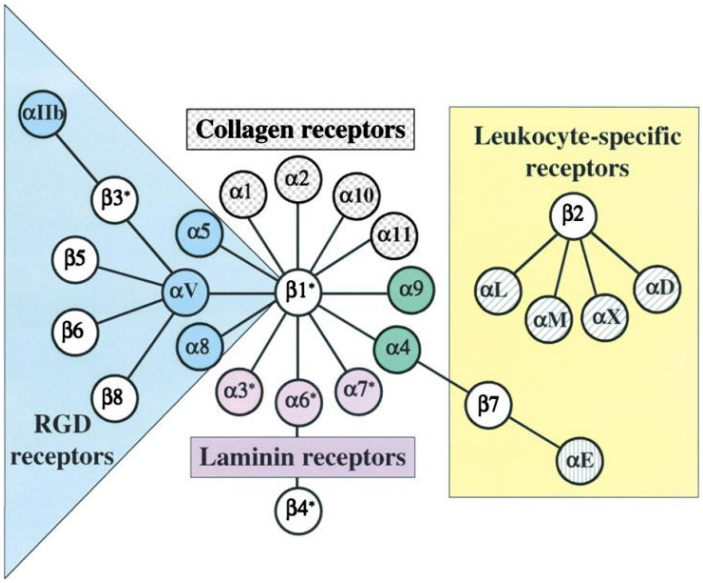

Figure8: Integrin heterodimer family
The integrin heterodimers can be grouped into several subclasses according to their ligand specificity for collagen, laminin or RGD motif containing ligands as well as their leukocyte restricted expression. All gray plaid and striped α subunits harbor α-inserted (αI) domains in the headpiece (modified from (Hynes, 2002)).

Integrins constitute a major family of cell surface receptors, which recognize as ligand ECM proteins such as collagen, laminin and fibronectin, expressed together with integrins in all metazoans. Integrins form obligate heterodimers composed of non-covalently associated α and β subunits, each being a transmembrane glycoprotein, where the majority of the domains of both subunits reside in the extracellular space and are required for ligand interaction (Humphries et al., 2006; Hynes, 2002). In mammals there are 18 α and 8 β subunits, which give rise to 24 distinct integrins heterodimers with specialized function and ligand binding activity (Figure8). Some integrin subunits like β1 form heterodimers with several different α subunits, whereas others such as β4 or β6 form only single heterodimers. Integrins can be grouped into four classes: first, RGD peptide recognizing integrins that bind molecules like fibronectin, vitronectin and others including latent TGFβ binding protein (LTBP) (see section 1.3.6) through an RGD motif; second, laminin binding receptors where the binding mode is still unknown; third, collagen receptors binding to a GFOGER peptide motif; forth, the LDV peptide recognizing integrins that bind fibronectin and other ligands such as vascular cell adhesion molecule (VCAM)1 (Humphries et al., 2006).

Integrins are regarded as molecular switches as they can reversibly change from a low to a high ligand affinity conformation, referred as integrin activation. Integrin activation, connection to the intracellular cytoskeleton and signaling is mediated by binding of multiple cytoskeletal and adaptor proteins to the rather short cytoplasmic tail of the β and less frequently to the α subunit. This allows reversible anchoring of the cellular actin cytoskeleton to the ECM and other cells.

Altogether, stable extracellular ligand binding stimulated upon intracellular signals (inside-out signal) results in recruitment of further intracellular signaling proteins to the integrins (outside-in signal), which therefore serve as signaling platform for bidirectional signaling across the plasma membrane. Thus, integrins control a variety of vital cell functions, such as adhesion, polarity, differentiation, migration and cell division, which are all critical for tissue morphogenesis and homeostasis. Indeed, deregulations in integrin signaling are hallmarks of many pathological conditions including adhesion related diseases such as junctional epidermolysis bullosa, Kindler syndrome (KS), Leukocyte adhesion deficiency type (LAD) I and III as well as cancer (see section 1.5.3 and 1.6.3) (Janes and Watt, 2006; Wilhelmsen et al., 2006; Winograd-Katz et al., 2014).

The expression pattern of integrins differs between tissues and cell types, where they exert distinct functions. Whereas β1 integrin heterodimers are expressed in almost all mammalian cells, others are highly restricted such as integrin β2 and β7 (only present on cells of the immune system) or β6 and β4 (limited to epithelial cells). The adhesive complexes also differ between the different integrin subtypes (see also section 1.2.5): β4 integrin anchors the intermediate filament to laminin in hemidesmosomes, allowing stable adhesion of the epithelia (Wilhelmsen et al., 2006). The integrins β1, β2 as well as β3 can form focal adhesion complexes and podosomes important for cell migration and tissue remodeling, respectively (Humphries et al., 2006; Linder and Kopp, 2005). The fact that integrins exert many non-redundant functions *in vivo* is reflected by the highly diverse mouse phenotypes upon deletion of individual integrin subunits: for example, β1 subunit deletion blocks embryo development already during the peri-implantation state, whereas β4 or αv loss lead to perinatal lethality and β2 or β7 deletion result in viable animals with defects in immune cells such as leukocytes (Bader et al., 1998; Fassler and Meyer, 1995; Scharffetter-Kochanek et al., 1998; van der Neut et al., 1996; Wagner et al., 1996).

1.2.1 Integrins in the skin

In skin integrin expression is largely confined to the basal layer of the epidermis and is down regulated during terminal differentiation. Also within the basal layer expression levels of the integrins vary, depending on their differentiation status; a hallmark of epithelial SC is their high level of β1 integrin heterodimer expression (Zhu et al., 1999). The most abundant integrins in skin are α2β1, α3β1 and α6β4, recognizing components of the basement membrane such as collagens and laminins. They are all highly expressed in the basal skin layer and mediate firm adhesion of the

kerationcytes to the basement membrane as well as to neighboring cells. Indeed, deletion of either complete β4 or skin specific β1 leads to severe skin blistering defects and barrier function (Piwko-Czuchra et al., 2009; Raghavan et al., 2000; van der Neut et al., 1996). While β4 null mice completely lose hemidesmosoms, in β1 deleted mice their stability is severely impaired. In addition, β1 deleted mice show an aberrant HF morphogenesis, due to impaired hair matrix cell adhesion and migration (Brakebusch et al., 2000; Raghavan et al., 2000).

In contrast, αvβ5 can be detected only at low levels in the skin and the αvβ5 null mice display no obvious phenotype (Huang et al., 2000). Thus, its function for skin homeostasis is still unclear. Interestingly, the expression of αvβ6 is restricted to epithelial cells, where it regulates epithelial remodeling during development, tissue repair and neoplasia. While during embryo development αvβ6 is highly expressed in the whole developing epidermis, in adult epithelial cells it is strongly downregulated with the exception of HF (Breuss et al., 1995; Breuss et al., 1993). There, αvβ6 integrin is highly expressed in the bulge (Tumbar et al., 2004) and the expression level correlates with the hair cycle, showing the highest expression in the early anagen and the lowest in telogen (Xie et al., 2012). During wound repair, the expression of αvβ6 is highly upregulated in the interfollicular epidermis and maintained until wound closure is completed (Eslami et al., 2009). Indeed, loss of β6 integrin leads to an accelerated wound closure (Xie et al., 2009). Although normal hair morphogenesis and hair cycle are not affected in β6 integrin null mice, after depilation keratinocyte proliferation is enhanced and hair cycle induction is accelerated, indicating an aberrant HF bulge SC activation (Xie et al., 2012). In addition, the β6 integrin null mice have revealed an unexpected role for this epithelial integrin in the downregulation of local inflammations, as they display increased numbers of macrophages in the skin and persistent accumulation of activated lymphocytes in the lung (Huang et al., 1996).

1.2.2 Integrin structure and activation

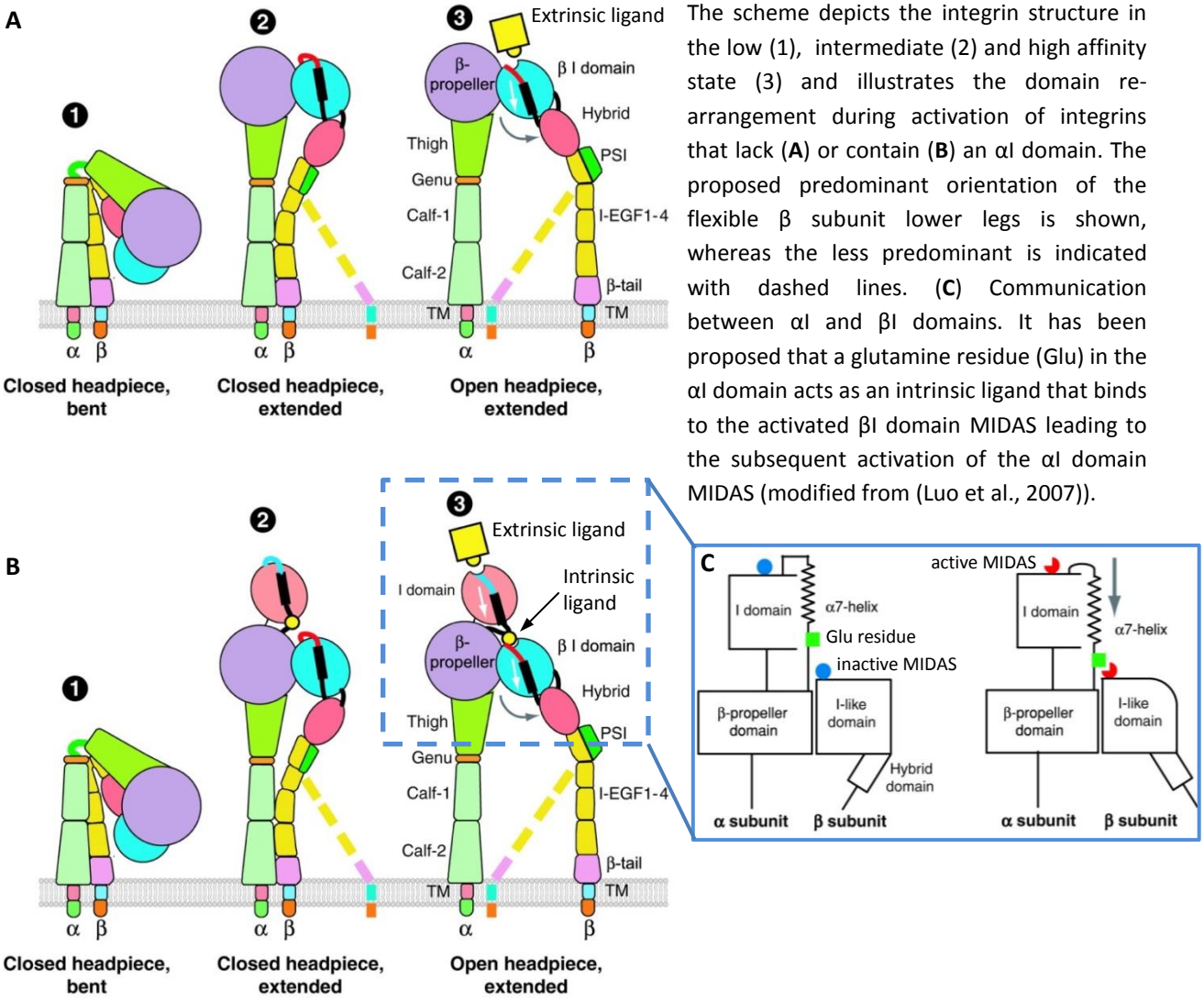

Figure9: Integrin activation
The scheme depicts the integrin structure in the low (1), intermediate (2) and high affinity state (3) and illustrates the domain re-arrangement during activation of integrins that lack (**A**) or contain (**B**) an αI domain. The proposed predominant orientation of the flexible β subunit lower legs is shown, whereas the less predominant is indicated with dashed lines. (**C**) Communication between αI and βI domains. It has been proposed that a glutamine residue (Glu) in the αI domain acts as an intrinsic ligand that binds to the activated βI domain MIDAS leading to the subsequent activation of the αI domain MIDAS (modified from (Luo et al., 2007)).

Both integrin subunits are composed of multiple, extended extracellular domains (~800 amino acids each) referred to as ectodomain, a 20 amino acids single pass transmembrane domain (TMD) and a short unstructured cytoplasmic "tail" domain, which generally ranges from 20-70 amino acids in length. The only exception is the β4 cytoplasmic tail being much larger (~1000 amino acids). Crystal structure analysis have revealed that the α subunit consists of several modules, subdivided into the more membrane proximal leg domain and the more distal, ligand-binding head domain (Figure9A,B). The most N-terminal β-sheet structure of the α ectodomain folds into a seven-bladed β-propeller domain. The α subunit leg contains three extended β-sandwich domains, the thigh domain in the upper and the two calf-1 and -2 domains in the lower leg. The thigh and

calf-1 domain are connect by a small Ca^{2+} binding loop, which serves as a flexible joint, termed "genu", for switchblade extension (discussed below).

Conversely, the structure of the β subunit is more complex. The headpiece of the β domain is formed by a plexin/semaphorin/integrin (PSI) domain that is interrupted by a β sandwich hybrid domain containing the β-inserted (βI) domain. In the folded β subunit headpiece the PSI domain is located below the hybrid-βI domain and bound to the lower headpiece by a disulfide bond. In addition, the βI domain contains two segments: the first allows forming the interface with the β-propeller and the second is essential for specific ligand binding, known as the specificity determining loop (SDL). One part of the βI domain directly binds to the β-propeller of the α subunit and both together form the ligand binding head of the integrin, which structurally shows strong similarity to the Gα/Gβ complex formation in G proteins. The lower β subunit leg part is built by four cysteine-rich integrin epidermal growth factor-like (I-EGF)1-4 domains and a short disulfide-bonded β-sheet tail (β-tail). The β leg pivot is located between the I-EGF domains 1 and 2 in close proximity to the α leg genu allowing the unbending of the integrin headpiece, which is an important prerequisite for ligand binding.

Integrins can exist in an equilibrium between two (β1 heterodimers) or three (αv, β2 and β3 heterodimers) different conformations with different ligand affinity (Luo et al., 2007; Nishida et al., 2006): a bent low-affinity (not bent in β1 heterodimers), half extended intermediate-affinity and an upright high-affinity state. The shift of this equilibrium from the first to the last conformation (i.e. integrin activation) can be induced either by the binding of extracellular ligands to integrin ectodomains or by the binding of integrin activatory proteins Talin and Kindlin to the cytoplasmic β tails (i.e. inside-out signaling, see section 1.2.4). In the bent conformation the headpiece is facing away from potential ligands and in close proximity to the plasma membrane with the hybrid domain deeply buried in the integrin leg interface. This low affinity state is stabilized by a close association of the integrin legs in the TMD and cytoplasmic tail region, forming hydrophobic and electrostatic interactions between the GFFKR and HDR(R/K)E sequence motifs in the membrane proximal region, which are highly conserved between all cytoplasmic integrin tails (De Melker et al., 1997; Hughes et al., 1996). It is proposed for some heterodimers that a salt bridge is formed between the arginine in the α and the aspartate in the β subunit and that disruption of this salt bridge can induce integrin tail separation and thus integrin activation (Hughes et al., 1996). For the intermediate-affinity state it is proposed that the integrin extends

the ectodomain while the headpiece is still closed and the integrin tails are not separated. In the high-affinity state the integrin headpiece is fully extended and open, placing the ligand binding site 150-200 Å away from the cell surface facing towards the ECM and thus increasing the ligand accessibility. Moreover, in the TMD the inhibitory salt bridge and the other interaction sites are disrupted allowing the integrin legs to separate by up to 70 Å. The equilibrium between the different conformations is integrin heterodimer dependent and could partially explain the different susceptibility of integrins to activation (Bazzoni et al., 1998).

Interestingly, nine of the α subunits contain an additional inserted αI domain, a 200 amino acid insertion into the 2 and 3 β-sheet of the β-propeller, also known as von Willebrand factor A domain. The αI domain is highly homologue to the βI domain but lacks the two additional segments (β-propeller interface and SDL). In these integrin heterodimers the αI domain provides the major integrin ligand interface and, similar to βI domain, it can switch between different conformations (Shimaoka et al., 2000). Upon ligand binding to the αI domain, it is proposed that a pseudo-substrate loop, harbored in the α subunit, binds to the β subunit βI domain which transmits the conformational change to the hybrid domain, leading to integrin activation (Figure9B,C).

Both I-domains harbor a highly conserved metal ion-dependent adhesion site (MIDAS) for divalent cation binding important for ligand binding (the integrin conformation regulation). Under physiological conditions the MIDAS is occupied by Mg^{2+}. In addition, the βI domain MIDAS is flanked by two Ca^{2+} binding sites which influence integrin-ligand affinity. One is termed ligand-induced metal ion–binding site (LIMBS), because this site is only formed in the ligand bound state and therefore stabilizes ligand binding. The other is known as adjacent to metal ion–dependent adhesion site (ADMIDAS) and has a rather inhibitory effect (Xiao et al., 2004). Because of these sites, integrin activation is influenced by divalent cations: Mg^{2+} has an activatory influence, high concentrations of Ca^{2+} are inhibitory and Mn^{2+} can induce a high affinity state of integrins through replacement of Ca^{2+} at the ADMIDAS site of the βI domain.

For integrin activation two models have been proposed: the ‘switchblade’ and the ‘deadbolt’ model. However, the exact mechanism remains elusive. In the first model the integrin headpiece is bended at the genu towards the plasma membrane in a ligand low-affinity state. The transition to a high ligand affinity state occurs by a switchblade-like opening of the ectodomain into an extended conformation with separated subunit legs, which allows adaptor protein recruitment. In

this model, integrin extension and subsequent leg separation are coupled with the swing-out of the hybrid domain.

The second model suggests that upon initial ligand binding the integrin remains V-shaped bended (low-affinity state) and only a piston-like movement of the TMD disrupts the locked orientation of the headpiece and β subunit, allowing full integrin extension (high-affinity state) (Arnaout et al., 2005; Xiong et al., 2003). Hence, transduction of outside-in signaling could already occur without ectodomain extension. However, mutations studies on the deadbolt region of the β tail domain have highly questioned this model, showing that bended integrin are resistant to inside-out activation and that the headpiece extension is essential for full length fibronectin accessibility (Zhu et al., 2007a).

Interestingly, integrin mutants with blocked TMD separation have revealed that tail separation is not necessary for full ectodomain extension, ligand binding and cell adhesion, but crucial for the propagation of outside-in signaling shown by impaired cell spreading, actin stress fiber and focal adhesion formation as well as focal adhesion kinase (FAK) activation (Zhu et al., 2007b). Thus the TMD separation is essential for outside-in signal transduction but not for integrin activation.

1.2.3 Integrin clustering and catch-bond mechanisms

The integrin adhesion to the ECM can be strengthened by lateral, non-covalent association of integrins at an adhesion site, referred to as integrin clustering (Cluzel et al., 2005; Shattil et al., 2010). The coordination of multiple weak binding integrin allows the formation of a strong adhesion bond in an additive manner. Besides integrin mediated adhesion, integrin clustering seems to be also essential for efficient integrin signaling (Bunch, 2010; Zhu et al., 2007b). But how clustering is mechanistically regulated, remains largely unclear. For example, it has been proposed that during the adhesion process the binding of one integrin to ECM can bring the cell surface closer to the ECM facilitating the association of further integrins which promote the formation of a cluster (Boettiger, 2012). But it is also possible that integrins form little clusters already in suspension which facilitate a stable adhesion formation upon initial contact with the ECM. Furthermore, Talin is proposed to play an important role for the integrin clustering process as a molecular lattice, due to its dimerization capacity and second integrin binding site (see section 1.2.4). Because α-Actinin and Filamin harbor multiple integrin binding sites, they could contribute

to integrin clustering as well. Finally, a recent study suggests that Kindlin could be more important for integrin clustering than integrin activation, but the molecular mechanism remains undefined (Ye et al., 2013).

Recent data underline a more important role for the integrin-actin-cytoskeleton-connection for integrin activation than previously assumed (Kong et al., 2009). It has been suggested, that integrin ligand interaction of at least certain heterodimers (α5β1, probably not αvβ3) might not follow normal kinetics of classical interactions. Usually, when a force is applied between two non-covalently interacting molecules, the half-life time of these bonds is decreased (slip-bond). For α5β1 integrin, it has been shown that instead the half-life time reaches a maximum between 10-30 pN force (catch-bond) before decreasing at higher force (slip-bond) (Kong et al., 2009). In a further publication, it has been shown that a second mechanism different from catch-bonding can be observed for α5β1 integrin (Kong et al., 2013): Here the integrin appears to retain a memory of a previously applied force, and thus will retain a prolonged half-life time of the ligand interaction after a cycle of contraction and relaxation (cyclic-mechanical reinforcement). However, how catch-bonds and cyclic-mechanical reinforcement are transmitted on the molecular level of the integrin, and which adaptor molecules are essentially required, remains to be elucidated.

1.2.4 Integrin activation is mediated by Talin and Kindlin

For integrin inside-out activation the key players are the cytoskeletal linker proteins Talin and Kindlin (Figure10) which are both essentially required for integrin activation and will be discussed below.

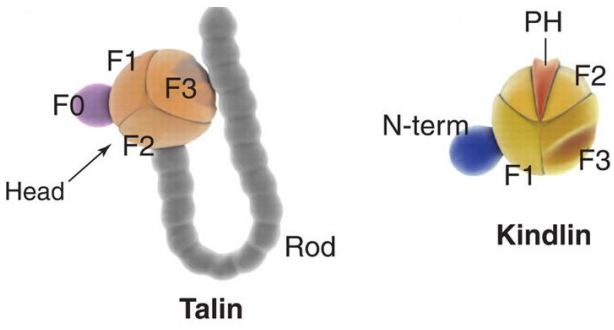

Figure10: Talin and Kindlin structure
Talin consists of a large rod and a head domain containing a four point one protein, ezrin, radixin, moesin (FERM) domain composed of three subdomains (F1-3) and a small F0 domain. In the inactive state the Talin rod domain is supposed to cover the integrin binding site in the F3 subdomain. Kindlins consist of a small N-terminal domain and a FERM which is highly similar to Talin but in addition harbors a pleckstrin homology (PH) domain in the F2 subdomain (modified from (Moser et al., 2009b)).

1.2.4.1 Talin

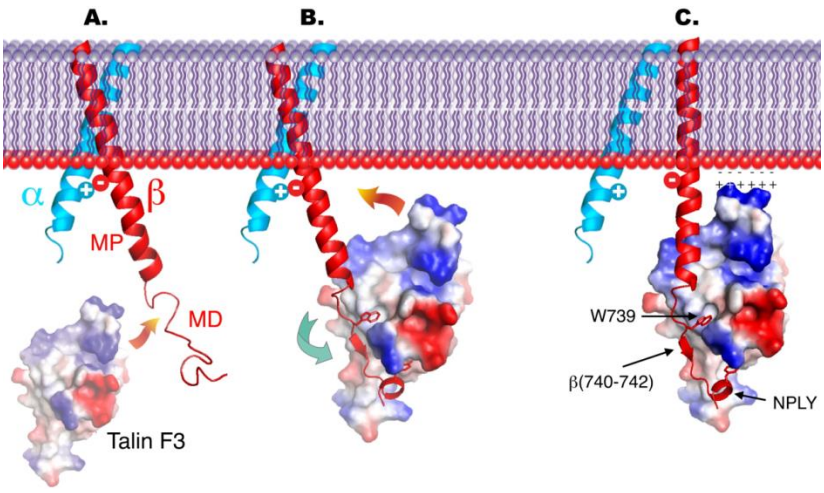

Figure11: Structural model of Talin induced β3 integrin activation
(**A**) In the inactive conformation the integrin heterodimers are connected via a salt bridge. (**B**) The Talin F3 domain binds to the NPLY motif in the membrane distal (MD) part of the β3-integrin tail resulting in a higher order of the cytoplasmic tail. (**C**) Subsequently, the Talin F3 domain electrostatically interacts with acidic lipid headgroups in the plasma membrane and a membrane proximal (MP) region of the cytoplasmic β tail, inducing the destabilization of the salt bridge, separation of the integrin tails and integrin activation (modified from (Wegener et al., 2007)).

Talin is a large cytoplasmic adaptor protein (~270 kDa) consisting of a N-terminal 47 kDa head domain with a four point one protein, ezrin, radixin, moesin (FERM) domain and a 220 kDa C-terminal flexible rod domain, which is composed of consecutive helical bundles with multiple binding sites for filamentous (f)-Actin binding protein Vinculin (Figure10) (Critchley and Gingras, 2008).

The FERM domain consists of three subdomains (F1, F2 and F3) and shares considerable sequence homology with the FERM domain of Kindlin. The F3 subdomain harbors a phosphotyrosine binding (PTB) fold that can directly bind to the membrane proximal NPxY motif in the cytoplasamtic β subunit tail (Wegener et al., 2007). Structural analysis of the β3 tail Talin head complex have revealed that the initial PTB NPLY binding only leads to separation of the integrin legs if Talin also binds to a more membrane proximal region of the β3 tail, leading to disruption of the inhibitory salt bridge (Figure11) (Wegener et al., 2007).

In addition, the Talin rod domain contains a second integrin binding site and a Talin/HIP1R/Sla2p actin tethering C-terminal homology (THATCH) domain at the very end, allowing Talin proteins to dimerize as well as to bind f-Actin directly (Senetar et al., 2004; Smith and McCann, 2007). The dimerization of two Talin molecules is proposed to promote integrin clustering. In support, calpain protease induced Talin head cleavage results in focal adhesion disassembly (Franco et al., 2004).

1.2.3.2 Kindlin

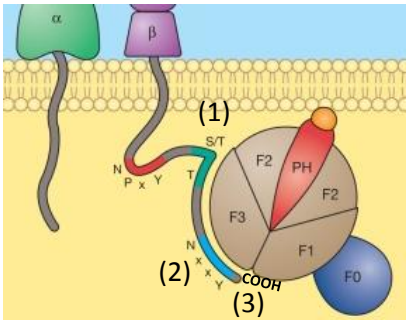

Figure12: Model for Kindlin binding to the cytoplasmic integrin tail
Kindlin is proposed to bind with its PH domain to phosphoinositides in the plasma membrane and with the FERM F3 subdomain to three distinct motifs in the cytoplasmic integrin β tail: a serine/threonine motif (1), the membrane distal NxxY motif (2) and COOH-terminus of the β integrin tail (modified from (Karakose et al., 2010)).

Kindlin are cytosolic proteins with a length of around 680 amino acids and a size of ~75 kDa and will be discussed in details in section 1.5. In contrast to Talin, the Kindlin FERM domain is divided by a pleckstrin homology (PH) domain in the F2 subdomain (Kloeker et al., 2004; Shi and Wu, 2008). The PH domain of Kindlin interacts with multiple phosphoinositides, especially with phosphatidylinositol-3,4,5-trisphosphate ($PI(3,4,5)P_3$), important for its membrane localization and to sustain integrin meditated adhesion and fibronectin deposition (Qu et al., 2011). Because Kindlins lack any rod domains, actin cytoskeleton linkage is mediated through direct binding to integrin-linked-kinase (ILK) and the filamin-binding protein Migfilin (Mackinnon et al., 2002; Tu et al., 2003). Also Kindlins have been shown to form dimers, however the function and physiological relevance remain unclear (Lai-Cheong et al., 2008).

Using integrin tail pull down assays, Kindlin has been shown to bind directly to the cytoplasmic tails of β1, β2, β3 β5 as well as β6 integrins. Interestingly, the Kindlin F3 FERM subdomain seems to interact with three distinct motifs in the cytoplasmic integrin tail (Figure12) (Bandyopadhyay et al., 2012; Fitzpatrick et al., 2014; Harburger et al., 2009; Moser et al., 2009a; Moser et al., 2008; Ussar et al., 2008). While Talin binds to the membrane proximal NPxY motif, Kindlin interacts with the membrane distal NxxY motif in the cytoplasmic β tail (Harburger et al., 2009). In addition, Kindlin interacts with a serine/threonine motif present between the NPxY and NxxY motifs of the β integrin cytoplasmic tail (Bottcher et al., 2012). A recent study revealed a third interaction site, where a carboxylate binding motif (h-G-h) in the Kindlin F3 region binds the COOH-terminus of the β integrin tail, which seems to have a crucial role for the Kindlin affinity to different integrin tails (Fitzpatrick et al., 2014).

Mutation of these critical residues in the cytoplasmic integrin tails leads to impaired Kindlin localization at adhesion structures as well as integrin activation defects, indicating that integrin binding is important for Kindlin localization and integrin mediated functions (Bandyopadhyay et al., 2012; Bottcher et al., 2012; Fitzpatrick et al., 2014; Moser et al., 2008).

1.2.4.3 Kindlin and Talin at the integrin tail

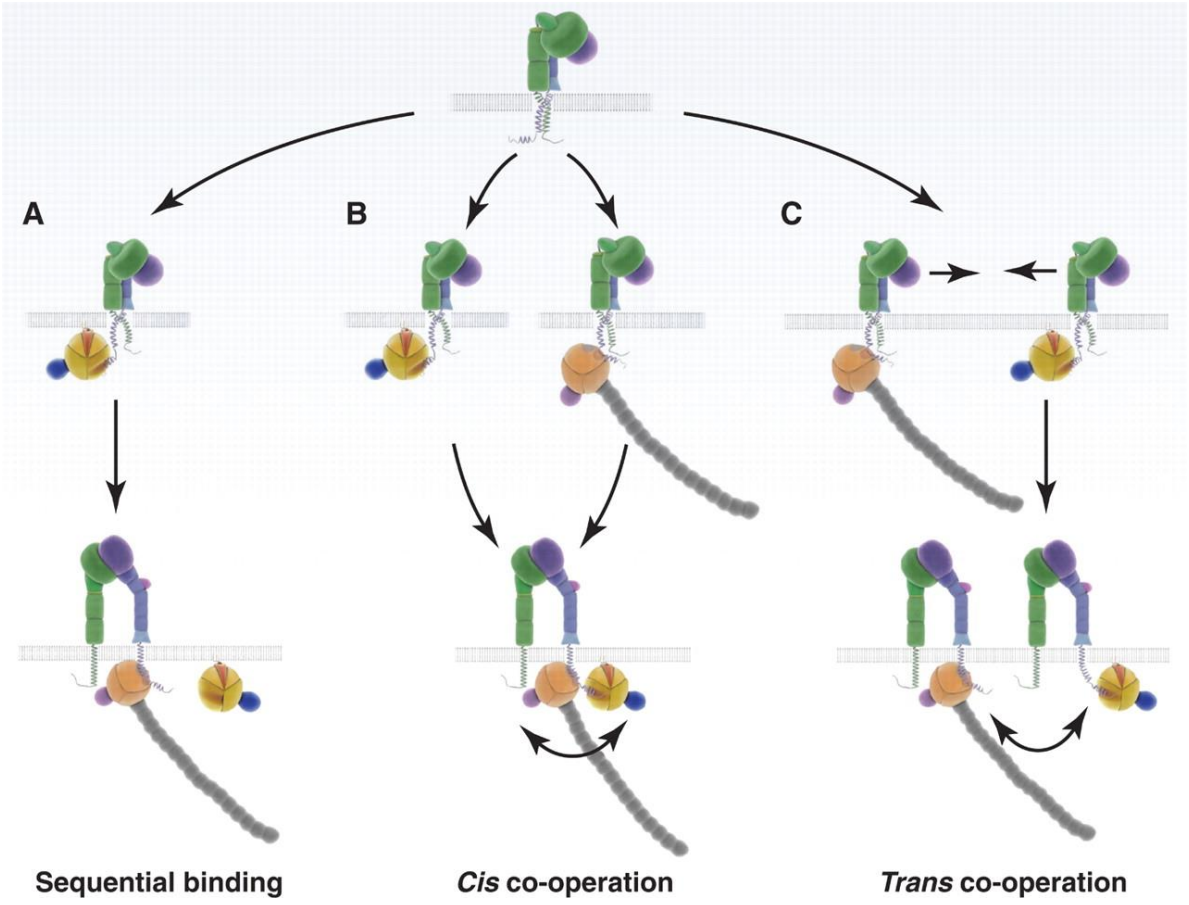

Figure13: Models for cooperatively of Kindlin-Talin binding to the integrin tail during integrin activation
(**A**) Sequential binding model: Kindlin binds first to the membrane distal NxxY motif and facilitates the recruitment of Talin, which leads to the displacement of Kindlin; (**B**) *Cis* co-operation model: Kindlin and Talin bind to their integrin tail binding sites and form a ternary complex, which induces integrin activation; (**C**) *Trans* co-operation model: Here Talin and Kindlin bind different integrin tails and upon clustering facilitate integrin activation (modified from (Moser et al., 2009b)).

How Kindlin and Talin interact with the cytoplasmic β integrin tail at the plasma membrane is still unclear and three binding models have been proposed: First, Kindlin binding could facilitate subsequent Talin recruitment, which in turn may leads to the Kindlin displacement (sequential binding model). Second, nuclear magnetic resonance (NMR), size-exclusion chromatography, surface plasmon resonance (SPR) experiments and ultracentrifugation studies indicate that both activators can bind simultaneously to β integrin cytoplasmic tails (Bledzka et al., 2012; Yates et al., 2012). Thus formation of a ternary complex could induce integrin activation (*cis* co-operation model). Third, Kindlin and Talin could be engaged at different integrin tails and cooperate in *trans*

in integrin nanocluster (*trans* co-operation model). In a recent study this model, however, has been excluded genetically (Meves et al., 2013).

The inside-out integrin activation seems to be tightly controlled at the level of integrin and activator interaction: First, structural analysis have revealed that Talin binding to β3 integrin tail is blocked upon phosphorylation of the NPxY tyrosine residue by sarcoma (Src) family kinases (Datta et al., 2002; Oxley et al., 2008). Similarly, phosphorylation of the NxxY motif of β tails has been shown to inhibit Kindlin binding (Bledzka et al., 2010). However, this seems to be integrin specific since mice that possess a double tyrosine-to-phenylalanine mutation in β1 tails display no phenotype characteristic for β1 integrin activation defects (Czuchra et al., 2006). Second, Talin exists in an auto-inhibited (closed) conformation in the cytoplasm with an intramolecular interaction between its head FERM and tail domain (Goksoy et al., 2008), masking several binding regions including the integrin β tail-binding sites. So far the activation mechanism of Talin remains elusive. However, it has been proposed that Talin binding to phosphatidylinositol-4,5-bisphosphate ($PI(4,5)P_2$) promotes a conformational change exposing the Talin head integrin binding site at the plasma membrane (Martel et al., 2001). Furthermore, the rat sarcoma (Ras)-like small GTPases Ras-related protein-1 (Rap1) has been shown to form an activating complex with its effector Rap1-interacting adapter molecule (RIAM) at the plasma membrane. This complex is able to recruit Talin and unmask its integrin binding site allowing integrin activation (Han et al., 2006b). It is still unclear if Kindlins needs to become activated *in vivo*, as well. A recent study in C. elegans proposes that when Kindlin binds to ILK a conformational change is induced, allowing Kindlin to bind to the cytoplasmic integrin tail (Qadota et al., 2012). It is currently unknown, if this mechanism holds true also for the mammalian Kindlin orthologues.

Taken together, a cell is only able to spread when integrins engage their ligand, become fully activated and stabilized in the high-affinity conformation and the integrin legs are separated through Kindlin and Talin interaction, allowing efficient FAK recruitment and activation and subsequently stable adhesion formation.

1.2.5 From integrin activation to mature integrin adhesions

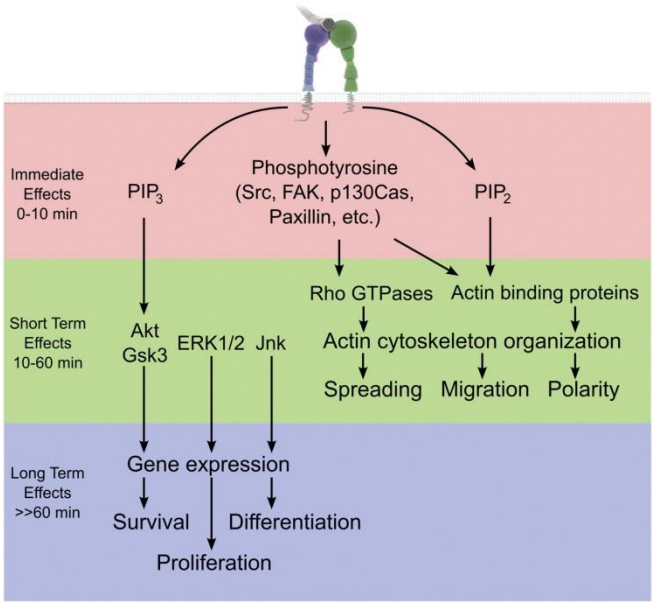

Figure14: Integrin outside-in signaling
Integrin outside-in signaling can be grouped in three temporally distinct phases: the **immediate effects** upon activation are the activation of lipid kinases and phosphorylation of specific protein substrates assisting focal adhesion maturation. Subsequent **short term effects** result in the activation of multiple signaling pathways and Rho family GTPases, which in concert with other actin regulatory proteins induce actin cytoskeleton remodeling influencing spreading, migration and cell polarity. The **long term effects** induce multiple signaling pathways influencing gene expression, proliferation, differentiation and survival (adapted from (Legate et al., 2009)).

The activation and clustering of integrins is able to induce a vast array of signaling events, termed outside-in signaling, which eventually results in the development of a nascent adhesion. Depending on the tissue, cell type, cellular context and environment, these nascent adhesion mature into focal adhesions, fibrillar adhesion, podosomes or invadopodia. All these integrin adhesion structures exert different functions in adhesion-mediated signaling, ECM remodeling as well as cell migration and invasion. Because the short cytoplasmic integrin tails lack any catalytic activity, integrins completely rely on the recruitment of effector proteins, termed focal adhesion proteins, to generate these distinct adhesion classes/types. In the last years multiple approaches, including proteomics, bioinformatics and immunohistochemistry, have identified 232 focal adhesion proteins which define the integrin adhesome (Schiller et al., 2013; Zaidel-Bar et al., 2007). These focal adhesion proteins can be further divided in 148 intrinsic (remain in the focal adhesion upon formation) and 84 transiently associated components. Functionally, they comprise various actin regulators, adaptor proteins that link cytoskeletal structures to the cytoplasmic tails of integrins and multiple signaling molecules (Winograd-Katz et al., 2014). Many of these focal adhesion proteins have been shown to bind the integrin tail directly serving as scaffolds for different sets of effector proteins. Thus, a differential recruitment of focal adhesion proteins allows transduction of highly diverse signals.

During adhesion formation the recruitment of focal adhesion proteins can be divided in three phases which differ in timing (Figure14): upon integrin activation, FAK and Src are activated and recruited to the integrin tail. In this priming phase within milliseconds the activated kinases start to phosphorylate multiple specific targets such as Paxillin as well as other kinases, which become activated themselves leading to signal amplification and propagation. Interestingly, in this phase the phosphorylation of integrin bound proteins can create new binding sites and promote the recruitment of further adaptor proteins like Crk and p130 Crk-associated substrate (p130Cas), generating highly divers signaling platforms (Zaidel-Bar et al., 2007). Moreover an enrichment of lipid second messengers, such as $PI(4,5)P_2$ and $PI(3,4,5)P_3$, is observed probably induced by the lipid kinase phosphatidylinositol 4-phosphate-5-kinase type I γ (PIPKIγ), which becomes recruited to focal adhesions by Talin (Di Paolo et al., 2002). Subsequently, the $PI(4,5)P_2$ rich plasma membrane facilitates the binding of further focal adhesion proteins, such as Numb, Src homology containing protein (Shc), Tensin as well as Talin, suggesting a positive feedback loop (Martel et al., 2001). Conversely, increased presence of $PI(3,4,5)P_3$ leads to rearrangement of focal adhesion bound α-Actinin and Vinculin. As a short term effect (within minutes), these signals translate into rearrangement of the actin cytoskeleton and myosin mediated force generation induced by the activation of Ras homolog (Rho) family GTPases and other actin regulatory proteins. Consequently, activation of rapidly-accelerated fibrosarcoma (Raf)/ extracellular signal-regulated kinase (ERK)/ mitogen-activated protein kinase (MAPK), Jun N-terminal kinase (Jnk) and Akt signaling pathways (long term effect), in concert with growth factor signaling such as TGFβ, epidermal growth factor (EGF), insulin growth factor (IGF) or platelet derived growth factor (PDGF), induces changes in gene transcription and cell behavior, and at the same time modulates cell survival, proliferation and differentiation (see also section 1.6.3).

1.3 TGFβ signaling

1.3.1 TGFβ superfamily members

TGFβ is part of a growth factor superfamily which modulates cell growth, differentiation, adhesion, migration, ECM synthesis and apoptosis (Massague, 1998; Siegel and Massague, 2003). Currently, it comprises 34 family members subcategorized into the groups of activins, inhibins, nodal, myostatin, BMPs and growth/differentiation factors (GDF). These different ligands are recognized by specific transmembrane type I and type II serine/threonine kinase receptors which form distinct heteromeric complexes upon ligand binding and subsequently activate distinct signal transducing Smad complexes in the cell (discussed below).

The TGFβ pathway seems to have developed in metazoans with the emerging need to control multicellular processes and thus is highly conserved in organisms ranging from C. elegans, Drosophila melanogaster, Xenopus laevis to mammals (Massague, 1998).

During embryo development, signaling of TGFβ family members is essential for tissue growth and morphogenesis such as vasculogenesis and angiogenesis, whereas in adult tissue it controls proliferation of epithelial, endothelial, immune cells and fibroblasts assuring tissue homeostasis (Guasch et al., 2007; Siegel and Massague, 2003; ten Dijke and Arthur, 2007). The number of target genes for a given TGFβ family member can range from just a few in embryonic SC to many hundreds in differentiated cells (Mullen et al., 2011). The strong cellular context dependency and apparent multifunctionality of TGFβ signaling was very puzzling in the early characterization: e.g. TGFβ is able to inhibit cell proliferation in many epithelial cells but can also enhance proliferation in fibroblast and cell growth in endothelial cells (Guasch et al., 2007; Xiao et al., 2012); it enhances SC pluripotency, but promotes differentiation in other cells (Park, 2011); in cancer development it suppresses pre-malignant cell proliferation, but at the same time promotes conversion to a metastatic phenotype (Chaudhury and Howe, 2009). All these different, partly opposing effects of TGFβ signaling indicate that the outcome of the TGFβ response is more dictated by the cellular context than by a determinate TGFβ signaling pathway. This multilayered signaling complexity of TGFβ in homeostasis and diseases only starts to be unraveled.

1.3.2 TGFβ receptors and ligands

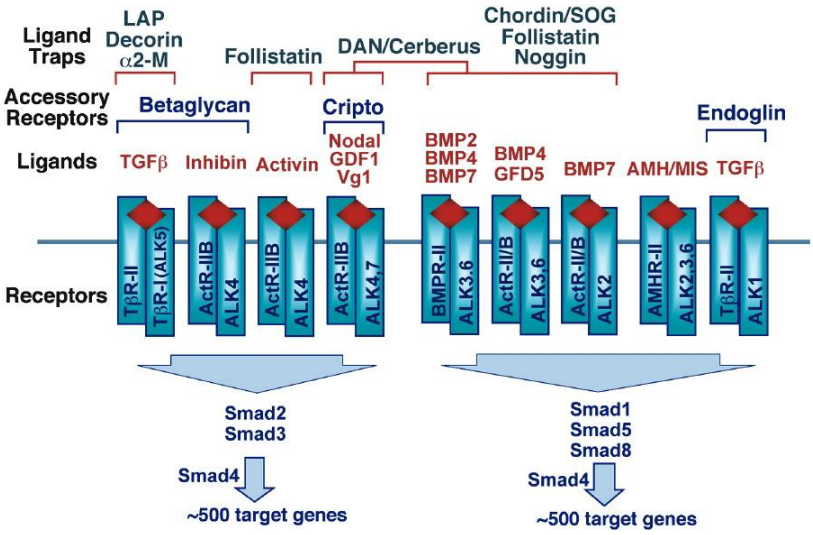

Figure15: TGFβ superfamily signal transduction

The scheme illustrates the TGFβ superfamily ligands and their associated ligand trap proteins recognizing different TGFβ type I and II receptors heterodimers. Some ligands require an accessory receptor for receptor binding. Activation of different TGFβ heterodimers can lead to highly diverse signal transduction through recruitment of different Smad transcription factors (modified from (Shi and Massague, 2003)).

Members of the TGFβ superfamily bind to two distinct receptor types, known as type II and type I receptors, which contain serine / threonine kinase domains in their intracellular part, required for signal transduction (Wrana et al., 1994). In mammalians, five type II receptors and seven type I receptors are known (Figure15). TGFβ receptor type II (TβRII), BMP receptor type II (BMPRII) and anti-müllerian hormone receptor type II (AMHRII) are specific for TGFβ-, BMP- and AMH-type ligands, respectively. In contrast, the activin type II and type IIB receptors (ActRII and ActRIIB) bind activins, but can also recognize other TGFβ-ligand superfamily members, including nodal and BMPs. The type I receptors can be grouped in the TGFβ specific TβR-I (activin receptor-like kinase (ALK)5) and ALK1, the BMP type I receptors BMPR-IA (ALK3), BMPR-IB (ALK6) and ALK2 as well as the activin, inhibin and nodal recognizing ALK4 and Alk7.

The access of ligands to the receptors is regulated by a large family of extracellular ligand trap proteins which retain ligands in the ECM, such as latency associated protein (LAP) for TGFβ, follistatin for activin and noggin for BMP as well as by cell surface proteins which act as co-receptors, including betaglycan (also known as TGFβ type III receptor) and endoglin (Figure15). The LAP-TGFβ ligand trap complex will be discussed in detail below (see section 1.3.5 and 1.3.6.2).

The type II receptor kinases are constitutively active and upon ligand binding the recruitment of type I receptor into hetero-tetrameric complexes is facilitated. The constitutively active type II receptor kinases subsequently phosphorylate the type I receptor kinases at the C-terminal GS domain, a highly conserved 30 amino acid sequence with a characteristic SGSGSG sequence directly upstream of the kinase domain (Wieser et al., 1995). This phosphorylation leads to a

conformational change resulting in type I receptor kinase activation and phosphorylation of intracellular targets. Thus, in the TGFβ signaling pathway, type I receptors act as downstream components of type II receptors and determine the specificity of the intracellular signals induced by TGFβ family cytokines.

1.3.3 Canonical Smad TGFβ signaling

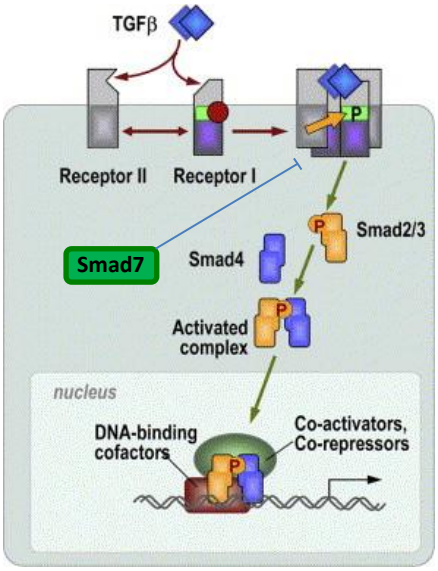

Figure16: The canonical TGFβ signal transduction
TGFβ binds the constitutive active type II receptor kinase leading to the recruitment and activation of type I receptor kinase, whereby the type II kinase phosphorylates and activates type I receptor. Subsequently, type I receptor phosphorylates receptor-bound R-Smad (Smad2/3) transcription factors at the C-terminal SSXS motif, inducing their release, association with the Co-Smad (Smad4) in the cytoplasm and translocation into the nucleus. I-Smad (Smad7) promote TGFβ receptor dephosphorylation and degradation, inhibiting TGFβ signal transduction. In the nucleus activated Smad complex interact with multiple co-activators and repressors generating distinct transcriptional responses (modified from (Massague and Gomis, 2006)).

Smads are the major signaling molecules downstream of the serine/threonine kinase receptors which can be divided in to three functional subgroups: the receptor-activated Smads (R-Smads), common mediator Smad (Co-Smad) and the inhibitory Smads (I-Smads). Structurally, all Smads are characterized by two conserved regions, the N-terminal Mad homology (MH)1 domain and the C-terminal MH2 domain which are joined by a short linker region of poorly conserved amino acid composition. While both MH domains play a role in gene transcription regulation, MH1 mediates direct DNA binding and nuclear import and MH2 Smad oligomerization. The R-Smads (Smad1, Smad2, Smad3, Smad5, and Smad8) are directly phosphorylated by the type I receptors on their C-terminal serine-serine-x-serine (SSXS) motif, leading to a conformational change in the MH2 domain which allows oligomerization with Co-Smad. The TGFβ superfamily cytokines can be classified into two subfamilies depending on the Smad signaling pathways they activate: while Smad2 and Smad3 are phosphorylated in response to the TGFβs and activin, Smad1, Smad5, and

Smad8 are phosphorylated in response to BMP. The Co-Smad, Smad4, assists the signal transduction from both the activin/TGFβ as well as BMP signaling pathways by oligomerizing with activated R-Smads, allowing nuclear translocation. In the nucleus the complex binds to Smad responsive elements (SRE) and cooperates with other transcription co-factors to either activate or repress target gene transcription (Feng and Derynck, 2005).

Smad6 and Smad7 function as I-Smads. They are induced by BMP and/or TGFβ/activin, respectively, and inhibit activation of R-Smads through competition for binding to activated TβR-I (Massague, 1998). Smad7 has been shown to promote dephosphorylation of activated type I receptor as well as its proteasomal degradation by recruiting Smad specific E3 ubiquitin protein ligase (Smurf) after endocytosis (Kavsak et al., 2000; Shi et al., 2004). In addition, attenuation of TGFβ signaling is mediated by either ubiquitination and subsequent proteasomal degradation of Smad2/3 (Lin et al., 2000) or dephosphorylation of the R-Smad/Co-Smad complex via the phosphatase PPM1A (Lin et al., 2006). The dephosphorylated Smads have been shown to translocate back into the cytoplasm to await the next round of signaling.

Interestingly, the TGFβ signaling does not only occur at the plasma membrane, but it is further regulated by endocytosis. TGFβ receptors belong to the family of serine/threonine kinase receptors that are rapidly internalized after ligand binding. Recent studies have shown that activated TGFβ receptors can follow two distinct internalization pathways which dictate downstream signal attenuation or activation (Di Guglielmo et al., 2003). First, the endocytosis via clathrin-coated vesicles and recruitment of Smad anchor for receptor activation (SARA) and Smad2 in early endosomes promote further signaling to the nucleus (TGFβ signaling enhancement), and second, the TGFβ receptor can be engulfed into caveolin-positive vesicles which further engage Smurf and Smad7 leading to rapid receptor degradation and TGFβ signaling attenuation.

Taken together, TGFβ signal transduction is regulated on multiple levels and most likely more will be identified in the near future. The expression pattern of different inhibitory and activatory Smads, TGFβ receptor subtypes and transcriptional co-factors are most likely determining the cell type specific response. However, how these different modes of TGFβ pathway regulation cooperate and influence each other leading to a cell context dependent specificity, are still open questions in the field.

1.3.4 Non-canonical Smad TGFβ signaling

In addition to the Smad depended signaling, TGFβ receptor activation is able to induce multiple signaling pathways such as phosphoinositide 3-kinase (PI3K), Ras, partitioning defective 6 (Par6), and Jnk/p38/ MAPK, referred to as non-canonical TGFβ pathway (Mu et al., 2012).

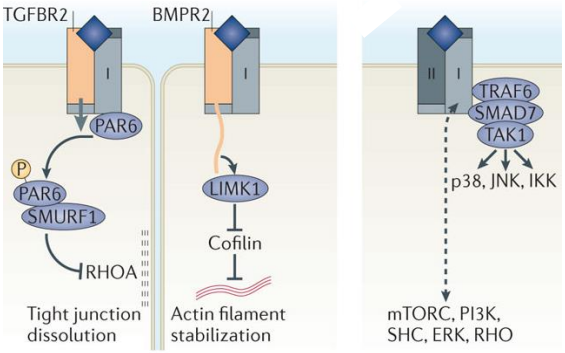

Figure17: The non-canonical TGFβ signal transduction
Activated TGFβ receptor type II (TGFBR2) can directly phosphorylate Par6 to recruit Smurf1 and target RhoA for degradation leading to disassembly of tight junctions in epithelial cells. BMP receptor type II (BMPR2) contains a long C-terminal tail that binds and activates LIMK1, thereby inhibiting Cofilin and stabilizing actin filaments. In addition, recruitment of TRAF6 and Smad7 to activated TGFβ receptors results in the activation of TAK1, which induces p38, JNK and IKK signaling. Furthermore, TGFβ and BMP receptors are proposed to activate several other signal transducers such as mTORC, PI3K, Shc, ERK and Rho (modified from (Massague, 2012)).

It has been shown that activated TGFβ receptor is able to directly phosphorylate the planar polarity protein Par6, a regulator of epithelial cell polarity and tight junction assembly (Figure17). Phosphorylated Par6 recruits the E3 ubiquitin ligase Smurf1 to tight junctions where it targets RhoA GTPase for degradation, thereby causing loss of tight junctions and polarized migration (Ozdamar et al., 2005). The C-terminal domain of BMPRII binds and promotes the activity of LIM kinase 1 (LIMK1), an inhibitor of the actin-depolymerizing factor Cofilin, thereby stabilizing actin filaments and inducing a loss of epithelial identity (Foletta et al., 2003).

In addition, TGFβ receptor activation induce MAPK and PI3K pathway involving tumor necrosis factor receptor-associated factor 6 (TRAF6), mammalian target of rapamycin (mTORC) and other mediator; however, detailed mechanistic insights are mostly missing. On the one hand, it has been proposed that TRAF6 in a complex with Smad7 bind to the TGFβ receptor, leading to the activation of TGFβ-activated kinase 1 (TAK1) and subsequently induction of the Jnk/p38/MAPK and IκB kinase (IKK)/ nuclear factor kappa-light-chain enhancer of activated B cell (NF-κB) pathway (Mao et al., 2011). On the other hand, TGFβ and BMP receptors can activate several other signal transducers such as mTORC, PI3K, ERK or RhoA. But whether these pathways are regulated through a direct TGFβ receptor induced activation or if it is the result of a collateral activation of other receptors upon TGFβ signaling, is currently unknown (Mu et al., 2012).

1.3.5 TGFβ synthesis and storage

After the identification of TGFβ1 in 1980s, two additional isoforms of TGFβ have been identified in mammals, TGFβ2 and TGFβ3, which show similar functions *in vitro*. However, *in vivo* mouse studies revealed that isoform specific complete deletion had very different influence on the HFs, indicating that each isoform has specific and non-redundant functions: TGFβ1 seems to promote catagen induction and its deletion results in increased epidermal proliferation and accelerated HF development. In contrast, TGFβ2 loss has no effect on epidermal cell proliferation, delays HF morphogenesis and inhibits bulge cell activation during anagen induction, whereas TGFβ3 null mice display no HF defects (Foitzik et al., 2000; Foitzik et al., 1999; Glick et al., 1994; Oshimori and Fuchs, 2012).

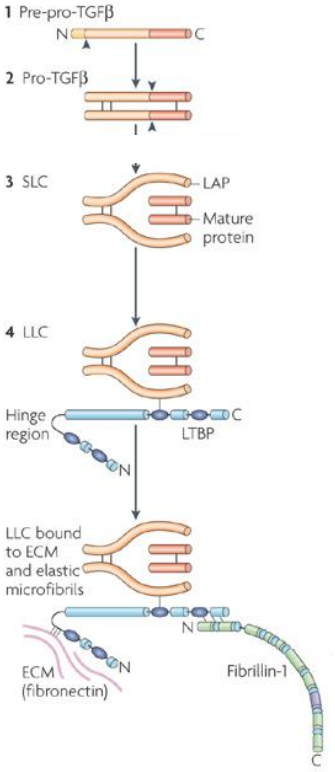

Figure18: Schematic model of synthesis, secretion and matrix deposition of TGFβ

TGFβ is synthesized as a pre-pro-protein, which undergoes proteolytic processing in the rough endoplasmic reticulum (**1**). Two monomers of TGFβ dimerize through disulfide bonds (**2**). The pro-TGFβ dimer is then cleaved by Furin convertase generating the small latent TGFβ complex (SLC), where LAP and TGFβ are connected by non-covalent bonds (**3**). Within secretory vesicles the large latent TGFβ complex (LLC) is formed by covalent attachment of LTBP through a disulfide bond (**4**). After secretion the N−terminal and hinge region of LTBP interact with ECM components such as fibronectin to which they can be covalently cross linked by transglutaminases. The C−terminal region of LTBP interacts non-covalently with the N−terminal region of Fibrillin−1 (modified from (ten Dijke and Arthur, 2007)).

The three isoforms are all encoded by separate genes and produced as an inactive complex (pro-TGFβ), consisting of a 25 kDa N-terminal pro-peptide, termed LAP and a covalently bound 12.5 kDa TGFβ at the C-terminus (Figure18). Because all LAP have sequence variations between the three TGFβ isoforms, they are grouped accordingly in LAP1, 2, 3. TGFβ is synthesized as a pre-pro-protein, which undergoes proteolytic processing in the rough endoplasmic reticulum. Subsequently, two TGFβ monomers dimerize through disulfide bonds and are then cleaved by Furin protease in the Golgi leading to the small latent TGFβ complex (SLC), in which LAP and TGFβ

are non-covalently connected through salt bridges and hydrophilic as well as hydrophobic interactions (Shi et al., 2011). In the subsequently secreted SLC, TGFβ is buried in the structure of LAP, preventing recognition of TGFβ by its high affinity receptor TβRI. In order to become biological active, TGFβ needs to be liberated (Annes et al., 2003), allowing a tight control of this potent cytokine in time and location.

Furthermore, in the majority of cases cells secrete TGFβ bound to the carrier protein LTBP as part of a large latency complex (LLC) important for association of TGFβ to the ECM. Only very few cells have been reported to produce and secrete a diffusible form of SLC, however the physiological relevance is unclear (Dallas et al., 1994). The LCC is stabilized through a covalent disulfide bond between the SLC and LTBP formed within secretory vesicles (Saharinen and Keski-Oja, 2000). LTBP is part of the superfamily of fibrillin-like ECM components that bind to several ECM proteins, such as Fibrillin-1 (ten Dijke and Arthur, 2007), fibronectin (Taipale et al., 1994) and vitronectin (Schoppet et al., 2002). The C-terminus and the hinge region of LTBP can be covalently cross linked to the ECM by transglutaminases (Nunes et al., 1997). In mammals, four isoforms with different features are expressed (LTBP1-4). Besides LTBP2, all other LTBPs can bind to all isoforms of TGFβ (Saharinen and Keski-Oja, 2000). A proper incorporation of LLC into the matrix is essential for an efficient TGFβ function as deletion of the N-terminal ECM binding motif of LTBP abolishes TGFβ liberation (Annes et al., 2004).

1.3.6 TGFβ release mechanisms

Although TGFβ can be released from the matrix by huge number of processes including heat, pH, reactive oxygen species (ROS) or various proteases (see section below), under physiological conditions RGD binding αv-class integrins represent the key activators for TGFβ activation *in vivo*. So far αvβ3, αvβ5, αvβ6 and αvβ8 have been shown to liberate TGFβ, while other RGD binding integrins, such as α5β1 or α8β1 cannot release TGFβ (Asano et al., 2005a, b; Mu et al., 2002; Munger et al., 1999). Furthermore, the observation that receptor-bound TGFβ induces αvβ3, αvβ5 and αvβ6 integrin expression suggests a positive feedback loop (Pechkovsky et al., 2008).

1.3.6.1 Integrin independent TGFβ release mechanisms

Conversion of TGFβ1 into its biologically active form can be mediated through proteolytic cleavage by plasmin, elastase and a variety of matrix metalloproteinases (MMPs) such as MMP-9 or MMP-2

(Taipale et al., 1994; Yu and Stamenkovic, 2000) as well as through destabilization of the LAP-TGFβ1 complex induced by ROS or harsh pH conditions (Barcellos-Hoff and Dix, 1996; Lyons et al., 1988). In addition, interaction between LAP1 and thrombospondin-1 (Murphy-Ullrich and Poczatek, 2000) and the mannose-6-phosphate receptor (Dennis and Rifkin, 1991) promote TGFβ1 activation independently of proteolytic cleavage. However, detailed mechanistic insights are still missing and the physiological relevance remains to be determined.

Surprisingly, in platelets a secreted furin-like proprotein convertase appears to activate TGFβ1 independently of any known mechanisms (Blakytny et al., 2004), suggesting that further and probably highly cell type specific TGFβ release mechanisms will be discovered in the near future.

1.3.6.2 Integrin mediated TGFβ release

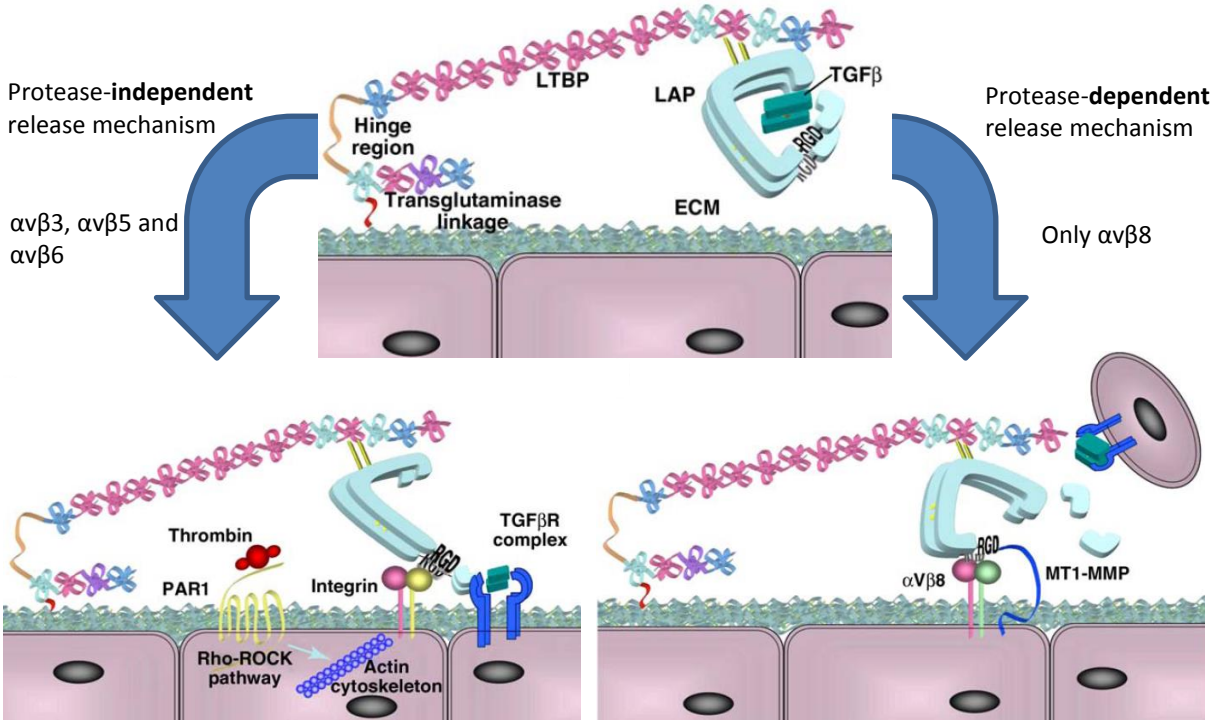

Figure19: Integrin mediated TGFβ release of different αv-class integrins
The LLC is tethered to the ECM on the surface of cells. TGFβ can be released by integrins via protease-independent and protease-dependent mechanisms. To unmask TGFβ, αv-class integrins bind to the RGD tripeptide motif in the LAP region. The interaction with αvβ3, αvβ5 or αvβ6 integrin induces a conformational change in the latent complex by generating an actin cytoskeleton depended pulling force, allowing TGFβ to access its receptors. Conversely, the αvβ8 integrin binds LAP, enabling the membrane bound protease MT1-MMP to cleave LAP and free TGFβ (modified from (Worthington et al., 2011)).

One key prerequisite of αv-class integrins is their ability to bind to the RGD integrin-binding motif in the LAP of the SLC and consequently, point mutations of LAP-RGD to LAP-RGE abolish integrin

mediated TGFβ liberation (Ludbrook et al., 2003; Munger et al., 1998; Munger et al., 1999). Although all TGFβ-releasing integrins interact with the RGD motif in the LAP, the release mechanism between the integrins differs (Figure19): for αvβ3, αvβ5 and αvβ6 integrin the TGFβ release is spatially restricted and controlled by cell contraction as well as dependent on an intact actin cytoskeleton (Munger et al., 1999; Wipff et al., 2007). Consequently, when cell contraction is enhanced by Thrombin, TGFβ release is increased. Collectively, these results propose a model for the TGFβ activation where integrin binds to and pulls on the LLC, inducing a conformational change in the LAP rendering the TGFβ now accessible for its high affinity receptor. Indeed, the recently solved crystal structure of the SLC of TGFβ confirmed that LAP-TGFβ is not accessible for TGFβ receptor and that mechanical force transmitted by αvβ6 integrins promotes a conformational change, required for TGFβ release (Shi et al., 2011). On the other hand, the intracellular signals required for αvβ6 integrin activation were not known so far.

Conversely, the αvβ8 integrin induced TGFβ release does not depend on actin-mediated cell contractility (Mu et al., 2002). Instead, the αvβ8 integrin release mechanism crucially depends on the proteolytic cleavage of LAP by cell surface metalloprotease MT1-MMP (also known as MMP14), leading to the release of TGFβ which then might act at more distant sites as well. Because the αvβ8 release mechanism has only been investigated in epithelial cells, further studies in αvβ8 expressing cells (e.g. brain or immune system) are required to test if this is a general mechanism for protease mediated TGFβ activation and which other proteases may be involved. Taken together, the integrin mediated TGFβ release represents a very elegant mechanism for specific and locally restricted TGFβ release and signaling activation.

The relevance of integrin mediated TGFβ release for *in vivo* development and homeostasis is further underlined by the observation that mice with the integrin-binding deficient LAP proteins (RGD motif mutated to RGE) recapitulate all major phenotypes of TGFβ1 null mice, including multi-organ inflammation and defects in vasculogenesis (Shull et al., 1992; Yang et al., 2007). This striking phenotype overlap with TGFβ deficient mice and phenotypes of mice lacking αv-class integrins (Aluwihare et al., 2009; Bader et al., 1998) demonstrates an essential interconnection of integrins with TGFβ signaling *in vivo*, while the role of non-integrin mediated release mechanisms remains less clear. Nevertheless, it is still possible that integrin dependent and independent TGFβ release mechanisms influence each other and potentially synergize during certain disease conditions. In line, in contrast to TGFβ1 and 3, TGFβ2 lacks an RGD site, thus other release mechanisms must be responsible for its activation.

1.4 Wnt signaling pathways

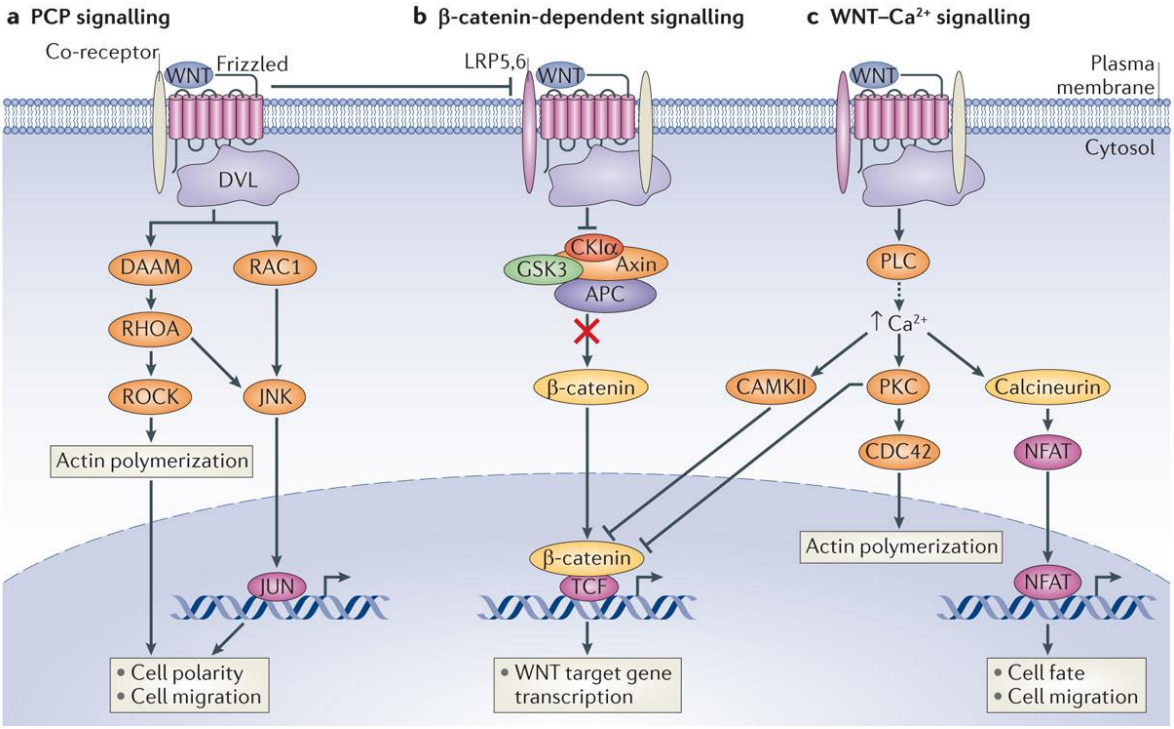

Figure20: Wnt signaling pathways

Simplified scheme displaying the canonical Wnt (**B**) and two main non-canonical Wnt pathways (**A**,**C**) induced by specific Wnt, Frizzled (Fzd) and Wnt co-receptors. (**A**) Planar cell polarity (PCP) signaling triggers activation of the small GTPases RhoA and Ras-related C3 botulinum toxin substrate (Rac1), inducing Rho-associated kinase (ROCK) and JNK, respectively, leading to actin polymerization and regulation of cell polarity and motility. (**B**) In the absence of Wnts β-catenin is constantly degraded via the destruction complex (comprising glycogen synthase kinase 3 (GSK3), casein kinase Iα (CKIα), Axin and adenomatosis polyposis coli (APC)) leading to repression of Wnt target gene transcription. Upon Wnt signaling, the destruction complex is inactivated, allowing β-catenin to accumulate in the nucleus and induce target gene transcription in complex with TCF. (**C**) The Wnt/Ca^{2+} pathway activate Ca^{2+} release, leading to the activation of calmodulin-dependent kinase II (CAMKII), protein kinase C (PKC) and Calcineurin. Calcineurin activates nuclear factor of activated T cells (NFAT), which regulates the transcription of genes controlling cell fate and cell migration. PCP and Wnt/Ca^{2+} pathways antagonize β-catenin signaling at various levels (modified from (Niehrs, 2012)).

One of the fundamental pathways directing cell proliferation, polarity, cell fate determination and SC maintenance in embryonic development as well as tissue homeostasis are the Wnt pathways (Logan and Nusse, 2004). In particular the fate of skin cells appears to be very sensitive to the precise levels of Wnt/β-catenin signaling: High Wnt/β-catenin signaling instructs keratinocytes to form hair, whereas intermediate to low levels of Wnt/β-catenin signaling specify the sebocyte and interfollicular epidermis lineages (Silva-Vargas et al., 2005). When this fine balance of Wnt/β-catenin signaling is deregulated, skin cells are promoted to form particular lineages, leading to

developmental defects as well as cancer (Lim and Nusse, 2013; MacDonald et al., 2009). There are several Wnt signaling pathways which depend on the specific surface receptors as well as Wnt ligands and mediate canonical Wnt signaling, non-canonical planar cell polarity signaling or non-canonical Wnt/Ca^{2+} signaling (Figure20). While the canonical pathway regulates gene transcription through the multifunctional adaptor protein β-catenin, the non-canonical planar polarity pathway modulates the actin cytoskeleton inducing cell shape changes and Wnt/Ca^{2+} pathway controls calcium levels in the cell (see section 1.4.5 and 1.4.6 for details).

1.4.1 Wnt ligands

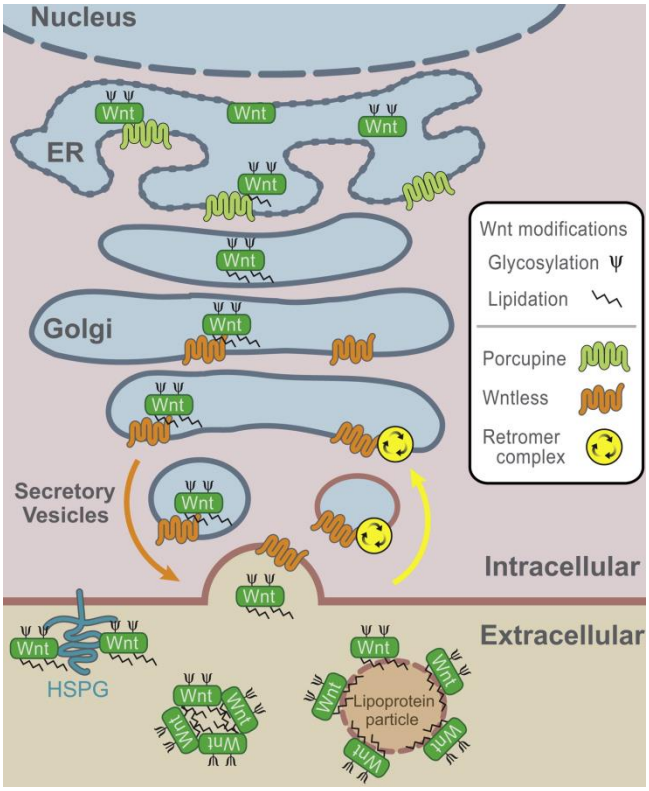

Figure 21: Wnt ligand synthesis and secretion
In the endoplasmatic reticulum (ER) Wnt ligands are glycosylated and lipid modified involving Porcupine. In the Golgi Wnts are escorted to the plasma membrane for secretion by Wntless, which is retrieved from endocytic vesicles and recycled back to the Golgi by the retromer complex. After secretion mature Wnts either bind to heparan sulfate proteoglycans (HSPGs) and lipoprotein particles or form multimers, which can modulate Wnt gradients and facilitate long-range Wnt signaling (modified from (MacDonald et al., 2009)).

Almost 30 year ago the first Wnt protein was identified and up today 19 Wnt genes have been described in the human and mouse genome mediating complex and specific Wnt signaling. While canonical Wnt signaling is induced by Wnt ligands such as Wnt1, 3, 3a, 8a, 8b, 10a or 10b, non-canonical Wnt signaling is mediated by Wnt4, 5b, 6, 7a, 7b, or 11. Interestingly, some Wnt ligands like Wnt5a are able to promote β-catenin dependent and independent Wnt signaling contingent on the receptor binding (see section 1.4.2) (Mikels and Nusse, 2006). All Wnt family members are glycolipoproteins with a size of ~40 kDa (350–400 amino acids) containing many conserved

cysteines and an N-terminal glycosylated signal peptide for secretion. The post-translational lipid modification and glycosylation of Wnt ligands is crucial for the secretion process (Takada et al., 2006). The multipass transmembrane O-acyltransferase Porcupine has been shown to palmitoylate and glycosylate Wnt proteins in the endoplasmatic reticulum (Figure21). For the subsequent Wnt transport from the Golgi to the plasma membrane, the seven-transmembrane domain protein Wntless is essential. Wntless is proposed to bind to Wnts and sort them to plasma membrane from where it is recycled via endocytic vesicles back to the Golgi by the retormer complex (Belenkaya et al., 2008). Of note, inhibition of Porcupine by chemical compounds such as IWP-2 abolishes Wnt ligand secretion and thus inhibits all Wnt signaling pathways (Chen et al., 2009).

Since single cell organisms are lacking Wnt genes, it has been speculated that they have been crucial for the development and evolution of multicellular organisms, as they are conserved in all metazoan animals including cnidarian and sponges (Kusserow et al., 2005; Petersen and Reddien, 2009). Indeed, Wnt proteins function as morphogens that can mediate short- and long-range signaling in tissues. The presence of lipid anchors in Wnt proteins appears contradictive for a role in long-range signaling, as lipid interaction would tether and trap Wnt proteins to the lipid membrane of the secreting or a neighboring cell. Thus, it has been speculated that after secretion, Wnt proteins either form diffusion competent micelle-like multimeric structures with the help of the membrane microdomain protein reggie-1/flotillin-2 (Katanaev et al., 2008) or bind to lipoprotein particles allowing long-range signaling (Panakova et al., 2005). However, the relevance of Wnt as a long-range spreading morphogen has been recently questioned by a study in Drosophila, showing that a membrane-trapped version of Wingless (the main Wnt in Drosophila) can also control development, without forming a secreted instructive gradient. Wingless fused to the transmembrane protein Neurotactin was expressed under the endogenous promoter leading to viable flies that produced normally patterned appendages of almost normal size (Alexandre et al., 2014). For short-range signaling, the heparan sulfate proteoglycans (HSPGs) low affinity Wnt co-receptors Dally and Dally-like protein have been proposed to regulate Wnt ligand diffusion, degradation as well as endocytosis/transcytosis (Baeg et al., 2001).

1.4.2 Wnt ligand receptors

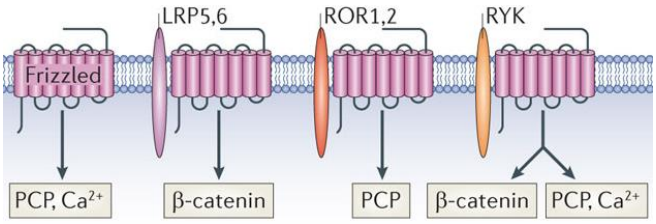

Figure22: Wnt signaling receptor complexes
The scheme illustrates different Wnt receptor complexes inducing canonical Wnt/β-catenin signaling (β-catenin) or non-canonical planar cell polarity signaling (PCP) or Wnt/Ca^{2+} signaling (Ca^{2+}) (modified from (Niehrs, 2012)).

After secretion and diffusion to the signal receiving cell, Wnt ligands bind to subtype specific Wnt receptors, leading to the different types of signaling (see section 1.4.5 and 1.4.6). The core receptor complex is composed by a seven-pass transmembrane-domain class Frizzled (Fzd) protein and its single-pass transmembrane co-receptor, the low-density lipoprotein receptor-related protein 5 or 6 (Lrp5/6) (Figure22) (Pinson et al., 2000; Tamai et al., 2000). Mammals have ten different Fzd genes which belong phylogenetically to the large family of G protein-coupled receptors (Bjarnadottir et al., 2006). They all contain large extracellular N-terminal cysteine-rich domain providing the primary binding platform for distinct Wnt ligands (Dann et al., 2001; Janda et al., 2012). If also the co-receptor Lrp5/6 can bind Wnts directly is still controversial (Tamai et al., 2000; Wu and Nusse, 2002). Of note, a single Wnt can interact with multiple Fzd proteins and at the same time several Fzd can interact with a specific Wnt. In addition, some Wnt ligands have been shown to bind to the receptor tyrosine kinase-like orphan receptor (Ror)2 and receptor-like tyrosine kinase (Ryk) (Figure22) (Hikasa et al., 2002; Lu et al., 2004). Thus, a particular Wnt may activate β-catenin and/or non-canonical pathways, depending on the receptor complex (van Amerongen et al., 2008).

1.4.3 β-catenin and Plakoglobin

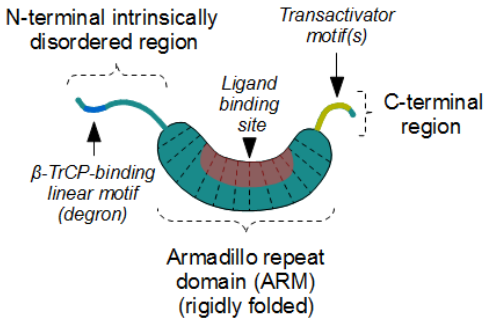

Figure23: Schematic β-catenin structure
The most important domains of β-catenin are indicated with associated function. The central β-catenin ligand binding site interacts with cadherin tails, Axin, APC as well as Tcf (Beta-catenin-structure by Bubus12 used under CC BY 3.0).

The central event during canonical Wnt signaling is the nuclear translocation of β-catenin, a member of the armadillo protein family. The central part of β-catenin harbors an armadillo (ARM) domain consisting of 40 very characteristic ARM repeats, whereas the N- and C-terminal parts are unstructured and flexible (Figure23) (Xing et al., 2008). The ARM repeats fold into a curved structure where the inner surface serves as ligand binding site for various interaction partners including the cytoplasmic cadherin tails, Axin, adenomatosis polyposis coli gene product (APC) and the transcription factors of the Tcf/Lef1 family (Behrens et al., 1996; Huber and Weis, 2001; Xing et al., 2003). Since the surface of the ARM domain can accommodate only one peptide motif at any given time, all these proteins compete for the same cellular pool of β-catenin molecules, which is a key feature of the canonical Wnt signaling pathway regulation.

While the C-terminal part mediates recruitment of transcriptional co-activators when β-catenin is bound to DNA, the N-terminal part is responsible for β-catenin turnover as it contains a short linear motif with several conserved sites, which bind to the β-transducin repeat containing E3 ubiquitin protein ligase (β-TrCP) when they are phosphorylated, inducing β-catenin degradation (see below). Notably, the deletion of the N-terminal part of β-catenin impairs the degradation, leading to its nuclear accumulation and increased Wnt/β-catenin signaling (Gat et al., 1998). Conversely, when the short C-terminal fragment is artificially fused to the β-catenin co-factor Tcf/Lef1, it can mimic the consequences of active Wnt signaling, indicating that the other β-catenin domains are not essential for target gene activation such as c-myc, Axin2 and Jagged1 (Vleminckx et al., 1999).

How increased cytoplasmic levels of β-catenin are translated into transcriptional changes in Wnt target genes, is incompletely understood. It has been proposed that the cytoplasmic-nuclear shuttling of β-catenin is partly mediated by a microtubule mediated active transport; however, the molecular mechanism remains elusive (Sugioka et al., 2011).

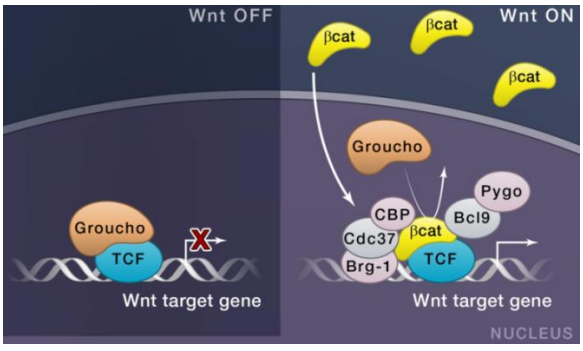

Figure24: β-catenin signaling in the nucleus
In the absence of Wnt/β-catenin signaling (Wnt OFF), Tcf together with the transcriptional co-repressor Groucho occupies and represses its Wnt-target genes. Upon Wnt signaling (Wnt ON), β-catenin accumulates in the cytoplasm, translocates into the nucleus where it displaces Groucho from Tcf, and recruits transcriptional co-activators as well as histone modifiers such as Brg-1, calcium-binding protein (CBP), Cdc47, B-cell chronic lymphocytic leukemia/ lymphoma (Bcl)9 and pygopus family PHD finger (Pygo) to promote target gene expression (modified from (Clevers and Nusse, 2012)).

In the absence of nuclear β-catenin the co-factor Tcf/Lef1 is bound to the DNA with transcriptional co-repressors such as C-terminal binding protein (CtBP), histone deacetylases and Groucho (Daniels and Weis, 2005), forming a mutimeric complex which inhibits Wnt target gene transcription (Figure24). Upon Wnt signaling activation nuclear β-catenin-Tcf/Lef1 complex facilitates the recruitment of additional transcriptional co-activators, such as the histone acetytransferase calcium-binding protein (CBP), B-cell chronic lymphocytic leukemia/lymphoma (Bcl)9 and pygopus family PHD finger (Pygo), leading to a multimeric complex with high transcriptional activation potential (Hecht et al., 2000; Stadeli and Basler, 2005). Intriguingly, it seems that not the absolute levels of β-catenin in the cell, but rather the fold changes activate Wnt signaling in the cell, indicating that very low level of β-catenin would be sufficient for Wnt activity modulation (Goentoro and Kirschner, 2009).

Of note, the β-catenin homologue Plakoglobin (also called γ-catenin) shares strikingly similar protein-domain architecture. Not only does their ARM domain resemble each other in both composition and ligand binding capacity, but also the N-terminal β-TrCP-binding motif is highly conserved in Plakoglobin, implying shared regulation and function with β-catenin in cell-cell adhesion and signaling (Sadot et al., 2000). Conversely, the sequence of the C-terminal segment differs, probably explaining the weaker transactivation activity of Plakoglobin towards classic β-catenin targets when bound to DNA (Maeda O et al., 2004). Indeed, Plakoglobin might act as a negative regulator of β-catenin, as it attenuates the expression of several Wnt target genes including c-myc (Williamson et al., 2006), and thus it is proposed to behave more as tumor suppressor in contrast to β-catenin (Zhurinsky et al., 2000).

1.4.4 Cell-cell adhesion in the context of β-catenin signaling

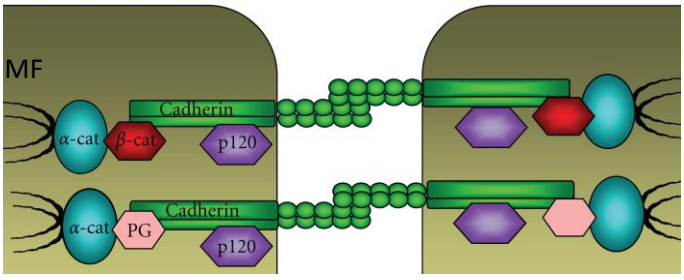

Figure25: β-catenin and Plakoglobin in adherens junctions

E-cadherin forms extracellular interactions with E-cadherin molecules on neighboring cells. Intracellular, β-catenin (β-cat) and Plakoglobin (PG) bind to cadherin tails mutually exclusive and engage α-catenin (α-cat) thereby connecting cadherins to actin microfilaments (MF). In addition, E-cadherins recruit p120-catenin which promotes cadherin dimerization (modified from (Aktary and Pasdar, 2012)).

In addition to its key role in the Wnt pathway, β-catenin as well as Plakoglobin are essential components of the cell-cell adherens junctions, necessary for the creation and maintenance of epithelial cell layers and barriers. Indeed, the majority of the β-catenin molecules in epithelial cells are retained at cell-cell junctions. β-catenin and plakoglobin bind in a mutually exclusive manner to the cytoplasmic domain of various cadherins, which constitute the core component of adherens junctions (Figure25) (Zhurinsky et al., 2000). Cadherins are single-pass transmembrane receptors that form homotypic interactions with cadherin proteins on neighboring cells through their extracellular cadherin repeat domains in the presence of Ca^{2+}. When bound to cadherin, β-catenin or Plakoglobin subsequently interact with the actin binding protein α-catenin at a different site linking the cadherins to the actin cytoskeleton. Another catenin family member p120 binds to a membrane more proximal domain of cadherin cytoplasmic tail, promoting cadherin dimerization and stability at the membrane (Meng and Takeichi, 2009).

Interestingly, in contrast to the short half-life of cytoplasmic β-catenin (minutes), referred to as signaling pool, the β-catenin engaged at cell-cell contacts is highly stable (adherens junction pool). It is still unclear how these two pools depend on and influence each other under physiological conditions. Of note, in many cancers and during wound healing loss of cadherin mediated adhesion during EMT leads to an increased β-catenin release and signaling (Heuberger and Birchmeier, 2010).

1.4.5 Canonical Wnt signaling pathway

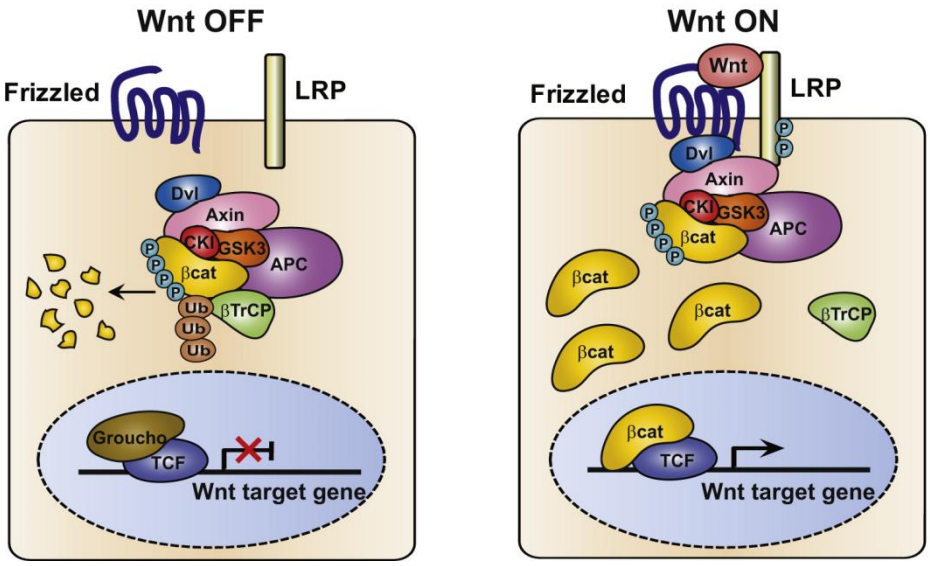

Figure26: The β-catenin destruction complex in the presence and absence of Wnt
In the absence of Wnt (Wnt OFF), the destruction complex resides in the cytoplasm where it binds, phosphorylates and ubiquitinates β-catenin by β-TrCP. Degradation of β-catenin by the proteasome is required to liberate β-catenin from the complex and thus "recycle" it. Consequently, cytosolic β-catenin levels are low and target gene expression is repressed. Wnt (Wnt ON) induces the association of the intact destruction complex with phosphorylated Lrp. After binding to LRP, the destruction complex still captures and phosphorylates β-catenin, but ubiquitination by β-TrCP is blocked. Newly synthesized β-catenin now accumulates in the cytoplasm and promotes Wnt signaling target gene expression (modified from (Li et al., 2012)).

Downstream of ligand bound-Wnt-receptor complex a destruction complex, which regulates the stability of cytoplasmic β-catenin, is considered as the core component of the canonical Wnt/β-catenin pathway (Figure26). This complex is composed by the scaffolding protein Axin, tumor suppressor APC, casein kinase 1 (CK1) and glycogen synthase kinase 3 (GSK3). As Axin interacts directly with all components, it is the central scaffold of the destruction complex and was shown to dictate its activity. The Axin turnover is mainly regulated by the poly-ADP-ribosylating enzyme Tankyrase, which targets Axin for proteasomal degradation (Huang et al., 2009). Of note, Tankyrase has emerged as a suitable target for Wnt signaling inhibition, as inhibition of its activity through chemical compounds such as IWR-1 enhances the stability of the destruction complex (Chen B et al., 2009).

In the absence of Wnt ligands, cytoplasmic β-catenin protein is constantly recruited to the destruction complex and sequentially phosphorylated by CK1 and GSK3 at specific serine residues in the N-terminal region. Phosphorylated β-catenin is subsequently recognized and ubiquitinated by the E3 ubiquitin ligase β-TrCP, and targeted for rapid destruction by the 26S proteasome (Aberle et al., 1997). This continuous degradation of cytosolic β-catenin prevents its accumulation in the nucleus. Upon Wnt-Fzd-Lrp5/6 complex formation the scaffold protein Dishevelled is recruited to the Fzd tail and starts to polymerize, promoting the clustering of several Wnt-Fzd-Lrp5/6 complexes, and thereby generating a dynamic scaffold for destruction complex recruitment and Lrp5/6 phosphorylation by GSK3 and CK1 (Schwarz-Romond et al., 2007). While it has been believed for a long time that the Axin recruitment to phosphorylated Lrp5/6 tails leads a disassembly of the destruction complex and thus inhibits the β-catenin phosphorylation and degradation (Roberts et al., 2011), new data demonstrate that the whole destruction complex is sequestered to the membrane. This re-localization inhibits the ubiquitination of β-catenin and subsequently leads to a saturation of the complex with phosphorylated β-catenin (Li et al., 2012). Newly synthesized cytoplasmic β-catenin is now able to accumulate in the nucleus where it induces target gene expression.

1.4.6 Non-canonical Wnt signaling pathways

In addition to the β-catenin dependent signaling pathways, in vertebrates β-catenin-independent (non-canonical) signaling pathways have been described. They control processes including inner ear planar cell polarity or tissue boundary formation, or dorsal-ventral patterning during gastrulation as well as cancer (Komiya and Habas, 2008). Non-canonical Wnt signaling can be activated by specific combinations of Wnt ligands and Fzd receptors in the absence of co-receptor Lrp5/6, or by specific receptors like Ror2. In the planar cell polarity pathway, Wnt5a specifically interacts with Ror2 inducing the recruitment of Dishevelled and Dishevelled-associated activator of morphogenesis 1 (DAAM1) (Figure20). This complex leads to the activation of the small G-protein Rho and Ras-related C3 botulinum toxin substrate (Rac1), promoting actin remodeling via Rho-associated kinase (ROCK) and JNK (Komiya and Habas, 2008). Of note, Wnt5a can also bind to the Wnt receptor complex Fzd4-Lrp5, promoting canonical Wnt signaling (Mikels and Nusse, 2006).

The Wnt/Ca^{2+} pathway instead regulates calcium release from the endoplasmic reticulum. Dishevelled activation upon Wnt ligand binding to Fzd receptor not only influences β-catenin stability (see section 1.4.5), but also induces phospholipase C (PLC) mediated cleavage of membrane bound $PI(4,5)P_2$ in diacyl-glycerol (DAG) and inositol trisphosphate (IP3). When IP3 binds its receptor on the endoplasmic reticulum, calcium is released which subsequently activates Ca^{2+}/calmodulin-dependent protein kinase (CAMkII) and protein kinase C (PkC). Subsequently, PkC can activate Cdc42, a regulator of the ventral patterning, and CAMkII induces activation of the transcription factor nuclear factor of activated T cells (NFAT), which regulates cell adhesion, migration and tissue separation (Figure20) (Komiya and Habas, 2008). The planar cell polarity pathway as well as the Wnt/Ca^{2+} pathway are able to antagonize canonical Wnt signaling although the mechanisms remain still poorly defined (MacDonald et al., 2009).

In addition, new non-canonical Wnt pathways seem to emerge recently. Upon Wnt ligand binding to the RYK, Dishevelled can be recruited to its cytoplasmic tail, leading to the protease mediated cleavage of the C-terminal tail of RYK which then translocates to the nucleus and induces neuronal differentiation (Lyu et al., 2008). So far it remains elusive, how the intracellular RYK fragment influences the transcriptional machinery in the nucleus.

1.4.7 Soluble Wnt agonists and antagonists:

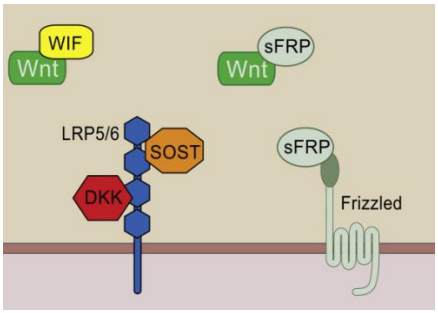

Figure27: Soluble Wnt antagonists
While Wif and sFRP bind directly to secreted Wnt ligands and/or Fzd competing for the Wnt receptor binding, Dkk and Wise (SOST) proteins interact with Lrp5/6 to prevent FZD-LRP complex formation (modified from (MacDonald et al., 2009)).

Lately, an increasing number of soluble Wnt ligand binding proteins have been identified, which act as Wnt signaling agonists or antagonists. The first identified Wnt antagonists were the sFRP comprising a whole family of Wnt binding proteins (sFRP1-5). Because their structure is highly homologous to the extracellular cysteine-rich domain of Fzd receptors, they compete with Wnt-Fzd complex formation (Figure27). Interestingly, some sFRPs exhibit a biphasic effect on Wnt activity in a concentration dependent manner: whereas at low concentrations sFRP1 enhances Wnt signaling activity, at high concentration it has an inhibitory effect; however the mechanism of these opposing functions remain unclear (Uren et al., 2000). Further known secreted Wnt antagonists are the structurally distinct Wif1 and the Dkk family (Dkk1-4) proteins (Fedi et al., 1999; Hsieh et al., 1999). Wif1 inhibits Wnt receptor interaction through direct interaction with Wnt ligands through its WIF domain. In contrast, Dkk family members inhibit canonical Wnt signaling by two different mechanisms: first, Dkk binding to Lrp5/6 prevents its interaction with Wnt-Fzd complexes and second, binding to the membrane-anchored Dkk receptor Kremen triggers the internalization of Lrp5/6 (Mao et al., 2002).

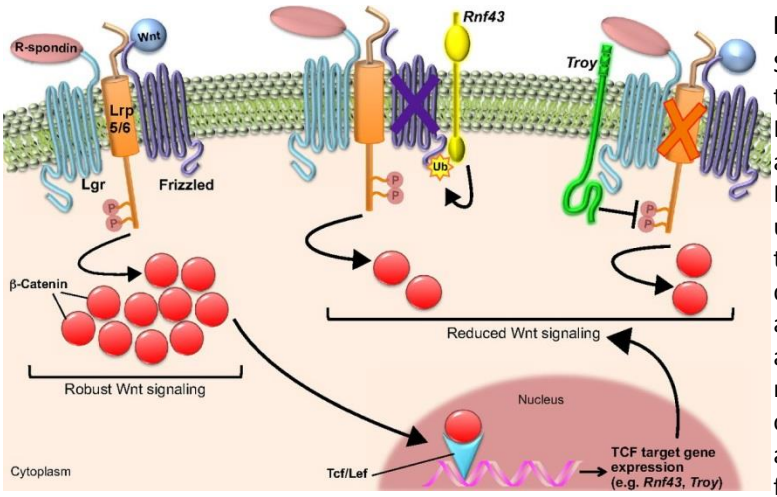

Figure28: Fine tuning Wnt signaling by Lgr and R-spondin proteins
Secreted R-spondin ligands can bind to Lgr receptors and facilitate Wnt-Lrp5/6-Fzd complex formation, amplifying Wnt signals. Conversely, Lgr bound R-spondin recruits the E3 ubiquitin ligase Rnf43 which ubiquitinates Fzd and promotes its degradation, dampening Wnt signaling. In addition, Troy was shown to associate with Lgr proteins and to be recruited to the Wnt receptor complex where it destabilizes Lrp, attenuating Wnt signaling (modified from (Barker et al., 2013)).

Among the agonists with a stimulatory influence towards canonical Wnt signaling, the growth factor R-spondins are most prominent (Figure28). It is currently unclear whether R-spondins are secreted locally, or whether they are delivered via the circulatory system from more distant sources (de Lau et al., 2012). Affected cells recognize R-spondin with leucine-rich repeat-containing G-protein-coupled receptors (Lgr) 4–6, a group of SC associated seven transmembrane domain surface receptors involved in progenitor and SC maintenance in multiple tissues (Barker et al., 2013; Carmon et al., 2011). The current model proposes that binding of R-spondin to Lgr recruits the E3 ubiquitin ligase ring finger protein 43 (Rnf43), which has been demonstrated to ubiquitinate Fzd receptor proteins, thereby targeting them for degradation (Koo et al., 2012). The Lgr-Rnf43 complex is rapidly cleared from the plasma membrane, which results in inhibition of Wnt receptor turnover and thus enhanced Wnt signaling (Hao et al., 2012). In addition, a further Wnt receptor stabilizing mechanism for Lgr-R-spondin function was described recently. In the absence of R-spondin, the tumor suppressor Troy directly interacts with Lgr and is recruited to a Wnt-Lgr receptor complex, leading to destabilization of Lrp co-receptor at the cell surface and reduced canonical Wnt signaling (Fafilek et al., 2013). Thus, Lgr proteins appear to be facultative components of the Wnt receptor complex that bind secreted R-spondin proteins to boost existing canonical Wnt signals selectively on responding cells. This might explain the restricted expression of Lrg5 on intestinal SC and Lrg6 on skin SC (see section 1.1.2), leading to a tightly controlled canonical Wnt signaling above threshold ensuring SC homeostasis *in vivo*.

1.4.8 Wnt and TGFβ signaling cross talk

TGFβ and Wnt/β-catenin signaling are interconnected at several levels through Smad proteins. In particular the TGFβ inhibitory protein Smad7 can promote and inhibit Wnt/β-catenin signaling through multiple pathways, and Smad7 is regulated at the same time by components of the Wnt/β-catenin signaling pathway. On the one hand, Smad7 in skin has been shown to promote degradation of β-catenin and consequently Wnt signaling inhibition through direct interaction and recruitment to the E3 ubiquitin ligase Smurf2, which also targets TGFβ receptor for degradation (Han et al., 2006a). Furthermore, in tumor cells Smad7 seems to promote β-catenin-E-cadherin complex formation and cell-cell adhesion, thereby inhibiting nuclear translocation of cytosolic β-catenin (Tang et al., 2008).

On the other hand, it has also been shown that Smad signaling can enhance Wnt signaling, as the Smad7 dependent E3 ubiquitin ligase Smurf2 also fosters the degradation of Axin and thus decreases the destruction complex activity (Kim and Jho, 2010). Conversely, Axin assists in the ubiquitin mediated degradation of Smad7 through serving as a scaffold for the E3 ligase Arkadia, indicating a negative feedback of Wnt signaling to Smad7 (Liu et al., 2006). Furthermore, a complex of β-catenin, Smad4 and its R-Smad was shown to protect β-catenin from degradation in the cytoplasm (Zhang et al., 2010). Phosphorylation of β-catenin at tyrosine 654 through activation of Src kinase(s) is induced by TGFβ, decreasing β-catenin binding to E-cadherin in cell-cell contacts and promoting its accumulation in the cytoplasm (Ulsamer et al., 2012). Besides influencing the protein stability of the respective other pathway, also direct cross talk at the level of gene transcription has been observed. In the nucleus Smad7 interacts with the β-catenin-Tcf/Lef1 complex, enhancing its transcriptional activity and inducing apoptosis in a TGFβ dependent manner (Edlund et al., 2005).

1.4.9 Wnt and Notch signaling are highly interconnected in skin

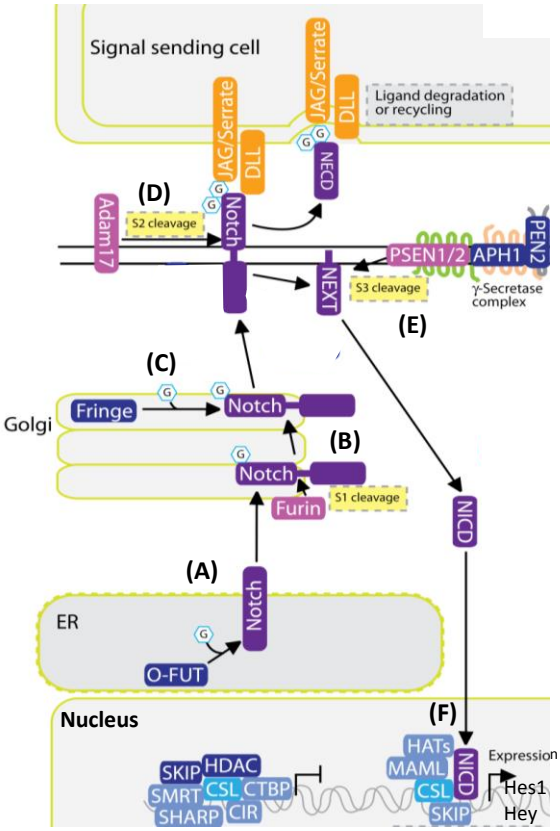

Figure29: Notch signaling pathway
(**A**) Notch is translated as a single polypeptide, which is fucosylated by the fucosyltransferase O-FUT in the endoplasmic reticulum (ER), facilitating Notch protein shuttling to the Golgi. (**B**) There, Notch is cleaved by a furin-like protease at the S1-cleavage site to generate the non-covalently linked Notch heterodimer, consisting of the extracellular portion and the intracellular portion. (**C**) Subsequently the heterodimer is glycosylated by several Fringe glycosyltransferase family members. (**D**) At the plasma membrane, Notch becomes available to interact with Notch ligand (Jag/Serrate and DLL) on a ligand-expressing cell. The interaction induces proteolytic cleavage of the Notch receptor by ADAM family metalloprotease at the S2 cleavage site, generating the intermediate Notch substrate NEXT. (**E**) NEXT is then cleaved by the γ-secretase complex, resulting in the release of the intracellular Notch fragment, which translocates to the nucleus, where it associates with the transcription factor RBP-J and other transcriptional co-activator and repressors (**F**) (modified from stem cell signaling pathway, Novus Biologicals).

Notch signaling controls a number of cellular processes including cell fate decision, proliferation, differentiation and survival/apoptosis (Andersson et al., 2011). In skin the Notch pathway plays an important role in regulating epidermal differentiation of HF, sebaceous gland and interfollicular epidermal lineages, reminiscent of the influence of Wnt/β-catenin signaling (Rangarajan et al., 2001). Genetic ablation or activation of the pathway reveals that Notch act as an epidermal tumor suppressor (Dotto, 2008). Mammals express four Notch proteins (Notch1- 4) and five Notch ligands, named Delta-like (DLL) 1, 3, 4, and Jagged (Serrate) 1 and 2. All four Notch proteins are highly similar in their structure: the extracellular domain of Notch possesses many EGF-like repeats which participate in ligand binding. The N-terminal EGF-like repeats are followed by cysteine-rich Notch/Lin12 repeats that prevent signaling in the absence of the ligand. The cytoplasmic region of Notch transduces the signal to the nucleus and contains a Rbp-associated molecule (RAM) domain, ankyrin repeats, nuclear localization signals, a transactivation domain and a PEST degradation sequence (Andersson et al., 2011). Although Notch is synthesized as a single precursor protein, it is cleaved in two parts during export to the cell surface and thus exists as a heterodimeric receptor (Blaumueller et al., 1997). All Notch ligands are single transmembrane domain proteins, presented on neighboring cells. Consequently, Notch signaling is transmitted by direct cell to cell contact, allowing distinct groups of cells to organize themselves into larger structures.

Notch signaling is initiated by a receptor ligand interaction between two neighboring cells, which leads to two successive proteolytic cleavage reactions (Figure29). The first is mediated by a disintegrin and metalloproteinase (ADAM) family metalloprotease at the extracellular part of the Notch receptors, generating an intermediate Notch extracellular truncation (NEXT), which is a substrate for the second proteolytic event mediated by the presenilin γ-secretase protein complex (Brou et al., 2000; Saxena et al., 2001). As a result of the second event, the Notch intracellular domain (NICD) is liberated from the membrane and translocates to the nucleus where it associates with the transcription factor RBP-J. Subsequently, the co-activators Mastermind and histone acetyltransferases are recruited to the complex and activate transcription of target genes, including Hes and Hey (Andersson et al., 2011; Mumm and Kopan, 2000). Interestingly, while the core signaling pathway of Notch is rather simple, there is considerable complexity in the regulation of the Notch receptor and ligands through post-translational modifications. For example the glycosyltransferase Fringe, resident in the Golgi, was shown to add carbohydrate chains to the extracellular domain of Notch, thereby altering the ability of ligands to activate the

receptor (Haines and Irvine, 2003). Similar to the Notch receptors, the ligands undergo controlled proteolysis, and there are indications that the cleaved ligand intracellular domains also participate in signaling (D'Souza et al., 2008). These diverse signal propagation modes, leading to simultaneous generation of distinct signals in the receiving and sending cells, qualify DLL-Notch signaling for patterning processes.

In adult skin all Notch proteins are expressed in the interfollicular epidermis and HF, especially in the hair bulb. Notch receptors become upregulated in the suprabasal keratinocyte layer and HF matrix, coinciding with cells that are initiating or are undergoing terminal differentiation. The Notch ligands Jagged1 and Jagged2 are detected in adult skin (Powell et al., 1998). While Jagged2 is restricted to the basal layer, Jagged1 is predominantly expressed in the suprabasal layers and only present in some basal cells. Similarly, in the HF Jagged2 is detected in the outer root sheath and basal hair bulb cells close to the dermal papilla, whereas Jagged1 is present in the more differentiated cells of the pericortex (Estrach et al., 2006). The highest Notch signaling activity is observed in the suprabasal interfollicular epidermis layer, HF pre-cortex and inner root sheath progenitor cells.

Due to multiple Notch receptor and ligands expressed in the epidermis, complete Notch inactivation is only achieved by targeting common Notch pathway components, such as γ-secretase, RBP-J or Mastermind. These studies have revealed that in the skin Notch activity is not required for embryonic HF morphogenesis and patterning, whereas in postnatal skin loss of Notch signaling leads to hyperproliferation of basal cells in the interfollicular epidermis, impaired sebaceous gland differentiation and conversion of cells from HF keratinocytes into cysts with interfollicular epidermis-like cells (Pan et al., 2004; Proweller et al., 2006; Yamamoto et al., 2003). Conversely, over activation of Notch signaling can be induced by overexpressing NICD in different epidermal layers. Overexpression of NICD in the suprabasal layers of the interfollicular epidermis and the HF inner root sheath leads to disturbed differentiation of HF lineages and hair loss as well as expansion of the differentiated cell compartment of the interfollicular epidermis (Uyttendaele et al., 2004). If NICD is overexpressed in the basal layer of the skin, the cell differentiation is severely impaired, leading to expansion of the interfollicular epidermal spinous layer, sebaceous glands and hair bulb base. In addition, HFs start to form abnormal clusters (Figure30) (Blanpain et al., 2006; Estrach et al., 2006).

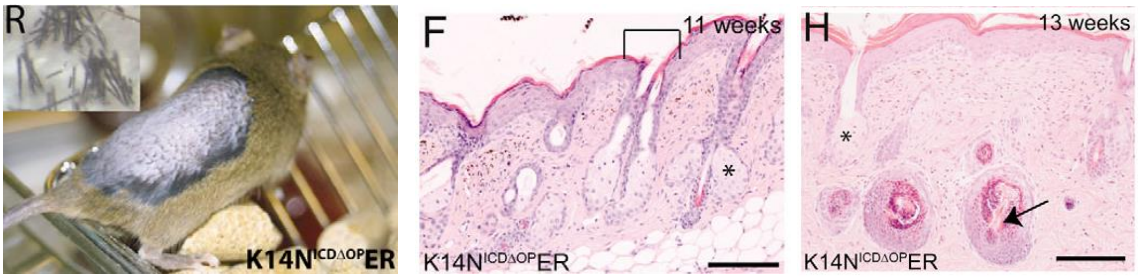

Figure30: Overexpression of NICD in the basal skin layer
Increased activation of NICD induces aberrant HF cluster formation, loss of spacing (left and middle) and to expansion of the sebaceous glands (asterisk) and hair bulb base (arrow). No ectopic HF formation can be observed (modified from (Estrach et al., 2006)).

In skin the Notch and Wnt pathway are highly interconnected. On the one hand, several Notch pathway genes are upregulated by β-catenin activation in the epidermis (Ambler and Watt, 2007); on the other hand the transcription of various Wnt ligands is regulated by Notch (Devgan et al., 2005; Hu et al., 2010). Intriguingly, Jagged1 was shown to be a direct target gene of canonical Wnt signaling and deletion of Jagged1 blocks β-catenin-induced ectopic HF formation, but not the ability of β-catenin to stimulate epidermal proliferation (Estrach et al., 2006). In line, overexpression of NICD promotes differentiation of β-catenin-induced HF; however, it does not induce ectopic HF formation alone (Estrach et al., 2006), placing Notch signaling downstream of Wnt. While Wnt signaling seems to have largely a positive effect on the Notch pathway, Notch activity seems to antagonize Wnt signaling in many cell types. Indeed, Wnt signaling becomes activated in tumors overexpressing dominant negative form of Mastermind, suppressing Notch signaling (Proweller et al., 2006). Conversely, Notch1 suppresses the expression of Wnt4 (Devgan et al., 2005), which inhibits canonical Wnt signaling by promoting the recruitment of β-catenin to cell-cell adhesion sites and thus reduces the β-catenin signaling pool (Bernard et al., 2008). In dermal papilla cells, Notch1 controls Wnt5a expression, which activates or represses canonical Wnt signaling depending on the expression of the Wnt receptor type (see section 1.4.2) (Hu et al., 2010). But Notch is also able to interfere with β-catenin signaling directly because non-cleaved NICD is able to bind β-catenin, serving as a protein trap at the membrane and thus suppressing β-catenin transcriptional activity (Hayward et al., 2005; Kwon et al., 2011). It is conceivable that more interaction points of Notch and Wnt pathway will be discovered in the future.

1.5 The Kindlin family

The Kindlins represent a class of focal adhesion proteins that belong to a family of three evolutionary conserved proteins in mammals (Kindlin-1, Kindlin-2 and Kindlin-3), encoded by three different genes, namely *KINDLIN-1* (chromosome 20p12.3), *KINDLIN-2* (chromosome 14q22.1) and *KINDLIN-3* (chromosome 11q13.1) (Siegel et al., 2003). The Kindlin genes are all composed by fifteen exons with the translation start in exon 2. Kindlins share considerable sequence and structural similarities. In mammals, Kindlin-2 has ~62% homology with Kindlin-1 and Kindlin-3 shares ~49% similarity with Kindlin-1 (Lai-Cheong et al., 2010; Siegel et al., 2003; Ussar et al., 2006).

Phylogeny analysis of the Kindlin paralogues suggests a single ancestral Kindlin protein present in even the earliest metazoan, which then underwent duplication events in insects and also genomic duplication in vertebrates, leading to the subfunctionalized Kindlin family with distinct expression pattern (Khan et al., 2011). Indeed, Kindlin orthologues can be found in C. elegans (unc112) and in Drosophila (Fermitin-1 and -2) (Bai et al., 2008; Rogalski et al., 2000). The Kindlin family members highly differ in their expression patters *in vivo*: Kindlin-3 is considered to be mainly restricted to the hematopoietic system, such as platelets and red blood cells, with the highest levels in megakaryocytes (Ussar et al., 2006), but expression has also been recently reported in endothelial tissues and breast cancer cells (Bialkowska et al., 2010; Sossey-Alaoui et al., 2014). Whereas Kindlin-2 is wildly expressed, Kindlin-1 is only present in epithelial cells from the skin, intestine, kidney and lung (Ussar et al., 2006). The latter two Kindlin paralogues show the highest sequence homology and are co-expressed in keratinocytes, where they seem to share a lot of redundant functions (He et al., 2011a; Kloeker et al., 2004; Ussar et al., 2008).

Functionally, Kindlins have revealed themselves as a novel class of adaptor molecules involved in integrin activation, integrin trafficking and adhesion turnover (Bottcher et al., 2012; Margadant et al., 2013; Montanez et al., 2008; Moser et al., 2008; Ussar et al., 2008). Due to the lack of catalytic domains, Kindlin function is exclusively mediated by protein-protein interactions. The initial link of Kindlins with integrin signaling was provided by studies on C. elegans embryos harboring homozygous mutations in unc112. These embryos develop a paralyzed, arrested elongation at twofold (PAT) lethal phenotype due to failure of organization of PAT3/β integrin in the body muscle wall (Rogalski et al., 2000). Following depletion studies in mouse resulted in integrin-mediated attachment and integrin activation defects in the affected organs for all three paralogues (Montanez et al., 2008; Moser et al., 2008; Ussar et al., 2008). In humans loss-of-

function mutations in *KINDLIN-1* and *KINDLIN-3* cause Kindler syndrome (KS) and leukocyte adhesion deficiency-III syndrome (LAD III), respectively, whereas no human disease has yet been associated with *KINDLIN-2* gene pathology (see section 1.5.3). Lately, an increasing number of new and homologue specific functions in multiple signaling pathways have been discovered, placing Kindlins as central signaling hubs in different cellular compartments, which will be discussed below.

1.5.1 Subcellular Kindlin localizations and specificities

It is still largely unknown, how Kindlins are selectively recruited and trafficked to distinct cell compartments. In cell culture Kindlins are strongly enriched at the integrin adhesion site, known as focal adhesions, while a large fraction resides in the cytoplasm (Herz et al., 2006; Kloeker et al., 2004; Lai-Cheong et al., 2008; Siegel et al., 2003). In keratinocytes Kindlin-1 and Kindlin-2 co-localize in focal adhesion structures, but in contrast to Kindlin-1, Kindlin-2 has been found to localize also at cell-cell adherens junctions in cardiac muscle cells (Dowling et al., 2008a; Dowling et al., 2008b), colon epithelial cells (Ussar et al., 2008) and keratinocytes (He et al., 2014), but not in podocytes (Qu et al., 2011). Kindlin-1 instead has been shown to localize at centrosomes in an integrin dependent manner upon phosphorylation, where it is involved in the mitotic spindle assembly (Patel et al., 2013). In osteoblasts Kindlin-3 is found predominantly at the sealing zone of podosomes, which are integrin mediated adhesion structures essential for bone resorption (Schmidt et al., 2011).

Notably, amongst the Kindlin family members only Kindlin-2 has a nuclear localization signal (Ussar et al., 2006) and nuclear localization was reported in various cell types including smooth muscle cells (Kato et al., 2004), breast cancer cells (Yu et al., 2012), but not in keratinocytes (Lai-Cheong et al., 2008). Although more and more nuclear Kindlin-2 functions are discovered, it remains elusive how Kindlin-2 nuclear trafficking is regulated and whether other Kindlin family members share similar nuclear functions.

One possible mechanism for Kindlin subcellular localization regulation is a differential binding affinity of the different Kindlins to various β tails with conserved NxxY motif. On the one hand, it has been shown that for example Kindlin-2 binds to β1 and β3 integrin tail with similar affinity, on the other hand binding to β2 is over 100 fold less efficient, indicating an impact of further integrin tail residues on Kindlin interaction. Indeed, the last three C-terminal residues in the β tail have

been identified to determine the Kindlin binding affinity (Bledzka et al., 2012). Of note, a recent study in zebra fish has further been able to show that the Kindlin binding affinity is determined by the amino acid spacing and the C-terminal COOH group, rather than by residue entities of the integrin tail (Fitzpatrick et al., 2014).

However, also the Kindlin isoforms can differ in their affinity to a β integrin tail. In contrast to Kindlin-2, Kindlin-1 is able to bind the β6 integrins and promotes its functions in TGFβ signaling, wound healing and cancer (see section 1.3.6 and 1.6.4) (Bandyopadhyay et al., 2012). But so far it remains largely elusive, how the selectivity between the integrin tails and Kindlin paralogues is achieved and most likely this has to be addressed with comparative co-crystallization studies of different Kindlin and integrin tails.

Taken together, these differences in Kindlin specificities for certain integrin isoforms appear as a reasonable consequence of the evolutionary splitting of the Kindlin family, allowing specific regulation of tissue specific integrin classes and associated signaling, and even differential regulation of integrins in the presence of different integrin isoforms. Furthermore, the different affinities of one Kindlin to the co-expressed integrin isoforms might lead to a differential preference of those integrins with higher affinities during early spreading and might allow regulation of Kindlin affinity via post-translational modifications.

1.5.2 Post-transcriptional modifications of Kindlins

The localization and function of Kindlins seem to be strongly regulated by post-transcriptional modifications, such as phosphorylation and cleavage. Bioinformatic analysis of the Kindlin sequence has predicted multiple highly conserved phosphorylation sites and it has become clear that Kindlins are prominent targets of multiple signaling kinases. For example, in keratinocytes a fraction of Kindlin-1 becomes phosphorylated by casein kinase-2, a serine/threonine kinase that is involved in cytoskeleton regulation (Herz et al., 2006), and in breast cancer cells Kindlin-1 phosphorylation at threonine 30 by the Polo-like kinase 1 (PLK1) controls Kindlin recruitment to centrosomes (Patel et al., 2013).

In platelets and leucocytes it has been shown that the integrin-Kindlin-3 interaction is regulated by calpain cleavage at tyrosine 373 in the N-terminal part of Kindlin-3 PH domain (Zhao et al., 2012). Expression of a calpain resistant Kindlin-3 mutant leads to stronger adhesion and inhibits cell migration by stabilizing its integrin tail association. Thus, calpain cleavage might promote one

process of Kindlin-3 removal from activated integrin to free binding sites for other integrin partners and allows reversibility of integrin-matrix interactions. Whether the function of other Kindlin isoforms is also controlled by protease mediated cleavage, is currently unknown.

In summary, although Kindlin proteins seem to be heavily modified in the cell, these post-transcriptional modifications remain poorly characterized. How these are regulated and which further modifications such as sumoylation or ubiquitination are involved in the modulation of Kindlin function, trafficking and localization are still open questions.

1.5.3 Kindlin pathogenesis and molecular function and signaling

1.5.3.1 Kindlin-1 and Kindler syndrome

Blistering

Premature aging

Skin atrophy Hyperkeratosis

Poikiloderma

Photosensitivity

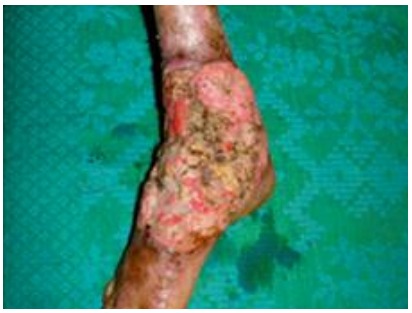

Squamous cell carcinoma

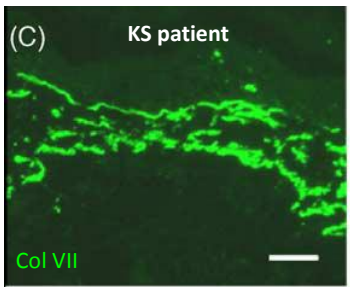

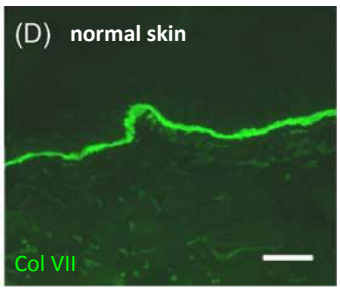

Basement membrane defect

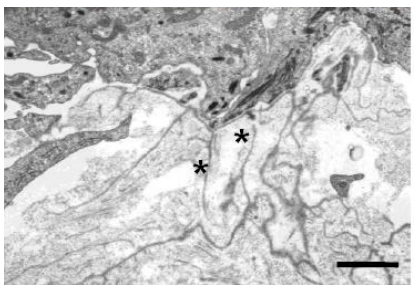

Reduplication of the lamina densa

Figure31: KS disease symptoms
Most common symptoms are displayed (modified from (Arita et al., 2007; Ashton et al., 2004; Fassihi et al., 2005; Mansur et al., 2007; Penagos et al., 2004)).

Although KS was first described in the year 1954 by Dr. Theresa Kindler as a subtype of bullous skin diseases characterized by skin blistering, hyperkeratosis, skin atrophy, and distinguished from the other diseases by premature skin aging photosensitivity, poikiloderma in sun exposed areas (Figure31), it took almost 50 years until loss-of-function mutations in the *KINDLIN-1* gene were identified as the cause of KS (Jobard et al., 2003; Kindler, 1954; Siegel et al., 2003). Since its discovery only slightly above 120 cases have been reported. However, due to the clinical symptom overlap with other skin blistering diseases, the true number might be higher (Intong and Murrell, 2012). To date, over 40 distinct *KINDLIN-1* mutations have been reported including large deletions, splice site, nonsense and frame shift mutations; all of them leading to premature termination codons and, consequently, to complete lack of Kindlin-1 in epithelial cells (Lai-Cheong et al., 2010). Interestingly, although the pathogenesis of the patients varies largely, all attempts to correlate the manifestation of a specific symptom or the severity of disease progression with a specific mutation in the Kindlin-1 gene, have failed so far. The first KS symptoms during infancy are characterized by trauma induced skin blistering, due to impaired integrin activity (Figure31) (Fassihi et al., 2005; Lai-Cheong et al., 2009; Penagos et al., 2004). With increasing age, further skin homeostasis abnormalities appear, including hyperkeratotic palms and soles, severe cutaneous atrophy especially on the dorsal side of hands and symptoms of premature aging such as cigarette paper-like wrinkling and webbing between fingers. Especially in sun exposed areas, KS patient very often develop poikiloderma (an aberrant hyperpigmentation of the skin) and erythema (redness of the skin) due to a photosensitivity (increased sensitivity to UV); however, the molecular basis for these pathologies are completely unknown (Ashton et al., 2004; Penagos et al., 2004). So far, it has only been described that in poikiloderma, melanocytes are highly proliferative and delocalized leading to secretion of melanin into the dermis which is then engulfed by resident macrophages, converting them to melanophages (Papa and Kligman, 1965). Because of the tight interdependence of bulge SC and HF melanocyte homeostasis, it can be speculated that loss of melanocyte hemostasis is due to aberrant bulge SC cross talk. Of note, colony-forming efficiency assays with serially cultivated primary keratinocytes isolated from KS patients indicate an accelerated depletion of SC and premature senescence, suggesting a SC maintenance defect which correlates with loss of SC marker expression in KS patient skin (Lai-

Cheong et al., 2009; Piccinni et al., 2013). However, the molecular mechanisms were unclear so far.

Intriguingly, despite the known functional redundancy between Kindlin-1 and -2 in KS patients or Kindlin-1 null mice, Kindlin-2 is unable to fully compensate for Kindlin-1 deficiency, suggesting that both Kindlins have functionally significant differences (He et al., 2011a; Ussar et al., 2008). In keratinocytes, depletion of Kindlin-1 leads to abnormal cell shape, increased migration, aberrant basement membrane deposition, adhesion and proliferation defects, while β1 integrin activation and cell adhesion are only mildly perturbed (He et al., 2011a; Herz et al., 2006; Lai-Cheong et al., 2009; Ussar et al., 2008). The aberrant cell shape and migration may in part be attributed to defective lamellipodium formation, resulting from abnormal signaling via Rho GTPase family (Has et al., 2009), as well as a partial loss of the epithelial identity (Qu et al., 2012). Although KS is mainly described as a skin fragility disorder, KS patients suffer from mucocutaneous malignancies (Wiebe et al., 2008) and ulcerative colitis-like intestinal problems from early on (Kern et al., 2007; Ussar et al., 2008), suggesting that this disease affects multiple kinds of epithelia. Unlike in the skin, two forms of Kindlin-1, arising from alternative splicing, can be detected in the colon (Kern et al., 2007); however, their individual function remains unknown. In addition, Kindlin-1 is also highly expressed in the kidney epithelial cells (Ussar et al., 2006), but no defects have been reported in KS patients and in Kindlin-1 null mice, suggesting that here Kindlin-1 loss is fully compensated for by Kindlin-2 during development.

Finally, KS patients have a higher risk of developing skin cancer at an early age (particularly squamous cell carcinomas (SCC) (Arita et al., 2007; Emanuel et al., 2006; Lotem et al., 2001; Mizutani et al., 2012), but how Kindlin-1 loss is able to promote tumorigenesis was unknown. Furthermore, the role of Kindlin-1 in carcinogenesis seems to be context dependent, because increased *KINDLIN-1* mRNA expression has been observed in up to 60% and 70% of lung breast and colon cancers, respectively (Sin et al., 2011; Weinstein et al., 2003). In addition, it is highly expressed in multiple pancreatic cancer cell lines, where it promotes migration and invasion (Mahawithitwong et al., 2013a). In such cancer entities, the oncogenic effect of Kindlin-1 seems to be strongly TGFβ signaling dependent, however the molecular mechanism remained unclear (Sin et al., 2011).

1.5.3.2 Kindlin-2

Because of its ubiquitous expression, Kindlin-2 seems to be important in multiple cell types and tissues, where it is implicated in disease condition such as fibrosis or cancer (discussed below).

In mice, loss of Kindlin-2 causes peri-implantation lethality before embryonic age 7.5 days, due to detachment of the endoderm and epiblast from the basement membrane because of severe adhesion defects (Dowling et al., 2008a; Montanez et al., 2008). Interestingly, Kindlin-2 is rapidly emerging as an important molecule in cardiac and muscle development, where it is highly expressed (Dowling et al., 2008a; Ussar et al., 2006). In these cells Kindlin-2 is not only involved in muscle elongation and fusion in an integrin dependent manner (Bai et al., 2008; Dowling et al., 2008a; Dowling et al., 2008b), but it also triggers cell differentiation by regulating myogenic regulatory factor Myogenin expression. Mechanistically, Kindlin-2 forms a complex with β-catenin and Tcf4 and binds to the Myogenin promoter in the nucleus to enhance its expression during myogenic differentiation (Yu et al., 2013a).

In skin Kindlin-2 seems to be important for the dermal fibroblast adhesion as well as for the keratinocytes cell-cell contact formation. During wound healing, Kindlin-2 becomes highly expressed in activated myofibroblasts, where it seems to be crucial for focal adhesion formation, organization of α-smooth muscle actin into stress fibers and force transmission (He et al., 2011b). Despite its low expression in the epidermis, a recent study using human keratinocytes organotypic cultures has revealed that Kindlin-2 contributes to cell–cell junctions formation and maintenance through RhoGTPase dependent regulation of the actin cytoskeleton at cadherin adhesion sites (He et al., 2014). Nevertheless, these results should be confirmed by conditional skin deletion of Kindlin-2 *in vivo*, in order to further elucidate why Kindlin-1 is not able to compensate for at cell-cell adhesion sites.

The disease kidney tubular intestinal fibrosis (TIF) is characterized by massive expansion of the cortical interstitium, activation of fibroblasts to myofibroblasts and progressive EMT of tubular epithelial cells (Bielesz et al., 2010). In affected mouse and human tubular epithelial cells, Kindlin-2 is highly expressed and promotes EMT by enhancing Erk1/2, Akt and TGFβ signaling: first, Kindlin-2 induces Ras activation through recruitment of son of sevenless homolog 1 (Sos1), which subsequently activates Erk1/2 and Akt signaling (Wei et al., 2014). Second, Kindlin-2 is able to activate the TGFβ pathway by binding C-terminally via the FERM domain with TβRI and N-terminally with Smad3 (Wei et al., 2013). How these distinct Kindlin-2 functions are regulated and influence each other in tubular epithelial cells, remains elusive.

In contrast to most other polarized cells, endothelial cells only express Kindlin-2 where it is essential for angiogenesis and blood vessel homeostasis. Besides controlling integrin mediated cell adhesion and migration during angiogenesis, Kindlin-2 triggers endocytosis and recycling of cell surface receptors, such as CD39 and CD73 via interaction with the clathrin complex, thereby modulating platelet responses and homeostasis (Pluskota et al., 2011; Pluskota et al., 2013).

For tumor development and progression, the role of Kindlin-2 seems to be tumor type dependent. Kindlin-2 expression was found to correlate with tumor invasion, lymph node metastasis and poor patient outcome in breast cancer (Gozgit et al., 2006), pancreatic ductal adenocarcinomas (Mahawithitwong et al., 2013b), malignant mesothelioma (An et al., 2010) and bladder cancer (Talaat et al., 2011). One major oncogenic effect of Kindlin-2 seems to be the promotion of EMT by activating the signaling pathways as described for TIF. In addition, Kindlin-2 was shown to trigger EMT and invasion in breast cancer by promoting Wnt signaling and target gene transcription through association with active β-catenin and Tcf4 (Yu et al., 2012) as well as by silencing microRNA200 (miR-200) family member miR-200b expression through CpG island hypermethylation in the nucleus (Yu et al., 2013b). Interestingly, in esophageal SCC Kindlin-2 has been shown to be a miR-200b target itself and decrease Kindlin-2 levels seems to be responsible for the tumor suppressive effect of miR-200b for cell invasion (Zhang et al., 2014).

Besides promoting proliferation, Kindlin-2 is also able to increase cell survival by stimulating Hedgehog signaling through interaction with Gli1 as well as expression of anti-apoptotic Bcl2 proteins (Gao et al., 2013; Gong et al., 2010; Shen et al., 2013). Interestingly, Kindlin-2 seems to enhance genome instability, a hallmark for cancer formation; however the molecular mechanism remains elusive (Zhao et al., 2013).

In sharp contrast, high Kindlin-2 expression in mesenchymal cancer cells seems to suppress invasion by inhibiting the secretion of the highly oncogenic urokinase-type plasminogen activator (uPA) (Shi and Wu, 2008). Furthermore, Kindlin-2 has been shown to impair tumor progression in serous epithelial ovarian cancer where it promotes mesenchymal to epithelial transition (MET) partly through upregulation of estrogen receptor and thus inhibits tumor cell dissemination (Ren et al., 2014).

Thus, similar to Kindlin-1, Kindlin-2 shows variable expression patterns in many human cancers with context dependent tumor promoting or suppressive effects. However, the involved signaling pathways and molecular mechanisms seem to highly differ between the two Kindlin paralogues.

Furthermore, many tumor types express more than one Kindlin isoform. A recent study indicates that Kindlin-1 and -2 have opposing function for lung cancer progression: while Kindlin-1 seems to inhibit EMT and to correlate with the differentiation status of non-small-cell lung cancer cells, high Kindlin-2 expression correlates with invasiveness and poor patient prognosis (Zhan et al., 2012). Whether comparable interdependencies occur in other epithelial cancer entities, and how deregulation of one isoform influences the other, has to be analyzed in comparative studies in the future.

Besides the expression in tumor cells, Kindlin-2 seems to be highly upregulated in the tumor stroma (Talaat et al., 2011). Consequently, dissecting the mutual influence of Kindlin family members in the tumor cell – tumor stroma cross talk will be an exciting challenge in the future.

1.5.3.3 Kindlin-3

Kindlin-3 is the most studied family member and its depletion affects the integrin function in all hematopoietic linages. In humans, pathogenic mutations in *KINDLIN-3* gene cause a rare hematopoietic disease known as LAD III, which results from the combined defects in β1, β2, and β3 integrin activation in platelets, neutrophils, lymphocytes as well as osteoclasts (Kuijpers et al., 2009; Malinin et al., 2009; Svensson et al., 2009). In addition, two other LAD subtypes (LAD I and II) have been described with different defects in the leukocyte adhesion cascade: while LAD I is due to structural defects in β2 integrin preventing firm adhesion, LAD II is caused by defects in a specific Golgi GDP-fucose transporter that lead to a loss of selectin ligands on the cell surface and a defective leukocyte rolling. However, the LAD I, II and III disease symptoms are very similar, as all patients suffer from impaired wound healing, marked leukocytosis, osteopetrosis and recurrent bacterial infections due to compromised inflammatory response (Hanna and Etzioni, 2012).

Kindlin-3 null mice die shortly after birth because of severe gastrointestinal, cutaneous, cerebral and bladder hemorrhages, caused by the defective platelet adhesion (Moser et al., 2008). Further analysis of Kindlin-3 deficient mice has been able to show that osteopetrosis is due to severe adhesion and spreading defects of osteoclasts leading to strongly reduced bone resorption (Schmidt et al., 2011). The defects in the inflammatory response upon Kindlin-3 loss are due to impaired β2 integrin activation in leukocytes (Moser et al., 2009a), essential for leukocyte adhesion to vessel wall endothelial cells and subsequent transmigration into tissues (Ley et al., 2007). Here, it has been shown that Kindlin-3 mediates firm arrest of leukocytes on the vessel wall

by fully activating β2 integrin (headpiece opening) from a Talin mediated intermediate active conformation (Lefort et al., 2012), which is especially important when integrin ligand expression is low (Moretti et al., 2013; Morrison et al., 2013). In addition, Kindlin-3 can increase adhesion stability by promoting a complex with β2 integrin and calcium selective ion channel Orai1 which induces a local Ca^{2+} influx at focal adhesion sites, leading to increased integrin clustering (Dixit et al., 2012). Although Kindlin-3 depleted leukocytes show severe adhesion and migration defects, Kindlin-3 seems not to be essential for contact dependent T-cell (Morrison et al., 2013) nor for natural killer cell activation and polarization (Gruda et al., 2012).

To date, there are only few reports pointing to a role of Kindlin-3 in cancerogenesis. A proteomic screening has revealed that Kindlin-3 is highly expressed in various B-cell malignancies including B-cell lymphoma, chronic lymphocytic leukemia and Hodgkin lymphoma (Boyd et al., 2003). However, the consequences of deregulated Kindlin-3 expression are elusive. Furthermore, a recent report indicates that in human breast tumors elevated Kindlin-3 levels increase β1 integrin activity and Twist induced vascular endothelial growth factor (VEGF) expression, promoting primary tumor growth, angiogenesis and lung metastasis formation (Sossey-Alaoui et al., 2014).

Taken together, while the role of Kindlin-3 in LAD III is well described, its involvement in other hematologic diseases remains unclear. In light of the recent findings that Kindlin-3 is also expressed outside the hematopoietic system (Bialkowska et al., 2010; Sossey-Alaoui et al., 2014), it will be intriguing to investigate its function in these cells and whether Kindlin-3 interferes with other Kindlin isoforms as well.

1.6 Skin cancer

1.6.1 Comparison of wound healing and cancer in the skin

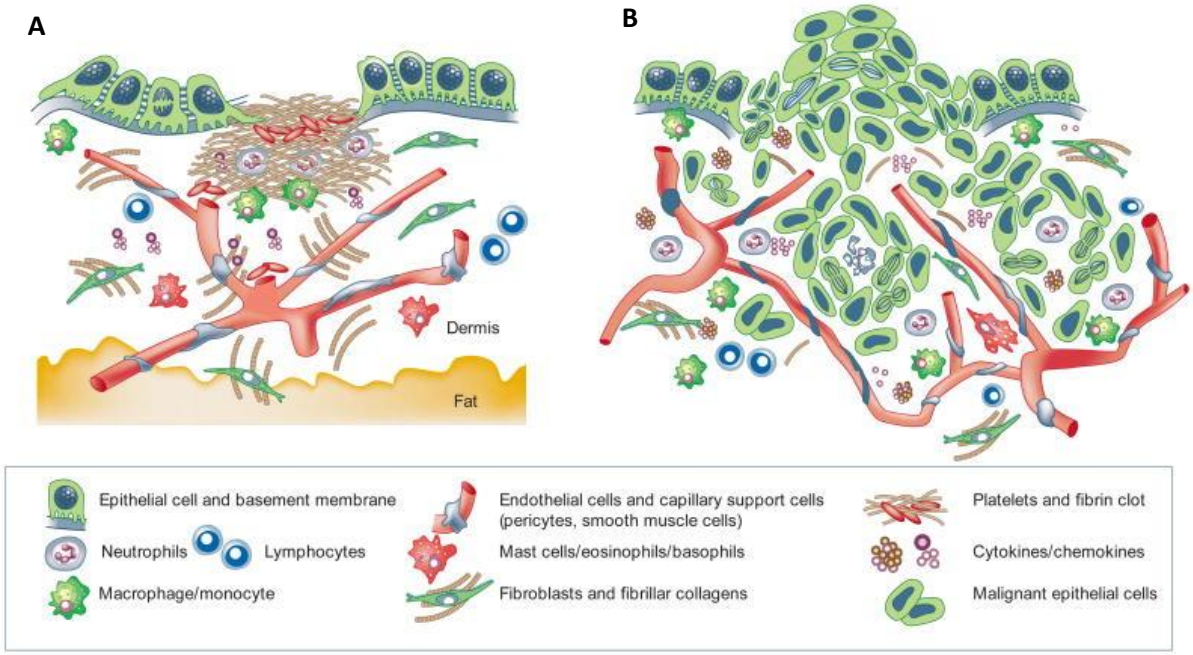

Figure32: Comparison of wound healing and invasive tumor growth
(**A**) Normal tissue is highly organized, where the basal keratinocytes are separated by the basement membrane from the dermis. Upon wounding activated platelets promote the formation of a fibrin clot and release cytokines and growth factors which facilitate the recruitment of immune cells and fibroblast, which become activated. These start to remodel the ECM and repair the dermal tissue before the keratinocytes start to re-epithelize the wound by a tightly controlled EMT-like process. After wound closure the increased cell proliferation, growth factor secretion and immune response are terminated and dermal fibroblasts are inactivated. (**B**) Invasive tumors are less organized. Neoplastic cells lose basement membrane and cell-cell contact in an uncontrolled manner and produce an array of cytokines and chemokines that attract and stimulate immune cells, fibroblasts and endothelial cells, promoting aberrant ECM remodeling and angiogenesis. In return, activated fibroblasts and infiltrating inflammatory cells secrete proteolytic enzymes, cytokines and chemokines, promoting neoplastic cell proliferation and invasion. In contrast to the wound healing response, signaling pathways controlling proliferation, ECM remodeling and angiogenesis remain constitutively active during tumor formation (modified from (Coussens and Werb, 2002)).

Wound healing is a highly dynamic process involving multiple interactions of epidermal cells, dermal fibroblasts and immune cells leading to a rapid wound closure and subsequent tissue repair. On the cellular level it involves de-differentiation, differentiation, migration, proliferation and apoptosis of various cell types to create the multilayered tissue that constitutes the skin.

The wound healing response starts immediately after injury with the development of a blood clot and a local inflammation, where immune cells prevent infection and remove debris (Figure32A). Subsequently, underlying dermal fibroblasts become activated to proliferate and to secret and

remodel the ECM. The fibroblasts of the hypodermis are mainly responsible for the ECM secretion for the early wound closure, whereas the upper dermal papillary fibroblast are only recruited during the later re-epithelialization step and are required for *de novo* HF formation (Driskell et al., 2013). For the re-epithelialization step keratinocytes at the periphery of the wound start migrating and proliferating in response to several growth factors, such as EGF, TGFα and keratinocyte growth factor (KGF). In an EMT-like process, migrating keratinocytes undergo several subcellular modifications including disassembly of hemidesmosomal links between epidermis and basement membrane, upregulation of fibronectin-binding integrins, rearrangement of the keratin filaments and dissolution of most desmosomes as well as cell polarization towards the wound, forming lamellipodia and focal contacts (Santoro and Gaudino, 2005). Once the overlaying keratinocytes have proliferated and migrated to repair the epidermis, they together with fibroblasts synthesize ECM proteins that are incorporated into the basement membrane. Further angiogenesis is stimulated locally to restore skin blood supply. Key signaling pathways during wound healing are Wnt/β-catenin, TGFβ, Hedgehog and Notch. After wounding, expression of multiple Wnt ligands is induced in the epithelium (Okuse et al., 2005). During the repair process Wnt/β-catenin signaling plays an important role in the construction of epithelial structures, particularly the HF as well as reconstitution of the dermal compartment, where it strongly influences fibroblast behavior (Cheon et al., 2002; Cheon et al., 2006; Ito et al., 2007). Of note, a recent study has shown that upon wounding recruited γδT cells activate Wnt signaling in dermal fibroblast, which is essential for the HF regeneration (Gay et al., 2013). The authors speculate that the low number of γδT cells in human skin compared to mice could explain why human skin scars but does not regenerate HFs. A prolonged or aberrant β-catenin activity in dermal fibroblast contributes to excessive fibrosis and scar formation (Cheon et al., 2005; Cheon et al., 2002). Similarly, prolonged TGFβ signaling is associated with hypertrophic scar formation and fibrosis. During cutaneous wound repair TGFβ signaling is highly activated and crucial in mediating the fibrotic mechanisms needed to restore the dermis as well as in modulating keratinocyte proliferation (Denton et al., 2009). Because TGFβ induces fibroblast contraction it is also proposed to promote wound closure (Martinez-Ferrer et al., 2010). The Hedgehog pathway and Notch pathway seem to participate in wound repair at multiple levels, such as angiogenesis, matrix production, and inflammation; however, molecular insights are largely missing (Bielefeld et al., 2013).

Whereas the wound healing process is a self-limiting process, tumor cells develop the capacity to expand, evolve and spread, promoted by a continuous inflammation (Figure32B). Tumors lose the

ability to respond to normal physiological regulatory feedback loops. Instead, tumors hijack and constitutively activate signaling pathways that are only transiently induced for wound repair, leading to striking similarities between the growth factors, cytokines and chemokines induced in healing wounds, and tumors (Chang et al., 2004). The similarities between the microenvironment of a healing wound and tumors, led the conclusion that "tumors are wounds that do not heal" (Dvorak, 1986). Indeed, chronic wounds are associated with increased risk for cancer (Coussens and Werb, 2002). Similarly, Wnt/β-catenin, TGFβ, Hedgehog and Notch are also key pathways in tumor formation and their deregulation give rise to distinct tumor entities, which will be discussed below.

1.6.2 Skin tumor entities

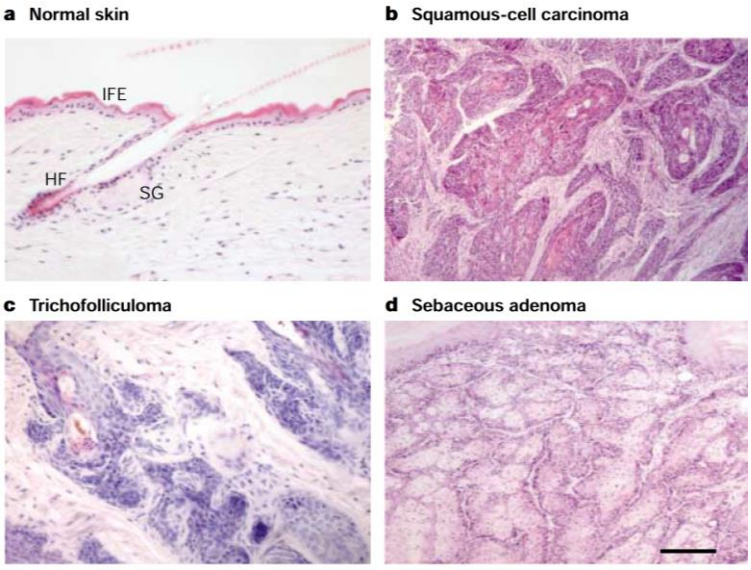

Figure33: Skin tumor entities
Mouse tissue H&E stainings of (**A**) normal skin, showing interfollicular epidermis (IFE), hair follicle (HF) and sebaceous gland (SG); (**B**) squamous-cell carcinoma, showing IFE differentiation; (**C**) trichofolliculoma, showing aberrant HF differentiation; (**D**) sebaceous adenoma, with numerous differentiated sebocytes. (**A**-**D**) scale bar: 100 μm; (modified from (Owens and Watt, 2003)).

In skin the tumor entity is mainly determined by the origin of the initiating cell: papillomas are derived from interfollicular epidermis or suprabasal cells, sebaceous adenoma arise from sebaceous gland and skin squamous-cell carcinoma (SCC) as well as trichofolliculomas originate from HF cells (Figure33A-D) (Perez-Losada and Balmain, 2003). While it has been assumed for a long time that basal cell carcinomas (BCCs) arise from HF cells, a recent study indicates that BCCs originate rather from interfollicular epidermis cells that are reprogrammed into an embryonic HF progenitor-like state (Youssef et al., 2012). In humans BCC and SCC are the most common non-melanoma skin cancers (Diepgen and Mahler, 2002), which will be discussed shortly below.

SCC is a malignant epidermal neoplasm that frequently manifests as a rough keratotic papule, a wart-like growth, or a fast growing tender protuberance, mostly with a central keratinous core. SCCs arise from multilayered epithelial cells, such as epidermis, oesophagus, cervix and the lining of the mouth leading to tumors with different frequency, entity and prognosis. The two major proto-oncogens or tumor suppressor genes responsible for SCC formation are K-ras and p53 respectively (White et al., 2011). Loss of the DNA damage sensor p53 and constitutive activity of K-ras, lead to uncontrolled proliferation and increased genome instability. P53 is mutated in more than 50% of all SCCs and mutations in p53 are frequently induced by UV exposure. Consequently, SCCs usually develop on sun exposed sites in the skin (Giglia-Mari and Sarasin, 2003).

BCC occurs more frequently than SCC (in a ratio 4:1) and thus is one of the most prevalent forms of skin cancer. BCCs can be superficial, nodular or morphoeic, which is associated with a more aggressive infiltrating growth pattern. These locally invasive skin tumors occur most commonly in sun exposed skin and are driven by UV induced mutations of genes encoding proteins in the Shh pathway. The most common mutations result in inactivation of Patched, which is the membrane receptor for Shh. In the absence of Shh ligand Patched inhibits signaling through smoothened, thus Patched inactivating mutations increase Shh signaling. Similar to SCC, also p53 is frequently mutated in BCC due to photo damage. However, p53 inactivation does not appear to be necessary for BCC formation in either mouse or human models (Fan et al., 1997; Grachtchouk et al., 2000).

1.6.3 Integrins and cancer

Due to the high similarity in many aspects of wound healing and tumor development, it is conceivable that integrins are crucial in both conditions. Indeed, loss of β1 integrin severely impairs wound repair in skin (Grose et al., 2002), and prevents the induction and maintenance of mammary tumors (White et al., 2004). In line, hyperactive integrins are associated with high skin tumor risk and dysfunctional integrins prevent skin tumor formation (see below).

Functionally, integrins are implicated in tumor cell proliferation, migration, adhesion and survival. In several tumor types, the expression of particular integrins correlates with increased disease progression and decreased patient survival. In tumors originating from epithelial cells, integrin expression pattern is often retained although the expression levels may be altered significantly between normal and tumor tissues. Most notably, the fibronectin receptors αvβ3, α5β1 and αvβ6, are usually expressed at very low levels in most adult epithelia, but can be highly upregulated in

some tumors, assisting adhesion, cell survival and proliferation on fibrotic tissue during invasion (see also section 1.6.4). Also switching of integrin heterodimer expression is frequently observed during tumor progression. In SCCs αvβ6 upregulation seems to correlate with αvβ5 downregulation, promoting cell survival (Janes and Watt, 2004).

Besides their expression, the integrin activity can be altered and indeed, several mutations in β1 integrin have been found in human SCC, influencing integrin activity and tumor development (Evans et al., 2004). Most prominently, a mutation in the β1 integrin I-like domain (T188I) was shown to constitutively activate β1 integrin, inducing sustained Erk-MAPK signaling independent of cell spreading and suppressing cell differentiation (Evans et al., 2003). In a chemical cancerogenesis mouse model, overexpression of T188I mutant β1 integrin in skin promotes tumor susceptibility and conversion of benign to malignant skin tumors (Ferreira et al., 2009). In addition to integrin activity, integrin recycling was revealed to have profound effects on tumor cell invasion. Ras-related in brain (Rab) GTPases direct integrins to the leading edge of invading tumors and coordinately regulate integrin and growth factor receptor recycling, enhancing growth factor signaling and invasiveness (Caswell et al., 2008; Caswell et al., 2007).

Not only integrins on the surface of tumor cells, but also the expression on tumor-associated cells can profoundly influence the malignant potential of a tumor, promoting ECM remodeling, angiogenesis and immune cell infiltration. Especially the cross talk of integrins and growth factor/cytokine receptors between tumor cell and tumor stroma is vital for many aspects of tumor progression. Integrins are able to directly or indirectly associate with growth factor or cytokine receptors, modulating the surface expression, ligand affinity and signaling of the receptors. A cooperative signaling occurs between integrins and members of the EGF receptor family: on the one hand, integrin ligand binding can induce EGF receptor phosphorylation independently of EGF, resulting in increased ERK-MAPK activation, tumor cell proliferation and survival (Moro et al., 2002). On the other hand, EGF has been suggested to increase integrin αvβ5 mediated migration by inducing Src kinase dependent phosphorylation of p130Cas and subsequent activation of GTPase Rap1 which increases Talin activation (see section 1.2.4.3) (Ricono JM et al., 2009). Furthermore, integrins can regulate the release of growth factor ligands from the ECM. The instrumental role of αv-class integrins in the activation of TGFβ, a well characterized promoter of tumor progression, is discussed in section 1.3.6.2.

Integrins and growth factor/cytokine receptor can also reciprocally regulate the surface expression and activity of one another. For example, the chemokine receptor CXCR4 increases cell

adhesion to fibronectin and collagen by promoting the activity of various β1 class integrins in small cell lung cancer cells (Hartmann et al., 2005). Moreover, activation of CXCR4 on various tumor cells increases the expression of integrins, such as α5β1 and αvβ3, increasing cell adhesion and invasion (Engl et al., 2006; Sun et al., 2007). Besides influencing growth factor/cytokine receptor, integrins have been shown to regulate the localization and activity of matrix-degrading proteases, such as MMP2 and uPA, important for tumor progression (see section 1.6.4).

One major hallmark for cancer cell progression is the loss of adhesion dependent growth control. Interestingly, integrins can have a profound influence on tumor survival, both in the presence and absence of ligands. In adherent cells, both β1- and αv-class integrin induce FAK and Src kinase activity and subsequent p130Cas phosphorylation, promoting survival signals through the Akt and Erk pathway. Furthermore, ligand bound integrins prevent pro-apoptotic signaling cascades initiated in detachment induced apoptosis (anoikis) (Frisch and Screaton, 2001), as well as integrin mediated death (IMD). In contrast to anoikis, IMD can also be induced in adherent cells by a subset of unligated integrins (shown for β1 and β3 integrin), which then bind and activate Caspase8, leading to apoptosis (Stupack et al., 2001). However, recent evidences also point to an anti-apoptotic role for unligated integrins in tumor cells. Unligated αvβ3 is able to induce cell survival signals by recruiting and activating Src and p130Cas in a FAK-independent manner (Desgrosellier et al., 2009). Also unligated αvβ6 integrin is able to promote survival signaling by suppressing anoikis in SCC cells (discussed below). Thus, increasing the expression of particular integrin heterodimers is an elegant strategy for tumor cells to be able to adapt to novel ECM environments during invasion or even escape adhesion dependent growth control.

1.6.4 αvβ6 integrin and cancer

Intriguingly, integrin αvβ6 is highly upregulated in various carcinomas of the lung, breast, pancreas, stomach, colon, ovary, salivary gland as well as oral and skin SCC (reviewed in (Bandyopadhyay and Raghavan, 2009)). In these cancers an increased expression of αvβ6 is often associated with a poor patient prognosis and enhanced cell invasion, cell survival, protease activity and EMT (Ahmed et al., 2002; Thomas et al., 2006). Mechanistic insights of how αvβ6 integrin promotes tumor progression and metastasis, only start to emerge recently.

On the one hand, αvβ6 integrin enhances spreading and migration of keratinocytes on fibronectin, tenascin C and vitronectin, all of which are components of the early wound matrix and often

upregulated in the tumor stroma. The αvβ6 integrin mediated cell motility was shown to be regulated by its interaction with HS1-associated protein X-1 (HAX1), which promotes αvβ6 clathrin-dependent endocytosis and invasion in SCC (Ramsay et al., 2007).

On the other hand, αvβ6 seems to play a role in the activity control of proteases, such as MMP9, 3 and uPA in various cancers, promoting ECM degradation as well as cell detachment from the basement membrane (Li et al., 2003; Thomas et al., 2001). Indeed, at the invading edge of colon cancer high αvβ6 levels are accompanied by the elevated expression of the pro-enzyme form of type IV collagenase and MMP9 (Yang GY et al., 2008). Interestingly, the MMP9 activity is modulated through direct ERK binding to the cytoplasmic β6 integrin tail, whereas activity of MMP3 has been reported to be modulated indirectly through binding of the Src family kinase FYN and subsequent FAK recruitment upon fibronectin binding. The induced activation of the ERK-MAPK pathway enhances MMP3 transcription (Li et al., 2003). But also a direct binding of uPA to the cytoplasmic tail of αvβ6 in ovarian cancer cells, but not in normal ovarian cells, has been shown to promote ECM degradation and to correlate with elevated TGFβ signaling (Saldanha et al., 2007).

How increased αvβ6 expression triggers EMT in different cancers is not fully understood. In colon carcinoma cells and oral SCC the EMT promoting effect of αvβ6 seems to be partly due to increased TGFβ1 release (see also section 1.6.5) (Bates et al., 2005; Ramos et al., 2009). Interestingly, deletion of the last 11 amino acids of the cytoplasmic β6 integrin tail abolishes the EMT promoting effect as well as the invasive activity of αvβ6 but not the αvβ6-dependent adhesion or migration (Morgan et al., 2011). A screening study for specific interaction partners to this unique terminal 11 amino acids β6 tail sequence has revealed that psoriasin (also known as S100A7) directly binds to it. The psoriasin-β6 tail interaction seems to be crucial for αvβ6 dependent invasiveness of carcinoma cells; however the molecular mechanism remains elusive (Morgan et al., 2011).

Upregulation of αvβ6 integrin is also able to generate adhesion independent survival signals, which are crucial for tumor cell invasion and subsequent metastasis formation. By switching the integrin profile from αvβ5 to αvβ6 high expression, oral SCC cells are able to upregulate Akt signaling independent of ligand binding, protecting them from anoikis (Janes and Watt, 2004). Whether non-transformed keratinocytes, which transiently upregulate αvβ6 integrin during wound healing, also become more resistant to apoptosis, is still an open question.

Taken together, αvβ6 promotes cancer progression on various levels ranging from enhanced adhesion and migration on various substrates to control of protease activity, EMT and cell survival. The selective expression in many types of cancer and reversion of oncogenic effects upon inhibition, by blocking antibody, shRNA or small peptides (Hsiao et al., 2010; Weinreb et al., 2004), positions αvβ6 as a suitable target for the development of cancer therapies.

1.6.5 The paradoxical role of TGFβ signaling in cancer

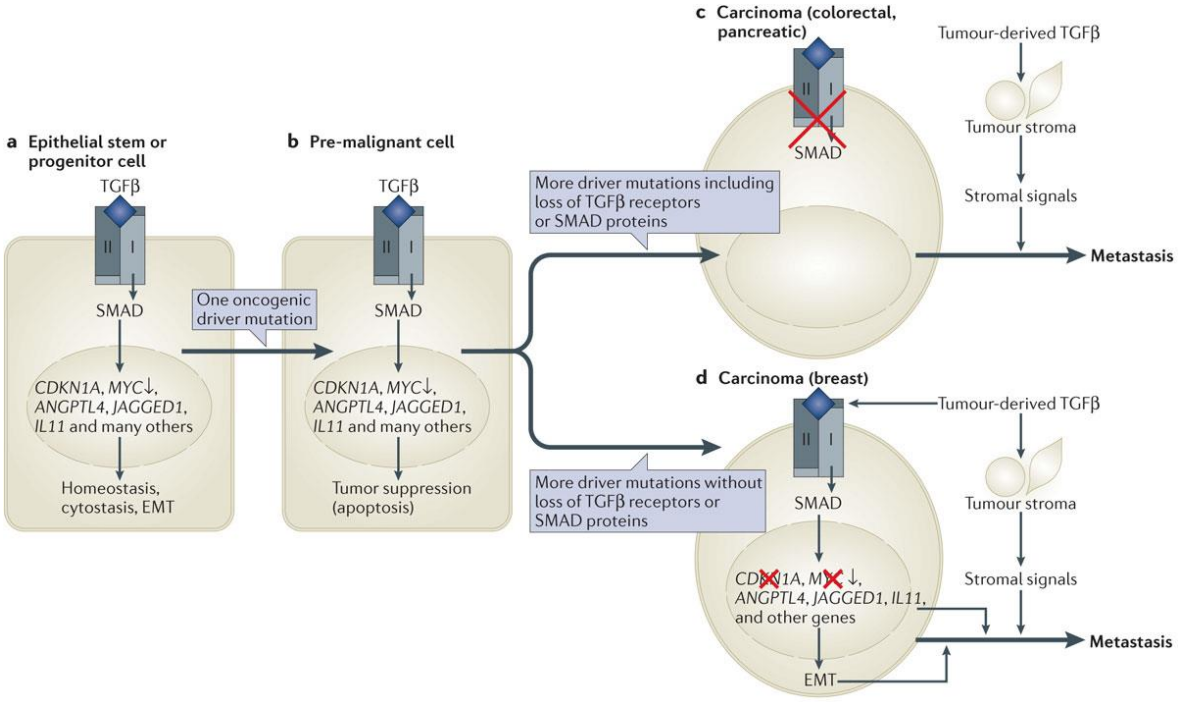

Figure34: The effect of TGFβ signaling on tumor initiation and progression
(**A**) TGFβ signaling via Smad transcription factor regulates multiple cytostatic genes and genes involved in homeostasis in normal epithelial cells. (**B**) Furthermore in pre-malignant epithelial cells, TGFβ signaling promotes apoptosis, thus acting as a tumor suppressor. During tumor progression, cells need to accumulate additional alterations to overcome the suppressive effect of TGFβ. (**C**) Tumor cells have been shown to acquire inactivating mutations in TGFβ receptor and/or Smad4 genes. As a consequence tumor cells are able to grow in a TGFβ-rich tumor stroma environment and at the same time benefit from pro-tumorigenic effects, such as TGFβ induction of stroma-derived cytokines promoting cell survival. (**D**) Alternatively, tumor cells can acquire mutations in TGFβ target genes, leading to loss of TGFβ mediated growth control, while retaining intact Smad signaling machinery. Thus cancer cells not only survive in a TGFβ-rich microenvironment, but also respond to TGFβ, resulting in canonical and non-canonical TGFβ signaling transduction promoting EMT and an invasive tumor cell behavior (modified from (Massague, 2012)).

TGFβ is a multifunctional cytokine which is produced by many different cell types and a loss of balance in TGFβ signaling has been implicated in the pathogenesis of many diseases including cancer, fibrosis autoimmune and vascular diseases (Blobe et al., 2000; Massague, 2008).

The effects of TGFβ during tumor development are paradoxical since it is a powerful tumor suppressor in the context of pre-malignant cells, but an enhancer of invasion and metastasis in the context of more advanced cancer cells (Massague, 2008). The tumor suppressive effect of TGFβ is based on its cytostatic pro-apoptotic and cell differentiation effect in a large variety of cell types. During the early stages of tumorigenesis when cells acquire oncogenic mutations, TGFβ inhibits cell cycle progression and triggers apoptosis (Bardeesy et al., 2006; Guasch et al., 2007). Key effector of the growth control in tumors is c-myc which is repressed through the canonical TGFβ pathway. Mechanistically upon TGFβ receptor activation, a preexisting complex of R-Smad and the transcription factors E2F4/5 and DP1 associate with Smad4 and translocate in the nucleus where it binds to a proximal element of the c-myc promoter suppressing its activation (Chen et al., 2002). At the same time, R-Smad and Smad4 are able to complex with forkhead box protein O (FoxO) transcription factors. In the nucleus these complexes bind to the promoters of several cyclin-dependent kinase inhibitors, including p15 and p21, promoting their transcription (Figure34A) (Gomis et al., 2006). Thus, activated R-Smad can act as a transcriptional repressor or activator, depending on the binding partner.

A detailed mechanism of how premalignant cells become programmed for apoptosis through TGFβ is still missing. The pro-apoptotic effect of TGFβ seems to involve multiple pathways including the induction of the death-associated protein (DAP)-kinase (Jang et al., 2002), the signaling factor growth arrest and DNA-damage inducible, beta (Gadd45b) (Yoo et al., 2003), the death receptor FAS (Kim et al., 2004) and the pro-apoptotic effector BIM (Ramesh et al., 2008). In addition, TGFβ inhibits the activation of the PI3K-Akt pro-survival pathway by inducing the 5' inositol phosphatase Src homology 2 (SH2) domain-containing 5' inositol phosphatase (SHIP) (Valderrama-Carvajal et al., 2002).

Besides promoting EMT (discussed below), TGFβ signaling can inhibit tumor progression by inducing cell differentiation and driving precursor cells into a less proliferative state (Derynck R and Akhurst RJ, 2007). For example, TGFβ modulates differentiation through inhibition of inhibitor of differentiation (Id) proteins that negatively regulate cell differentiation by interfering with pro-differentiation transcription factors, such as basic helix-loop-helix (bHLH) (Ruzinova and Benezra, 2003).

In many different tumor entities, such as skin cancer, breast cancers or head or neck SCC, loss of TGFβ induced proliferation control is one prominent feature (Massague, 2008).

In line, transgenic mice expressing a dominant negative TβRII or lacking TβRII in the epidermis or mammary glands show increased tumor formation and metastatic progression (Bottinger et al., 1997; Go et al., 1999; Guasch et al., 2007). Furthermore, deletion of TGFβ1 in the skin leads to increased tumor susceptibility and promotes malignant conversion metastasis formation, while TGFβ1 overexpression suppresses initial tumor formation but is able to promote the progression and invasiveness in chemical cancerogenesis mouse models (Cui et al., 1996; Glick et al., 1994; Mohammed et al., 2010).

Once pre-malignant cells eliminate the sensitivity to the tumor suppressive effect of the TGFβ pathway, cancer cells can benefit from a TGFβ-rich microenvironment that favors tumor progression through EMT promotion, deregulated inflammation as well as enhanced fibroblast activation in the tumor stroma (Figure34B-D) (Yang et al., 2010). Indeed, loss of TGFβ tumor suppressive responses has been shown to occur by inactivating mutations in TβRII and Smad4, leading to a complete inactivation or more downstream by mutation of essential tumor suppressive Smad target, such as cyclin-dependent kinase inhibitor 2B (CDKN2B) and c-myc, whereas the potentially remaining Smad signaling capacity is able to promote EMT (Figure34) (Massague, 2008). In contrast to the spatially and temporally tight controlled EMT during embryonic development or wound healing, this process is more disorganized in advanced cancer. TGFβ induces EMT by canonical as well as non-canonical TGFβ signaling. R-Smad activation promotes expression of the zinc-finger binding proteins Snail and Slug which promote EMT by inhibiting E-cadherin transcription (Vincent et al., 2009). Independent of Smad signaling, EMT is promoted by the TGFβ induced activation of the p38/MAPK pathway (Bakin et al., 2002), RhoA signaling (Bhowmick et al., 2001), PI3K activity (Kattla et al., 2008) or phosphorylation of Par6 through the activated TGFβ receptor kinase (Ozdamar et al., 2005).

Taken together under normal physiological conditions or during onset of tumor formation, TGFβ exerts cytostatic effects and functions as a tumor suppressor, whereas at later stages of cancer progression it functions as a tumor promoter assisting in metastatic progression by inducing EMT and modulating the tumor microenvironment.

1.6.6 Wnt signaling in cancer

Mutations in the Wnt pathway are often observed in cancer, especially in tissues which depend on Wnt signaling for self-renewal or repair. Indeed, the Wnt pathway has turned out as an essential player for tumor growth and progression (Beronja et al., 2013; Malanchi et al., 2008). It has been estimated that approximately 10% of all tissue samples sequenced from all cancers display mutations in the CTNNB1 gene (Forbes et al., 2011). Most of these mutations are located within the β-TrCP binding motif of the N-terminal β-catenin segment in various tissues, leading to stabilized β-catenin and increased Wnt signaling (Chan et al., 1999; Morin et al., 1997; Rubinfeld et al., 1997). Indeed, sustained activation of canonical Wnt signaling in adult epidermis promotes HF derived pilomatricomas (benign skin tumor derived from hair matrix) and trichofolliculomas (benign HF tumor) in transgenic mice and humans (Chan et al., 1999; Gat et al., 1998; Lo Celso et al., 2004; Silva-Vargas et al., 2005). Also in melanoma oncogenic β-catenin stabilizing mutations are frequent found (Rubinfeld et al., 1997). In addition, mutations are also frequently seen in the β-catenin recruiting motifs of APC as well as Axin2 (Liu et al., 2000; Morin et al., 1997). Strikingly, the majority of colorectal cancers carry inactivating APC mutations resulting in increased β-catenin stability (Korinek et al., 1997; Morin et al., 1997; Rowan et al., 2000). Of note, hereditary loss-of-function mutations of APC cause a condition known as familial adenomatous polyposis (FAP) (Groden et al., 1991). Affected individuals develop multiple polyps in the large intestine, which eventually progress to malignancy.

Surprisingly, also the inhibition of Wnt/β-catenin signaling can promote some types of cancers. In skin, mutation of the β-catenin binding site in Lef1 induces the formation of sebaceous gland tumors in transgenic mice (Niemann et al., 2002) and humans (Takeda et al., 2006). These data suggest that an optimal level of Wnt/β-catenin signaling exists that is required for tissue homeostasis, and that either hyperactivation or attenuation of signaling can lead to tumor formation.

2 Aim of the thesis

My PhD project focused on the role of Kindlin-1 in skin homeostasis and tumor development. Kindlin-1 belongs to focal adhesion protein family of three members (Kindlin-1, -2 and -3). All Kindlins are involved in cell substrate adhesion by regulating the activity of the cell surface adhesion receptors integrin and linking them to the actin cytoskeleton via recruitment of adaptor proteins such as ILK. In epithelial cells Kindlin-1 and -2 are co-expressed, while Kindlin-3 is only expressed in hematopoietic cells. In humans loss-of-function mutations in *KINDLIN-1* and *KINDLIN-3* impair the integrin function in the affected organs causing Kindler syndrome (KS) and leukocyte adhesion deficiency III syndrome, respectively. KS is a rare skin genodermatosis characterized by trauma induced skin blistering, areas of cutaneous atrophy and hyperkeratosis, pigmentation defects, photosensitivity, premature skin aging and an increased risk for skin cancer. Especially the increased risk for skin cancer in KS patients is highly unexpected, as hyperactive integrins are associated with high skin tumor risk and dysfunctional integrins prevent skin tumor formation. This contradiction has strongly suggested that the absence of Kindlin-1 triggers novel, integrin-independent oncogenic function(s) that are sufficient to induce skin tumors early in the life of KS patients.

To explore these novel Kindlin functions *in vivo*, the **first aim** was to generate and characterize a suitable mouse model for the human KS disease, allowing to monitor the consequences of Kindlin-1 loss at different developmental stages and especially at older age.

By comparing the Kindlin-1 mouse model with transgenic mice expressing a Kindlin-binding deficient β1 integrin mutants in the skin, the contribution of the major skin integrin to the KS phenotype should be dissected as a **second aim**.

My **third aim** was to analyze the impact of Kindlin-1 loss on the different cutaneous epithelial stem cell lineages and their homeostasis. Further, the affected molecular skin signaling pathways were investigated employing and establishing numerous *in vitro* and *in vivo* assays.

The **forth aim** comprised the investigation of whether the increased tumor risk in KS patients could be recapitulated in a chemical cancerogenesis mouse model and to thoroughly analyze and quantify the developing tumors by histology. In addition, I identified the molecular mechanism contributing to the increased skin cancer risk in mice and humans.

After defining the role of Kindlin-1 in skin stem cell homeostasis and identifying novel Kindlin-1 regulated signaling pathways in skin, as **fifth aim**, these findings were compared to the function of Kindlin-3 for hematopoietic stem and precursor cells in the bone marrow.

3 Short summary of manuscripts

3.1 Kindlin-1 controls Wnt and TGF-β availability to regulate cutaneous stem cell proliferation

Emanuel Rognoni, Moritz Widmaier, Madis Jakobson, Raphael Ruppert, Siegfried Ussar, Despoina Katsougkri, Ralph T. Böttcher, Joey E. Lai-Cheong, Daniel B. Rifkin, John McGrath, Reinhard Fässler

Kindlin-1 is an integrin tail binding protein that controls integrin activation, which is important for cell adhesion to the extracellular matrix. Mutations in the Kindlin-1 (*KINDLIN-1*) gene cause Kindler syndrome in humans, which is characterized by skin blisters, pigmentation defects, skin atrophy and increased skin tumor susceptibility. Of note, the increased tumor risk is highly unexpected, as hyperactive integrins are associated with high skin tumor risk and dysfunctional integrins prevent skin tumor formation.

This contradiction prompted us to develop a mouse model for an epidermal specific deletion of Kindlin-1, enabling us for the first time to fully recapitulate the human Kindler syndrome disease in mice and explore the role of Kindlin-1 in tumor development. Following the progression of Kindler syndrome disease during the whole life span of the animals, we were able to show that Kindlin-1 controls epithelial stem cell homeostasis and consequently loss of Kindlin-1 led to enlarged and hyperactive stem cell compartments and aberrant stem cell commitment, resulting in severe hair follicle abnormalities. *In vivo* and *ex vivo* studies of Kindlin-1 deleted keratinocytes revealed, in addition to the expected β1 integrin associated adhesion defect, a severe deregulation of the Wnt/β-catenin and TGFβ signaling pathway, both important for skin epithelial stem cell quiescence, self-renewal and differentiation.

Mechanistically, we identified that (1) Kindlin-1 controls adhesion of epidermal cells primarily by β1 integrin and (2) in stem cells Kindlin-1 inhibits proliferation by inducing αvβ6 integrin-mediated TGFβ release and (3) triggers cutaneous epithelial stem cell commitment by regulating Wnt ligand expression and preventing aberrant Wnt/β-catenin signaling in an integrin independent manner.

The relevance of our findings is underscored by the fact that we confirmed similar defects in TGFβ and Wnt signaling pathways in human Kindler syndrome patients.

3.2 Loss of Kindlin-1 causes skin atrophy and lethal neonatal intestinal epithelial dysfunction

Siegfried Ussar, Markus Moser, Moritz Widmaier, **Emanuel Rognoni**, Christian Harrer, Orsolya Genzel-Boroviczeny, Reinhard Fässler

The human disease Kindler syndrome is caused by mutations in the (*KINDLIN-1*) gene and is characterized by skin blistering, pigmentation defects, skin atrophy and cancer. Kindlin-1 belongs to a family (Kindlin-1, -2 and -3) of focal adhesion proteins which bind to the cytoplasmic tails of several integrins and promote the activation of these cell surface receptors, essential for cell adhesion to the extracellular matrix, migration, proliferation as well as survival.

In this study we generated a constitutive Kindlin-1 null mouse which develops some symptoms of the human Kindler syndrome disease including skin blisters and atrophy. Surprisingly, Kindlin-1 null mice die shortly after birth due to an ulcerative colitis-like intestinal dysfunction. Similar to the skin, the intestinal epithelial cells express the Kindlin isoforms Kindlin-1 and -2.

Mechanistically, loss of Kindlin-1 leads to impaired intestinal epithelial integrin function, which cannot be compensated by Kindlin-2, resulting in a shear stress promoted detachment of the intestinal epithelium and subsequent induction of a severe inflammatory response in the whole intestine. Of note, a recent study reports that also human subjects with Kindler syndrome showed ulcerative colitis-like symptoms confirming our mouse findings; however, the human intestinal symptoms are less severe.

In summary, this mouse model enables us to study the development of the ulcerative colitis-like intestinal dysfunction in Kindler syndrome disease, underlining that loss of Kindlin-1 affects integrin activity in multiple epithelial structures beyond the skin epidermis.

3.3 Kindlin-3 mediated integrin adhesion is dispensable for quiescent hematopoietic stem cells but required to maintain activated hematopoietic stem and precursor cells

Raphael Ruppert, Markus Moser, Markus Sperandio, **Emanuel Rognoni**, Martin Orban, Wen-Hsin Liu, Ansgar Schulz, Robert A. J. Oostendorp, Steffen Massberg, and Reinhard Fässler

The Kindlin family consists of three members (Kindlin-1, -2 and -3) which bind to the cytoplasmic tail of most integrin β subunits, which compose a family cell surface receptors essential for cell adhesion, migration, survival and proliferation.

Interestingly, the expression of Kindlin-3 is restricted to the hematopoietic system and mutation of the *KINDLIN-3* gene in human leads to leukocyte adhesion deficiency type III (LAD III), while constitutive deletion of Kindlin-3 in mice is embryonic lethal, due to severe hemorrhages in multiple organs. Both hematological disorders are characterized by impaired adhesion and migration of multiple blood cell linages because of impaired integrin function. Kindlin-3 is highly expressed in hematopoietic stem and precursor cells, but in contrast to mature blood lineages, such as leukocytes, platelets and osteoclasts, the influence of Kindlin-3 loss in these compartments is unknown. After embryonic development, all mature blood cell linages are generated and maintained by a pool of hematopoietic stem cells residing in specialized niche compartments in the bone marrow. Quiescence, retention, restricted activation and differentiation of the hematopoietic stem cells is controlled by a complex cross talk between the hematopoietic stem cell and multiple niche environment factors including extracellular matrix components, adhesion molecules such as integrins, CD44 or selectins, growth factors, cytokines and morphogenes.

In this study, we generated chimeric mice by transplanting fetal liver cells from Kindlin-3 wild type and knockout animals into lethally irradiated wild type recipients, circumventing the early postnatal lethality of Kindlin-3 null mice. Upon transplantation we show that hematopoietic precursor cells depleted for Kindlin-3 are severely impaired in their bone marrow homing ability because of attenuated integrin mediated adhesion to the endothelial cells of the vessels. Also the homing competent fraction of Kindlin-3 deficient hematopoietic stem cells can only be retained for a while. The defective integrin activation leads to premature release of activated Kindlin-3 deficient hematopoietic precursor cells into the circulation causing a lack of mature effector cells, such as platelets, neutrophils and erythrocytes, which in turn leads to a sustained angiopoietic

feedback signal fueling stem cell activation. Thus, Kindlin-3 deficient hematopoietic stem cells never enter quiescence and are eventually lost due to exhaustion. Interestingly, in the presence of unaffected wild type hematopoietic stem cells which guarantee normal blood effector cell homeostasis, Kindlin-3 deficient hematopoietic stem cells can enter quiescence and be retained in the bone marrow.

In summary, we conclude that after homing, Kindlin-3 is dispensable to maintain hematopoietic stem cell quiescence in the bone marrow niche. In sharp contrast, Kindlin-3 mediated integrin activity is absolutely essential for the retention and function of activated hematopoietic stem precursor cells in the bone marrow compartment. Of note, a blood sample from a LAD III patient revealed a highly increased number of circulating hematopoietic stem precursor cells, indicating that Kindlin-3 loss impairs hematopoietic stem cell and precursor cell homeostasis also in humans.

3.4 Integrins synergistically induce the MAL/SRF target gene ISG15 to ISGylate cytoskeletal and focal adhesion proteins necessary for cancer cell invasion

Michaela-Rosemarie Hermann, **Emanuel Rognoni**, Madis Jakobson, Moritz Widmaier, Assa Yeroslaviz, Roy Zent, Guido Posern, Ferdinand Hofstädter and Reinhard Fässler

Integrins are cell surface adhesion receptors important for adhesion and migration. Depending on the bound ligand and engaged integrin heterodimer, they mediate different short-term signaling effects, involving recruitment of intracellular signaling proteins and long-term changes, resulting in actin cytoskeleton rearrangement, gene transcription modulation as well as promotion of cell survival and proliferation. How different integrin heterodimers execute individual long-term effects and whether they influence each other, is largely unknown. To answer this question for the fibronectin binding αv- and β1-class integrins, we generated single integrin class expressing cell lines by reconstituting pan integrin knockout fibroblast with similar levels of only αv (αv-cells) or β1 (β1-cells), while cells reconstituted with both integrin subtypes (αv/β1-cells) represented the wild type situation.

In this study, we report that αv- and/or β1-class integrin expressing cells differ in their monomeric globular (g)-Actin pool levels correlating with low nuclear megakaryocyte acute leukemia protein

(MAL) levels and MAL/ serum response factor (SRF) signaling in αv single, intermediate in β1 and high in αv/β1 double expressing cells. The pool of free g-Actin is controlled by numerous actin binding proteins such as Thymosin β4 and Cofilin as well as integrin mediated activation of small Rho family GTPases, which stimulate g-Actin polymerization into filamentous (f)-Actin structures. Free cytosolic g-Actin associates with MAL and inhibits its nuclear translocation and association with SRF. Once g-Actin is sequestered into f-Actin structures, free MAL is able to translocate into the nucleus and to associate with SRF inducing transcription of MAL target genes, including cytoskeletal proteins like actin and multiple integrin associated focal adhesion proteins.

We show that αv- and β1-class integrins synergistically induce MAL/SRF activity and target gene expression through modulation of the free g-Actin pool. Indeed, g-Actin is significantly more sequestered and f-Actin less severed in β1-cells and even more αv/β1-cells compared to αv-cells. Among the known targets of MAL, we identified the particularly interesting ubiquitin-like interferon-stimulated gene 15 (ISG15) to be regulated by integrin-MAL signaling and independent of interferon, as previously described. ISG15 binds covalently to specific lysine residues of targets proteins influencing their function directly or interfering with protein ubiquitination at multiple levels, eventually modulating proteasomal degradation and protein stability. Following mass spectrometry analysis of ISG15 modified proteins revealed have ISGylation of many proteins that are transcriptionally regulated by MAL/SRF signaling, including multiple integrins, actin, focal adhesion and actin binding proteins and the newly identified MAL targets Talin and Eplin.

The increased ISGylation of these proteins in αv/β1-cells promotes invasiveness of mouse fibroblasts and human breast cancer cells and is correlated with poor patient survival. By dissecting the fibronectin binding αv and β1 integrin class functions, we have revealed a novel autoregulatory feed-forward loop connecting integrin adhesion, MAL/SRF and ISG15, which modulates adhesion and actin cytoskeleton remodeling, essential for cell spreading, migration and invasion.

3.5 Integrin-linked kinase at a glance

Moritz Widmaier, **Emanuel Rognoni**, Korana Radovanac, S. Babak Azimifar, Reinhard Fässler

Integrin-linked-kinase (ILK) is a focal adhesion protein which is ubiquitously expressed and is involved in multiple cellular processes including actin rearrangement, cell polarization, spreading, migration, proliferation and survival.

ILK is able to bind to the cytoplasmic tail of the integrin β subunit directly or via Kindlin mediated recruitment and in the last years ILK has emerged as a central hub of focal adhesion signaling through its interaction with multiple proteins listed in the review. The ILK function is mainly influenced by its two most prominent binding partners the adaptor proteins Pinch and Parvin, forming a ternary complex termed ILK-Pinch-Parvin (IPP) complex. Because Parvin as well as Pinch constitute protein families of two or three members respectively, which differ in functions and expression patterns, each IPP complex can execute different functions which are summarized in the review.

Besides the prominent localization of ILK at focal adhesion sites, in different cell types, ILK seems to play an important role at cell-cell adherens junctions, influencing the cell-cell contact formation and recruitment of tight junction proteins. At centrosomes, ILK controls centrosome function and centrosome clustering during mitotic spindle organization, and in the nucleus it has been shown to regulate the expression of several genes. Furthermore, in β1 integrin containing nascent adhesion sites, ILK is essential for capturing microtubule tips and connecting them to the cortical actin network, allowing exocytosis of caveolar carriers at the plasma membrane. In this review, we have summarized the novel ILK functions at the different subcellular compartments and illustrated the proposed molecular mechanisms.

Novel insights of the ILK crystal structure as well as transgenic mouse studies targeting critical residues of the putative ILK kinase domain, demonstrated that this domain lacks any catalytic activity. To illustrate these findings, we compared the kinase center of the structurally related bona fide kinase protein kinase A (PkA) with the putative ILK kinase domain highlighting the structural hurdles within the ILK kinase domain which inhibit phosphorylation of any substrate.

Taken together, while an increasing number of new ILK interaction partners, subcellular localizations and functions are emerging, mechanistical details for these functions are often lacking behind. Now that the kinase function of ILK could be finally ruled out, its prominent role in cancer has to be redefined, which we discussed at the end of the review.

4 References

Aberle, H., Bauer, A., Stappert, J., Kispert, A., and Kemler, R. (1997). beta-catenin is a target for the ubiquitin-proteasome pathway. The EMBO journal *16*, 3797-3804.

Ahmed, N., Riley, C., Rice, G.E., Quinn, M.A., and Baker, M.S. (2002). Alpha(v)beta(6) integrin-A marker for the malignant potential of epithelial ovarian cancer. The journal of histochemistry and cytochemistry : official journal of the Histochemistry Society *50*, 1371-1380.

Aktary, Z., and Pasdar, M. (2012). Plakoglobin: role in tumorigenesis and metastasis. International journal of cell biology *2012*, 189521.

Alexandre, C., Baena-Lopez, A., and Vincent, J.P. (2014). Patterning and growth control by membrane-tethered Wingless. Nature *505*, 180-185.

Alonso, L., and Fuchs, E. (2003). Stem cells in the skin: waste not, Wnt not. Genes & development *17*, 1189-1200.

Aluwihare, P., Mu, Z., Zhao, Z., Yu, D., Weinreb, P.H., Horan, G.S., Violette, S.M., and Munger, J.S. (2009). Mice that lack activity of alphavbeta6- and alphavbeta8-integrins reproduce the abnormalities of Tgfb1- and Tgfb3-null mice. Journal of cell science *122*, 227-232.

Ambler, C.A., and Watt, F.M. (2007). Expression of Notch pathway genes in mammalian epidermis and modulation by beta-catenin. Developmental dynamics : an official publication of the American Association of Anatomists *236*, 1595-1601.

An, Z., Dobra, K., Lock, J.G., Stromblad, S., Hjerpe, A., and Zhang, H. (2010). Kindlin-2 is expressed in malignant mesothelioma and is required for tumor cell adhesion and migration. International journal of cancer Journal international du cancer *127*, 1999-2008.

Andersson, E.R., Sandberg, R., and Lendahl, U. (2011). Notch signaling: simplicity in design, versatility in function. Development *138*, 3593-3612.

Andl, T., Reddy, S.T., Gaddapara, T., and Millar, S.E. (2002). WNT signals are required for the initiation of hair follicle development. Developmental cell *2*, 643-653.

Annes, J.P., Chen, Y., Munger, J.S., and Rifkin, D.B. (2004). Integrin alphaVbeta6-mediated activation of latent TGF-beta requires the latent TGF-beta binding protein-1. The Journal of cell biology *165*, 723-734.

Annes, J.P., Munger, J.S., and Rifkin, D.B. (2003). Making sense of latent TGFbeta activation. Journal of cell science *116*, 217-224.

Arai, F., and Suda, T. (2008). Quiescent stem cells in the niche. In StemBook (Cambridge (MA)).

Arita, K., Wessagowit, V., Inamadar, A.C., Palit, A., Fassihi, H., Lai-Cheong, J.E., Pourreyron, C., South, A.P., and McGrath, J.A. (2007). Unusual molecular findings in Kindler syndrome. The British journal of dermatology *157*, 1252-1256.

Arnaout, M.A., Mahalingam, B., and Xiong, J.P. (2005). Integrin structure, allostery, and bidirectional signaling. Annual review of cell and developmental biology *21*, 381-410.

Arwert, E.N., Hoste, E., and Watt, F.M. (2012). Epithelial stem cells, wound healing and cancer. Nature reviews Cancer *12*, 170-180.

Asano, Y., Ihn, H., Yamane, K., Jinnin, M., Mimura, Y., and Tamaki, K. (2005a). Increased expression of integrin alpha(v)beta3 contributes to the establishment of autocrine TGF-beta signaling in scleroderma fibroblasts. Journal of immunology *175*, 7708-7718.

Asano, Y., Ihn, H., Yamane, K., Jinnin, M., Mimura, Y., and Tamaki, K. (2005b). Involvement of alphavbeta5 integrin-mediated activation of latent transforming growth factor beta1 in autocrine transforming growth factor beta signaling in systemic sclerosis fibroblasts. Arthritis and rheumatism *52*, 2897-2905.

Ashton, G.H., McLean, W.H., South, A.P., Oyama, N., Smith, F.J., Al-Suwaid, R., Al-Ismaily, A., Atherton, D.J., Harwood, C.A., Leigh, I.M.*, et al.* (2004). Recurrent mutations in kindlin-1, a novel keratinocyte focal contact protein, in the autosomal recessive skin fragility and photosensitivity disorder, Kindler syndrome. The Journal of investigative dermatology *122*, 78-83.

Bader, B.L., Rayburn, H., Crowley, D., and Hynes, R.O. (1998). Extensive vasculogenesis, angiogenesis, and organogenesis precede lethality in mice lacking all alpha v integrins. Cell *95*, 507-519.

Baeg, G.H., Lin, X., Khare, N., Baumgartner, S., and Perrimon, N. (2001). Heparan sulfate proteoglycans are critical for the organization of the extracellular distribution of Wingless. Development *128*, 87-94.

Bai, J., Binari, R., Ni, J.Q., Vijayakanthan, M., Li, H.S., and Perrimon, N. (2008). RNA interference screening in Drosophila primary cells for genes involved in muscle assembly and maintenance. Development *135*, 1439-1449.

Bakin, A.V., Rinehart, C., Tomlinson, A.K., and Arteaga, C.L. (2002). p38 mitogen-activated protein kinase is required for TGFbeta-mediated fibroblastic transdifferentiation and cell migration. Journal of cell science *115*, 3193-3206.

Bandyopadhyay, A., and Raghavan, S. (2009). Defining the role of integrin alphavbeta6 in cancer. Current drug targets *10*, 645-652.

Bandyopadhyay, A., Rothschild, G., Kim, S., Calderwood, D.A., and Raghavan, S. (2012). Functional differences between kindlin-1 and kindlin-2 in keratinocytes. Journal of cell science *125*, 2172-2184.

Barcellos-Hoff, M.H., and Dix, T.A. (1996). Redox-mediated activation of latent transforming growth factor-beta 1. Molecular endocrinology *10*, 1077-1083.

Bardeesy, N., Cheng, K.H., Berger, J.H., Chu, G.C., Pahler, J., Olson, P., Hezel, A.F., Horner, J., Lauwers, G.Y., Hanahan, D.*, et al.* (2006). Smad4 is dispensable for normal pancreas development yet critical in progression and tumor biology of pancreas cancer. Genes & development *20*, 3130-3146.

Barker, N., Tan, S., and Clevers, H. (2013). Lgr proteins in epithelial stem cell biology. Development *140*, 2484-2494.

Bates, R.C., Bellovin, D.I., Brown, C., Maynard, E., Wu, B., Kawakatsu, H., Sheppard, D., Oettgen, P., and Mercurio, A.M. (2005). Transcriptional activation of integrin beta6 during the epithelial-mesenchymal transition defines a novel prognostic indicator of aggressive colon carcinoma. The Journal of clinical investigation *115*, 339-347.

Bazzoni, G., Ma, L., Blue, M.L., and Hemler, M.E. (1998). Divalent cations and ligands induce conformational changes that are highly divergent among beta1 integrins. The Journal of biological chemistry *273*, 6670-6678.

Behrens, J., von Kries, J.P., Kuhl, M., Bruhn, L., Wedlich, D., Grosschedl, R., and Birchmeier, W. (1996). Functional interaction of beta-catenin with the transcription factor LEF-1. Nature *382*, 638-642.

Belenkaya, T.Y., Wu, Y., Tang, X., Zhou, B., Cheng, L., Sharma, Y.V., Yan, D., Selva, E.M., and Lin, X. (2008). The retromer complex influences Wnt secretion by recycling wntless from endosomes to the trans-Golgi network. Developmental cell *14*, 120-131.

Bernard, P., Fleming, A., Lacombe, A., Harley, V.R., and Vilain, E. (2008). Wnt4 inhibits beta-catenin/TCF signalling by redirecting beta-catenin to the cell membrane. Biology of the cell / under the auspices of the European Cell Biology Organization *100*, 167-177.

Beronja, S., Janki, P., Heller, E., Lien, W.H., Keyes, B.E., Oshimori, N., and Fuchs, E. (2013). RNAi screens in mice identify physiological regulators of oncogenic growth. Nature *501*, 185-190.

Bhowmick, N.A., Ghiassi, M., Bakin, A., Aakre, M., Lundquist, C.A., Engel, M.E., Arteaga, C.L., and Moses, H.L. (2001). Transforming growth factor-beta1 mediates epithelial to mesenchymal transdifferentiation through a RhoA-dependent mechanism. Molecular biology of the cell *12*, 27-36.

Bialkowska, K., Ma, Y.Q., Bledzka, K., Sossey-Alaoui, K., Izem, L., Zhang, X., Malinin, N., Qin, J., Byzova, T., and Plow, E.F. (2010). The integrin co-activator Kindlin-3 is expressed and functional in a non-hematopoietic cell, the endothelial cell. The Journal of biological chemistry *285*, 18640-18649.

Bielefeld, K.A., Amini-Nik, S., and Alman, B.A. (2013). Cutaneous wound healing: recruiting developmental pathways for regeneration. Cellular and molecular life sciences : CMLS *70*, 2059-2081.

Bielesz, B., Sirin, Y., Si, H., Niranjan, T., Gruenwald, A., Ahn, S., Kato, H., Pullman, J., Gessler, M., Haase, V.H*., et al.* (2010). Epithelial Notch signaling regulates interstitial fibrosis development in the kidneys of mice and humans. The Journal of clinical investigation *120*, 4040-4054.

Bitgood, M.J., and McMahon, A.P. (1995). Hedgehog and Bmp genes are coexpressed at many diverse sites of cell-cell interaction in the mouse embryo. Developmental biology *172*, 126-138.

Bjarnadottir, T.K., Gloriam, D.E., Hellstrand, S.H., Kristiansson, H., Fredriksson, R., and Schioth, H.B. (2006). Comprehensive repertoire and phylogenetic analysis of the G protein-coupled receptors in human and mouse. Genomics *88*, 263-273.

Blakytny, R., Ludlow, A., Martin, G.E., Ireland, G., Lund, L.R., Ferguson, M.W., and Brunner, G. (2004). Latent TGF-beta1 activation by platelets. Journal of cellular physiology *199*, 67-76.

Blanpain, C., and Fuchs, E. (2006). Epidermal stem cells of the skin. Annual review of cell and developmental biology *22*, 339-373.

Blanpain, C., Lowry, W.E., Geoghegan, A., Polak, L., and Fuchs, E. (2004). Self-renewal, multipotency, and the existence of two cell populations within an epithelial stem cell niche. Cell *118*, 635-648.

Blanpain, C., Lowry, W.E., Pasolli, H.A., and Fuchs, E. (2006). Canonical notch signaling functions as a commitment switch in the epidermal lineage. Genes & development *20*, 3022-3035.

Blaumueller, C.M., Qi, H., Zagouras, P., and Artavanis-Tsakonas, S. (1997). Intracellular cleavage of Notch leads to a heterodimeric receptor on the plasma membrane. Cell *90*, 281-291.

Bledzka, K., Bialkowska, K., Nie, H., Qin, J., Byzova, T., Wu, C., Plow, E.F., and Ma, Y.Q. (2010). Tyrosine phosphorylation of integrin beta3 regulates kindlin-2 binding and integrin activation. The Journal of biological chemistry *285*, 30370-30374.

Bledzka, K., Liu, J., Xu, Z., Perera, H.D., Yadav, S.P., Bialkowska, K., Qin, J., Ma, Y.Q., and Plow, E.F. (2012). Spatial coordination of kindlin-2 with talin head domain in interaction with integrin beta cytoplasmic tails. The Journal of biological chemistry *287*, 24585-24594.

Blobe, G.C., Schiemann, W.P., and Lodish, H.F. (2000). Role of transforming growth factor beta in human disease. The New England journal of medicine *342*, 1350-1358.

Boettiger, D. (2012). Mechanical control of integrin-mediated adhesion and signaling. Current opinion in cell biology *24*, 592-599.

Bottcher, R.T., Stremmel, C., Meves, A., Meyer, H., Widmaier, M., Tseng, H.Y., and Fassler, R. (2012). Sorting nexin 17 prevents lysosomal degradation of beta1 integrins by binding to the beta1-integrin tail. Nature cell biology *14*, 584-592.

Bottinger, E.P., Jakubczak, J.L., Haines, D.C., Bagnall, K., and Wakefield, L.M. (1997). Transgenic mice overexpressing a dominant-negative mutant type II transforming growth factor beta receptor show enhanced tumorigenesis in the mammary gland and lung in response to the carcinogen 7,12-dimethylbenz-[a]-anthracene. Cancer research *57*, 5564-5570.

Boyd, R.S., Adam, P.J., Patel, S., Loader, J.A., Berry, J., Redpath, N.T., Poyser, H.R., Fletcher, G.C., Burgess, N.A., Stamps, A.C.*, et al.* (2003). Proteomic analysis of the cell-surface membrane in chronic lymphocytic leukemia: identification of two novel proteins, BCNP1 and MIG2B. Leukemia *17*, 1605-1612.

Brakebusch, C., Grose, R., Quondamatteo, F., Ramirez, A., Jorcano, J.L., Pirro, A., Svensson, M., Herken, R., Sasaki, T., Timpl, R.*, et al.* (2000). Skin and hair follicle integrity is crucially dependent on beta 1 integrin expression on keratinocytes. The EMBO journal *19*, 3990-4003.

Breuss, J.M., Gallo, J., DeLisser, H.M., Klimanskaya, I.V., Folkesson, H.G., Pittet, J.F., Nishimura, S.L., Aldape, K., Landers, D.V., Carpenter, W.*, et al.* (1995). Expression of the beta 6 integrin subunit in development, neoplasia and tissue repair suggests a role in epithelial remodeling. Journal of cell science *108 (Pt 6)*, 2241-2251.

Breuss, J.M., Gillett, N., Lu, L., Sheppard, D., and Pytela, R. (1993). Restricted distribution of integrin beta 6 mRNA in primate epithelial tissues. The journal of histochemistry and cytochemistry : official journal of the Histochemistry Society *41*, 1521-1527.

Brou, C., Logeat, F., Gupta, N., Bessia, C., LeBail, O., Doedens, J.R., Cumano, A., Roux, P., Black, R.A., and Israel, A. (2000). A novel proteolytic cleavage involved in Notch signaling: the role of the disintegrin-metalloprotease TACE. Molecular cell *5*, 207-216.

Brownell, I., Guevara, E., Bai, C.B., Loomis, C.A., and Joyner, A.L. (2011). Nerve-derived sonic hedgehog defines a niche for hair follicle stem cells capable of becoming epidermal stem cells. Cell stem cell *8*, 552-565.

Bunch, T.A. (2010). Integrin alphaIIbbeta3 activation in Chinese hamster ovary cells and platelets increases clustering rather than affinity. The Journal of biological chemistry *285*, 1841-1849.

Carmon, K.S., Gong, X., Lin, Q., Thomas, A., and Liu, Q. (2011). R-spondins function as ligands of the orphan receptors LGR4 and LGR5 to regulate Wnt/beta-catenin signaling. Proceedings of the National Academy of Sciences of the United States of America *108*, 11452-11457.

Caswell, P.T., Chan, M., Lindsay, A.J., McCaffrey, M.W., Boettiger, D., and Norman, J.C. (2008). Rab-coupling protein coordinates recycling of alpha5beta1 integrin and EGFR1 to promote cell migration in 3D microenvironments. The Journal of cell biology *183*, 143-155.

Caswell, P.T., Spence, H.J., Parsons, M., White, D.P., Clark, K., Cheng, K.W., Mills, G.B., Humphries, M.J., Messent, A.J., Anderson, K.I.*, et al.* (2007). Rab25 associates with alpha5beta1 integrin to promote invasive migration in 3D microenvironments. Developmental cell *13*, 496-510.

Chan, E.F., Gat, U., McNiff, J.M., and Fuchs, E. (1999). A common human skin tumour is caused by activating mutations in beta-catenin. Nature genetics *21*, 410-413.

Chang, H.Y., Sneddon, J.B., Alizadeh, A.A., Sood, R., West, R.B., Montgomery, K., Chi, J.T., van de Rijn, M., Botstein, D., and Brown, P.O. (2004). Gene expression signature of fibroblast serum response predicts human cancer progression: similarities between tumors and wounds. PLoS biology *2*, E7.

Chaudhury, A., and Howe, P.H. (2009). The tale of transforming growth factor-beta (TGFbeta) signaling: a soigne enigma. IUBMB life *61*, 929-939.

Chen, B., Dodge, M.E., Tang, W., Lu, J., Ma, Z., Fan, C.W., Wei, S., Hao, W., Kilgore, J., Williams, N.S.*, et al.* (2009). Small molecule-mediated disruption of Wnt-dependent signaling in tissue regeneration and cancer. Nature chemical biology *5*, 100-107.

Chen, C.R., Kang, Y., Siegel, P.M., and Massague, J. (2002). E2F4/5 and p107 as Smad cofactors linking the TGFbeta receptor to c-myc repression. Cell *110*, 19-32.

Cheon, S., Poon, R., Yu, C., Khoury, M., Shenker, R., Fish, J., and Alman, B.A. (2005). Prolonged beta-catenin stabilization and tcf-dependent transcriptional activation in hyperplastic cutaneous wounds. Laboratory investigation; a journal of technical methods and pathology *85*, 416-425.

Cheon, S.S., Cheah, A.Y., Turley, S., Nadesan, P., Poon, R., Clevers, H., and Alman, B.A. (2002). beta-Catenin stabilization dysregulates mesenchymal cell proliferation, motility, and invasiveness and causes aggressive fibromatosis and hyperplastic cutaneous wounds. Proceedings of the National Academy of Sciences of the United States of America *99*, 6973-6978.

Cheon, S.S., Wei, Q., Gurung, A., Youn, A., Bright, T., Poon, R., Whetstone, H., Guha, A., and Alman, B.A. (2006). Beta-catenin regulates wound size and mediates the effect of TGF-beta in cutaneous healing. FASEB journal : official publication of the Federation of American Societies for Experimental Biology *20*, 692-701.

Clayton, E., Doupe, D.P., Klein, A.M., Winton, D.J., Simons, B.D., and Jones, P.H. (2007). A single type of progenitor cell maintains normal epidermis. Nature *446*, 185-189.

Clevers, H., and Nusse, R. (2012). Wnt/beta-catenin signaling and disease. Cell *149*, 1192-1205.

Cluzel, C., Saltel, F., Lussi, J., Paulhe, F., Imhof, B.A., and Wehrle-Haller, B. (2005). The mechanisms and dynamics of (alpha)v(beta)3 integrin clustering in living cells. The Journal of cell biology *171*, 383-392.

Cotsarelis, G., Sun, T.T., and Lavker, R.M. (1990). Label-retaining cells reside in the bulge area of pilosebaceous unit: implications for follicular stem cells, hair cycle, and skin carcinogenesis. Cell *61*, 1329-1337.

Coussens, L.M., and Werb, Z. (2002). Inflammation and cancer. Nature *420*, 860-867.

Critchley, D.R., and Gingras, A.R. (2008). Talin at a glance. Journal of cell science *121*, 1345-1347.

Cui, W., Fowlis, D.J., Bryson, S., Duffie, E., Ireland, H., Balmain, A., and Akhurst, R.J. (1996). TGFbeta1 inhibits the formation of benign skin tumors, but enhances progression to invasive spindle carcinomas in transgenic mice. Cell *86*, 531-542.

Czuchra, A., Meyer, H., Legate, K.R., Brakebusch, C., and Fassler, R. (2006). Genetic analysis of beta1 integrin "activation motifs" in mice. The Journal of cell biology *174*, 889-899.

D'Souza, B., Miyamoto, A., and Weinmaster, G. (2008). The many facets of Notch ligands. Oncogene *27*, 5148-5167.

Dallas, S.L., Park-Snyder, S., Miyazono, K., Twardzik, D., Mundy, G.R., and Bonewald, L.F. (1994). Characterization and autoregulation of latent transforming growth factor beta (TGF beta) complexes in osteoblast-like cell lines. Production of a latent complex lacking the latent TGF beta-binding protein. The Journal of biological chemistry *269*, 6815-6821.

Daniels, D.L., and Weis, W.I. (2005). Beta-catenin directly displaces Groucho/TLE repressors from Tcf/Lef in Wnt-mediated transcription activation. Nature structural & molecular biology *12*, 364-371.

Dann, C.E., Hsieh, J.C., Rattner, A., Sharma, D., Nathans, J., and Leahy, D.J. (2001). Insights into Wnt binding and signalling from the structures of two Frizzled cysteine-rich domains. Nature *412*, 86-90.

DasGupta, R., and Fuchs, E. (1999). Multiple roles for activated LEF/TCF transcription complexes during hair follicle development and differentiation. Development *126*, 4557-4568.

Datta, A., Huber, F., and Boettiger, D. (2002). Phosphorylation of beta3 integrin controls ligand binding strength. The Journal of biological chemistry *277*, 3943-3949.

de Lau, W.B., Snel, B., and Clevers, H.C. (2012). The R-spondin protein family. Genome biology *13*, 242.

De Melker, A.A., Kramer, D., Kuikman, I., and Sonnenberg, A. (1997). The two phenylalanines in the GFFKR motif of the integrin alpha6A subunit are essential for heterodimerization. The Biochemical journal *328 (Pt 2)*, 529-537.

Dennis, P.A., and Rifkin, D.B. (1991). Cellular activation of latent transforming growth factor beta requires binding to the cation-independent mannose 6-phosphate/insulin-like growth factor type

II receptor. Proceedings of the National Academy of Sciences of the United States of America *88*, 580-584.
Denton, C.P., Khan, K., Hoyles, R.K., Shiwen, X., Leoni, P., Chen, Y., Eastwood, M., and Abraham, D.J. (2009). Inducible lineage-specific deletion of TbetaRII in fibroblasts defines a pivotal regulatory role during adult skin wound healing. The Journal of investigative dermatology *129*, 194-204.
Deschene, E.R., Myung, P., Rompolas, P., Zito, G., Sun, T.Y., Taketo, M.M., Saotome, I., and Greco, V. (2014). beta-Catenin activation regulates tissue growth non-cell autonomously in the hair stem cell niche. Science *343*, 1353-1356.
Desgrosellier, J.S., Barnes, L.A., Shields, D.J., Huang, M., Lau, S.K., Prevost, N., Tarin, D., Shattil, S.J., and Cheresh, D.A. (2009). An integrin alpha(v)beta(3)-c-Src oncogenic unit promotes anchorage-independence and tumor progression. Nature medicine *15*, 1163-1169.
Devgan, V., Mammucari, C., Millar, S.E., Brisken, C., and Dotto, G.P. (2005). p21WAF1/Cip1 is a negative transcriptional regulator of Wnt4 expression downstream of Notch1 activation. Genes & development *19*, 1485-1495.
Di Guglielmo, G.M., Le Roy, C., Goodfellow, A.F., and Wrana, J.L. (2003). Distinct endocytic pathways regulate TGF-beta receptor signalling and turnover. Nature cell biology *5*, 410-421.
Di Paolo, G., Pellegrini, L., Letinic, K., Cestra, G., Zoncu, R., Voronov, S., Chang, S., Guo, J., Wenk, M.R., and De Camilli, P. (2002). Recruitment and regulation of phosphatidylinositol phosphate kinase type 1 gamma by the FERM domain of talin. Nature *420*, 85-89.
Diepgen, T.L., and Mahler, V. (2002). The epidemiology of skin cancer. The British journal of dermatology *146 Suppl 61*, 1-6.
Dixit, N., Kim, M.H., Rossaint, J., Yamayoshi, I., Zarbock, A., and Simon, S.I. (2012). Leukocyte function antigen-1, kindlin-3, and calcium flux orchestrate neutrophil recruitment during inflammation. Journal of immunology *189*, 5954-5964.
Dotto, G.P. (2008). Notch tumor suppressor function. Oncogene *27*, 5115-5123.
Dowling, J.J., Gibbs, E., Russell, M., Goldman, D., Minarcik, J., Golden, J.A., and Feldman, E.L. (2008a). Kindlin-2 is an essential component of intercalated discs and is required for vertebrate cardiac structure and function. Circulation research *102*, 423-431.
Dowling, J.J., Vreede, A.P., Kim, S., Golden, J., and Feldman, E.L. (2008b). Kindlin-2 is required for myocyte elongation and is essential for myogenesis. BMC cell biology *9*, 36.
Driskell, R.R., Lichtenberger, B.M., Hoste, E., Kretzschmar, K., Simons, B.D., Charalambous, M., Ferron, S.R., Herault, Y., Pavlovic, G., Ferguson-Smith, A.C*., et al.* (2013). Distinct fibroblast lineages determine dermal architecture in skin development and repair. Nature *504*, 277-281.
Dvorak, H.F. (1986). Tumors: wounds that do not heal. Similarities between tumor stroma generation and wound healing. The New England journal of medicine *315*, 1650-1659.
Edlund, S., Lee, S.Y., Grimsby, S., Zhang, S., Aspenstrom, P., Heldin, C.H., and Landstrom, M. (2005). Interaction between Smad7 and beta-catenin: importance for transforming growth factor beta-induced apoptosis. Molecular and cellular biology *25*, 1475-1488.
Emanuel, P.O., Rudikoff, D., and Phelps, R.G. (2006). Aggressive squamous cell carcinoma in Kindler syndrome. Skinmed *5*, 305-307.
Engl, T., Relja, B., Marian, D., Blumenberg, C., Muller, I., Beecken, W.D., Jones, J., Ringel, E.M., Bereiter-Hahn, J., Jonas, D*., et al.* (2006). CXCR4 chemokine receptor mediates prostate tumor cell adhesion through alpha5 and beta3 integrins. Neoplasia *8*, 290-301.
Eslami, A., Gallant-Behm, C.L., Hart, D.A., Wiebe, C., Honardoust, D., Gardner, H., Hakkinen, L., and Larjava, H.S. (2009). Expression of integrin alphavbeta6 and TGF-beta in scarless vs scar-forming wound healing. The journal of histochemistry and cytochemistry : official journal of the Histochemistry Society *57*, 543-557.

Estrach, S., Ambler, C.A., Lo Celso, C., Hozumi, K., and Watt, F.M. (2006). Jagged 1 is a beta-catenin target gene required for ectopic hair follicle formation in adult epidermis. Development *133*, 4427-4438.

Evans, R.D., Jones, J., Taylor, C., and Watt, F.M. (2004). Sequence variation in the I-like domain of the beta1 integrin subunit in human oral squamous cell carcinomas. Cancer letters *213*, 189-194.

Evans, R.D., Perkins, V.C., Henry, A., Stephens, P.E., Robinson, M.K., and Watt, F.M. (2003). A tumor-associated beta 1 integrin mutation that abrogates epithelial differentiation control. The Journal of cell biology *160*, 589-596.

Fafilek, B., Krausova, M., Vojtechova, M., Pospichalova, V., Tumova, L., Sloncova, E., Huranova, M., Stancikova, J., Hlavata, A., Svec, J.*, et al.* (2013). Troy, a tumor necrosis factor receptor family member, interacts with lgr5 to inhibit wnt signaling in intestinal stem cells. Gastroenterology *144*, 381-391.

Fan, H., Oro, A.E., Scott, M.P., and Khavari, P.A. (1997). Induction of basal cell carcinoma features in transgenic human skin expressing Sonic Hedgehog. Nature medicine *3*, 788-792.

Fassihi, H., Wessagowit, V., Jones, C., Dopping-Hepenstal, P., Denyer, J., Mellerio, J.E., Clark, S., and McGrath, J.A. (2005). Neonatal diagnosis of Kindler syndrome. Journal of dermatological science *39*, 183-185.

Fassler, R., and Meyer, M. (1995). Consequences of lack of beta 1 integrin gene expression in mice. Genes & development *9*, 1896-1908.

Fedi, P., Bafico, A., Nieto Soria, A., Burgess, W.H., Miki, T., Bottaro, D.P., Kraus, M.H., and Aaronson, S.A. (1999). Isolation and biochemical characterization of the human Dkk-1 homologue, a novel inhibitor of mammalian Wnt signaling. The Journal of biological chemistry *274*, 19465-19472.

Feng, X.H., and Derynck, R. (2005). Specificity and versatility in tgf-beta signaling through Smads. Annual review of cell and developmental biology *21*, 659-693.

Ferreira, M., Fujiwara, H., Morita, K., and Watt, F.M. (2009). An activating beta1 integrin mutation increases the conversion of benign to malignant skin tumors. Cancer research *69*, 1334-1342.

Fitzpatrick, P., Shattil, S.J., and Ablooglu, A.J. (2014). C-terminal COOH of Integrin beta1 Is Necessary for beta1 Association with the Kindlin-2 Adapter Protein. The Journal of biological chemistry *289*, 11183-11193.

Foitzik, K., Lindner, G., Mueller-Roever, S., Maurer, M., Botchkareva, N., Botchkarev, V., Handjiski, B., Metz, M., Hibino, T., Soma, T.*, et al.* (2000). Control of murine hair follicle regression (catagen) by TGF-beta1 in vivo. FASEB journal : official publication of the Federation of American Societies for Experimental Biology *14*, 752-760.

Foitzik, K., Paus, R., Doetschman, T., and Dotto, G.P. (1999). The TGF-beta2 isoform is both a required and sufficient inducer of murine hair follicle morphogenesis. Developmental biology *212*, 278-289.

Foletta, V.C., Lim, M.A., Soosairajah, J., Kelly, A.P., Stanley, E.G., Shannon, M., He, W., Das, S., Massague, J., and Bernard, O. (2003). Direct signaling by the BMP type II receptor via the cytoskeletal regulator LIMK1. The Journal of cell biology *162*, 1089-1098.

Forbes, S.A., Bindal, N., Bamford, S., Cole, C., Kok, C.Y., Beare, D., Jia, M., Shepherd, R., Leung, K., Menzies, A.*, et al.* (2011). COSMIC: mining complete cancer genomes in the Catalogue of Somatic Mutations in Cancer. Nucleic acids research *39*, D945-950.

Franco, S.J., Rodgers, M.A., Perrin, B.J., Han, J., Bennin, D.A., Critchley, D.R., and Huttenlocher, A. (2004). Calpain-mediated proteolysis of talin regulates adhesion dynamics. Nature cell biology *6*, 977-983.

Frisch, S.M., and Screaton, R.A. (2001). Anoikis mechanisms. Current opinion in cell biology *13*, 555-562.

Fuchs, E. (2008). Skin stem cells: rising to the surface. The Journal of cell biology *180*, 273-284.
Fujiwara, H., Ferreira, M., Donati, G., Marciano, D.K., Linton, J.M., Sato, Y., Hartner, A., Sekiguchi, K., Reichardt, L.F., and Watt, F.M. (2011). The basement membrane of hair follicle stem cells is a muscle cell niche. Cell *144*, 577-589.
Gao, J., Khan, A.A., Shimokawa, T., Zhan, J., Stromblad, S., Fang, W., and Zhang, H. (2013). A feedback regulation between Kindlin-2 and GLI1 in prostate cancer cells. FEBS letters *587*, 631-638.
Gat, U., DasGupta, R., Degenstein, L., and Fuchs, E. (1998). De Novo hair follicle morphogenesis and hair tumors in mice expressing a truncated beta-catenin in skin. Cell *95*, 605-614.
Gay, D., Kwon, O., Zhang, Z., Spata, M., Plikus, M.V., Holler, P.D., Ito, M., Yang, Z., Treffeisen, E., Kim, C.D*., et al.* (2013). Fgf9 from dermal gammadelta T cells induces hair follicle neogenesis after wounding. Nature medicine *19*, 916-923.
Ghazizadeh, S., and Taichman, L.B. (2001). Multiple classes of stem cells in cutaneous epithelium: a lineage analysis of adult mouse skin. The EMBO journal *20*, 1215-1222.
Giglia-Mari, G., and Sarasin, A. (2003). TP53 mutations in human skin cancers. Human mutation *21*, 217-228.
Glick, A.B., Lee, M.M., Darwiche, N., Kulkarni, A.B., Karlsson, S., and Yuspa, S.H. (1994). Targeted deletion of the TGF-beta 1 gene causes rapid progression to squamous cell carcinoma. Genes & development *8*, 2429-2440.
Go, C., Li, P., and Wang, X.J. (1999). Blocking transforming growth factor beta signaling in transgenic epidermis accelerates chemical carcinogenesis: a mechanism associated with increased angiogenesis. Cancer research *59*, 2861-2868.
Goentoro, L., and Kirschner, M.W. (2009). Evidence that fold-change, and not absolute level, of beta-catenin dictates Wnt signaling. Molecular cell *36*, 872-884.
Goksoy, E., Ma, Y.Q., Wang, X., Kong, X., Perera, D., Plow, E.F., and Qin, J. (2008). Structural basis for the autoinhibition of talin in regulating integrin activation. Molecular cell *31*, 124-133.
Gomis, R.R., Alarcon, C., He, W., Wang, Q., Seoane, J., Lash, A., and Massague, J. (2006). A FoxO-Smad synexpression group in human keratinocytes. Proceedings of the National Academy of Sciences of the United States of America *103*, 12747-12752.
Gong, X., An, Z., Wang, Y., Guan, L., Fang, W., Stromblad, S., Jiang, Y., and Zhang, H. (2010). Kindlin-2 controls sensitivity of prostate cancer cells to cisplatin-induced cell death. Cancer letters *299*, 54-62.
Gozgit, J.M., Pentecost, B.T., Marconi, S.A., Otis, C.N., Wu, C., and Arcaro, K.F. (2006). Use of an aggressive MCF-7 cell line variant, TMX2-28, to study cell invasion in breast cancer. Molecular cancer research : MCR *4*, 905-913.
Grachtchouk, M., Mo, R., Yu, S., Zhang, X., Sasaki, H., Hui, C.C., and Dlugosz, A.A. (2000). Basal cell carcinomas in mice overexpressing Gli2 in skin. Nature genetics *24*, 216-217.
Greco, V., Chen, T., Rendl, M., Schober, M., Pasolli, H.A., Stokes, N., Dela Cruz-Racelis, J., and Fuchs, E. (2009). A two-step mechanism for stem cell activation during hair regeneration. Cell stem cell *4*, 155-169.
Groden, J., Thliveris, A., Samowitz, W., Carlson, M., Gelbert, L., Albertsen, H., Joslyn, G., Stevens, J., Spirio, L., Robertson, M*., et al.* (1991). Identification and characterization of the familial adenomatous polyposis coli gene. Cell *66*, 589-600.
Grose, R., Hutter, C., Bloch, W., Thorey, I., Watt, F.M., Fassler, R., Brakebusch, C., and Werner, S. (2002). A crucial role of beta 1 integrins for keratinocyte migration in vitro and during cutaneous wound repair. Development *129*, 2303-2315.

Gruda, R., Brown, A.C., Grabovsky, V., Mizrahi, S., Gur, C., Feigelson, S.W., Achdout, H., Bar-On, Y., Alon, R., Aker, M.*, et al.* (2012). Loss of kindlin-3 alters the threshold for NK cell activation in human leukocyte adhesion deficiency-III. Blood *120*, 3915-3924.

Guasch, G., Schober, M., Pasolli, H.A., Conn, E.B., Polak, L., and Fuchs, E. (2007). Loss of TGFbeta signaling destabilizes homeostasis and promotes squamous cell carcinomas in stratified epithelia. Cancer cell *12*, 313-327.

Haines, N., and Irvine, K.D. (2003). Glycosylation regulates Notch signalling. Nature reviews Molecular cell biology *4*, 786-797.

Han, G., Li, A.G., Liang, Y.Y., Owens, P., He, W., Lu, S., Yoshimatsu, Y., Wang, D., Ten Dijke, P., Lin, X.*, et al.* (2006a). Smad7-induced beta-catenin degradation alters epidermal appendage development. Developmental cell *11*, 301-312.

Han, J., Lim, C.J., Watanabe, N., Soriani, A., Ratnikov, B., Calderwood, D.A., Puzon-McLaughlin, W., Lafuente, E.M., Boussiotis, V.A., Shattil, S.J.*, et al.* (2006b). Reconstructing and deconstructing agonist-induced activation of integrin alphaIIbbeta3. Current biology : CB *16*, 1796-1806.

Hanna, S., and Etzioni, A. (2012). Leukocyte adhesion deficiencies. Annals of the New York Academy of Sciences *1250*, 50-55.

Hao, H.X., Xie, Y., Zhang, Y., Charlat, O., Oster, E., Avello, M., Lei, H., Mickanin, C., Liu, D., Ruffner, H.*, et al.* (2012). ZNRF3 promotes Wnt receptor turnover in an R-spondin-sensitive manner. Nature *485*, 195-200.

Harburger, D.S., Bouaouina, M., and Calderwood, D.A. (2009). Kindlin-1 and -2 directly bind the C-terminal region of beta integrin cytoplasmic tails and exert integrin-specific activation effects. The Journal of biological chemistry *284*, 11485-11497.

Hartmann, T.N., Burger, J.A., Glodek, A., Fujii, N., and Burger, M. (2005). CXCR4 chemokine receptor and integrin signaling co-operate in mediating adhesion and chemoresistance in small cell lung cancer (SCLC) cells. Oncogene *24*, 4462-4471.

Has, C., Herz, C., Zimina, E., Qu, H.Y., He, Y., Zhang, Z.G., Wen, T.T., Gache, Y., Aumailley, M., and Bruckner-Tuderman, L. (2009). Kindlin-1 Is required for RhoGTPase-mediated lamellipodia formation in keratinocytes. The American journal of pathology *175*, 1442-1452.

Hayward, P., Brennan, K., Sanders, P., Balayo, T., DasGupta, R., Perrimon, N., and Martinez Arias, A. (2005). Notch modulates Wnt signalling by associating with Armadillo/beta-catenin and regulating its transcriptional activity. Development *132*, 1819-1830.

He, Y., Esser, P., Heinemann, A., Bruckner-Tuderman, L., and Has, C. (2011a). Kindlin-1 and -2 have overlapping functions in epithelial cells implications for phenotype modification. The American journal of pathology *178*, 975-982.

He, Y., Esser, P., Schacht, V., Bruckner-Tuderman, L., and Has, C. (2011b). Role of kindlin-2 in fibroblast functions: implications for wound healing. The Journal of investigative dermatology *131*, 245-256.

He, Y., Sonnenwald, T., Sprenger, A., Hansen, U., Dengjel, J., Bruckner-Tuderman, L., Schmidt, G., and Has, C. (2014). RhoA activation by CNFy restores cell-cell adhesion in kindlin-2-deficient keratinocytes. The Journal of pathology.

Hecht, A., Vleminckx, K., Stemmler, M.P., van Roy, F., and Kemler, R. (2000). The p300/CBP acetyltransferases function as transcriptional coactivators of beta-catenin in vertebrates. The EMBO journal *19*, 1839-1850.

Herz, C., Aumailley, M., Schulte, C., Schlotzer-Schrehardt, U., Bruckner-Tuderman, L., and Has, C. (2006). Kindlin-1 is a phosphoprotein involved in regulation of polarity, proliferation, and motility of epidermal keratinocytes. The Journal of biological chemistry *281*, 36082-36090.

Heuberger, J., and Birchmeier, W. (2010). Interplay of cadherin-mediated cell adhesion and canonical Wnt signaling. Cold Spring Harbor perspectives in biology *2*, a002915.

Hikasa, H., Shibata, M., Hiratani, I., and Taira, M. (2002). The Xenopus receptor tyrosine kinase Xror2 modulates morphogenetic movements of the axial mesoderm and neuroectoderm via Wnt signaling. Development *129*, 5227-5239.

Horsley, V., O'Carroll, D., Tooze, R., Ohinata, Y., Saitou, M., Obukhanych, T., Nussenzweig, M., Tarakhovsky, A., and Fuchs, E. (2006). Blimp1 defines a progenitor population that governs cellular input to the sebaceous gland. Cell *126*, 597-609.

Hsiao, J.R., Chang, Y., Chen, Y.L., Hsieh, S.H., Hsu, K.F., Wang, C.F., Tsai, S.T., and Jin, Y.T. (2010). Cyclic alphavbeta6-targeting peptide selected from biopanning with clinical potential for head and neck squamous cell carcinoma. Head & neck *32*, 160-172.

Hsieh, J.C., Kodjabachian, L., Rebbert, M.L., Rattner, A., Smallwood, P.M., Samos, C.H., Nusse, R., Dawid, I.B., and Nathans, J. (1999). A new secreted protein that binds to Wnt proteins and inhibits their activities. Nature *398*, 431-436.

Hu, B., Lefort, K., Qiu, W., Nguyen, B.C., Rajaram, R.D., Castillo, E., He, F., Chen, Y., Angel, P., Brisken, C.*, et al.* (2010). Control of hair follicle cell fate by underlying mesenchyme through a CSL-Wnt5a-FoxN1 regulatory axis. Genes & development *24*, 1519-1532.

Huang, S.M., Mishina, Y.M., Liu, S., Cheung, A., Stegmeier, F., Michaud, G.A., Charlat, O., Wiellette, E., Zhang, Y., Wiessner, S.*, et al.* (2009). Tankyrase inhibition stabilizes axin and antagonizes Wnt signalling. Nature *461*, 614-620.

Huang, X., Griffiths, M., Wu, J., Farese, R.V., Jr., and Sheppard, D. (2000). Normal development, wound healing, and adenovirus susceptibility in beta5-deficient mice. Molecular and cellular biology *20*, 755-759.

Huang, X.Z., Wu, J.F., Cass, D., Erle, D.J., Corry, D., Young, S.G., Farese, R.V., Jr., and Sheppard, D. (1996). Inactivation of the integrin beta 6 subunit gene reveals a role of epithelial integrins in regulating inflammation in the lung and skin. The Journal of cell biology *133*, 921-928.

Huber, A.H., and Weis, W.I. (2001). The structure of the beta-catenin/E-cadherin complex and the molecular basis of diverse ligand recognition by beta-catenin. Cell *105*, 391-402.

Huelsken, J., Vogel, R., Erdmann, B., Cotsarelis, G., and Birchmeier, W. (2001). beta-Catenin controls hair follicle morphogenesis and stem cell differentiation in the skin. Cell *105*, 533-545.

Hughes, P.E., Diaz-Gonzalez, F., Leong, L., Wu, C., McDonald, J.A., Shattil, S.J., and Ginsberg, M.H. (1996). Breaking the integrin hinge. A defined structural constraint regulates integrin signaling. The Journal of biological chemistry *271*, 6571-6574.

Humphries, J.D., Byron, A., and Humphries, M.J. (2006). Integrin ligands at a glance. Journal of cell science *119*, 3901-3903.

Hynes, R.O. (2002). Integrins: bidirectional, allosteric signaling machines. Cell *110*, 673-687.

Intong, L.R., and Murrell, D.F. (2012). Inherited epidermolysis bullosa: new diagnostic criteria and classification. Clinics in dermatology *30*, 70-77.

Ito, M., Liu, Y., Yang, Z., Nguyen, J., Liang, F., Morris, R.J., and Cotsarelis, G. (2005). Stem cells in the hair follicle bulge contribute to wound repair but not to homeostasis of the epidermis. Nature medicine *11*, 1351-1354.

Ito, M., Yang, Z., Andl, T., Cui, C., Kim, N., Millar, S.E., and Cotsarelis, G. (2007). Wnt-dependent de novo hair follicle regeneration in adult mouse skin after wounding. Nature *447*, 316-320.

Jaks, V., Barker, N., Kasper, M., van Es, J.H., Snippert, H.J., Clevers, H., and Toftgard, R. (2008). Lgr5 marks cycling, yet long-lived, hair follicle stem cells. Nature genetics *40*, 1291-1299.

Janda, C.Y., Waghray, D., Levin, A.M., Thomas, C., and Garcia, K.C. (2012). Structural basis of Wnt recognition by Frizzled. Science *337*, 59-64.

Janes, S.M., and Watt, F.M. (2004). Switch from alphavbeta5 to alphavbeta6 integrin expression protects squamous cell carcinomas from anoikis. The Journal of cell biology *166*, 419-431.

Janes, S.M., and Watt, F.M. (2006). New roles for integrins in squamous-cell carcinoma. Nature reviews Cancer *6*, 175-183.

Jang, C.W., Chen, C.H., Chen, C.C., Chen, J.Y., Su, Y.H., and Chen, R.H. (2002). TGF-beta induces apoptosis through Smad-mediated expression of DAP-kinase. Nature cell biology *4*, 51-58.

Jensen, K.B., Collins, C.A., Nascimento, E., Tan, D.W., Frye, M., Itami, S., and Watt, F.M. (2009). Lrig1 expression defines a distinct multipotent stem cell population in mammalian epidermis. Cell stem cell *4*, 427-439.

Jensen, K.B., Driskell, R.R., and Watt, F.M. (2010). Assaying proliferation and differentiation capacity of stem cells using disaggregated adult mouse epidermis. Nature protocols *5*, 898-911.

Jiang, T.X., Jung, H.S., Widelitz, R.B., and Chuong, C.M. (1999). Self-organization of periodic patterns by dissociated feather mesenchymal cells and the regulation of size, number and spacing of primordia. Development *126*, 4997-5009.

Jobard, F., Bouadjar, B., Caux, F., Hadj-Rabia, S., Has, C., Matsuda, F., Weissenbach, J., Lathrop, M., Prud'homme, J.F., and Fischer, J. (2003). Identification of mutations in a new gene encoding a FERM family protein with a pleckstrin homology domain in Kindler syndrome. Human molecular genetics *12*, 925-935.

Karakose, E., Schiller, H.B., and Fassler, R. (2010). The kindlins at a glance. Journal of cell science *123*, 2353-2356.

Katanaev, V.L., Solis, G.P., Hausmann, G., Buestorf, S., Katanayeva, N., Schrock, Y., Stuermer, C.A., and Basler, K. (2008). Reggie-1/flotillin-2 promotes secretion of the long-range signalling forms of Wingless and Hedgehog in Drosophila. The EMBO journal *27*, 509-521.

Kato, K., Shiozawa, T., Mitsushita, J., Toda, A., Horiuchi, A., Nikaido, T., Fujii, S., and Konishi, I. (2004). Expression of the mitogen-inducible gene-2 (mig-2) is elevated in human uterine leiomyomas but not in leiomyosarcomas. Human pathology *35*, 55-60.

Kattla, J.J., Carew, R.M., Heljic, M., Godson, C., and Brazil, D.P. (2008). Protein kinase B/Akt activity is involved in renal TGF-beta1-driven epithelial-mesenchymal transition in vitro and in vivo. American journal of physiology Renal physiology *295*, F215-225.

Kavsak, P., Rasmussen, R.K., Causing, C.G., Bonni, S., Zhu, H., Thomsen, G.H., and Wrana, J.L. (2000). Smad7 binds to Smurf2 to form an E3 ubiquitin ligase that targets the TGF beta receptor for degradation. Molecular cell *6*, 1365-1375.

Kern, J.S., Herz, C., Haan, E., Moore, D., Nottelmann, S., von Lilien, T., Greiner, P., Schmitt-Graeff, A., Opitz, O.G., Bruckner-Tuderman, L.*, et al.* (2007). Chronic colitis due to an epithelial barrier defect: the role of kindlin-1 isoforms. The Journal of pathology *213*, 462-470.

Khan, A.A., Janke, A., Shimokawa, T., and Zhang, H. (2011). Phylogenetic analysis of kindlins suggests subfunctionalization of an ancestral unduplicated kindlin into three paralogs in vertebrates. Evolutionary bioinformatics online *7*, 7-19.

Kim, S., and Jho, E.H. (2010). The protein stability of Axin, a negative regulator of Wnt signaling, is regulated by Smad ubiquitination regulatory factor 2 (Smurf2). The Journal of biological chemistry *285*, 36420-36426.

Kim, S.G., Jong, H.S., Kim, T.Y., Lee, J.W., Kim, N.K., Hong, S.H., and Bang, Y.J. (2004). Transforming growth factor-beta 1 induces apoptosis through Fas ligand-independent activation of the Fas death pathway in human gastric SNU-620 carcinoma cells. Molecular biology of the cell *15*, 420-434.

Kindler, T. (1954). Congenital poikiloderma with traumatic bulla formation and progressive cutaneous atrophy. The British journal of dermatology *66*, 104-111.

Kloeker, S., Major, M.B., Calderwood, D.A., Ginsberg, M.H., Jones, D.A., and Beckerle, M.C. (2004). The Kindler syndrome protein is regulated by transforming growth factor-beta and involved in integrin-mediated adhesion. The Journal of biological chemistry *279*, 6824-6833.

Kloepper, J.E., Tiede, S., Brinckmann, J., Reinhardt, D.P., Meyer, W., Faessler, R., and Paus, R. (2008). Immunophenotyping of the human bulge region: the quest to define useful in situ markers for human epithelial hair follicle stem cells and their niche. Experimental dermatology *17*, 592-609.

Komiya, Y., and Habas, R. (2008). Wnt signal transduction pathways. Organogenesis *4*, 68-75.

Kong, F., Garcia, A.J., Mould, A.P., Humphries, M.J., and Zhu, C. (2009). Demonstration of catch bonds between an integrin and its ligand. The Journal of cell biology *185*, 1275-1284.

Kong, F., Li, Z., Parks, W.M., Dumbauld, D.W., Garcia, A.J., Mould, A.P., Humphries, M.J., and Zhu, C. (2013). Cyclic mechanical reinforcement of integrin-ligand interactions. Molecular cell *49*, 1060-1068.

Koo, B.K., Spit, M., Jordens, I., Low, T.Y., Stange, D.E., van de Wetering, M., van Es, J.H., Mohammed, S., Heck, A.J., Maurice, M.M*., et al.* (2012). Tumour suppressor RNF43 is a stem-cell E3 ligase that induces endocytosis of Wnt receptors. Nature *488*, 665-669.

Korinek, V., Barker, N., Morin, P.J., van Wichen, D., de Weger, R., Kinzler, K.W., Vogelstein, B., and Clevers, H. (1997). Constitutive transcriptional activation by a beta-catenin-Tcf complex in APC-/- colon carcinoma. Science *275*, 1784-1787.

Kuijpers, T.W., van de Vijver, E., Weterman, M.A., de Boer, M., Tool, A.T., van den Berg, T.K., Moser, M., Jakobs, M.E., Seeger, K., Sanal, O*., et al.* (2009). LAD-1/variant syndrome is caused by mutations in FERMT3. Blood *113*, 4740-4746.

Kusserow, A., Pang, K., Sturm, C., Hrouda, M., Lentfer, J., Schmidt, H.A., Technau, U., von Haeseler, A., Hobmayer, B., Martindale, M.Q*., et al.* (2005). Unexpected complexity of the Wnt gene family in a sea anemone. Nature *433*, 156-160.

Kwon, C., Cheng, P., King, I.N., Andersen, P., Shenje, L., Nigam, V., and Srivastava, D. (2011). Notch post-translationally regulates beta-catenin protein in stem and progenitor cells. Nature cell biology *13*, 1244-1251.

Lai-Cheong, J.E., Parsons, M., and McGrath, J.A. (2010). The role of kindlins in cell biology and relevance to human disease. The international journal of biochemistry & cell biology *42*, 595-603.

Lai-Cheong, J.E., Parsons, M., Tanaka, A., Ussar, S., South, A.P., Gomathy, S., Mee, J.B., Barbaroux, J.B., Techanukul, T., Almaani, N*., et al.* (2009). Loss-of-function FERMT1 mutations in kindler syndrome implicate a role for fermitin family homolog-1 in integrin activation. The American journal of pathology *175*, 1431-1441.

Lai-Cheong, J.E., Ussar, S., Arita, K., Hart, I.R., and McGrath, J.A. (2008). Colocalization of kindlin-1, kindlin-2, and migfilin at keratinocyte focal adhesion and relevance to the pathophysiology of Kindler syndrome. The Journal of investigative dermatology *128*, 2156-2165.

Lefort, C.T., Rossaint, J., Moser, M., Petrich, B.G., Zarbock, A., Monkley, S.J., Critchley, D.R., Ginsberg, M.H., Fassler, R., and Ley, K. (2012). Distinct roles for talin-1 and kindlin-3 in LFA-1 extension and affinity regulation. Blood *119*, 4275-4282.

Legate, K.R., Wickstrom, S.A., and Fassler, R. (2009). Genetic and cell biological analysis of integrin outside-in signaling. Genes & development *23*, 397-418.

Ley, K., Laudanna, C., Cybulsky, M.I., and Nourshargh, S. (2007). Getting to the site of inflammation: the leukocyte adhesion cascade updated. Nature reviews Immunology *7*, 678-689.

Li, V.S., Ng, S.S., Boersema, P.J., Low, T.Y., Karthaus, W.R., Gerlach, J.P., Mohammed, S., Heck, A.J., Maurice, M.M., Mahmoudi, T*., et al.* (2012). Wnt signaling through inhibition of beta-catenin degradation in an intact Axin1 complex. Cell *149*, 1245-1256.

Li, X., Yang, Y., Hu, Y., Dang, D., Regezi, J., Schmidt, B.L., Atakilit, A., Chen, B., Ellis, D., and Ramos, D.M. (2003). Alphavbeta6-Fyn signaling promotes oral cancer progression. The Journal of biological chemistry *278*, 41646-41653.

Lien, W.H., Polak, L., Lin, M., Lay, K., Zheng, D., and Fuchs, E. (2014). In vivo transcriptional governance of hair follicle stem cells by canonical Wnt regulators. Nature cell biology *16*, 179-190.
Lim, X., and Nusse, R. (2013). Wnt signaling in skin development, homeostasis, and disease. Cold Spring Harbor perspectives in biology *5*.
Lim, X., Tan, S.H., Koh, W.L., Chau, R.M., Yan, K.S., Kuo, C.J., van Amerongen, R., Klein, A.M., and Nusse, R. (2013). Interfollicular epidermal stem cells self-renew via autocrine Wnt signaling. Science *342*, 1226-1230.
Lin, K.K., Chudova, D., Hatfield, G.W., Smyth, P., and Andersen, B. (2004). Identification of hair cycle-associated genes from time-course gene expression profile data by using replicate variance. Proceedings of the National Academy of Sciences of the United States of America *101*, 15955-15960.
Lin, X., Duan, X., Liang, Y.Y., Su, Y., Wrighton, K.H., Long, J., Hu, M., Davis, C.M., Wang, J., Brunicardi, F.C*., et al.* (2006). PPM1A functions as a Smad phosphatase to terminate TGFbeta signaling. Cell *125*, 915-928.
Lin, X., Liang, M., and Feng, X.H. (2000). Smurf2 is a ubiquitin E3 ligase mediating proteasome-dependent degradation of Smad2 in transforming growth factor-beta signaling. The Journal of biological chemistry *275*, 36818-36822.
Linder, S., and Kopp, P. (2005). Podosomes at a glance. Journal of cell science *118*, 2079-2082.
Liu, W., Dong, X., Mai, M., Seelan, R.S., Taniguchi, K., Krishnadath, K.K., Halling, K.C., Cunningham, J.M., Boardman, L.A., Qian, C*., et al.* (2000). Mutations in AXIN2 cause colorectal cancer with defective mismatch repair by activating beta-catenin/TCF signalling. Nature genetics *26*, 146-147.
Liu, W., Rui, H., Wang, J., Lin, S., He, Y., Chen, M., Li, Q., Ye, Z., Zhang, S., Chan, S.C*., et al.* (2006). Axin is a scaffold protein in TGF-beta signaling that promotes degradation of Smad7 by Arkadia. The EMBO journal *25*, 1646-1658.
Lo Celso, C., Prowse, D.M., and Watt, F.M. (2004). Transient activation of beta-catenin signalling in adult mouse epidermis is sufficient to induce new hair follicles but continuous activation is required to maintain hair follicle tumours. Development *131*, 1787-1799.
Logan, C.Y., and Nusse, R. (2004). The Wnt signaling pathway in development and disease. Annual review of cell and developmental biology *20*, 781-810.
Lotem, M., Raben, M., Zeltser, R., Landau, M., Sela, M., Wygoda, M., and Tochner, Z.A. (2001). Kindler syndrome complicated by squamous cell carcinoma of the hard palate: successful treatment with high-dose radiation therapy and granulocyte-macrophage colony-stimulating factor. The British journal of dermatology *144*, 1284-1286.
Lu, W., Yamamoto, V., Ortega, B., and Baltimore, D. (2004). Mammalian Ryk is a Wnt coreceptor required for stimulation of neurite outgrowth. Cell *119*, 97-108.
Ludbrook, S.B., Barry, S.T., Delves, C.J., and Horgan, C.M. (2003). The integrin alphavbeta3 is a receptor for the latency-associated peptides of transforming growth factors beta1 and beta3. The Biochemical journal *369*, 311-318.
Luo, B.H., Carman, C.V., and Springer, T.A. (2007). Structural basis of integrin regulation and signaling. Annual review of immunology *25*, 619-647.
Lyle, S., Christofidou-Solomidou, M., Liu, Y., Elder, D.E., Albelda, S., and Cotsarelis, G. (1998). The C8/144B monoclonal antibody recognizes cytokeratin 15 and defines the location of human hair follicle stem cells. Journal of cell science *111 (Pt 21)*, 3179-3188.
Lyons, R.M., Keski-Oja, J., and Moses, H.L. (1988). Proteolytic activation of latent transforming growth factor-beta from fibroblast-conditioned medium. The Journal of cell biology *106*, 1659-1665.
Lyu, J., Yamamoto, V., and Lu, W. (2008). Cleavage of the Wnt receptor Ryk regulates neuronal differentiation during cortical neurogenesis. Developmental cell *15*, 773-780.

MacDonald, B.T., Tamai, K., and He, X. (2009). Wnt/beta-catenin signaling: components, mechanisms, and diseases. Developmental cell *17*, 9-26.
Mackinnon, A.C., Qadota, H., Norman, K.R., Moerman, D.G., and Williams, B.D. (2002). C. elegans PAT-4/ILK functions as an adaptor protein within integrin adhesion complexes. Current biology : CB *12*, 787-797.
Mahawithitwong, P., Ohuchida, K., Ikenaga, N., Fujita, H., Zhao, M., Kozono, S., Shindo, K., Ohtsuka, T., Aishima, S., Mizumoto, K.*, et al.* (2013a). Kindlin-1 expression is involved in migration and invasion of pancreatic cancer. International journal of oncology *42*, 1360-1366.
Mahawithitwong, P., Ohuchida, K., Ikenaga, N., Fujita, H., Zhao, M., Kozono, S., Shindo, K., Ohtsuka, T., Mizumoto, K., and Tanaka, M. (2013b). Kindlin-2 expression in peritumoral stroma is associated with poor prognosis in pancreatic ductal adenocarcinoma. Pancreas *42*, 663-669.
Malanchi, I., Peinado, H., Kassen, D., Hussenet, T., Metzger, D., Chambon, P., Huber, M., Hohl, D., Cano, A., Birchmeier, W.*, et al.* (2008). Cutaneous cancer stem cell maintenance is dependent on beta-catenin signalling. Nature *452*, 650-653.
Malinin, N.L., Zhang, L., Choi, J., Ciocea, A., Razorenova, O., Ma, Y.Q., Podrez, E.A., Tosi, M., Lennon, D.P., Caplan, A.I.*, et al.* (2009). A point mutation in KINDLIN3 ablates activation of three integrin subfamilies in humans. Nature medicine *15*, 313-318.
Mansur, A.T., Elcioglu, N.H., Aydingoz, I.E., Akkaya, A.D., Serdar, Z.A., Herz, C., Bruckner-Tuderman, L., and Has, C. (2007). Novel and recurrent KIND1 mutations in two patients with Kindler syndrome and severe mucosal involvement. Acta dermato-venereologica *87*, 563-565.
Mao, B., Wu, W., Davidson, G., Marhold, J., Li, M., Mechler, B.M., Delius, H., Hoppe, D., Stannek, P., Walter, C.*, et al.* (2002). Kremen proteins are Dickkopf receptors that regulate Wnt/beta-catenin signalling. Nature *417*, 664-667.
Mao, R., Fan, Y., Mou, Y., Zhang, H., Fu, S., and Yang, J. (2011). TAK1 lysine 158 is required for TGF-beta-induced TRAF6-mediated Smad-independent IKK/NF-kappaB and JNK/AP-1 activation. Cellular signalling *23*, 222-227.
Margadant, C., Kreft, M., Zambruno, G., and Sonnenberg, A. (2013). Kindlin-1 regulates integrin dynamics and adhesion turnover. PloS one *8*, e65341.
Martel, V., Racaud-Sultan, C., Dupe, S., Marie, C., Paulhe, F., Galmiche, A., Block, M.R., and Albiges-Rizo, C. (2001). Conformation, localization, and integrin binding of talin depend on its interaction with phosphoinositides. The Journal of biological chemistry *276*, 21217-21227.
Martinez-Ferrer, M., Afshar-Sherif, A.R., Uwamariya, C., de Crombrugghe, B., Davidson, J.M., and Bhowmick, N.A. (2010). Dermal transforming growth factor-beta responsiveness mediates wound contraction and epithelial closure. The American journal of pathology *176*, 98-107.
Massague, J. (1998). TGF-beta signal transduction. Annual review of biochemistry *67*, 753-791.
Massague, J. (2008). TGFbeta in Cancer. Cell *134*, 215-230.
Massague, J. (2012). TGFbeta signalling in context. Nature reviews Molecular cell biology *13*, 616-630.
Massague, J., and Gomis, R.R. (2006). The logic of TGFbeta signaling. FEBS letters *580*, 2811-2820.
Meng, W., and Takeichi, M. (2009). Adherens junction: molecular architecture and regulation. Cold Spring Harbor perspectives in biology *1*, a002899.
Meves, A., Stremmel, C., Bottcher, R.T., and Fassler, R. (2013). beta1 integrins with individually disrupted cytoplasmic NPxY motifs are embryonic lethal but partially active in the epidermis. The Journal of investigative dermatology *133*, 2722-2731.
Mikels, A.J., and Nusse, R. (2006). Purified Wnt5a protein activates or inhibits beta-catenin-TCF signaling depending on receptor context. PLoS biology *4*, e115.

Mizutani, H., Masuda, K., Nakamura, N., Takenaka, H., Tsuruta, D., and Katoh, N. (2012). Cutaneous and laryngeal squamous cell carcinoma in mixed epidermolysis bullosa, kindler syndrome. Case reports in dermatology *4*, 133-138.

Mohammed, J., Ryscavage, A., Perez-Lorenzo, R., Gunderson, A.J., Blazanin, N., and Glick, A.B. (2010). TGFbeta1-induced inflammation in premalignant epidermal squamous lesions requires IL-17. The Journal of investigative dermatology *130*, 2295-2303.

Montanez, E., Ussar, S., Schifferer, M., Bosl, M., Zent, R., Moser, M., and Fassler, R. (2008). Kindlin-2 controls bidirectional signaling of integrins. Genes & development *22*, 1325-1330.

Moretti, F.A., Moser, M., Lyck, R., Abadier, M., Ruppert, R., Engelhardt, B., and Fassler, R. (2013). Kindlin-3 regulates integrin activation and adhesion reinforcement of effector T cells. Proceedings of the National Academy of Sciences of the United States of America *110*, 17005-17010.

Morgan, M.R., Jazayeri, M., Ramsay, A.G., Thomas, G.J., Boulanger, M.J., Hart, I.R., and Marshall, J.F. (2011). Psoriasin (S100A7) associates with integrin beta6 subunit and is required for alphavbeta6-dependent carcinoma cell invasion. Oncogene *30*, 1422-1435.

Morin, P.J., Sparks, A.B., Korinek, V., Barker, N., Clevers, H., Vogelstein, B., and Kinzler, K.W. (1997). Activation of beta-catenin-Tcf signaling in colon cancer by mutations in beta-catenin or APC. Science *275*, 1787-1790.

Moriyama, M., Osawa, M., Mak, S.S., Ohtsuka, T., Yamamoto, N., Han, H., Delmas, V., Kageyama, R., Beermann, F., Larue, L*., et al.* (2006). Notch signaling via Hes1 transcription factor maintains survival of melanoblasts and melanocyte stem cells. The Journal of cell biology *173*, 333-339.

Moro, L., Dolce, L., Cabodi, S., Bergatto, E., Boeri Erba, E., Smeriglio, M., Turco, E., Retta, S.F., Giuffrida, M.G., Venturino, M*., et al.* (2002). Integrin-induced epidermal growth factor (EGF) receptor activation requires c-Src and p130Cas and leads to phosphorylation of specific EGF receptor tyrosines. The Journal of biological chemistry *277*, 9405-9414.

Morris, R.J., Liu, Y., Marles, L., Yang, Z., Trempus, C., Li, S., Lin, J.S., Sawicki, J.A., and Cotsarelis, G. (2004). Capturing and profiling adult hair follicle stem cells. Nature biotechnology *22*, 411-417.

Morrison, V.L., MacPherson, M., Savinko, T., Lek, H.S., Prescott, A., and Fagerholm, S.C. (2013). The beta2 integrin-kindlin-3 interaction is essential for T-cell homing but dispensable for T-cell activation in vivo. Blood *122*, 1428-1436.

Moser, M., Bauer, M., Schmid, S., Ruppert, R., Schmidt, S., Sixt, M., Wang, H.V., Sperandio, M., and Fassler, R. (2009a). Kindlin-3 is required for beta2 integrin-mediated leukocyte adhesion to endothelial cells. Nature medicine *15*, 300-305.

Moser, M., Legate, K.R., Zent, R., and Fassler, R. (2009b). The tail of integrins, talin, and kindlins. Science *324*, 895-899.

Moser, M., Nieswandt, B., Ussar, S., Pozgajova, M., and Fassler, R. (2008). Kindlin-3 is essential for integrin activation and platelet aggregation. Nature medicine *14*, 325-330.

Mu, D., Cambier, S., Fjellbirkeland, L., Baron, J.L., Munger, J.S., Kawakatsu, H., Sheppard, D., Broaddus, V.C., and Nishimura, S.L. (2002). The integrin alpha(v)beta8 mediates epithelial homeostasis through MT1-MMP-dependent activation of TGF-beta1. The Journal of cell biology *157*, 493-507.

Mu, Y., Gudey, S.K., and Landstrom, M. (2012). Non-Smad signaling pathways. Cell and tissue research *347*, 11-20.

Mullen, A.C., Orlando, D.A., Newman, J.J., Loven, J., Kumar, R.M., Bilodeau, S., Reddy, J., Guenther, M.G., DeKoter, R.P., and Young, R.A. (2011). Master transcription factors determine cell-type-specific responses to TGF-beta signaling. Cell *147*, 565-576.

Muller-Rover, S., Handjiski, B., van der Veen, C., Eichmuller, S., Foitzik, K., McKay, I.A., Stenn, K.S., and Paus, R. (2001). A comprehensive guide for the accurate classification of murine hair follicles in distinct hair cycle stages. The Journal of investigative dermatology *117*, 3-15.

Mumm, J.S., and Kopan, R. (2000). Notch signaling: from the outside in. Developmental biology *228*, 151-165.
Munger, J.S., Harpel, J.G., Giancotti, F.G., and Rifkin, D.B. (1998). Interactions between growth factors and integrins: latent forms of transforming growth factor-beta are ligands for the integrin alphavbeta1. Molecular biology of the cell *9*, 2627-2638.
Munger, J.S., Huang, X., Kawakatsu, H., Griffiths, M.J., Dalton, S.L., Wu, J., Pittet, J.F., Kaminski, N., Garat, C., Matthay, M.A.*, et al.* (1999). The integrin alpha v beta 6 binds and activates latent TGF beta 1: a mechanism for regulating pulmonary inflammation and fibrosis. Cell *96*, 319-328.
Murphy-Ullrich, J.E., and Poczatek, M. (2000). Activation of latent TGF-beta by thrombospondin-1: mechanisms and physiology. Cytokine & growth factor reviews *11*, 59-69.
Niehrs, C. (2012). The complex world of WNT receptor signalling. Nature reviews Molecular cell biology *13*, 767-779.
Niemann, C., Owens, D.M., Hulsken, J., Birchmeier, W., and Watt, F.M. (2002). Expression of DeltaNLef1 in mouse epidermis results in differentiation of hair follicles into squamous epidermal cysts and formation of skin tumours. Development *129*, 95-109.
Nijhof, J.G., Braun, K.M., Giangreco, A., van Pelt, C., Kawamoto, H., Boyd, R.L., Willemze, R., Mullenders, L.H., Watt, F.M., de Gruijl, F.R.*, et al.* (2006). The cell-surface marker MTS24 identifies a novel population of follicular keratinocytes with characteristics of progenitor cells. Development *133*, 3027-3037.
Nishida, N., Xie, C., Shimaoka, M., Cheng, Y., Walz, T., and Springer, T.A. (2006). Activation of leukocyte beta2 integrins by conversion from bent to extended conformations. Immunity *25*, 583-594.
Nishimura, E.K., Jordan, S.A., Oshima, H., Yoshida, H., Osawa, M., Moriyama, M., Jackson, I.J., Barrandon, Y., Miyachi, Y., and Nishikawa, S. (2002). Dominant role of the niche in melanocyte stem-cell fate determination. Nature *416*, 854-860.
Nishimura, E.K., Suzuki, M., Igras, V., Du, J., Lonning, S., Miyachi, Y., Roes, J., Beermann, F., and Fisher, D.E. (2010). Key roles for transforming growth factor beta in melanocyte stem cell maintenance. Cell stem cell *6*, 130-140.
Nunes, I., Gleizes, P.E., Metz, C.N., and Rifkin, D.B. (1997). Latent transforming growth factor-beta binding protein domains involved in activation and transglutaminase-dependent cross-linking of latent transforming growth factor-beta. The Journal of cell biology *136*, 1151-1163.
Ohyama, M., Terunuma, A., Tock, C.L., Radonovich, M.F., Pise-Masison, C.A., Hopping, S.B., Brady, J.N., Udey, M.C., and Vogel, J.C. (2006). Characterization and isolation of stem cell-enriched human hair follicle bulge cells. The Journal of clinical investigation *116*, 249-260.
Okuse, T., Chiba, T., Katsuumi, I., and Imai, K. (2005). Differential expression and localization of WNTs in an animal model of skin wound healing. Wound repair and regeneration : official publication of the Wound Healing Society [and] the European Tissue Repair Society *13*, 491-497.
Osawa, M. (2008). Melanocyte stem cells. In StemBook (Cambridge (MA)).
Oshimori, N., and Fuchs, E. (2012). Paracrine TGF-beta signaling counterbalances BMP-mediated repression in hair follicle stem cell activation. Cell stem cell *10*, 63-75.
Owens, D.M., and Watt, F.M. (2003). Contribution of stem cells and differentiated cells to epidermal tumours. Nature reviews Cancer *3*, 444-451.
Oxley, C.L., Anthis, N.J., Lowe, E.D., Vakonakis, I., Campbell, I.D., and Wegener, K.L. (2008). An integrin phosphorylation switch: the effect of beta3 integrin tail phosphorylation on Dok1 and talin binding. The Journal of biological chemistry *283*, 5420-5426.
Ozdamar, B., Bose, R., Barrios-Rodiles, M., Wang, H.R., Zhang, Y., and Wrana, J.L. (2005). Regulation of the polarity protein Par6 by TGFbeta receptors controls epithelial cell plasticity. Science *307*, 1603-1609.

Pan, Y., Lin, M.H., Tian, X., Cheng, H.T., Gridley, T., Shen, J., and Kopan, R. (2004). gamma-secretase functions through Notch signaling to maintain skin appendages but is not required for their patterning or initial morphogenesis. Developmental cell *7*, 731-743.
Panakova, D., Sprong, H., Marois, E., Thiele, C., and Eaton, S. (2005). Lipoprotein particles are required for Hedgehog and Wingless signalling. Nature *435*, 58-65.
Papa, C.M., and Kligman, A.M. (1965). The behavior of melanocytes in inflammation. The Journal of investigative dermatology *45*, 465-473.
Park, K.S. (2011). TGF-beta Family Signaling in Embryonic Stem Cells. International journal of stem cells *4*, 18-23.
Patel, H., Zich, J., Serrels, B., Rickman, C., Hardwick, K.G., Frame, M.C., and Brunton, V.G. (2013). Kindlin-1 regulates mitotic spindle formation by interacting with integrins and Plk-1. Nature communications *4*, 2056.
Paus, R., and Foitzik, K. (2004). In search of the "hair cycle clock": a guided tour. Differentiation; research in biological diversity *72*, 489-511.
Paus, R., Muller-Rover, S., Van Der Veen, C., Maurer, M., Eichmuller, S., Ling, G., Hofmann, U., Foitzik, K., Mecklenburg, L., and Handjiski, B. (1999). A comprehensive guide for the recognition and classification of distinct stages of hair follicle morphogenesis. The Journal of investigative dermatology *113*, 523-532.
Pechkovsky, D.V., Scaffidi, A.K., Hackett, T.L., Ballard, J., Shaheen, F., Thompson, P.J., Thannickal, V.J., and Knight, D.A. (2008). Transforming growth factor beta1 induces alphavbeta3 integrin expression in human lung fibroblasts via a beta3 integrin-, c-Src-, and p38 MAPK-dependent pathway. The Journal of biological chemistry *283*, 12898-12908.
Penagos, H., Jaen, M., Sancho, M.T., Saborio, M.R., Fallas, V.G., Siegel, D.H., and Frieden, I.J. (2004). Kindler syndrome in native Americans from Panama: report of 26 cases. Archives of dermatology *140*, 939-944.
Perez-Losada, J., and Balmain, A. (2003). Stem-cell hierarchy in skin cancer. Nature reviews Cancer *3*, 434-443.
Petersen, C.P., and Reddien, P.W. (2009). Wnt signaling and the polarity of the primary body axis. Cell *139*, 1056-1068.
Piccinni, E., Di Zenzo, G., Maurelli, R., Dellambra, E., Teson, M., Has, C., Zambruno, G., and Castiglia, D. (2013). Induction of senescence pathways in Kindler syndrome primary keratinocytes. The British journal of dermatology *168*, 1019-1026.
Pinson, K.I., Brennan, J., Monkley, S., Avery, B.J., and Skarnes, W.C. (2000). An LDL-receptor-related protein mediates Wnt signalling in mice. Nature *407*, 535-538.
Piwko-Czuchra, A., Koegel, H., Meyer, H., Bauer, M., Werner, S., Brakebusch, C., and Fassler, R. (2009). Beta1 integrin-mediated adhesion signalling is essential for epidermal progenitor cell expansion. PloS one *4*, e5488.
Plikus, M.V., and Chuong, C.M. (2008). Complex hair cycle domain patterns and regenerative hair waves in living rodents. The Journal of investigative dermatology *128*, 1071-1080.
Plikus, M.V., Mayer, J.A., de la Cruz, D., Baker, R.E., Maini, P.K., Maxson, R., and Chuong, C.M. (2008). Cyclic dermal BMP signalling regulates stem cell activation during hair regeneration. Nature *451*, 340-344.
Pluskota, E., Dowling, J.J., Gordon, N., Golden, J.A., Szpak, D., West, X.Z., Nestor, C., Ma, Y.Q., Bialkowska, K., Byzova, T.*, et al.* (2011). The integrin coactivator kindlin-2 plays a critical role in angiogenesis in mice and zebrafish. Blood *117*, 4978-4987.
Pluskota, E., Ma, Y., Bledzka, K.M., Bialkowska, K., Soloviev, D.A., Szpak, D., Podrez, E.A., Fox, P.L., Hazen, S.L., Dowling, J.J.*, et al.* (2013). Kindlin-2 regulates hemostasis by controlling endothelial

cell-surface expression of ADP/AMP catabolic enzymes via a clathrin-dependent mechanism. Blood *122*, 2491-2499.
Powell, B.C., Passmore, E.A., Nesci, A., and Dunn, S.M. (1998). The Notch signalling pathway in hair growth. Mechanisms of development *78*, 189-192.
Proweller, A., Tu, L., Lepore, J.J., Cheng, L., Lu, M.M., Seykora, J., Millar, S.E., Pear, W.S., and Parmacek, M.S. (2006). Impaired notch signaling promotes de novo squamous cell carcinoma formation. Cancer research *66*, 7438-7444.
Qadota, H., Moerman, D.G., and Benian, G.M. (2012). A molecular mechanism for the requirement of PAT-4 (integrin-linked kinase (ILK)) for the localization of UNC-112 (Kindlin) to integrin adhesion sites. The Journal of biological chemistry *287*, 28537-28551.
Qu, H., Tu, Y., Shi, X., Larjava, H., Saleem, M.A., Shattil, S.J., Fukuda, K., Qin, J., Kretzler, M., and Wu, C. (2011). Kindlin-2 regulates podocyte adhesion and fibronectin matrix deposition through interactions with phosphoinositides and integrins. Journal of cell science *124*, 879-891.
Qu, H., Wen, T., Pesch, M., and Aumailley, M. (2012). Partial loss of epithelial phenotype in kindlin-1-deficient keratinocytes. The American journal of pathology *180*, 1581-1592.
Rabbani, P., Takeo, M., Chou, W., Myung, P., Bosenberg, M., Chin, L., Taketo, M.M., and Ito, M. (2011). Coordinated activation of Wnt in epithelial and melanocyte stem cells initiates pigmented hair regeneration. Cell *145*, 941-955.
Raghavan, S., Bauer, C., Mundschau, G., Li, Q., and Fuchs, E. (2000). Conditional ablation of beta1 integrin in skin. Severe defects in epidermal proliferation, basement membrane formation, and hair follicle invagination. The Journal of cell biology *150*, 1149-1160.
Ramesh, S., Qi, X.J., Wildey, G.M., Robinson, J., Molkentin, J., Letterio, J., and Howe, P.H. (2008). TGF beta-mediated BIM expression and apoptosis are regulated through SMAD3-dependent expression of the MAPK phosphatase MKP2. EMBO reports *9*, 990-997.
Ramos, D.M., Dang, D., and Sadler, S. (2009). The role of the integrin alpha v beta6 in regulating the epithelial to mesenchymal transition in oral cancer. Anticancer research *29*, 125-130.
Ramsay, A.G., Keppler, M.D., Jazayeri, M., Thomas, G.J., Parsons, M., Violette, S., Weinreb, P., Hart, I.R., and Marshall, J.F. (2007). HS1-associated protein X-1 regulates carcinoma cell migration and invasion via clathrin-mediated endocytosis of integrin alphavbeta6. Cancer research *67*, 5275-5284.
Rangarajan, A., Talora, C., Okuyama, R., Nicolas, M., Mammucari, C., Oh, H., Aster, J.C., Krishna, S., Metzger, D., Chambon, P*., et al.* (2001). Notch signaling is a direct determinant of keratinocyte growth arrest and entry into differentiation. The EMBO journal *20*, 3427-3436.
Rawles, M.E. (1947). Origin of pigment cells from the neural crest in the mouse embryo. Physiological zoology *20*, 248-266.
Ren, C., Du, J., Xi, C., Yu, Y., Hu, A., Zhan, J., Guo, H., Fang, W., Liu, C., and Zhang, H. (2014). Kindlin-2 inhibits serous epithelial ovarian cancer peritoneal dissemination and predicts patient outcomes. Biochemical and biophysical research communications *446*, 187-194.
Roberts, D.M., Pronobis, M.I., Poulton, J.S., Waldmann, J.D., Stephenson, E.M., Hanna, S., and Peifer, M. (2011). Deconstructing the sscatenin destruction complex: mechanistic roles for the tumor suppressor APC in regulating Wnt signaling. Molecular biology of the cell *22*, 1845-1863.
Rogalski, T.M., Mullen, G.P., Gilbert, M.M., Williams, B.D., and Moerman, D.G. (2000). The UNC-112 gene in Caenorhabditis elegans encodes a novel component of cell-matrix adhesion structures required for integrin localization in the muscle cell membrane. The Journal of cell biology *150*, 253-264.
Rompolas, P., Mesa, K.R., and Greco, V. (2013). Spatial organization within a niche as a determinant of stem-cell fate. Nature *502*, 513-518.

Rowan, A.J., Lamlum, H., Ilyas, M., Wheeler, J., Straub, J., Papadopoulou, A., Bicknell, D., Bodmer, W.F., and Tomlinson, I.P. (2000). APC mutations in sporadic colorectal tumors: A mutational "hotspot" and interdependence of the "two hits". Proceedings of the National Academy of Sciences of the United States of America *97*, 3352-3357.

Rubinfeld, B., Robbins, P., El-Gamil, M., Albert, I., Porfiri, E., and Polakis, P. (1997). Stabilization of beta-catenin by genetic defects in melanoma cell lines. Science *275*, 1790-1792.

Ruzinova, M.B., and Benezra, R. (2003). Id proteins in development, cell cycle and cancer. Trends in cell biology *13*, 410-418.

Sadot, E., Simcha, I., Iwai, K., Ciechanover, A., Geiger, B., and Ben-Ze'ev, A. (2000). Differential interaction of plakoglobin and beta-catenin with the ubiquitin-proteasome system. Oncogene *19*, 1992-2001.

Saharinen, J., and Keski-Oja, J. (2000). Specific sequence motif of 8-Cys repeats of TGF-beta binding proteins, LTBPs, creates a hydrophobic interaction surface for binding of small latent TGF-beta. Molecular biology of the cell *11*, 2691-2704.

Saldanha, R.G., Molloy, M.P., Bdeir, K., Cines, D.B., Song, X., Uitto, P.M., Weinreb, P.H., Violette, S.M., and Baker, M.S. (2007). Proteomic identification of lynchpin urokinase plasminogen activator receptor protein interactions associated with epithelial cancer malignancy. Journal of proteome research *6*, 1016-1028.

Santoro, M.M., and Gaudino, G. (2005). Cellular and molecular facets of keratinocyte reepithelization during wound healing. Experimental cell research *304*, 274-286.

Saxena, M.T., Schroeter, E.H., Mumm, J.S., and Kopan, R. (2001). Murine notch homologs (N1-4) undergo presenilin-dependent proteolysis. The Journal of biological chemistry *276*, 40268-40273.

Scharffetter-Kochanek, K., Lu, H., Norman, K., van Nood, N., Munoz, F., Grabbe, S., McArthur, M., Lorenzo, I., Kaplan, S., Ley, K*., et al.* (1998). Spontaneous skin ulceration and defective T cell function in CD18 null mice. The Journal of experimental medicine *188*, 119-131.

Schiller, H.B., Hermann, M.R., Polleux, J., Vignaud, T., Zanivan, S., Friedel, C.C., Sun, Z., Raducanu, A., Gottschalk, K.E., Thery, M*., et al.* (2013). beta1- and alphav-class integrins cooperate to regulate myosin II during rigidity sensing of fibronectin-based microenvironments. Nature cell biology *15*, 625-636.

Schmidt, S., Nakchbandi, I., Ruppert, R., Kawelke, N., Hess, M.W., Pfaller, K., Jurdic, P., Fassler, R., and Moser, M. (2011). Kindlin-3-mediated signaling from multiple integrin classes is required for osteoclast-mediated bone resorption. The Journal of cell biology *192*, 883-897.

Schneider, M.R., Schmidt-Ullrich, R., and Paus, R. (2009). The hair follicle as a dynamic miniorgan. Current biology : CB *19*, R132-142.

Schoppet, M., Chavakis, T., Al-Fakhri, N., Kanse, S.M., and Preissner, K.T. (2002). Molecular interactions and functional interference between vitronectin and transforming growth factor-beta. Laboratory investigation; a journal of technical methods and pathology *82*, 37-46.

Schwarz-Romond, T., Fiedler, M., Shibata, N., Butler, P.J., Kikuchi, A., Higuchi, Y., and Bienz, M. (2007). The DIX domain of Dishevelled confers Wnt signaling by dynamic polymerization. Nature structural & molecular biology *14*, 484-492.

Senetar, M.A., Foster, S.J., and McCann, R.O. (2004). Intrasteric inhibition mediates the interaction of the I/LWEQ module proteins Talin1, Talin2, Hip1, and Hip12 with actin. Biochemistry *43*, 15418-15428.

Sharov, A., Tobin, D.J., Sharova, T.Y., Atoyan, R., and Botchkarev, V.A. (2005). Changes in different melanocyte populations during hair follicle involution (catagen). The Journal of investigative dermatology *125*, 1259-1267.

Shattil, S.J., Kim, C., and Ginsberg, M.H. (2010). The final steps of integrin activation: the end game. Nature reviews Molecular cell biology *11*, 288-300.

Shen, Z., Ye, Y., Kauttu, T., Seppanen, H., Vainionpaa, S., Wang, S., Mustonen, H., and Puolakkainen, P. (2013). Novel focal adhesion protein kindlin-2 promotes the invasion of gastric cancer cells through phosphorylation of integrin beta1 and beta3. Journal of surgical oncology *108*, 106-112.

Shi, M., Zhu, J., Wang, R., Chen, X., Mi, L., Walz, T., and Springer, T.A. (2011). Latent TGF-beta structure and activation. Nature *474*, 343-349.

Shi, W., Sun, C., He, B., Xiong, W., Shi, X., Yao, D., and Cao, X. (2004). GADD34-PP1c recruited by Smad7 dephosphorylates TGFbeta type I receptor. The Journal of cell biology *164*, 291-300.

Shi, X., and Wu, C. (2008). A suppressive role of mitogen inducible gene-2 in mesenchymal cancer cell invasion. Molecular cancer research : MCR *6*, 715-724.

Shi, Y., and Massague, J. (2003). Mechanisms of TGF-beta signaling from cell membrane to the nucleus. Cell *113*, 685-700.

Shimaoka, M., Shifman, J.M., Jing, H., Takagi, J., Mayo, S.L., and Springer, T.A. (2000). Computational design of an integrin I domain stabilized in the open high affinity conformation. Nature structural biology *7*, 674-678.

Shull, M.M., Ormsby, I., Kier, A.B., Pawlowski, S., Diebold, R.J., Yin, M., Allen, R., Sidman, C., Proetzel, G., Calvin, D*., et al.* (1992). Targeted disruption of the mouse transforming growth factor-beta 1 gene results in multifocal inflammatory disease. Nature *359*, 693-699.

Sick, S., Reinker, S., Timmer, J., and Schlake, T. (2006). WNT and DKK determine hair follicle spacing through a reaction-diffusion mechanism. Science *314*, 1447-1450.

Siegel, D.H., Ashton, G.H., Penagos, H.G., Lee, J.V., Feiler, H.S., Wilhelmsen, K.C., South, A.P., Smith, F.J., Prescott, A.R., Wessagowit, V*., et al.* (2003). Loss of kindlin-1, a human homolog of the Caenorhabditis elegans actin-extracellular-matrix linker protein UNC-112, causes Kindler syndrome. American journal of human genetics *73*, 174-187.

Siegel, P.M., and Massague, J. (2003). Cytostatic and apoptotic actions of TGF-beta in homeostasis and cancer. Nature reviews Cancer *3*, 807-821.

Silva-Vargas, V., Lo Celso, C., Giangreco, A., Ofstad, T., Prowse, D.M., Braun, K.M., and Watt, F.M. (2005). Beta-catenin and Hedgehog signal strength can specify number and location of hair follicles in adult epidermis without recruitment of bulge stem cells. Developmental cell *9*, 121-131.

Sin, S., Bonin, F., Petit, V., Meseure, D., Lallemand, F., Bieche, I., Bellahcene, A., Castronovo, V., de Wever, O., Gespach, C*., et al.* (2011). Role of the focal adhesion protein kindlin-1 in breast cancer growth and lung metastasis. Journal of the National Cancer Institute *103*, 1323-1337.

Slominski, A., Wortsman, J., Plonka, P.M., Schallreuter, K.U., Paus, R., and Tobin, D.J. (2005). Hair follicle pigmentation. The Journal of investigative dermatology *124*, 13-21.

Smith, S.J., and McCann, R.O. (2007). A C-terminal dimerization motif is required for focal adhesion targeting of Talin1 and the interaction of the Talin1 I/LWEQ module with F-actin. Biochemistry *46*, 10886-10898.

Snippert, H.J., Haegebarth, A., Kasper, M., Jaks, V., van Es, J.H., Barker, N., van de Wetering, M., van den Born, M., Begthel, H., Vries, R.G*., et al.* (2010). Lgr6 marks stem cells in the hair follicle that generate all cell lineages of the skin. Science *327*, 1385-1389.

Soma, T., Tsuji, Y., and Hibino, T. (2002). Involvement of transforming growth factor-beta2 in catagen induction during the human hair cycle. The Journal of investigative dermatology *118*, 993-997.

Sossey-Alaoui, K., Pluskota, E., Davuluri, G., Bialkowska, K., Das, M., Szpak, D., Lindner, D.J., Downs-Kelly, E., Thompson, C.L., and Plow, E.F. (2014). Kindlin-3 enhances breast cancer progression and metastasis by activating Twist-mediated angiogenesis. FASEB journal : official publication of the Federation of American Societies for Experimental Biology *28*, 2260-2271.

Stadeli, R., and Basler, K. (2005). Dissecting nuclear Wingless signalling: recruitment of the transcriptional co-activator Pygopus by a chain of adaptor proteins. Mechanisms of development *122*, 1171-1182.

Stenn, K.S., and Paus, R. (2001). Controls of hair follicle cycling. Physiological reviews *81*, 449-494.

Stupack, D.G., Puente, X.S., Boutsaboualoy, S., Storgard, C.M., and Cheresh, D.A. (2001). Apoptosis of adherent cells by recruitment of caspase-8 to unligated integrins. The Journal of cell biology *155*, 459-470.

Sugioka, K., Mizumoto, K., and Sawa, H. (2011). Wnt regulates spindle asymmetry to generate asymmetric nuclear beta-catenin in C. elegans. Cell *146*, 942-954.

Sun, Y.X., Fang, M., Wang, J., Cooper, C.R., Pienta, K.J., and Taichman, R.S. (2007). Expression and activation of alpha v beta 3 integrins by SDF-1/CXC12 increases the aggressiveness of prostate cancer cells. The Prostate *67*, 61-73.

Svensson, L., Howarth, K., McDowall, A., Patzak, I., Evans, R., Ussar, S., Moser, M., Metin, A., Fried, M., Tomlinson, I.*, et al.* (2009). Leukocyte adhesion deficiency-III is caused by mutations in KINDLIN3 affecting integrin activation. Nature medicine *15*, 306-312.

Taipale, J., Miyazono, K., Heldin, C.H., and Keski-Oja, J. (1994). Latent transforming growth factor-beta 1 associates to fibroblast extracellular matrix via latent TGF-beta binding protein. The Journal of cell biology *124*, 171-181.

Takada, R., Satomi, Y., Kurata, T., Ueno, N., Norioka, S., Kondoh, H., Takao, T., and Takada, S. (2006). Monounsaturated fatty acid modification of Wnt protein: its role in Wnt secretion. Developmental cell *11*, 791-801.

Takeda, H., Lyle, S., Lazar, A.J., Zouboulis, C.C., Smyth, I., and Watt, F.M. (2006). Human sebaceous tumors harbor inactivating mutations in LEF1. Nature medicine *12*, 395-397.

Talaat, S., Somji, S., Toni, C., Garrett, S.H., Zhou, X.D., Sens, M.A., and Sens, D.A. (2011). Kindlin-2 expression in arsenite- and cadmium-transformed bladder cancer cell lines and in archival specimens of human bladder cancer. Urology *77*, 1507 e1501-1507.

Tamai, K., Semenov, M., Kato, Y., Spokony, R., Liu, C., Katsuyama, Y., Hess, F., Saint-Jeannet, J.P., and He, X. (2000). LDL-receptor-related proteins in Wnt signal transduction. Nature *407*, 530-535.

Tang, Y., Liu, Z., Zhao, L., Clemens, T.L., and Cao, X. (2008). Smad7 stabilizes beta-catenin binding to E-cadherin complex and promotes cell-cell adhesion. The Journal of biological chemistry *283*, 23956-23963.

Taylor, G., Lehrer, M.S., Jensen, P.J., Sun, T.T., and Lavker, R.M. (2000). Involvement of follicular stem cells in forming not only the follicle but also the epidermis. Cell *102*, 451-461.

ten Dijke, P., and Arthur, H.M. (2007). Extracellular control of TGFbeta signalling in vascular development and disease. Nature reviews Molecular cell biology *8*, 857-869.

Thomas, G.J., Lewis, M.P., Hart, I.R., Marshall, J.F., and Speight, P.M. (2001). AlphaVbeta6 integrin promotes invasion of squamous carcinoma cells through up-regulation of matrix metalloproteinase-9. International journal of cancer Journal international du cancer *92*, 641-650.

Thomas, G.J., Nystrom, M.L., and Marshall, J.F. (2006). Alphavbeta6 integrin in wound healing and cancer of the oral cavity. Journal of oral pathology & medicine : official publication of the International Association of Oral Pathologists and the American Academy of Oral Pathology *35*, 1-10.

Trempus, C.S., Morris, R.J., Bortner, C.D., Cotsarelis, G., Faircloth, R.S., Reece, J.M., and Tennant, R.W. (2003). Enrichment for living murine keratinocytes from the hair follicle bulge with the cell surface marker CD34. The Journal of investigative dermatology *120*, 501-511.

Tu, Y., Wu, S., Shi, X., Chen, K., and Wu, C. (2003). Migfilin and Mig-2 link focal adhesions to filamin and the actin cytoskeleton and function in cell shape modulation. Cell *113*, 37-47.

Tumbar, T., Guasch, G., Greco, V., Blanpain, C., Lowry, W.E., Rendl, M., and Fuchs, E. (2004). Defining the epithelial stem cell niche in skin. Science *303*, 359-363.
Ulsamer, A., Wei, Y., Kim, K.K., Tan, K., Wheeler, S., Xi, Y., Thies, R.S., and Chapman, H.A. (2012). Axin pathway activity regulates in vivo pY654-beta-catenin accumulation and pulmonary fibrosis. The Journal of biological chemistry *287*, 5164-5172.
Uren, A., Reichsman, F., Anest, V., Taylor, W.G., Muraiso, K., Bottaro, D.P., Cumberledge, S., and Rubin, J.S. (2000). Secreted frizzled-related protein-1 binds directly to Wingless and is a biphasic modulator of Wnt signaling. The Journal of biological chemistry *275*, 4374-4382.
Ussar, S., Moser, M., Widmaier, M., Rognoni, E., Harrer, C., Genzel-Boroviczeny, O., and Fassler, R. (2008). Loss of Kindlin-1 causes skin atrophy and lethal neonatal intestinal epithelial dysfunction. PLoS genetics *4*, e1000289.
Ussar, S., Wang, H.V., Linder, S., Fassler, R., and Moser, M. (2006). The Kindlins: subcellular localization and expression during murine development. Experimental cell research *312*, 3142-3151.
Uyttendaele, H., Panteleyev, A.A., de Berker, D., Tobin, D.T., and Christiano, A.M. (2004). Activation of Notch1 in the hair follicle leads to cell-fate switch and Mohawk alopecia. Differentiation; research in biological diversity *72*, 396-409.
Valderrama-Carvajal, H., Cocolakis, E., Lacerte, A., Lee, E.H., Krystal, G., Ali, S., and Lebrun, J.J. (2002). Activin/TGF-beta induce apoptosis through Smad-dependent expression of the lipid phosphatase SHIP. Nature cell biology *4*, 963-969.
van Amerongen, R., Mikels, A., and Nusse, R. (2008). Alternative wnt signaling is initiated by distinct receptors. Science signaling *1*, re9.
van der Neut, R., Krimpenfort, P., Calafat, J., Niessen, C.M., and Sonnenberg, A. (1996). Epithelial detachment due to absence of hemidesmosomes in integrin beta 4 null mice. Nature genetics *13*, 366-369.
van Genderen, C., Okamura, R.M., Farinas, I., Quo, R.G., Parslow, T.G., Bruhn, L., and Grosschedl, R. (1994). Development of several organs that require inductive epithelial-mesenchymal interactions is impaired in LEF-1-deficient mice. Genes & development *8*, 2691-2703.
Van Mater, D., Kolligs, F.T., Dlugosz, A.A., and Fearon, E.R. (2003). Transient activation of beta -catenin signaling in cutaneous keratinocytes is sufficient to trigger the active growth phase of the hair cycle in mice. Genes & development *17*, 1219-1224.
Vidal, V.P., Chaboissier, M.C., Lutzkendorf, S., Cotsarelis, G., Mill, P., Hui, C.C., Ortonne, N., Ortonne, J.P., and Schedl, A. (2005). Sox9 is essential for outer root sheath differentiation and the formation of the hair stem cell compartment. Current biology : CB *15*, 1340-1351.
Vincent, T., Neve, E.P., Johnson, J.R., Kukalev, A., Rojo, F., Albanell, J., Pietras, K., Virtanen, I., Philipson, L., Leopold, P.L.*, et al.* (2009). A SNAIL1-SMAD3/4 transcriptional repressor complex promotes TGF-beta mediated epithelial-mesenchymal transition. Nature cell biology *11*, 943-950.
Vleminckx, K., Kemler, R., and Hecht, A. (1999). The C-terminal transactivation domain of beta-catenin is necessary and sufficient for signaling by the LEF-1/beta-catenin complex in Xenopus laevis. Mechanisms of development *81*, 65-74.
Wagner, N., Lohler, J., Kunkel, E.J., Ley, K., Leung, E., Krissansen, G., Rajewsky, K., and Muller, W. (1996). Critical role for beta7 integrins in formation of the gut-associated lymphoid tissue. Nature *382*, 366-370.
Watt, F.M., and Jensen, K.B. (2009). Epidermal stem cell diversity and quiescence. EMBO molecular medicine *1*, 260-267.
Wegener, K.L., Partridge, A.W., Han, J., Pickford, A.R., Liddington, R.C., Ginsberg, M.H., and Campbell, I.D. (2007). Structural basis of integrin activation by talin. Cell *128*, 171-182.

Wei, X., Wang, X., Xia, Y., Tang, Y., Li, F., Fang, W., and Zhang, H. (2014). Kindlin-2 regulates renal tubular cell plasticity by activation of Ras and its downstream signaling. American journal of physiology Renal physiology *306*, F271-278.

Wei, X., Xia, Y., Li, F., Tang, Y., Nie, J., Liu, Y., Zhou, Z., Zhang, H., and Hou, F.F. (2013). Kindlin-2 mediates activation of TGF-beta/Smad signaling and renal fibrosis. Journal of the American Society of Nephrology : JASN *24*, 1387-1398.

Weinreb, P.H., Simon, K.J., Rayhorn, P., Yang, W.J., Leone, D.R., Dolinski, B.M., Pearse, B.R., Yokota, Y., Kawakatsu, H., Atakilit, A.*, et al.* (2004). Function-blocking integrin alphavbeta6 monoclonal antibodies: distinct ligand-mimetic and nonligand-mimetic classes. The Journal of biological chemistry *279*, 17875-17887.

Weinstein, E.J., Bourner, M., Head, R., Zakeri, H., Bauer, C., and Mazzarella, R. (2003). URP1: a member of a novel family of PH and FERM domain-containing membrane-associated proteins is significantly over-expressed in lung and colon carcinomas. Biochimica et biophysica acta *1637*, 207-216.

White, A.C., Tran, K., Khuu, J., Dang, C., Cui, Y., Binder, S.W., and Lowry, W.E. (2011). Defining the origins of Ras/p53-mediated squamous cell carcinoma. Proceedings of the National Academy of Sciences of the United States of America *108*, 7425-7430.

White, D.E., Kurpios, N.A., Zuo, D., Hassell, J.A., Blaess, S., Mueller, U., and Muller, W.J. (2004). Targeted disruption of beta1-integrin in a transgenic mouse model of human breast cancer reveals an essential role in mammary tumor induction. Cancer cell *6*, 159-170.

Widelitz, R.B., Jiang, T.X., Chen, C.W., Stott, N.S., Jung, H.S., and Chuong, C.M. (1999). Wnt-7a in feather morphogenesis: involvement of anterior-posterior asymmetry and proximal-distal elongation demonstrated with an in vitro reconstitution model. Development *126*, 2577-2587.

Wiebe, C.B., Petricca, G., Hakkinen, L., Jiang, G., Wu, C., and Larjava, H.S. (2008). Kindler syndrome and periodontal disease: review of the literature and a 12-year follow-up case. Journal of periodontology *79*, 961-966.

Wieser, R., Wrana, J.L., and Massague, J. (1995). GS domain mutations that constitutively activate T beta R-I, the downstream signaling component in the TGF-beta receptor complex. The EMBO journal *14*, 2199-2208.

Wilhelmsen, K., Litjens, S.H., and Sonnenberg, A. (2006). Multiple functions of the integrin alpha6beta4 in epidermal homeostasis and tumorigenesis. Molecular and cellular biology *26*, 2877-2886.

Williamson, L., Raess, N.A., Caldelari, R., Zakher, A., de Bruin, A., Posthaus, H., Bolli, R., Hunziker, T., Suter, M.M., and Muller, E.J. (2006). Pemphigus vulgaris identifies plakoglobin as key suppressor of c-Myc in the skin. The EMBO journal *25*, 3298-3309.

Winograd-Katz, S.E., Fassler, R., Geiger, B., and Legate, K.R. (2014). The integrin adhesome: from genes and proteins to human disease. Nature reviews Molecular cell biology *15*, 273-288.

Wipff, P.J., Rifkin, D.B., Meister, J.J., and Hinz, B. (2007). Myofibroblast contraction activates latent TGF-beta1 from the extracellular matrix. The Journal of cell biology *179*, 1311-1323.

Woo, W.M., and Oro, A.E. (2011). SnapShot: hair follicle stem cells. Cell *146*, 334-334 e332.

Worthington, J.J., Klementowicz, J.E., and Travis, M.A. (2011). TGFbeta: a sleeping giant awoken by integrins. Trends in biochemical sciences *36*, 47-54.

Wrana, J.L., Attisano, L., Wieser, R., Ventura, F., and Massague, J. (1994). Mechanism of activation of the TGF-beta receptor. Nature *370*, 341-347.

Wu, C.H., and Nusse, R. (2002). Ligand receptor interactions in the Wnt signaling pathway in Drosophila. The Journal of biological chemistry *277*, 41762-41769.

Wu, C.I., Hoffman, J.A., Shy, B.R., Ford, E.M., Fuchs, E., Nguyen, H., and Merrill, B.J. (2012). Function of Wnt/beta-catenin in counteracting Tcf3 repression through the Tcf3-beta-catenin interaction. Development *139*, 2118-2129.

Xiao, L., Du, Y., Shen, Y., He, Y., Zhao, H., and Li, Z. (2012). TGF-beta 1 induced fibroblast proliferation is mediated by the FGF-2/ERK pathway. Frontiers in bioscience *17*, 2667-2674.

Xiao, T., Takagi, J., Coller, B.S., Wang, J.H., and Springer, T.A. (2004). Structural basis for allostery in integrins and binding to fibrinogen-mimetic therapeutics. Nature *432*, 59-67.

Xie, Y., Gao, K., Hakkinen, L., and Larjava, H.S. (2009). Mice lacking beta6 integrin in skin show accelerated wound repair in dexamethasone impaired wound healing model. Wound repair and regeneration : official publication of the Wound Healing Society [and] the European Tissue Repair Society *17*, 326-339.

Xie, Y., McElwee, K.J., Owen, G.R., Hakkinen, L., and Larjava, H.S. (2012). Integrin beta6-deficient mice show enhanced keratinocyte proliferation and retarded hair follicle regression after depilation. The Journal of investigative dermatology *132*, 547-555.

Xing, Y., Clements, W.K., Kimelman, D., and Xu, W. (2003). Crystal structure of a beta-catenin/axin complex suggests a mechanism for the beta-catenin destruction complex. Genes & development *17*, 2753-2764.

Xing, Y., Takemaru, K., Liu, J., Berndt, J.D., Zheng, J.J., Moon, R.T., and Xu, W. (2008). Crystal structure of a full-length beta-catenin. Structure *16*, 478-487.

Xiong, J.P., Stehle, T., Goodman, S.L., and Arnaout, M.A. (2003). New insights into the structural basis of integrin activation. Blood *102*, 1155-1159.

Yamamoto, N., Tanigaki, K., Han, H., Hiai, H., and Honjo, T. (2003). Notch/RBP-J signaling regulates epidermis/hair fate determination of hair follicular stem cells. Current biology : CB *13*, 333-338.

Yang, L., Pang, Y., and Moses, H.L. (2010). TGF-beta and immune cells: an important regulatory axis in the tumor microenvironment and progression. Trends in immunology *31*, 220-227.

Yang, Z., Mu, Z., Dabovic, B., Jurukovski, V., Yu, D., Sung, J., Xiong, X., and Munger, J.S. (2007). Absence of integrin-mediated TGFbeta1 activation in vivo recapitulates the phenotype of TGFbeta1-null mice. The Journal of cell biology *176*, 787-793.

Yates, L.A., Fuzery, A.K., Bonet, R., Campbell, I.D., and Gilbert, R.J. (2012). Biophysical analysis of Kindlin-3 reveals an elongated conformation and maps integrin binding to the membrane-distal beta-subunit NPXY motif. The Journal of biological chemistry *287*, 37715-37731.

Ye, F., Petrich, B.G., Anekal, P., Lefort, C.T., Kasirer-Friede, A., Shattil, S.J., Ruppert, R., Moser, M., Fassler, R., and Ginsberg, M.H. (2013). The mechanism of kindlin-mediated activation of integrin alphaIIbbeta3. Current biology : CB *23*, 2288-2295.

Yoo, J., Ghiassi, M., Jirmanova, L., Balliet, A.G., Hoffman, B., Fornace, A.J., Jr., Liebermann, D.A., Bottinger, E.P., and Roberts, A.B. (2003). Transforming growth factor-beta-induced apoptosis is mediated by Smad-dependent expression of GADD45b through p38 activation. The Journal of biological chemistry *278*, 43001-43007.

Youssef, K.K., Lapouge, G., Bouvree, K., Rorive, S., Brohee, S., Appelstein, O., Larsimont, J.C., Sukumaran, V., Van de Sande, B., Pucci, D*., et al.* (2012). Adult interfollicular tumour-initiating cells are reprogrammed into an embryonic hair follicle progenitor-like fate during basal cell carcinoma initiation. Nature cell biology *14*, 1282-1294.

Yu, Q., and Stamenkovic, I. (2000). Cell surface-localized matrix metalloproteinase-9 proteolytically activates TGF-beta and promotes tumor invasion and angiogenesis. Genes & development *14*, 163-176.

Yu, Y., Qi, L., Wu, J., Wang, Y., Fang, W., and Zhang, H. (2013a). Kindlin 2 regulates myogenic related factor myogenin via a canonical Wnt signaling in myogenic differentiation. PloS one *8*, e63490.

Yu, Y., Wu, J., Guan, L., Qi, L., Tang, Y., Ma, B., Zhan, J., Wang, Y., Fang, W., and Zhang, H. (2013b). Kindlin 2 promotes breast cancer invasion via epigenetic silencing of the microRNA200 gene family. International journal of cancer Journal international du cancer *133*, 1368-1379.

Yu, Y., Wu, J., Wang, Y., Zhao, T., Ma, B., Liu, Y., Fang, W., Zhu, W.G., and Zhang, H. (2012). Kindlin 2 forms a transcriptional complex with beta-catenin and TCF4 to enhance Wnt signalling. EMBO reports *13*, 750-758.

Zaidel-Bar, R., Itzkovitz, S., Ma'ayan, A., Iyengar, R., and Geiger, B. (2007). Functional atlas of the integrin adhesome. Nature cell biology *9*, 858-867.

Zhan, J., Zhu, X., Guo, Y., Wang, Y., Wang, Y., Qiang, G., Niu, M., Hu, J., Du, J., Li, Z*., et al.* (2012). Opposite role of Kindlin-1 and Kindlin-2 in lung cancers. PloS one *7*, e50313.

Zhang, H.F., Zhang, K., Liao, L.D., Li, L.Y., Du, Z.P., Wu, B.L., Wu, J.Y., Xu, X.E., Zeng, F.M., Chen, B*., et al.* (2014). miR-200b suppresses invasiveness and modulates the cytoskeletal and adhesive machinery in esophageal squamous cell carcinoma cells via targeting Kindlin-2. Carcinogenesis *35*, 292-301.

Zhang, M., Wang, M., Tan, X., Li, T.F., Zhang, Y.E., and Chen, D. (2010). Smad3 prevents beta-catenin degradation and facilitates beta-catenin nuclear translocation in chondrocytes. The Journal of biological chemistry *285*, 8703-8710.

Zhao, T., Guan, L., Yu, Y., Pei, X., Zhan, J., Han, L., Tang, Y., Li, F., Fang, W., and Zhang, H. (2013). Kindlin-2 promotes genome instability in breast cancer cells. Cancer letters *330*, 208-216.

Zhao, Y., Malinin, N.L., Meller, J., Ma, Y., West, X.Z., Bledzka, K., Qin, J., Podrez, E.A., and Byzova, T.V. (2012). Regulation of cell adhesion and migration by Kindlin-3 cleavage by calpain. The Journal of biological chemistry *287*, 40012-40020.

Zhu, A.J., Haase, I., and Watt, F.M. (1999). Signaling via beta1 integrins and mitogen-activated protein kinase determines human epidermal stem cell fate in vitro. Proceedings of the National Academy of Sciences of the United States of America *96*, 6728-6733.

Zhu, J., Boylan, B., Luo, B.H., Newman, P.J., and Springer, T.A. (2007a). Tests of the extension and deadbolt models of integrin activation. The Journal of biological chemistry *282*, 11914-11920.

Zhu, J., Carman, C.V., Kim, M., Shimaoka, M., Springer, T.A., and Luo, B.H. (2007b). Requirement of alpha and beta subunit transmembrane helix separation for integrin outside-in signaling. Blood *110*, 2475-2483.

Zhurinsky, J., Shtutman, M., and Ben-Ze'ev, A. (2000). Plakoglobin and beta-catenin: protein interactions, regulation and biological roles. Journal of cell science *113 (Pt 18)*, 3127-3139.

5 Acknowledgements

This work would not have been possible without the help and dedication of many people in and outside the lab.

First of all I am deeply grateful to my mentor Prof. Reinhard Fässler, whose door was always open for discussions and advices. His continuous support, trust and enthusiasm were crucial for this work. In addition, he gave me the freedom to develop my own ideas and concepts, as well as the possibility to work and participate on very diverse projects in the lab. In the lab, he created an outstanding scientific infrastructure and intellectually stimulating environment with many talented scientists, which fostered my own creativity. These multiple experiences enabled me to grow and develop as a young scientist.

Second, I want to thank Prof. Ralf Huss, who agreed to be the second referee of my thesis, as well as the other thesis committee members, Prof. Martin Biel, Prof. Karl-Peter Hopfner, Prof. Stefan Zahler and Prof. Angelika Vollmar, for taking their time to review my work.

Third, I want to appreciate the many collaborators, in particular Prof. John McGrath, Dr. Joey Lai-Cheong and Prof. Daniel Rifkin, who provided essential material and data for the Kindlin-1 project. The fruitful discussions with Prof. Ralf Paus, Prof. Roy Zent and Prof. Ambra Pozzi during important phases of the Kindlin-1 project contributed to the successful outcome.

Forth, I want to thank all the lab mates who directly or indirectly contributed to my work. In particular, my special gratitude goes to Moritz Widmaier who continuously supported this work with ideas, motivating discussions and by always lending a helping hand, if needed. He helped me out in all most difficult moments of the project and I will never forget his encouragements. Further, I am very pleased that I had the opportunity to collaborate closely with Dr. Madis Jakobson, Michaela Hermann and Raphael Ruppert on my and their projects. Thank you for the exciting scientific adventures and unlimited assistance. The sometimes endless and enthusiastic discussions as well as the incredible team spirit were unique to this lab. Especially in the beginning of my PhD, the former lab mates Dr. Sara Wickström and Dr. Eloi Montanez were extremely generous with their time for discussion and support.

Fifth, I am thankful to Simone Bach, Klaus Weber, Ines Lach-Kusevic and Dr. Armin Lambacher for all the technical support which was often needed during the project. From our animal facility, I want to express my gratitude to Dr. Heinz Brandstetter and Dr. Corinna Mörth as well as the animal caretaker Jens Paessler and Florian Thieme, who were always very supportive.

Most importantly, I want to thank my family, especially my parents, my brother Lorenz Rognoni and my partner Larissa Butschek. Without their boundless support and trust in me during all lab and life crises, I would never have come so far. My infinitive thanks to you!

6 Curriculum vitae

Personal Data

Full Name: Emanuel Rognoni
Born: in Berlin, Germany, on November 23rd, 1982
Nationality: German / Italian
Address: Hochstr. 21
D-81669 Munich
Germany

Telephone number: +49 89 44452002
Email address: rognoni@biochem.mpg.de

Education

March 2008- current:	PhD thesis at the Max-Planck-Institute of Biochemistry
July 2007:	Degree Master of Science in Biochemistry
August 2005:	Degree Bachelor of Science in Biochemistry
Since October 2002:	Study of Biochemistry at the TU-Munich
1995 – 2002:	High School Paul-Natrop in Berlin (main subjects: natural sciences)
1989-1995:	Elementary School in Berlin

Working experience

March, 1st, 2008 - current:
PhD thesis at the Max Planck Institute of Biochemistry, Department of Molecular Medicine (Prof. Dr. Reinhard Fässler) *"Role of Kindlin-1 in cutaneous epithelial stem cells and skin cancerogenesis"*

February 1st - July 31st, 2005:
Master Thesis at the university hospital "Rechts der Isar", Department of experimental oncology (Munich): *"Characterization of the oncolytic adenovirus Ad-Delo3-RGD in pancreas tumor cell lines"*

June 12th – July 12th, 2006:
Internship at the university hospital Santa Lucia IRCCS in Rome, Department of Neurochemistry (Italy): *"SOD1 localization in mitochondria of a cellular model for familiar Amyotrophic Lateral Sclerosis"*

Mai 1st - August 30th, 2005:
Bachelor Thesis at the university hospital "Rechts der Isar", Department of experimental oncology (Munich): *"Characterization of the adenovirus dl520 in the bladder cancer cell line EJ-28 and its affect in combination with different cytostatic drugs"*

August 1st - September 30th, 2004:
Summer Internship at the Albert Einstein College of Medicine in New York, Department of Cell Biology (USA): *"Expression, purification and characterization of yeast proteins of the ribosomal complex and analysis of their interaction with pulldown assays"*

Languages

German and Italian:	bilingual
English:	fluent (nine years at school and improved during several school exchanges and travels in English-speaking countries)
French:	good (seven years at school)

Publications

Rognoni E, Widmaier M, Jakobson M, Ruppert R, Ussar S, Katsougkri D, Böttcher RT, Lai-Cheong JE, Rifkin DB, McGrath JA, Fässler R. Kindlin-1 controls Wnt and TGF-β availability to regulate cutaneous stem cell proliferation. *Nat Med.* 2014, 20(4), 350-9.

Fraccaroli A, Franco CA, **Rognoni E**, Neto F, Rehberg M, Aszodi A, Wedlich-Söldner R, Pohl U, Gerhardt H, Montanez E. Visualization of endothelial actin cytoskeleton in the mouse retina. *PLoS One.* 2012, 7(10), e47488.

Ussar S, Moser M, Widmaier M, **Rognoni E**, Harrer C, Genzel-Boroviczeny O, Fässler R. Loss of Kindlin-1 causes skin atrophy and lethal neonatal intestinal epithelial dysfunction *PLoS Genet.* 2008, 4(12), e1000289.

Widmaier M, **Rognoni E**, Radovanac K, Azimifar SB, Fässler R. Integrin-linked kinase at a glance. *J Cell Sci.* 2012, 125(Pt 8), 1839-1843.

Holzmüller R, Mantwill K, Haczek C, **Rognoni E**, Anton M, Kasajima A, Weichert W, Treue D, Lage H, Schuster T, Schlegel J, Gänsbacher B, Holm PS. YB-1 dependent virotherapy in combination with temozolomide as a multimodal therapy approach to eradicate malignant glioma. *Int J Cancer*. 2011, 129(5), 1265-1276.

Rognoni E, Widmaier M, Haczek C, Mantwill K, Holzmüller R, Gansbacher B, Kolk A, Schuster T, Schmid RM, Saur D, Kaszubiak A, Lage H, Holm PS. Adenovirus-based virotherapy enabled by cellular YB-1 expression in vitro and in vivo. *Cancer Gene Ther.* 2009; 16(10), 753-763.

Fellowships and Awards

2014,	MPIB Junior Research Award
2014,	EMBO Long-Term Fellowship
2013,	Max-Planck-Institute of Biochemistry picture award
2012,	Eugene M. Farber Travel Award for Young Investigators
2008-2012,	Max-Planck Institute of Biochemistry Fellowship

Conference presentations

2012, Montagna Symposium on the Biology of the Skin (*Portland, OR, USA*) Poster presenter

2011, Fibronectin, Integrins and Related Molecules Gordon Conference (*Lucca, Italy*) Poster presenter

2010, 33rd Annual Meeting of the German Society for Cell Biology, DGZ (*Regensburg, Germany)* Poster present

7 Appendix

The appendix includes reprints of the **paper I** to **V**. The supplementary materials (Figures, tables and movies) for each paper, which are not printed, can be found on the enclosed CD.

7.1 Paper I

Kindlin-1 controls Wnt and TGF-β availability to regulate cutaneous stem cell proliferation

Emanuel Rognoni, Moritz Widmaier, Madis Jakobson, Raphael Ruppert, Siegfried Ussar, Despoina Katsougkri, Ralph T. Böttcher, Joey E. Lai-Cheong, Daniel B. Rifkin, John McGrath, Reinhard Fässler

Supplementary material

PDF file

Supplementary Figures 1-8

Supplementary Table 1, *P*-values for relative amount of SC subpopulations over time analyzed by FACS

Supplementary Table 3, Wnt ligand and receptor transcript analysis

Supplementary Table 4, List of qPCR oligonucleotides

Extended Experimental Procedure

Supplemental References

Excel file

Supplementary Table 2, Microarray data with significant gene expression changes of ≥ 2 fold

Kindlin-1 controls Wnt and TGF-β availability to regulate cutaneous stem cell proliferation

Emanuel Rognoni[1], Moritz Widmaier[1], Madis Jakobson[1], Raphael Ruppert[1], Siegfried Ussar[1], Despoina Katsougkri[1], Ralph T Böttcher[1], Joey E Lai-Cheong[2,3], Daniel B Rifkin[4], John A McGrath[3] & Reinhard Fässler[1]

Kindlin-1 is an integrin tail binding protein that controls integrin activation. Mutations in the *FERMT-1* gene, which encodes for Kindlin-1, lead to Kindler syndrome in man, which is characterized by skin blistering, premature skin aging and skin cancer of unknown etiology. Here we show that loss of Kindlin-1 in mouse keratinocytes recapitulates Kindler syndrome and also produces enlarged and hyperactive stem cell compartments, which lead to hyperthickened epidermis, ectopic hair follicle development and increased skin tumor susceptibility. Mechanistically, Kindlin-1 controls keratinocyte adhesion through β_1-class integrins and proliferation and differentiation of cutaneous epithelial stem cells by promoting $\alpha_v\beta_6$ integrin–mediated transforming growth factor-β (TGF-β) activation and inhibiting Wnt–β-catenin signaling through integrin-independent regulation of Wnt ligand expression. Our findings assign Kindlin-1 the previously unknown and essential task of controlling cutaneous epithelial stem cell homeostasis by balancing TGF-β–mediated growth-inhibitory signals and Wnt–β-catenin–mediated growth-promoting signals.

Kindler syndrome (KS) is an autosomal-recessive disease caused by loss-of-function mutations in the *FERMT-1* gene, which encodes Kindlin-1. The skin is the principal affected organ in individuals with KS and displays trauma-induced blisters, photosensitivity, pigmentation defects and increased risk for malignancies[1,2].

The Kindlins belong to a family of evolutionary conserved proteins, which are found primarily at cell-matrix adhesion sites, where they bind the cytoplasmic tail of β subunit–containing integrins and increase integrin affinity for ligands (also called integrin activation)[3–5]. In addition, they are also present at cell-cell adhesion sites, in the cytoplasm and in the nucleus, where their functions are unknown[6,7]. Epidermal and hair follicle (HF) keratinocytes express Kindlin-1 and Kindlin-2. However, despite their striking sequence similarity, Kindlin-1 and Kindlin-2 cannot compensate for each other, indicating that they have specialized functions[3,8].

Epidermal keratinocytes express several integrins, most notably members of the β_1 subunit–containing subfamily[9]. Keratinocytes of the HF bulge express high levels of β_1 and $\alpha_v\beta_6$ integrin[10]. The HF bulge harbors dormant stem cells (SCs) that periodically become activated to sustain the hair cycle[11,12]. The alternation of bulge SC activation and dormancy is regulated by a tight interplay of antagonistic signaling pathways. SC dormancy is achieved by bone morphogenic protein (BMP) and TGF-β signaling, whereas SC activation is elicited by shutting down BMP and TGF-β signaling and activating canonical Wnt–β-catenin signaling. Perturbations of these cell growth–regulating signaling pathways or of integrin signaling can profoundly alter SC homeostasis and tumor incidence[13–16]. It has been shown, for example, that increased integrin expression or activity is associated with an increased risk for squamous cell carcinoma[16–18]. Conversely, loss of β_1 subunit–containing integrin expression in skin (M. Sibilia, Medical University of Vienna, Austria, personal communication) or other tissues such as the mammary gland markedly reduces tumor susceptibility[19]. Moreover, it has been shown recently that Kindlin-2 can stabilize β-catenin and induce Wnt signaling in certain tumor cell lines[20]. It is therefore enigmatic why patients with KS suffer from an increased tumor risk[2,21,22] despite Kindlin-1 loss and compromised integrin functions in their keratinocytes[3,23,24]. This discrepancy suggests that Kindlin-1 harbors potent tumor-suppressor function(s) in keratinocytes that operate independently of the abundant and oncogenic β_1-class integrins. In this study we identified oncogenic signaling pathways that are tightly controlled by Kindlin-1.

RESULTS

Kindlin-1 loss in epidermis and HFs leads to KS-like defects

To circumvent the lethal ulcerative colitis of a constitutive *Fermt-1* gene ablation[3], we efficiently deleted the *Fermt-1* gene in keratinocytes by breeding mice with floxed *Fermt-1* with Keratin-5 (K5)-Cre transgenic mice[25] (resulting in Kind1-K5 mice; **Fig. 1a–c** and **Supplementary Fig. 1a–c**). Kindlin-1 loss persisted and did not affect Kindlin-2 expression in these mice (**Supplementary Fig. 1b**). Heterozygous Kind1-K5 mice or mice with homozygous floxed *Fermt-1* used as control strains had no apparent phenotype. Homozygous Kind1-K5 mice were born within the expected Mendelian ratio, were fertile and gained weight normally (**Supplementary Fig. 1d**).

[1]Department of Molecular Medicine, Max Planck Institute of Biochemistry, Martinsried, Germany. [2]Department of Dermatology, King Edward VII Hospital, Windsor, UK. [3]St. John's Institute of Dermatology, King's College London (Guy's Campus), London, UK. [4]New York University, Langone School of Medicine, New York, New York, USA. Correspondence should be addressed to R.F. (faessler@biochem.mpg.de).

Received 14 November 2013; accepted 3 February 2014; published online 30 March 2014; doi:10.1038/nm.3490

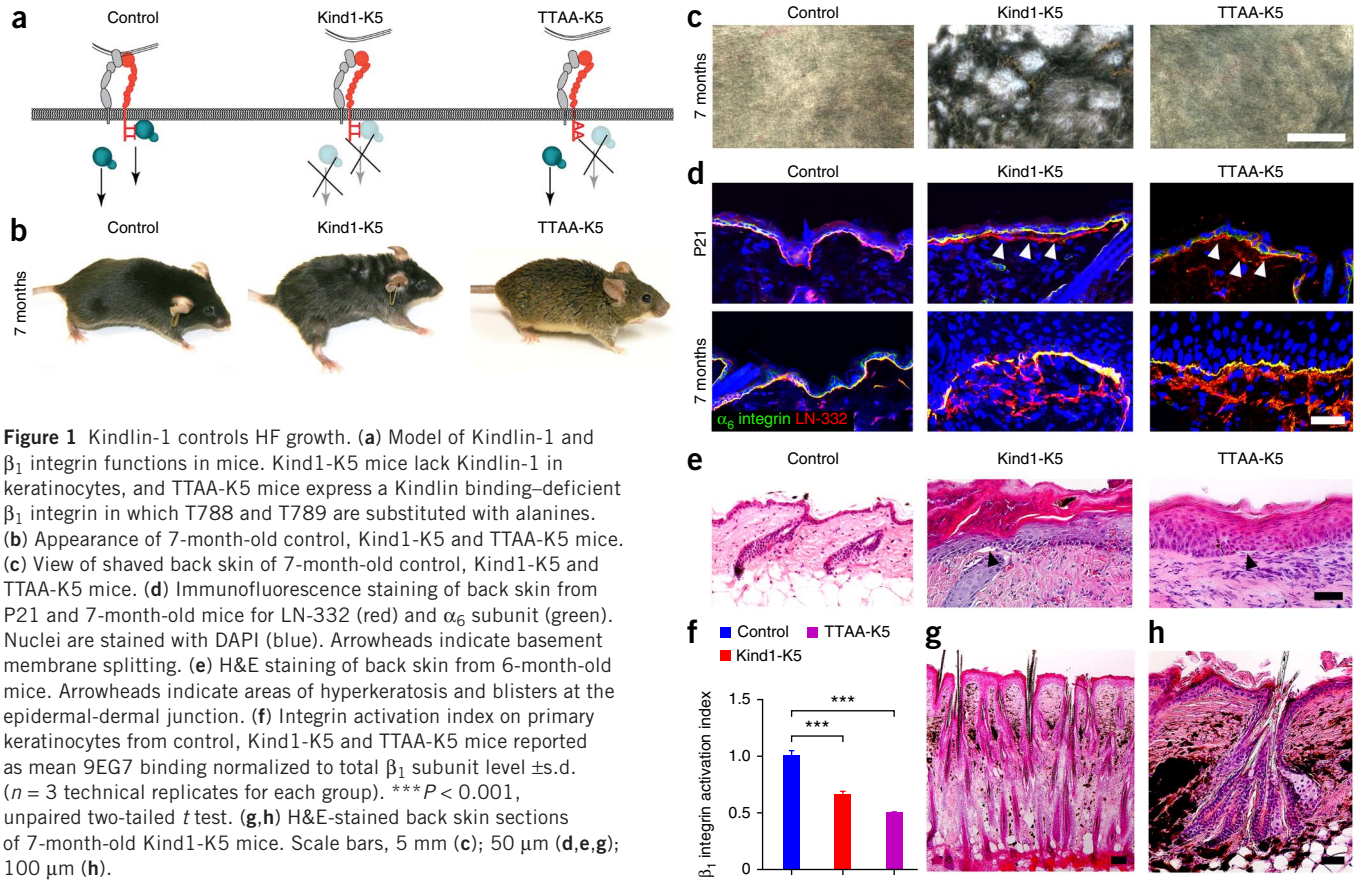

Figure 1 Kindlin-1 controls HF growth. (**a**) Model of Kindlin-1 and β_1 integrin functions in mice. Kind1-K5 mice lack Kindlin-1 in keratinocytes, and TTAA-K5 mice express a Kindlin binding–deficient β_1 integrin in which T788 and T789 are substituted with alanines. (**b**) Appearance of 7-month-old control, Kind1-K5 and TTAA-K5 mice. (**c**) View of shaved back skin of 7-month-old control, Kind1-K5 and TTAA-K5 mice. (**d**) Immunofluorescence staining of back skin from P21 and 7-month-old mice for LN-332 (red) and α_6 subunit (green). Nuclei are stained with DAPI (blue). Arrowheads indicate basement membrane splitting. (**e**) H&E staining of back skin from 6-month-old mice. Arrowheads indicate areas of hyperkeratosis and blisters at the epidermal-dermal junction. (**f**) Integrin activation index on primary keratinocytes from control, Kind1-K5 and TTAA-K5 mice reported as mean 9EG7 binding normalized to total β_1 subunit level ±s.d. ($n = 3$ technical replicates for each group). $^{***}P < 0.001$, unpaired two-tailed t test. (**g**,**h**) H&E-stained back skin sections of 7-month-old Kind1-K5 mice. Scale bars, 5 mm (**c**); 50 µm (**d**,**e**,**g**); 100 µm (**h**).

The first histologic phenotype emerged at around postnatal day (P) 21 in the back skin of Kind1-K5 mice, with basement membrane splitting, small blisters at the dermal-epidermal junction and aberrant accumulation of F-actin and cell-cell adhesion proteins at the basal side of basal keratinocytes (**Fig. 1d**,**e** and **Supplementary Fig. 1e**). We also observed the same defects in mice expressing Kindlin binding–deficient β_1 subunits in keratinocytes (**Fig. 1a**) due to substitutions of T788 and T789 to alanine in the β_1 subunit cytoplasmic domain (TTAA-K5 mice)[26], indicating that they are caused by malfunctioning β_1-class integrins (**Fig. 1f**). The blisters and basement membrane defects triggered a regenerative response with granulocyte, monocyte and T cell infiltrates in the dermis of the back skin of Kind1-K5 and TTAA-K5 mice (**Supplementary Fig. 1f–h**).

At P60, Kind1-K5 mice showed progressive melanin deposits, first in the tail and then in the entire back skin (**Fig. 1g**,**h** and **Supplementary Fig. 1i**), resembling poikiloderma in KS. At around 3 months of age, Kind1-K5 mice developed an irregular hair coat with small patches of densely clustered hair (**Fig. 1b**) that increased in size with age and appeared as meanders on the shaved back skin (**Fig. 1c**). At 6–8 months of age, Kind1-K5 mice began to lose hair, and patches with dense hair and alopecia alternated on their hair coat (**Supplementary Fig. 1j**). TTAA-K5 mice developed neither pigmentation defects nor densely packed hairs (**Fig. 1b**,**c**,**e**). Kind1-K5 mice also developed areas of atrophy next to areas of hyperkeratosis in the tail and back skin, whereas TTAA-K5 mice displayed hyperkeratotic areas only (**Fig. 1e** and **Supplementary Fig. 2a**). Although the number of Ki67-positive cells was higher in the epidermis of Kind1-K5 and TTAA-K5 mice compared to control littermates (**Supplementary Fig. 2b–d**), keratinocyte differentiation and apoptosis were unaffected in both mouse strains (**Supplementary Fig. 2e–i**).

These results show that Kindlin-1 deletion in the mouse epidermis recapitulates human KS and additionally induces an aberrant hair coat, which does not develop in TTAA-K5 mice, indicating that the aberrant hair coat is caused by Kindlin-1–specific and β_1 class– and inflammation-independent mechanisms.

Kindlin-1 loss disturbs the hair cycle and induces ectopic HFs

Back skin histology of 6-month-old Kind1-K5 mice revealed two different HF abnormalities: (i) areas with isolated and densely packed HFs (**Fig. 1g**) separated by 1–15 interfollicular epithelium (IFE) cells compared to the 37 ± 10 (mean ± s.d., $n = 4$ mice per genotype) IFE cells observed between control HFs, and (ii) HFs with multiple hair shafts and bulges that clustered together and contained hair strands exiting the skin through a single hair canal (**Fig. 1h**).

A detailed hair cycle analysis revealed that HF morphogenesis and the first hair cycle proceeded normally in the skin of Kind1-K5 mice (**Supplementary Fig. 3a**). At P50, HFs from control and Kind1-K5 mice entered telogen (resting phase of the hair cycle). Whereas HFs from control mice remained in a long telogen until P80 before a new hair cycle was initiated (**Supplementary Fig. 3a**), HFs from Kind1-K5 mice immediately re-entered anagen (growth phase of the hair cycle) (**Fig. 2a–c**), which was visible by the formation of a hair germ and the expression of the transcription factor CCAAT displacement protein (CDP)[27]. We never observed premature anagen induction in TTAA-K5 mice (**Supplementary Fig. 3b**).

Whole-mount staining of the tail epidermis at P80 showed HFs from control mice with prominent sebaceous glands, normal-sized Keratin-15 (Krt-15)-positive bulges and small hair germs with few CDP$^+$ cells (**Fig. 2d**). The tail skin of Kind1-K5 mice contained small ectopic HFs originating from pre-existing HFs and the IFE (**Fig. 2d**,**e**).

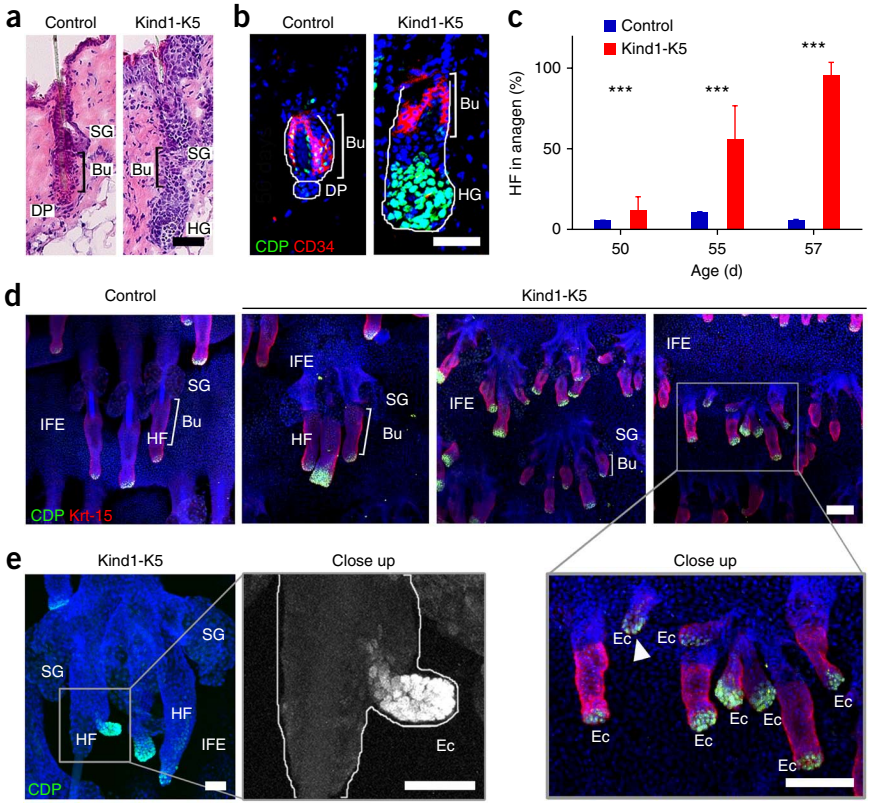

Figure 2 Premature anagen induction and ectopic HF development in skin from Kind1-K5 mice. (**a**) H&E-stained back skin sections of P56 mice. (**b**) Immunostaining of HFs from P56 mice for CD34 (red) and CDP (green). Nuclei are stained with DAPI (blue). (**c**) The percentage of anagen HFs at the indicated time points (mean ± s.d., $n = 4$ mice per genotype, ≥8 10× objective fields were counted). ***$P < 0.001$, unpaired two-tailed t test. (**d**) Immunostaining of tail epidermal whole mounts for CDP (green), Krt-15 (red) and DAPI (blue) of P80 mice. Of note, there is ectopic HF growth in the IFE of Kind1-K5 mice. (**e**) Ectopic HF outgrowth from a pre-existing HF of tail whole mount skin in a 6-month-old Kind1-K5 mouse stained for CDP (green) and DAPI (blue). Scale bars, 50 µm (**a**,**b**); 100 µm (**d**,**e**). Bu, bulge; SG, sebaceous gland; HG, hair germ; DP, dermal papilla; Ec, ectopic HF.

Ectopic HF- and IFE-derived HFs were also present in the back skin of Kind1-K5 mice and expressed the dermal papilla marker alkaline phosphatase (**Supplementary Fig. 3c**,**d**). Of note, whereas HF numbers increased after P50 in the back skin of Kind1-K5 mice, their number began declining after 1 year of age (**Supplementary Fig. 3i**).

These findings show that Kindlin-1 deficiency leads to a premature onset of anagen, the formation of ectopic HFs in the IFE and from pre-existing HFs and a decline in HF numbers at old age.

Kindlin-1 regulates cutaneous epithelial SC homeostasis

The ectopic HFs in Kind1-K5 mice pointed to a perturbed SC homeostasis. The epidermis contains different SC populations that reside in different niches[11]. Whereas bulge SCs express CD34, Krt-15, nephronectin (Npnt)[28] and high levels of α_6 integrin (**Fig. 3a**), reliable mouse IFE SC markers are still missing[11,29]. Immunostaining revealed higher numbers of CD34$^+$ bulge cells in back skin (**Supplementary Fig. 3e**) and enlarged Krt-15$^+$ bulges in tail whole mounts of Kind1-K5 mice at P80 compared to controls (**Fig. 3b** and **Supplementary Fig. 3f**). Krt-15$^+$ cells were also present in the infundibulum and IFE of Kind1-K5 mice (**Fig. 3b**) but were not present in control mice. Npnt expression expanded into the sebaceous gland, the infundibulum and the outer root sheath (**Fig. 3b**,**c**), and *Npnt* mRNA levels were higher in FACS-sorted bulge and infundibulum–junctional zone cells of Kind1-K5 mice compared to controls (**Supplementary Fig. 3h**). Also, the leucine-rich repeats and immunoglobulin-like domains 1 (Lrig1)-positive SC population of the infundibulum–junctional zone[30] extended toward the infundibulum and lower hair shaft of back and tail skin HFs of Kind1-K5 mice (**Fig. 3d** and **Supplementary Fig. 3g**).

Despite normal hair cycles and hair counts until P50 (**Supplementary Fig. 3a**,**i**), FACS quantifications of keratinocytes from mouse skin at P40 revealed significantly more SCs in the bulge, upper isthmus and infundibulum–junctional zone of Kind1-K5 mice compared to controls (**Fig. 3e**,**f**). A time-course analysis showed that the expansion of the SC compartments was already visible at P21, peaked at P50–P80 and then began declining to become markedly smaller in 12-month-old Kind1-K5 mice (**Fig. 3g** and **Supplementary Table 1**).

In line with normal hair coat development, SC subpopulations were unaffected in TTAA-K5 mice, at least until 1 year of age (**Supplementary Fig. 3j**).

To test whether elevated proliferation caused the enlarged bulges, we performed BrdU label-retaining cell (LRC) assays. After 10 days of chase, significantly more bulge cells were BrdU$^+$ in tail whole mounts of Kind1-K5 mice compared to controls, whereas after 32 days, 70 days and 5.5 months, significantly fewer bulge cells were BrdU$^+$ in Kind1-K5 mice (**Fig. 3h**,**i**).

These findings demonstrate that Kindlin-1 deficiency elevates cutaneous epithelial SC proliferation, numbers and compartments in a β_1 class–independent manner.

Kindlin-1 triggers $\alpha_v\beta_6$ integrin–mediated TGF-β release in skin

To determine whether Kindlin-1 loss alters integrin surface levels, we analyzed integrin profiles on primary keratinocytes using FACS. The levels of β_1 and β_4 integrin subunits were slightly lower and the levels of β_5 and β_8 integrin subunits were slightly higher in cells from Kind1-K5 mice compared to controls. Detection of β_3 integrin subunits was not evident in either genotype. We also noted clearly elevated β_6 subunit levels in Kindlin-1–deficient keratinocytes (**Fig. 4a**), as were *Itgb6* (encoding the β_6 integrin subunit) mRNA levels in FACS-sorted cutaneous SCs (**Supplementary Fig. 4a**). Immunostaining showed β_6 subunit expression extending from the bulge and outer root sheath to the infundibulum and IFE of Kind1-K5 mice (**Fig. 4b**).

Next we investigated β_6 subunit–dependent cell spreading and focal adhesion formation. Although keratinocytes from Kind1-K5 mice spread normally on fibronectin, they displayed severely impaired adhesion, spreading, clustering of paxillin in focal adhesion-like structures and assembly of F-actin stress fibers when plated on surfaces coated with $\alpha_v\beta_6$-specific antibodies or α_v-specific peptidomimetic cyclic RGD (cRGD) (**Fig. 4c**,**d** and **Supplementary Fig. 4b**,**c**),

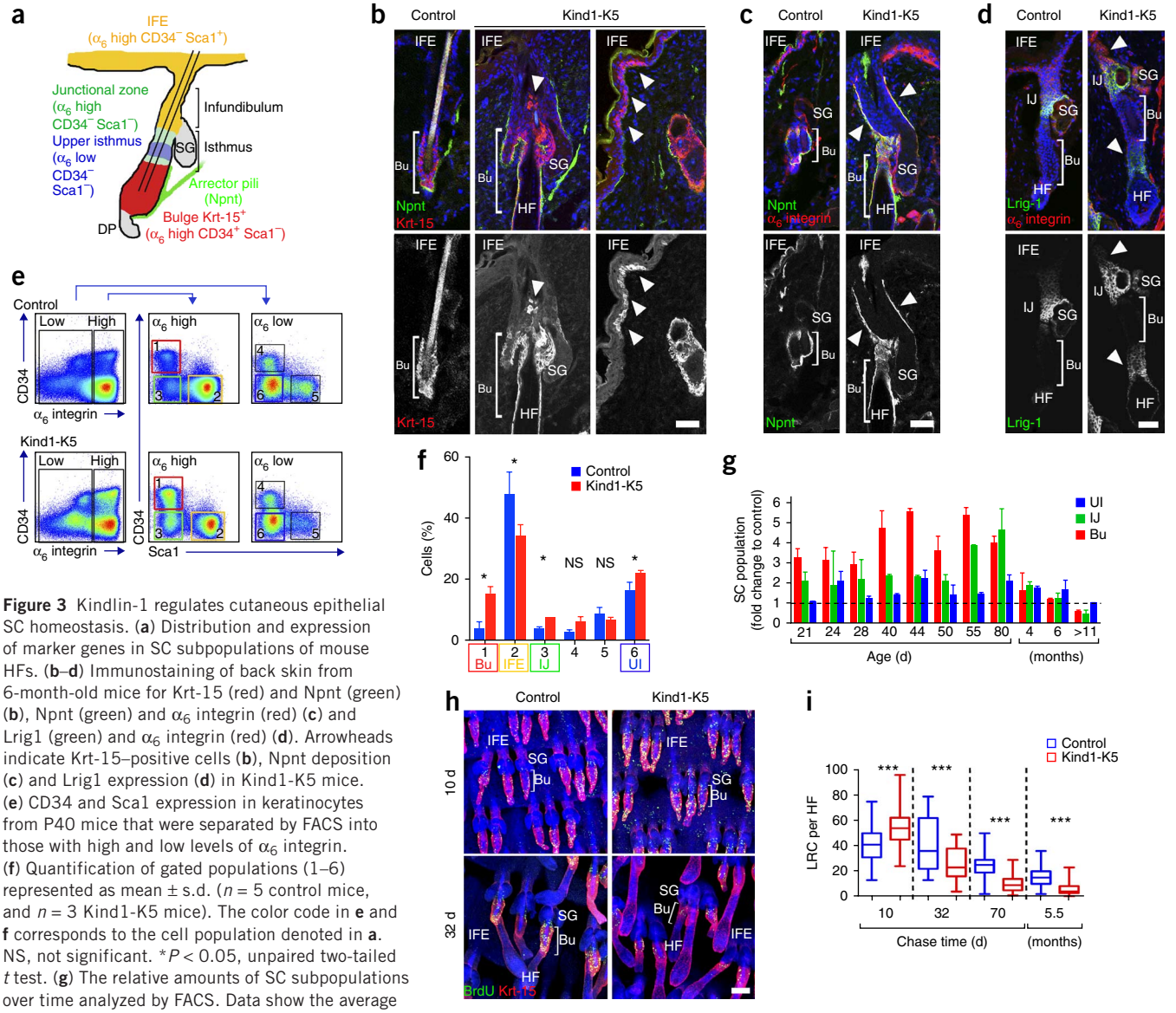

Figure 3 Kindlin-1 regulates cutaneous epithelial SC homeostasis. (**a**) Distribution and expression of marker genes in SC subpopulations of mouse HFs. (**b**–**d**) Immunostaining of back skin from 6-month-old mice for Krt-15 (red) and Npnt (green) (**b**), Npnt (green) and α_6 integrin (red) (**c**) and Lrig1 (green) and α_6 integrin (red) (**d**). Arrowheads indicate Krt-15–positive cells (**b**), Npnt deposition (**c**) and Lrig1 expression (**d**) in Kind1-K5 mice. (**e**) CD34 and Sca1 expression in keratinocytes from P40 mice that were separated by FACS into those with high and low levels of α_6 integrin. (**f**) Quantification of gated populations (1–6) represented as mean ± s.d. ($n = 5$ control mice, and $n = 3$ Kind1-K5 mice). The color code in **e** and **f** corresponds to the cell population denoted in **a**. NS, not significant. $^*P < 0.05$, unpaired two-tailed t test. (**g**) The relative amounts of SC subpopulations over time analyzed by FACS. Data show the average fold increase (±s.d.) relative to control mice (n and P values are listed in **Supplementary Table 1**). (**h**) BrdU (green)-retaining cells in Krt-15 (red)-stained tail whole mounts after the indicated chase times. (**i**) Numbers of LRCs per HF after the indicated chasing periods quantified as boxplots (10 d: $n = 5$ control, and $n = 3$ Kind1-K5; 32 d: $n = 3$ control, and $n = 4$ Kind1-K5; 80 d: $n = 4$ control, and $n = 3$ Kind1-K5). The boxplot whisker ends show the minimum and maximum distribution, and the middle line reports the median. $^{***}P < 0.001$, Mann-Whitney U test. Nuclei are stained with DAPI (blue) (**b**–**d**,**h**). Scale bars, 50 μm (**b**–**d**); 100 μm (**h**). UI, upper isthmus; IJ, infundibulum junctional zone.

indicating that $\alpha_v\beta_6$ integrins in keratinocytes from Kind1-K5 mice are nonfunctional. We confirmed the $\alpha_v\beta_6$ specificity of these defects by treating keratinocytes from control mice with the β_6-blocking antibody 10D5, which phenocopied the spreading defects of Kindlin-1–deficient cells on cRGD surfaces (**Supplementary Fig. 4d**).

Active $\alpha_v\beta_6$ integrins can release TGF-β from the latency associated protein (LAP)[31], which in turn suppresses the proliferation of bulge SCs[10,12,32,33]. We tested $\alpha_v\beta_6$-dependent TGF-β release by seeding keratinocytes together with transformed mink lung epithelial cells (tMLECs), which are able to report TGF-β–induced luciferase on a latent TGF-β binding protein-1 (LTBP-1)–LAP–TGF-β1–rich matrix[34] (**Fig. 4e**). Keratinocytes from control mice efficiently induced the luciferase reporter, which could be inhibited with the $\alpha_v\beta_6$ blocking antibody 10D5 or the TGF-β neutralizing antibody 1D11. In sharp contrast, keratinocytes from Kind1-K5 mice were unable to release TGF-β, confirming that their $\alpha_v\beta_6$ integrins are nonfunctional (**Fig. 4e**). In line with this *in vitro* result, TGF-β signaling was also severely impaired in bulge cells of Kind1-K5 mice *in vivo*, in which phosphorylated Smad2 and Smad3 (pSmad2/3) was detectable neither before nor after premature anagen induction (**Fig. 4f** and **Supplementary Fig. 4g**). Signaling by BMP through phosphorylation of Smad1, Smad5 and Smad8 (pSmad1/5/8), which also suppresses bulge cell proliferation[35,36], was unaffected (**Supplementary Fig. 4h**). Treatment of Kindlin-1–deficient keratinocytes with soluble TGF-β1 induced robust Smad2 phosphorylation and reduced cell proliferation (**Supplementary Fig. 4e**,**f**), indicating that TGF-β1 signals are efficiently transduced. The severe dysfunction of $\alpha_v\beta_6$ integrins was not compensated by Kindlin-2 because of the inability of Kindlin-2 to bind β_6 tails (**Fig. 4g**). Most notably, subjects with KS showed a similar TGF-β defect as Kind1-K5 mice, with elevated expression

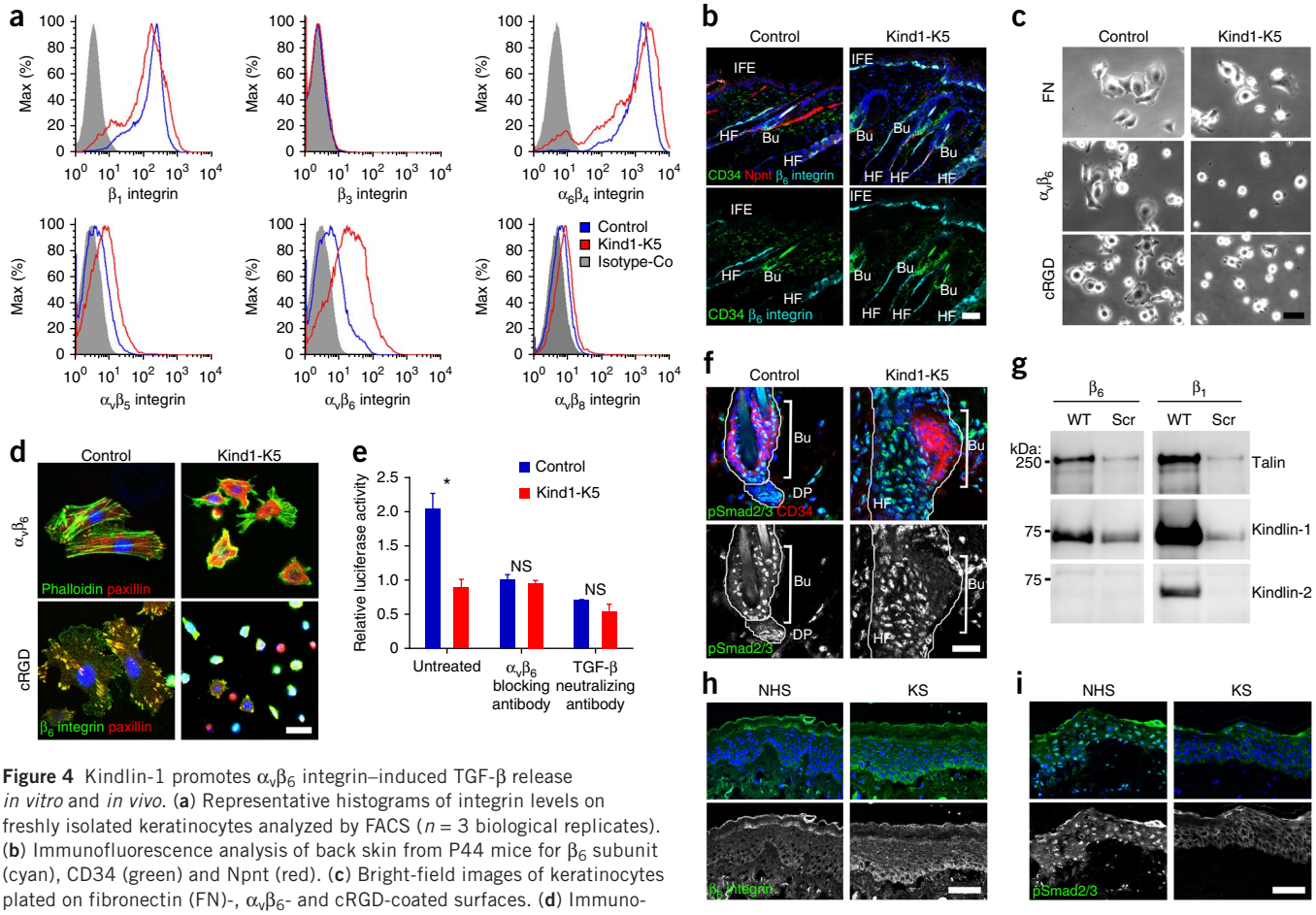

Figure 4 Kindlin-1 promotes $\alpha_v\beta_6$ integrin–induced TGF-β release *in vitro* and *in vivo*. (**a**) Representative histograms of integrin levels on freshly isolated keratinocytes analyzed by FACS ($n = 3$ biological replicates). (**b**) Immunofluorescence analysis of back skin from P44 mice for β_6 subunit (cyan), CD34 (green) and Npnt (red). (**c**) Bright-field images of keratinocytes plated on fibronectin (FN)-, $\alpha_v\beta_6$- and cRGD-coated surfaces. (**d**) Immunostaining of keratinocytes plated on $\alpha_v\beta_6$- and cRGD-coated surfaces for paxillin (red) and F-actin or β_6 integrin (green). (**e**) TGF-β release from the extracellular matrix by keratinocytes from control or Kind1-K5 mice in the absence or presence of the indicated blocking antibodies monitored with the tMLEC reporter cell line. Luciferase activity is reported as mean ± s.e.m. ($n = 3$ biological replicates per genotype). NS, not significant. $^*P < 0.05$, unpaired two-tailed *t* test. (**f**) Immunostaining of a HF from the back skin of 4-month-old mice for pSmad2/3 (green) and CD34 (red). (**g**) Streptavidin bead pulldown assay with biotinylated wild-type (WT) integrin tails or scrambled (Scr) peptides from keratinocyte lysates (representative blot from three independent experiments). (**h**,**i**) Immunofluorescence staining of skin sections from control individuals and individuals with KS for β_6 integrin (**h**) and pSmad2/3 (**i**). Nuclei are stained with DAPI (blue) (**b**,**d**,**f**,**h**,**i**). Scale bars, 50 μm (**b**,**c**,**h**,**i**) and 25 μm (**d**,**f**). NHS, normal human skin; Isotype-Co, isotype control.

of β_6 subunits and reduced nuclear pSmad2/3 in large areas of basal epidermal keratinocytes (**Fig. 4h**,**i**), whereas pSmad1/5/8 was unaffected (**Supplementary Fig. 4i**).

These findings indicate that Kindlin-1 is essential for β_6 subunit–containing integrin–mediated cell adhesion, cell spreading and TGF-β release required for SC quiescence.

Kindlin-1 curbs Wnt–β-catenin signaling in skin

Premature anagen induction, ectopic HF development and expansion of SC compartments also develop in mice with elevated Wnt–β-catenin signaling in keratinocytes[37–40], and reduced HF spacing and aberrant hair orientation occur in mice overexpressing the β-catenin cofactor Lef1 (ref. 41) or mice with increased Notch signaling[42]. In the skin of control mice, β-catenin levels were high at cell-cell junctions, low in the nucleus and absent at the basal side of basal keratinocytes. In contrast, in the epidermis of Kind1-K5 mice, β-catenin also accumulated at basal sides of basal keratinocytes, in the nuclei of a large number of IFE cells and in catagen HFs (**Fig. 5a** and **Supplementary Fig. 5d**). Furthermore, Kind1-K5 mice showed β-catenin in the nuclei of developing hair germs during premature anagen induction (**Supplementary Fig. 5a**,**b**) and extended Lef1 expression from the normal site in hair germs to the bulge and IFE at all stages analyzed (**Fig. 5a** and **Supplementary Fig. 5a**,**c**,**d**). Notably, at P50, shortly before bulges from Kind1-K5 mice induced premature anagen, they showed high nuclear Lef1 levels, indicating a premature onset of Wnt signaling. In control mice, Lef1 was absent in telogen bulges and became highly expressed in the nuclei of hair germ cells and weakly expressed in the cytoplasm of IFE cells (**Fig. 5a** and **Supplementary Fig. 5a**). The numbers of nuclear Notch effector Notch intracellular domain (NICD)-containing cells and NICD-induced *Hes1* mRNA levels were unaltered in hair germs and the pericortex, but both were higher in the IFE of Kind1-K5 mice compared to controls at all time points analyzed (**Fig. 5b** and **Supplementary Fig. 5e–g**).

Next we determined Wnt–β-catenin signaling by intercrossing Kind1-K5 and control mice with TOPgal reporter mice, which express β-galactosidase under a TCF-Lef–controlled minimal c-Fos promotor[43]. In HFs from control mice, TOPgal activities were high in the pericortex during anagen, low during catagen and lost in telogen, with some residual activity in club hairs. In Kind1-K5 mice, the high TOPgal activity in the pericortex and bulb of anagen HFs persisted

throughout catagen, decreased in telogen (**Fig. 5c** and **Supplementary Fig. 5i**) and was strongly re-induced in the following anagen stage (**Supplementary Fig. 5h**). Furthermore, we observed a patch-like distribution of TOPgal in the IFE of Kind1-K5 mice, which was absent in controls (**Fig. 5c**). Notably, the IFE of humans with KS showed similar abnormalities in β-catenin–LEF1 expression, with weak nuclear β-catenin expression in the basal cell layer and a patch-like distribution of nuclear LEF1, whereas normal human skin contained β-catenin exclusively in cell-cell contacts and LEF1 in the cytoplasm (**Fig. 5d** and **Supplementary Fig. 5j**).

These findings demonstrate that loss of Kindlin-1 induces nuclear translocation of β-catenin–Lef1 in KS and mouse skin, leading to elevated Wnt–β-catenin signaling and premature anagen onset of HFs in Kind1-K5 mice.

Kindlin-1 regulates Wnt ligand expression

To find an explanation for the increased Wnt–β-catenin signaling in the absence of Kindlin-1, we compared the skin transcriptome between healthy individuals and subjects with KS using microarray analyses. As we expected, *FERMT-1* expression was absent in skin from subjects with KS, and the levels of mRNAs encoding inflammatory proteins were high (**Fig. 5e**; the complete list is given in **Supplementary Table 2**). Unexpectedly, the levels of several Wnt signaling components, most notably *WNT5A*, were high in individuals with KS compared to healthy individuals (**Fig. 5e**). Immunostaining confirmed the aberrant expression of WNT5A in basal keratinocytes of individuals with KS (**Fig. 5f**). Quantitative PCR (qPCR) and *in situ* hybridization of tail whole mounts from Kind1-K5 mice corroborated high *Wnt5a* mRNA levels in hair bulbs, ectopic HFs and patches of the IFE, which overlapped with high TOPgal activities (**Fig. 5g** and **Supplementary Fig. 6a–c**). qPCR of all known Wnt ligands and receptors revealed that the levels of several canonical (*Wnt1*, *Wnt2b*, *Wnt3a* and *Wnt9b*) and noncanonical (*Wnt6* and *Wnt2*) Wnts were also significantly higher in keratinocytes from Kind1-K5 mice compared to controls, whereas the levels of *Wnt4*, *Wnt7a*, *Wnt9a*, *Wnt10a* and *Wnt16* were significantly lower (**Fig. 5g** and **Supplementary Table 3**). The expression of several Frizzled (Fzd) receptors was higher in Kind1-K5 mice compared to controls, most notably *Fzd4* and *Fzd5* and to a lesser extent the Fzd co-receptor *Lrp6*. We also performed qPCR of FACS-sorted bulge cells and *in situ* hybridization of tail whole mounts from Kind1-K5 mice and confirmed the high *Fzd4* mRNA levels and patch-like expression of Fzd4 in the IFE (**Supplementary Fig. 6d,e**).

Transfection of Kindlin-1–deficient keratinocytes with SuperTOPFlash reporter revealed that the elevated Wnt signaling was cell autonomous (**Fig. 5h,i**) and that Lef1 was limiting the extent of Wnt signaling (**Supplementary Fig. 6f**). Overexpression of Wnt4, which triggers translocation of β-catenin to cell-cell junctions, thereby preventing nuclear accumulation of β-catenin and Wnt–β-catenin signaling[44], decreased SuperTOPFlash activity in Kindlin-1–deficient keratinocytes compared to GFP-transfected controls (**Fig. 5h**). Overexpression of Wnt5a, which together with Lrp5 and Fzd4 efficiently activates the canonical Wnt–β-catenin signaling pathway[45], further increased the activity of the SuperTOPFlash reporter in Kindlin-1–deficient cells but not in control cells in which Fzd4 expression was low (**Fig. 5h** and **Supplementary Fig. 6d,e**).

Re-expression of similar quantities of Kindlin-1–GFP or the integrin binding–deficient Kindlin-1^{Q611A,W612A}–GFP but not Kindlin-2 attenuated the increased SuperTOPFlash activities and levels of Wnt4 and Wnt5a in Kindlin-1–deficient keratinocytes (**Fig. 5i** and **Supplementary Fig. 6g–j**), indicating that inhibition of Wnt–β-catenin signaling is Kindlin-1 specific and does not require integrin binding. To exclude a role for nuclear Kindlin-1, we expressed Kindlin-1–GFP fused to two SV40 nuclear localization signals (NLSs) in Kind1-null cells. Although most of the protein localized to the nucleus, the elevated SuperTOPFlash activity was only partially rescued (**Fig. 5i**), probably because of Kind1-NLS-GFP spillovers into the cytoplasm (**Supplementary Fig. 6j**).

To corroborate that elevated Wnt protein secretion and high Wnt–β-catenin signaling underlie premature HF anagen induction in Kind1-K5 mice, we treated them at P49, shortly before telogen onset (**Fig. 5j** and **Supplementary Fig. 7a**), with IWP-2, which blocks Wnt protein secretion by inhibiting porcupine-mediated palmitylation of Wnts[46], or with IWR-1, which inhibits tankyrases, thereby stabilizing the β-catenin destruction complex[46,47]. Both compounds efficiently blocked premature anagen induction in Kind1-K5 mice and decreased SuperTOPFlash activities *in vitro* (**Fig. 5j** and **Supplementary Fig. 7a,b**). In line with previous reports[42], inhibition of Wnt signaling also reduced aberrant Notch activities in Kind1-K5 keratinocytes *in vitro* and *in vivo*, which in turn normalized *Wnt4* levels[48] (**Supplementary Fig. 7c–g**).

Together these findings demonstrate that Kindlin-1 inhibits Wnt–β-catenin signaling by regulating the transcription of Wnt ligands and receptors in a cell-autonomous and integrin-independent manner.

Loss of Kindlin-1 increases skin tumor susceptibility

The low TGF-β levels and augmented Wnt signaling in humans with KS and Kind1-K5 mice are oncogenic threats[49,50]. To test this hypothesis, we used the two-stage carcinogenesis protocol and treated mice with 7,12-dimethylbenz[a]anthracene (DMBA) and 12-*O*-tetradecanoylphorbol-13-acetate (TPA) for 25 weeks. Kind1-K5 mice developed tumors earlier and had more tumors than control mice (**Fig. 6a–c**). Of note, tumor sizes were similar between Kind1-K5 and control mice (**Fig. 6d**), which could be due to different skin lesion subtypes. Indeed, histology of the tumor lesions revealed that hyperkeratotic and exophytic papillomas dominated in control mice, whereas HF-derived trichofolliculoma-like lesions, sebaceous papillomas, mixed papillomas and basal cell carcinoma–like lesions dominated in Kind1-K5 mice (**Fig. 6e** and **Supplementary Fig. 8a**). In line with uncurbed Wnt signaling, we observed more cells with nuclear β-catenin and Lef1 expression in tumors from Kind1-K5 mice (**Supplementary Fig. 8b–d**).

Figure 5 Kindlin-1 controls Wnt–β-catenin signaling. (**a**) Immunofluorescence staining for β-catenin (green) in HFs (P44) (left) and the IFE (P55) (middle) and for Lef1 and CD34 (red) in HFs and the IFE (4 months) (right) from control and Kind1-K5 mice. Arrowheads indicate aberrant β-catenin (left) or Lef1 (right) localization. (**b**) IFE immunofluorescence staining for NICD (green) from P44 control and Kind1-K5 mice. (**c**) TOPgal reporter activity in tail HFs (left) and the IFE (right) from 3-month-old control and Kind1-K5 mice. Arrowheads indicate HFs with abnormal TOPgal activity. β-gal, β-galactosidase. (**d**) Immunofluorescence staining of human skin from control individuals and individuals with KS for β-catenin (left) and LEF1 (right). (**e**) Skin gene expression profile of NHS ($n = 3$) and KS ($n = 3$) assessed with microarray and shown as a volcano plot. Genes with at least twofold change in KS were plotted according to the $\log_2$ fold change (*x* axis) and the $\log_{10}$ *P* value (*y* axis), unpaired two-tailed *t* test. (**f**) Immunofluorescence staining for WNT5A (green) in the skin of control individuals and individuals with KS. (**g**) Volcano plot of the qPCR-determined gene expression profile of keratinocytes from control and Kind1-K5 mice. Mean expressions relative to *Gapdh* of Wnt ligands (circle, red) and receptors (triangle, green) were plotted according to the $\log_2$ fold change (*x* axis) and $\log_{10}$ *P* value (*y* axis) ($n = 3$ biological replicates per genotype; the ± s.e.m. values are listed in **Supplementary Table 3**). (**h**) Transient overexpression of GFP, Wnt4 and Wnt5a in floxed keratinocytes (WT) and Kindlin-1–deficient keratinocytes previously treated with adenovirus expressing Cre recombinase (KO) expressing the TOPFlash reporter. Values are corrected for the *Renilla* control and are represented as mean ± s.e.m. fold increase relative to WT cells ($n = 5$ WT and KO biological replicates). $^*P < 0.05$, $^{**}P < 0.01$, unpaired two-tailed *t* test. (**i**) TOPFlash reporter activity in KO cells stably re-expressing Kindlin-1–GFP, integrin binding–deficient Kindlin-1^{Q611A,W612A}–GFP (Kind1-QW/AA-GFP), NLS-tagged Kindlin-1–GFP or Kindlin-2–GFP. Values are corrected for the *Renilla* control, are represented as fold increase relative to WT cells and are reported as mean ± s.e.m. ($n = 21$ WT and KO; $n = 13$ Kind1-GFP; $n = 9$ Kind1-QW/AA-GFP; $n = 5$ Kind1-NLS-GFP and Kind2-GFP; all biological replicates). NS, not significant. $^*P < 0.05$, $^{**}P < 0.01$, $^{***}P < 0.001$, unpaired two-tailed *t* test. (**j**) H&E staining of control and Kind1-K5 mice at 1 d (P50) and after treatment (P56) with the indicated Wnt inhibitor. Nuclei are stained with DAPI (blue) (**a**,**b**,**d**,**f**). All scale bars, 50 μm.

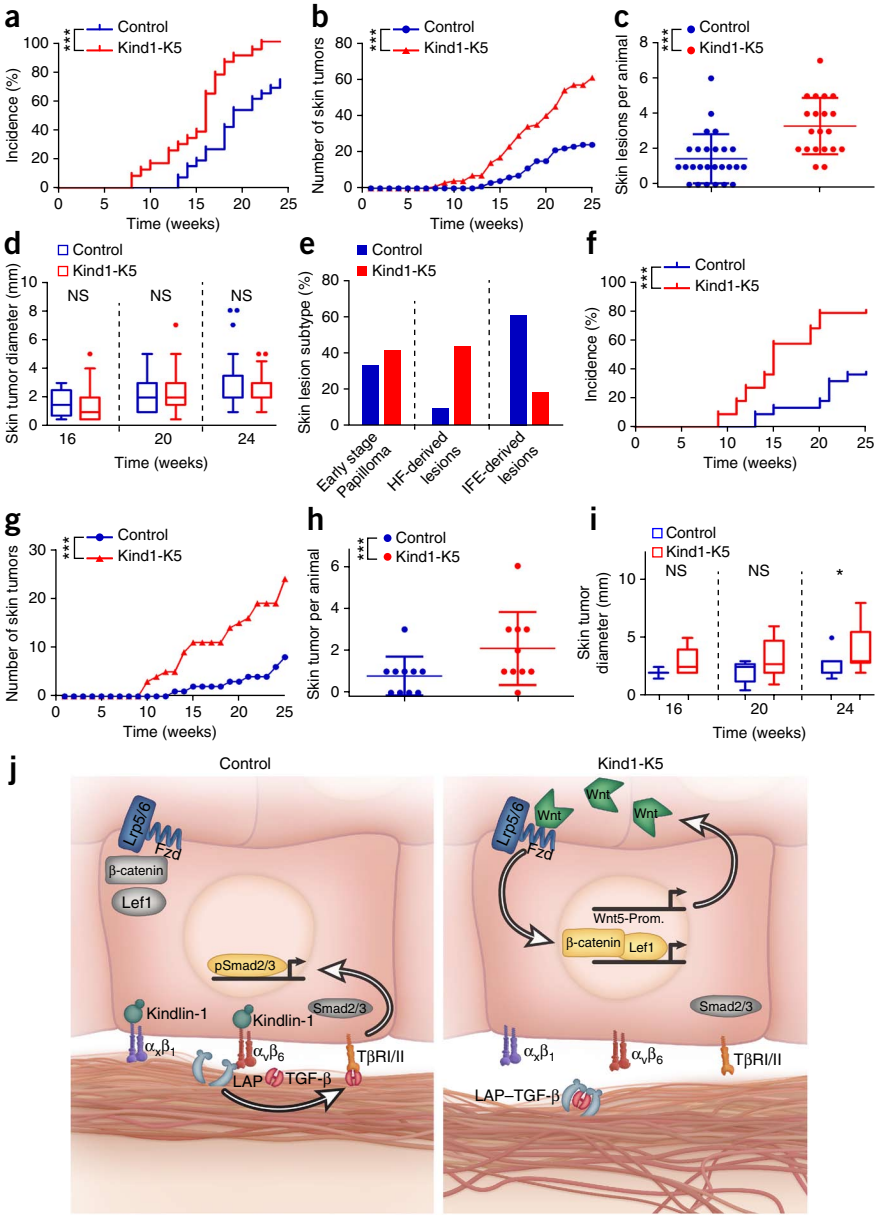

Figure 6 Loss of Kindlin-1 increases skin tumor incidence. (**a**–**e**) Two-stage carcinogenesis ($n = 26$ control mice and $n = 23$ Kind1-K5 mice). (**a**–**c**) Tumor incidence (P value by log-rank test) (**a**), burden (P value by Wilcoxon t test) (**b**) and skin lesions per animal (reported as mean ± s.d., P value by Mann-Whitney U test) after 25 weeks of treatment (**c**). $^{***}P < 0.001$. (**d**) Tumor growth reported by diameter shown in a boxplot, where the whisker ends are at the 1.5-interquartile range, and the middle lines represent the median. NS, not significant; P values by Mann-Whitney U test. (**e**) The percentage of skin lesion subtypes from control ($n = 25$ lesions) and Kind1-K5 ($n = 47$ lesions) mice that were staged by histology and immunofluorescence analysis (**Supplementary Fig. 8a**). (**f**–**i**) One-stage carcinogenesis with DMBA ($n = 10$ control mice and $n = 10$ Kind1-K5 mice monitored as in **a**–**d**). (**f**–**i**) Tumor incidence (P value by log-rank test) (**f**), skin lesion number (P value by Wilcoxon t test) (**g**), frequency (reported as mean ± s.d., P value by Mann-Whitney U test) (**h**) and size (reported as boxplot, where the whisker ends are at the 1.5-interquartile range, and the middle lines represent the median; P value by Mann-Whitney U test) (**i**). NS, not significant. $^{*}P < 0.05$, $^{***}P < 0.001$. (**j**) Molecular functions of Kindlin-1. In normal cells (left), Kindlin-1 activates β_1-class integrins and $\alpha_v\beta_6$ integrin to facilitate adhesion and TGF-β liberation from LAP, respectively. Free TGF-β activates TGF-β receptors (TβRI/II), leading to nuclear translocation of pSmad2/3, which promotes SC quiescence. In Kindlin-1–deficient cells (right), activation of β_1-class integrins and $\alpha_v\beta_6$ is impaired, leading to adhesion defects and loss of TGF-β–mediated SC quiescence. In addition, dysregulated Wnt ligand expression leading to elevation of Wnt5a levels leads to canonical Wnt–β-catenin signaling through the Lrp5/6–Fzd4 complex. Wnt5-Prom, Wnt5 promotor.

A single DMBA treatment induced more and slightly larger tumors in Kind1-K5 mice compared to controls (**Fig. 6f**–**i**), indicating that the hyperproliferative state of keratinocytes in Kind1-K5 mice was sufficient to promote tumor development. Furthermore, the tumors in the Kind1-K5 mice originated primarily from HFs and sebaceous glands containing hyperactive SCs.

DISCUSSION

Loss-of-function mutations in the *FERMT-1* gene cause KS, which is characterized by skin blistering at birth, premature skin aging, pigmentation defects and increased incidence of skin cancer. The ability of Kindlin-1 to activate integrins and link them to the F-actin cytoskeleton explains the development of skin blisters and basement membrane splitting followed by an inflammatory response. However, the notion that skin tumor development is promoted by hyperactive integrins and inhibited by compromised integrins indicates that Kindlin-1 loss activates oncogenic functions, inhibits tumor-suppressor functions or both. The task of this study was to identify such pathway(s).

Deletion of Kindlin-1 in skin epithelial cells with the K5-Cre driver line leads to small skin blistering, basement membrane defects, chronic skin inflammation, progressive pigmentation defects and skin atrophy and is hence similar to KS. Unexpectedly, Kind1-K5 mice also develop enlarged cutaneous epithelial SC compartments, hyperactive bulge SCs, distorted HF cycles and ectopic HFs (**Supplementary Fig. 8e**). In line with high SC proliferation, treatment with both DMBA and TPA as well as with DMBA only induces a significantly higher tumor incidence and tumor burden in Kind1-K5 mice. Moreover, the majority of the tumors are basal cell carcinoma– and trichofolliculoma-like lesions, suggesting that the tumors originate predominantly from HF bulge SCs.

In search for a mechanistic explanation for the dysregulated SC and tumor cell proliferation in Kind1-K5 mice, we identified two Kindlin-1–regulated signaling pathways with opposing functions on bulge SC quiescence (**Fig. 6j**). Kindlin-1 binding to the cytoplasmic tail of β_6 subunit–containing integrin[51] triggers $\alpha_v\beta_6$ integrin binding to the RGD motif of LAP, thereby liberating TGF-β and inducing TGF-β receptor signaling and cutaneous epithelial SC quiescence. These findings are supported by a report showing that loss of β_6

subunit–containing integrin impairs TGF-β signaling and elevates bulge SC activity *in vivo*[32].

Despite the sequence similarities of Kindlin-1 and Kindlin-2 (ref. 52) and their expression in keratinocytes from control and Kind1-K5 mice, Kindlin-2 can only partially compensate for Kindlin-1 at β_1 subunit–containing integrin adhesion sites. Furthermore, Kindlin-2 is unable to bind β_6 subunit tails, which prevents it from releasing TGF-β1 and suppressing SC proliferation. Interestingly, other TGF-β isoforms such as TGF-β2 activate HF stem cells by antagonizing BMP in the bulge[53]. In contrast to LAP1, however, LAP2 lacks the $\alpha v\beta_6$-binding RGD motif[54], and hence the release of TGF-β2 and BMP signaling are not affected by Kindlin-1 loss.

It is particularly interesting that high Kindlin-1 levels have also been associated with high TGF-β1 signaling in metastatic breast cancers[55]. Although it was not investigated how Kindlin-1 regulates TGF-β1 signaling, this observation, together with our findings, suggests that different tumor stages may benefit from different Kindlin-1 levels: in early stage tumors, low TGF-β signaling supports tumor growth, whereas in late stage tumors, high TGF-β signaling promotes the epithelial-to-mesenchymal transition and metastatic progression[56]. If this is the case, subjects with KS suffering from an increased tumor risk may be protected from metastasis.

We also found elevated Wnt–β-catenin signaling in cutaneous epithelial cells of Kind1-K5 mice and the epidermis of subjects with KS, which is inevitably associated with a high tumor risk and severe SC and hair cycle defects[13,50]. The defect leads to ectopic HF formation and aberrant hair cycling and is due to aberrant expression of several Wnt ligands, most notably Wnt5a, which probably act in an autocrine manner. Notably, chemical compounds that inhibit Wnt protein secretion or Wnt–β-catenin signaling prevent the hair cycle and Wnt signaling defects in keratinocytes from Kind1-K5 mice.

Wnt5a is best known for the ability to activate the noncanonical Wnt signaling pathway. However, Wnt5a can also elicit canonical Wnt–β-catenin signaling. The decision of which signaling pathway is induced is dictated by the type of cell surface receptor to which Wnt5a is binding: Wnt5a binding to the Ror2 receptor tyrosine kinase inhibits the transcriptional activity of β-catenin and thus canonical signaling, whereas Wnt5a binding to Fzd4 and the Lrp5/6 co-receptors leads to β-catenin stabilization and canonical Wnt signaling[45]. Interestingly, Wnt–β-catenin signaling can activate Notch[42], which is also elevated in keratinocytes from Kind1-K5 mice and may contribute at least in part to the Kind1-K5 mouse phenotype, for example, by suppressing *Wnt4* expression[48] and the recruitment of β-catenin to cell-cell junctions[44]. Clearly, the dysregulated expression of Wnt proteins and their receptors in Kind1-K5 mice strongly suggests that Kindlin-1 safeguards the skin and HFs against an overshooting activation of the important and at the same time potentially harmful canonical Wnt–β-catenin signals.

In summary, our results show that Kindlin-1 loss results in a combination of defects caused by the dysregulation of distinct pathways: the compromised β_1 integrins impair adhesion and induce an inflammatory response, the impaired TGF-β liberation from LAP leads to HF SC hyperproliferation, and the increased Wnt signaling abrogates the resting phase of the hair cycle, expands the SC compartments and, together with impaired TGF-β signaling and inflammation, contributes to the increased tumor risk. The high epithelial SC activity eventually leads to SC exhaustion and skin atrophy later in life, which is another hallmark of KS. It is also conceivable that the ability of Kindlin-1 to shuttle between integrin sites, where it mediates adhesion, migration and TGF-β release, and the cytoplasm, where it curbs Wnt–β-catenin signaling, may also contribute to physiologic SC homeostasis and hair development (**Fig. 6j**); mobilization of bulge SCs has little or no integrin-ligand engagement and therefore uses Kindlin-1 to prevent Wnt–β-catenin signaling and their activation. Once activated bulge SCs move to the hair germ, they engage integrins to ensure downward growth and therefore have less Kindlin-1 in the cytoplasm to inhibit Wnt–β-catenin signaling.

METHODS

Methods and any associated references are available in the online version of the paper.

Note: Any Supplementary Information and Source Data files are available in the online version of the paper.

ACKNOWLEDGMENTS

We thank J. Polleux for generating gold nanoarrays, S. Bach for expert technical assistance, C. Mein (Barts and the London Genome Centre) for generating the human microarray data and R. Zent and R. Paus for carefully reading the manuscript. We thank M. Aumailley (University of Cologne), R. Grosschedl (Max Planck Institute (MPI) Immunobiology), S. Violette (Biogen Idec), D. Sheppard (University of California, San Francisco) and M. Wegner (University of Erlangen) for providing antibodies and I. Thesleff (University of Helsinki), R. Kageyama (Kyoto University), A. Kispert (University of Hannover) and J. Behrens (University of Erlangen) for sending essential constructs. This work was funded by the US National Institutes of Health (CA034282) to D.B.R., the Wellcome Trust (PhD studentship to J.E.L.-C.) and the UK National Institute for Health Research (NIHR) Biomedical Research Centre based at Guy's and St. Thomas' National Health Service Foundation Trust and King's College London to J.A.M., the Advanced European Research Council (ERC) Grant (ERC Grant Agreement 322652) and the Max Planck Society to R.F.

AUTHOR CONTRIBUTIONS

R.F. initiated the project. R.F. and E.R. designed the experiments and wrote the paper. E.R., D.K., M.W., M.J., R.R., S.U., R.T.B. and J.E.L.-C. performed experiments. E.R., M.W., M.J. and R.F. analyzed data. D.B.R. and J.A.M. provided important reagents and/or analytical tools. All authors read and approved the manuscript.

COMPETING FINANCIAL INTERESTS

The authors declare no competing financial interests.

1. Meves, A., Stremmel, C., Gottschalk, K. & Fässler, R. The Kindlin protein family: new members to the club of focal adhesion proteins. *Trends Cell Biol.* **19**, 504–513 (2009).
2. Lai-Cheong, J.E. *et al.* Kindler syndrome: a focal adhesion genodermatosis. *Br. J. Dermatol.* **160**, 233–242 (2009).
3. Ussar, S. *et al.* Loss of Kindlin-1 causes skin atrophy and lethal neonatal intestinal epithelial dysfunction. *PLoS Genet.* **4**, e1000289 (2008).
4. Montanez, E. *et al.* Kindlin-2 controls bidirectional signaling of integrins. *Genes Dev.* **22**, 1325–1330 (2008).
5. Moser, M., Nieswandt, B., Ussar, S., Pozgajova, M. & Fässler, R. Kindlin-3 is essential for integrin activation and platelet aggregation. *Nat. Med.* **14**, 325–330 (2008).
6. Dowling, J.J., Vreede, A.P., Kim, S., Golden, J. & Feldman, E.L. Kindlin-2 is required for myocyte elongation and is essential for myogenesis. *BMC Cell Biol.* **9**, 36 (2008).
7. Lai-Cheong, J.E., Ussar, S., Arita, K., Hart, I.R. & McGrath, J.A. Colocalization of kindlin-1, kindlin-2, and migfilin at keratinocyte focal adhesion and relevance to the pathophysiology of Kindler syndrome. *J. Invest. Dermatol.* **128**, 2156–2165 (2008).
8. He, Y., Esser, P., Heinemann, A., Bruckner-Tuderman, L. & Has, C. Kindlin-1 and -2 have overlapping functions in epithelial cells implications for phenotype modification. *Am. J. Pathol.* **178**, 975–982 (2011).
9. Watt, F.M. Role of integrins in regulating epidermal adhesion, growth and differentiation. *EMBO J.* **21**, 3919–3926 (2002).
10. Tumbar, T. *et al.* Defining the epithelial stem cell niche in skin. *Science* **303**, 359–363 (2004).
11. Watt, F.M. & Jensen, K.B. Epidermal stem cell diversity and quiescence. *EMBO Mol. Med.* **1**, 260–267 (2009).
12. Woo, W.M. & Oro, A.E. SnapShot: hair follicle stem cells. *Cell* **146**, 334–334 (2011).

13. Arwert, E.N., Hoste, E. & Watt, F.M. Epithelial stem cells, wound healing and cancer. *Nat. Rev. Cancer* **12**, 170–180 (2012).
14. Alonso, L. & Fuchs, E. Stem cells in the skin: waste not, Wnt not. *Genes Dev.* **17**, 1189–1200 (2003).
15. Watt, F.M. & Fujiwara, H. Cell–extracellular matrix interactions in normal and diseased skin. *Cold Spring Harb. Perspect. Biol.* **3**, a005124 (2011).
16. Janes, S.M. & Watt, F.M. New roles for integrins in squamous-cell carcinoma. *Nat. Rev. Cancer* **6**, 175–183 (2006).
17. Evans, R.D. *et al.* A tumor-associated β1 integrin mutation that abrogates epithelial differentiation control. *J. Cell Biol.* **160**, 589–596 (2003).
18. Ferreira, M., Fujiwara, H., Morita, K. & Watt, F.M. An activating β1 integrin mutation increases the conversion of benign to malignant skin tumors. *Cancer Res.* **69**, 1334–1342 (2009).
19. White, D.E. *et al.* Targeted disruption of β1-integrin in a transgenic mouse model of human breast cancer reveals an essential role in mammary tumor induction. *Cancer Cell* **6**, 159–170 (2004).
20. Yu, Y. *et al.* Kindlin 2 forms a transcriptional complex with β-catenin and TCF4 to enhance Wnt signalling. *EMBO Rep.* **13**, 750–758 (2012).
21. Arita, K. *et al.* Unusual molecular findings in Kindler syndrome. *Br. J. Dermatol.* **157**, 1252–1256 (2007).
22. Emanuel, P.O., Rudikoff, D. & Phelps, R.G. Aggressive squamous cell carcinoma in Kindler syndrome. *Skinmed* **5**, 305–307 (2006).
23. Lai-Cheong, J.E. *et al.* Loss-of-function FERMT1 mutations in kindler syndrome implicate a role for fermitin family homolog-1 in integrin activation. *Am. J. Pathol.* **175**, 1431–1441 (2009).
24. Has, C. *et al.* Kindlin-1 is required for RhoGTPase-mediated lamellipodia formation in keratinocytes. *Am. J. Pathol.* **175**, 1442–1452 (2009).
25. Brakebusch, C. *et al.* Skin and hair follicle integrity is crucially dependent on β1 integrin expression on keratinocytes. *EMBO J.* **19**, 3990–4003 (2000).
26. Böttcher, R.T. *et al.* Sorting nexin 17 prevents lysosomal degradation of β1 integrins by binding to the β1-integrin tail. *Nat. Cell Biol.* **14**, 584–592 (2012).
27. Braun, K.M. *et al.* Manipulation of stem cell proliferation and lineage commitment: visualisation of label-retaining cells in wholemounts of mouse epidermis. *Development* **130**, 5241–5255 (2003).
28. Fujiwara, H. *et al.* The basement membrane of hair follicle stem cells is a muscle cell niche. *Cell* **144**, 577–589 (2011).
29. Alonso, L. & Fuchs, E. Stem cells of the skin epithelium. *Proc. Natl. Acad. Sci. USA* **100** (suppl. 1), 11830–11835 (2003).
30. Jensen, K.B. *et al.* Lrig1 expression defines a distinct multipotent stem cell population in mammalian epidermis. *Cell Stem Cell* **4**, 427–439 (2009).
31. Munger, J.S. *et al.* The integrin $\alpha_v\beta_6$ binds and activates latent TGFβ1: a mechanism for regulating pulmonary inflammation and fibrosis. *Cell* **96**, 319–328 (1999).
32. Xie, Y., McElwee, K.J., Owen, G.R., Häkkinen, L. & Larjava, H.S. Integrin β6-deficient mice show enhanced keratinocyte proliferation and retarded hair follicle regression after depilation. *J. Invest. Dermatol.* **132**, 547–555 (2012).
33. Li, L. & Bhatia, R. Stem cell quiescence. *Clin. Cancer Res.* **17**, 4936–4941 (2011).
34. Annes, J.P., Chen, Y., Munger, J.S. & Rifkin, D.B. Integrin $\alpha_v\beta_6$-mediated activation of latent TGF-β requires the latent TGF-β binding protein-1. *J. Cell Biol.* **165**, 723–734 (2004).
35. Kobielak, K., Stokes, N., de la Cruz, J., Polak, L. & Fuchs, E. Loss of a quiescent niche but not follicle stem cells in the absence of bone morphogenetic protein signaling. *Proc. Natl. Acad. Sci. USA* **104**, 10063–10068 (2007).
36. Zhang, J. *et al.* Bone morphogenetic protein signaling inhibits hair follicle anagen induction by restricting epithelial stem/progenitor cell activation and expansion. *Stem Cells* **24**, 2826–2839 (2006).
37. Gat, U., DasGupta, R., Degenstein, L. & Fuchs, E. *De novo* hair follicle morphogenesis and hair tumors in mice expressing a truncated β-catenin in skin. *Cell* **95**, 605–614 (1998).
38. Lo Celso, C., Prowse, D.M. & Watt, F.M. Transient activation of β-catenin signaling in adult mouse epidermis is sufficient to induce new hair follicles but continuous activation is required to maintain hair follicle tumours. *Development* **13**, 1787–1799 (2004).
39. Lowry, W.E. *et al.* Defining the impact of β-catenin/Tcf transactivation on epithelial stem cells. *Genes Dev.* **19**, 1596–1611 (2005).
40. Silva-Vargas, V. *et al.* β-catenin and Hedgehog signal strength can specify number and location of hair follicles in adult epidermis without recruitment of bulge stem cells. *Dev. Cell* **9**, 121–131 (2005).
41. Zhou, P., Byrne, C., Jacobs, J. & Fuchs, E. Lymphoid enhancer factor 1 directs hair follicle patterning and epithelial cell fate. *Genes Dev.* **9**, 700–713 (1995).
42. Estrach, S. *et al.* Jagged 1 is a β-catenin target gene required for ectopic hair follicle formation in adult epidermis. *Development* **133**, 4427–4438 (2006).
43. DasGupta, R. & Fuchs, E. Multiple roles for activated LEF/TCF transcription complexes during hair follicle development and differentiation. *Development* **126**, 4557–4568 (1999).
44. Bernard, P., Fleming, A., Lacombe, A., Harley, V.R. & Vilain, E. Wnt4 inhibits β-catenin/TCF signalling by redirecting β-catenin to the cell membrane. *Biol. Cell* **100**, 167–177 (2008).
45. Mikels, A.J. & Nusse, R. Purified Wnt5a protein activates or inhibits β-catenin–TCF signaling depending on receptor context. *PLoS Biol.* **4**, e115 (2006).
46. Chen, B. *et al.* Small molecule–mediated disruption of Wnt-dependent signaling in tissue regeneration and cancer. *Nat. Chem. Biol.* **5**, 100–107 (2009).
47. Huang, S.M. *et al.* Tankyrase inhibition stabilizes axin and antagonizes Wnt signalling. *Nature* **461**, 614–620 (2009).
48. Devgan, V., Mammucari, C., Millar, S.E., Brisken, C. & Dotto, G.P. p21WAF1/Cip1 is a negative transcriptional regulator of Wnt4 expression downstream of Notch1 activation. *Genes Dev.* **19**, 1485–1495 (2005).
49. Guasch, G. *et al.* Loss of TGFβ signaling destabilizes homeostasis and promotes squamous cell carcinomas in stratified epithelia. *Cancer Cell* **12**, 313–327 (2007).
50. Beronja, S. *et al.* RNAi screens in mice identify physiological regulators of oncogenic growth. *Nature* **501**, 185–190 (2013).
51. Bandyopadhyay, A., Rothschild, G., Kim, S., Calderwood, D.A. & Raghavan, S. Functional differences between kindlin-1 and kindlin-2 in keratinocytes. *J. Cell Sci.* **125**, 2172–2184 (2012).
52. Ussar, S., Wang, H.V., Linder, S., Fässler, R. & Moser, M. The Kindlins: subcellular localization and expression during murine development. *Exp. Cell Res.* **312**, 3142–3151 (2006).
53. Oshimori, N. & Fuchs, E. Paracrine TGF-β signaling counterbalances BMP-mediated repression in hair follicle stem cell activation. *Cell Stem Cell* **10**, 63–75 (2012).
54. Annes, J.P. *et al.* Making sense of latent TGFβ activation. *J. Cell Sci.* **116**, 217–224 (2003).
55. Sin, S. *et al.* Role of the focal adhesion protein kindlin-1 in breast cancer growth and lung metastasis. *J. Natl. Cancer Inst.* **103**, 1323–1337 (2011).
56. Chaudhury, A. & Howe, P.H. The tale of transforming growth factor-β (TGFβ) signaling: a soigné enigma. *IUBMB Life* **61**, 929–939 (2009).

ONLINE METHODS

Mouse strains. The conditional *Fermt-1*$^{flox/flox}$ mice carry a *loxP*-flanked ATG-containing exon 2 (**Supplementary Fig. 1a**) and were generated by electroporation of R1 embryonic stem cells using standard procedures[57]. Homologous recombination was verified with Southern blots, and positive embryonic stem cell clones were used to generate chimeric mice. Mice were crossed with transgenic mice carrying a deleter-flp recombinase to remove the neomycin cassette and with mice carrying deleter-Cre (to confirm the null phenotype) or K5-Cre transgenes, respectively[58]. For all animal studies, transgenic mice were backcrossed eight times to C57BL/6 mice. The TTAA-K5 transgenic mice were obtained through an intercross of mice carrying alanine substitutions of T788 and T789 in the cytoplasmic domain of β_1 integrin[26] with *Itgb1*-floxed mice and K5-Cre transgenic mice. The TOPgal Wnt reporter mice[43] were intercrossed with Kind1-K5 mice. For all *in vivo* experiments, genders were distributed randomly between the genotypes. Mice were housed in a special pathogen-free mouse facility, and all animal experiments were carried out according to the rules of and approved by the government of Upper Bavaria.

DMBA and TPA tumor experiment. Cutaneous two-stage chemical carcinogenesis was performed as previously described[59] using topical applications of 100 nmol (25 µg) DMBA (Sigma) in 100 µl of acetone and twice weekly applications of 10 nmol (6.1 µg) TPA (Sigma) in 200 µl of acetone or only acetone for 25 weeks. The tumor model was terminated after 25 weeks of TPA promotion because of the critical skin health condition of Kind1-K5 mice. For tumor experiments, control animals were treated with acetone or TPA only. For all animal studies, 7-week-old mice were randomized after genotyping, and sample size was estimated by nonparametric Wilcoxon test (*U* test). The number and size of tumors were recorded once per week after the start of promotion (week 0). All mice were euthanized at the end of the experiment. Skin lesions were analyzed by histology and graded as described previously[59–61].

Subjects with KS. Individuals with KS gave their informed written consent under protocols approved by St. Thomas' Hospital Ethics Committee (COREC number 06/Q0702/154), and the study was conducted according to the Declaration of Helsinki Principles. For immunofluorescence (IF) analysis, biopsies were taken from age- and site-matched controls (NHS) and subjects with KS with the following mutations: KS patient 1 (3-year-old Indian girl; homozygous nonsense mutation +/+ p.Glu516X) and KS patient 2 (22-year-old Panamanian woman; homozygous nonsense mutation +/+ p.Arg271X).

RNA for microarray analysis was isolated from upper-arm biopsies taken from three subjects with KS; KS patient A, a 22-year-old Omani woman with the homozygous nonsense mutation +/+ p.Arg271X; KS patient B, a 7-year-old Indian girl with the homozygous nonsense mutation +/+ p.Try616X; and KS patient C, a 19-year-old Omani woman with the nonsense mutation +/+ p.Try616X. Control skin RNA was isolated from four age-, site- and sex-matched biopsies.

Gene expression microarray. Total RNA was extracted using the RNeasy Fibrous Tissue Mini kit (Qiagen), and quantity and quality were measured on a Nanodrop spectrophotometer (Nanodrop, Wilmington, DE, USA). For whole-genome Illumina expression analysis, total RNA from each skin biopsy was hybridized to an Illumina Human-Ref-6 v2 BeadChip expression array (Illumina, San Diego, CA, USA). The Illumina HumanRef-6 v2 BeadChips were scanned with an Illumina Bead Array Reader confocal scanner.

The microarray data analysis was performed using Illumina's BeadStudio Data Analysis Software (Illumina). The expression signals for all genes from each individual were grouped in KS and NHS and averaged. In order to identify statistically significant differentially regulated genes, a prefiltering set was determined for significantly higher (≥2-fold change) and lower (≤0.5-fold change) expression intensity between KS and NHS skin samples. Bonferroni's correction was applied to each *P* value to obtain an adjusted *P* value to identify differentially expressed mRNAs with high statistical significance (**Supplementary Table 2**). The microarray data have been submitted to NCBI under the GEO accession number GSE47642.

FACS analysis. FACS analysis and sorting was performed as previously described[62]. A suspension of primary keratinocytes in FACS-PBS (PBS with 1% BSA) was incubated for 1 h with primary antibodies on ice and then washed twice with FACS-PBS. Cell viability was assessed by 7-aminoactinomycin labeling (BD Biosciences) or ethidium monoazide staining (Invitrogen). FACS analysis was carried out using a FACSCantoTMII cytometer (BD Biosciences) and cell sorting with an AriaFACSII high-speed sorter (BD Biosciences), both of which were equipped with FACS DiVa software (BD Biosciences). Purity of the sorted cells was determined by post-sort FACS analysis and typically exceeded 95%. Integrin surface FACS analysis of primary keratinocytes was carried out as previously described[63]. Data analysis was conducted using the FlowJo program (version 9.4.10).

Real-time PCR and Notch target gene inhibition. Total RNA from total skin or FACS-sorted keratinocytes was extracted with the RNeasy Mini extraction kit (Qiagen) following the manufacturer's instructions. For Notch target gene inhibition analysis, cells were plated on fibronectin- and collagen I–coated six-well plates (1.2×10^6 cells per well) and were treated the next day with 2.5 µM N-[N-(3,5-difluorophenacetyl)-L-alanyl]-S-phenylglycine t-butyl ester (DAPT; Selleckchem, S2215) in full keratinocyte growth medium (KGM) for 24 h before total RNA isolation. cDNA was prepared with an iScript cDNA Synthesis Kit (Biorad). Real-time PCR was performed with an iCycler (Biorad). Each sample was measured in triplicate, and values were normalized to *Gapdh*. The PCR primers used are listed in **Supplementary Table 4**.

Antibodies and inhibitors. The following antibodies or molecular probes were used at the indicated concentrations for western blot (W), IF, immunohistochemistry (IHC) or flow cytometry (FACS): Kindlin-1 (home made[3]; W: 1:5,000, IF of tissue: 1:1,000), Kindlin-2 (Sigma; K3269; W: 1:1,000), talin (Sigma; 8D4; W: 1:1,000), GAPDH (Calbiochem; 6C5; W: 1:10,000), phalloidin–Alexa 488 (Invitrogen; A12379; IF tissue: 1:500; IF of cells: 1:800), integrin α_M (Mac-1) (eBioscience; M1/70; IF of tissue: 1:200), GR1 (Ly6g) (eBioscience; RB6-8C5; IF of tissue: 1:200), CD4 (PharMing; H129.19; IF of tissue: 1:200), CD19 (PharMing; 1D3; IF of tissue: 1:200), integrin α_x (CD11c) (BD Bioscience; HL3; IF of tissue: 1:200), desmoplakin (Fritzgerald Industries International; 20R-DP002; IF tissue: 1:500), integrin α_6 (Itga6) (PharMingen; GoH3; IF of tissue: 1:200, FACS: 1:500), laminin-332 (a gift from M. Aumailley, University of Cologne, Germany; IF of tissue: 1:500), Keratin-10 (Krt-10) (Covance; PRB-159P; IHC: 1:600), Keratin-15 (Krt-15) (a gift from R. Grosschedl; MPI Immunobiology, Freiburg, Germany; IF: 1:500), Lef1 (a gift from R. Grosschedl, MPI Immunobiology, Freiburg, Germany; IF of tissue: 1:500), Loricrin (Lor) (Covance; PRB-145P; IF: 1:500), Ki67 (Dianova; M7249; IHC: 1:100), cleaved caspase-3 (Asp175, cCaspase3) (Cell Signaling; 9661; IF of tissue: 1:200), CD34 (BD Bioscience; RAM34; IF of tissue: 1:200, FACS: 1:100), Sca1 (BioLegend; D7; IF of tissue: 1:200, FACS: 1:200), Lrig1 (R&D Systems, AF3688; IF: 1:500), BrdU (Abcam; ab6326; IF: 1:500), Keratin-5 (Krt-5) (Covance; PRB-160P; IF: 1:1,000), Keratin-6 (Krt-6) (Covance; PRB-169; IF: 1:500), CDP (Santa Cruz; sc-13024; IF: 1:500), integrin β_1 (BD Biosciences; Ha2/5; FACS: 1:200), integrin β_3 (BD Bioscience; 2C3.G2; FACS: 1:200), integrin β_4 (BD Biosciences; 346-11A; FACS: 1:200), integrin β_6 CH2A1 (Itgb6) (a gift from S. Violette, Biogen Idec; IF of mouse tissue: 1:500), integrin β_6 (Itgb6) (Chemicon; 10D5; IF of human tissue: 1:200, FACS: 1:200, IF of cells: 1:500), integrin β_5 (Itgb5) (a gift from D. Sheppard, University of California, USA; FACS: 1:200), integrin β_8 (Itgb8) (Santa Cruz; sc-25714; FACS: 1:200), paxillin (BD Bioscience; 610051; IF: 1:500); pSMAD2/3 (Santa Cruz, sc11769; IF: 1:200), pSmad2 (Millipore; AB3849; W: 1:2,000), total Smad2/3 (Santa Cruz; sc-8332; W: 1:1,000), pSMAD1/5/8 (Millipore; AB3848; IF of tissue: 1:200), Sox9 (a gift from M. Wegner, University of Erlangen, Germany; IF of tissue: 1:500), trichohyalin (AE15) (Abcam; ab58755; IF of tissue: 1:500), activated Notch1 (NICD) (Abcam, ab8925; IF of tissue: 1:200) and pan-laminin (Sigma; L9393; IF of tissue: 1:500). The following secondary antibodies were used: goat anti–rabbit Alexa 488 (A11008), goat anti–human Alexa 488 (A11013), goat anti–mouse Alexa 488 (A11029), donkey anti–goat Alexa 488 (A11055), goat anti–guinea pig Alexa 594 (A11076), goat anti–mouse Alexa 546 (A11003), goat anti–rabbit Alexa 546 (A11010) (all from Invitrogen; FACS: 1:500, IF: 1:500), streptavidin-Cy5 (Dianova; 016170084; FACS: 1:400), goat anti–rat horseradish peroxidase (HRP) (Dianova; 712035150; W: 1:10,000), goat anti–mouse HRP (172-1011) and goat anti–rabbit HRP (172-1019) (all from Biorad; W: 1:10,000). For mouse monoclonal primary antibodies the M.O.M. (Mouse on Mouse) kit

doi:10.1038/nm.3490

(Vector Labs) was used according to the manufacturer's protocol. Mast cells were stained for mast cell heparin with avidin-FITC (Invitrogen; 43-4411; IF of tissue: 1:100) as previously described[64]. Nuclei were stained with DAPI (Sigma).

The Notch signaling inhibitor DAPT (Selleckchem; S2215) was dissolved in ethanol at 25 μg $μl^{-1}$. The Wnt inhibitors IWP-2 (Calbiochem; 681671) and IWR-1 (Sigma; I0161) were dissolved in DMSO at 2.5 μg $μl^{-1}$ (IWP-2) or 10 μg $μl^{-1}$ (IWR-1).

BrdU labeling. The LRC assay was performed as previously described[27]. Briefly, 10-day-old mice were injected four times with 50 mg kg^{-1} body weight BrdU every 12 h to label mitotic cells, and then mice were maintained for the indicated chase periods. To determine LRCs per HF bulge, tail epidermal whole mounts were prepared, *z* projections were acquired using a Leica SP5 confocal microscope (20× objective), and BrdU-positive cells were counted from ≥30 HFs per animal from different whole mounts.

Cell culture. The TGF-β reporter cell line tMLEC and LTBP1–TGF-β matrix–producing CHO-LTBP1 cells were used as described previously[34]. Primary keratinocytes were isolated at P21 or at the indicated time points as described previously[65]. To generate clonal keratinocyte cell lines, primary cells from *Fermt-1*$^{flox/flox}$ mice were spontaneously immortalized, single clones were picked, and Kindlin-1 ablation was induced by transient transfection with an adenovirus expressing Cre recombinase. Keratinocytes were cultured in KGM containing 8% chelated FCS (Invitrogen) and 45 μM Ca^{2+} in a 5% CO_2 humidified atmosphere on plastic dishes coated with a mixture of 30 μg ml^{-1} collagen I (Advanced BioMatrix) and 10 μg ml^{-1} fibronectin (Invitrogen).

Inhibition of premature anagen induction and increased Notch signaling. At telogen onset (P49), back skin of control and Kind1-K5 mice was shaved, and 100 μl of 200 μM IWR-1 or IWP-2 (diluted in PBS) was subcutaneously injected every 24 h into a marked skin region. 100 μl DMSO diluted in PBS was used for control experiments. At P56, the treated back skin was isolated, sectioned and stained with H&E. Ten serially sectioned HFs per animal were counted. To analyze Notch signaling, back skin sections were stained for NICD, and NICD-positive nuclei were quantified.

Constructs and transfections. Wnt4 expression constructs were gifts from A. Kispert (University of Hannover, Germany), and the human β-catenin expression construct was a gift from J. Behrens (University of Erlangen, Germany). Human WNT5A (ID18032), LEF1 (ID16709), pHes1-luc (ID43806), SuperTOPFlash (ID17165) and FOPFlash (ID12457) reporter plasmids were purchased from Addgene. The pEGFP-C1 expression vector was acquired from Clontech.

GFP-tagged Kindlin-1, Kindlin-2 and Kindlin-1–QWAA expression constructs were described previously[3], and the Kindlin1-NLS construct was generated by fusing SV40 NLS motifs to the N terminus of Kindlin-1. The expression cassettes were driven by a CAG promotor and flanked by two inverted terminal repeat sites recognized by sleeping beauty transposase 100× (SB100×)[66] and transiently co-transfected with the SB100× vector in a 1:1 ratio using Lipofectamine 2000 (Invitrogen) following the manufacturer's instructions. After two passages, cells stably expressing the GFP fusion protein were FACS sorted for equal expression levels, which was further confirmed by western blotting.

Histology and immunostainings. Small pieces from back skin were either fixed in paraformaldehyde (PFA) and embedded in paraffin or frozen on dry ice in cryo-matrix (Thermo) and sectioned. Tail skin whole mounts were prepared and immunostained as described[27]. Immunohistochemistry (H&E, DAB, Oil Red O, alkaline phosphatase (AP) and β-gal) of skin sections and tail whole mounts and immunofluorescence staining of tissue sections were carried out as described[25]. To better visualize the blue β-gal stain, the epidermal whole mount was overlaid with a grayscale image. Immunostaining of human skin sections for $β_6$ integrin followed published protocols[67].

HF bulge sizes were quantified in epidermal tail whole mounts stained for Krt-15, and *z* projections were collected with a confocal microscope using a 20× objective. The length and diameter of a Krt-15–positive bulge area was measured with the ImageJ software (version 1.41n), and bulge volumes were calculated using the circular cylinder formula ($v = π \times r^2 \times h$, where *v* is the volume, *r* is the radius, and *h* is the height). The HF numbers were quantified in serial sections of comparable back skin regions from at least three mice per genotype and the indicated ages. HFs per 10× objective field of H&E-stained sections were counted. HFs in anagen and early HF development were staged as described previously[68,69].

Images were collected by confocal microscopy (DMIRE2 or SP5, Leica) with a 10×, 20× numerical aperture (NA) 1.4 or 40× oil objective using Leica Confocal software (version 2.5 build 1227) or by bright field microscopy (Axioskop, Carl Zeiss with a 10× NA 0.3, 20× NA 0.5 or 40× NA 0.75 objective) and DC500 camera with IM50 software (Leica).

***In situ* hybridization.** Antisense riboprobes for mouse *Fzd4* (SpeI-EcoRI fragment of mouse FZD4 3′ untranslated region), *Wnt5a* (gift from I. Thesleff, University of Helsinki, Finland) and Hes1 (gift from R. Kageyama, Kyoto University, Japan) were synthesized with T7 RNA polymerase (New England BioLabs) and DIG (digoxigenin) RNA Labeling Mix according to the manufacturer's instructions (Roche). Isolated tail skin epidermis was fixed in 4% PFA in PBS, washed in PBS for 5 min twice and then washed twice for 15 min in PBS with 0.1% active diethylpyrocarbonate followed by 15 min equilibration in 5× saline-sodium citrate (SSC). Samples were first prehybridized for 1 h at 58 °C in 50% formamide, 5× SSC and 40 μg ml^{-1} salmon sperm DNA, then hybridized for 16 h at 58 °C with 400 ng ml^{-1} of DIG-labeled probe in prehybridization mix and washed twice for 30 min in 2× SSC at room temperature, followed by a 60-min wash at 65 °C in 2× SSC and then a 60-min wash at 65 °C in 0.2× SSC. The tissues were washed in Tris-buffered saline (TBS) for 5 min three times, blocked in 0.5% blocking reagent (Roche) in 0.1% Tween 20 and TBS (TBST) for 90 min at room temperature and then incubated in 1:5,000-diluted anti-DIG AP (Roche) in 0.5% blocking reagent in TBST at 4 °C overnight. After three 60-min washes in TBST, tissues were incubated in NTMT (100 mM NaCl, 100 mM Tris, pH 9.5, 50 mM $MgCl_2$ and 0.1% Tween 20) for 10 min at room temperature. Color was developed using BM Purple AP substrate precipitating reagent (Roche) at 37 °C. The reaction was stopped for 15 min with TE buffer (10 mM Tris and 1 mM EDTA, pH 8.0), and samples were mounted with 70% glycerol.

Peptide pulldowns. Pulldowns were performed with $β_1$ WT tail peptide (HDRR EFAKFEKEKMNAKWDTGENPIYKSAVTTVVNPKYEGK-OH), $β_1$ scrambled peptide (EYEFEPDKVDTGAKGTKMAKNEKKFRNYTVHNIWESRKV AP-OH), $β_6$ WT tail peptide (HDRKEVAKFEAERSKAKWQTGTNPLYRGST STFKNVTYKHREKHKAGLSSDG-OH) and $β_6$ scrambled peptide (KTDHAV QGDKKLSHKKNRGTSKATFPKVRHYETEEWAALESGYGSRTFKNSR-OH). All peptides were desthiobiotinylated. Before use, peptides were immobilized on 35 μl Dynabeads MyOne Streptavidine C1 (10 mg ml^{-1}; Invitrogen) for 3 h at 4 °C.

Keratinocytes were lysed on ice in Mammalian Protein Extraction Reagent (Thermo Scientific), and 1 mg of cell lysate was incubated with the indicated peptides for 4 h at 4 °C. After three washes with lysis buffer, the beads were boiled in SDS-PAGE sample buffer, and the supernatant was loaded on 8% SDS-PAGE gels.

Preparation of $α_vβ_6$ antibody–coated coverslips. Antibody coating was carried out as described[70]. Briefly, glass slides (24 mm × 24 mm; Menzel) were sterilized, coated with collagen I (Advanced BioMatrix) for 1 h at 37 °C, air dried, covered with nitrocellulose dissolved in methanol and air dried again. Slides were incubated with $α_vβ_6$-specific antibody (10D5; 10 μg ml^{-1}; Chemicon) diluted in PBS overnight at 4 °C in a humidity chamber, washed once with PBS and blocked with 1% BSA for 1 h at room temperature.

Generation of dense gold nanoarrays functionalized with cRGD. In a typical synthesis, 7 mg ml^{-1} of polystyrene$_{154}$-block-poly(2-vinylpyridine)$_{33}$ (PS_{154}-*b*-$P2VP_{33}$; Polymer Source) was dissolved at room temperature in p-xylene (Sigma) and stirred for 2 d. Hydrogen tetrachloroaurate (III) trihydrate ($HAuCl_4 \cdot 3H_2O$; Sigma) was added to the block co-polymer solution (1 $HAuCl_4$ per 2 P2VP units) and stirred for 2 d in a sealed glass vessel. Glass coverslips (Carl Roth) were cleaned in a piranha solution for at least 2 h and rinsed extensively with MilliQ water and dried under a stream of nitrogen. Micellar monolayers were prepared by dip coating a glass coverslip into previously prepared solutions with a constant

velocity equal to 24 mm min^{-1}. The dip-coated glass slides were exposed to oxygen plasma (150 W, 0.15 mbar, 45 min; PVA TEPLA 100 Plasma System). To prevent nonspecific protein adsorption or cell binding, the glass background was covalently modified with silane-terminated polyethylene glycol (PEG; molecular weight 2,000) (ref. 71). Thiol-terminated cRGD was synthesized as described before[72]. The gold nanoparticles were then functionalized with this ligand by incubating the PEG-functionalized substrates in 100 µl of a 50 µM aqueous solution. The substrates were then rinsed thoroughly, incubated overnight with water and finally dried with nitrogen.

Spreading assay. A single-cell suspension with 1.0×10^5 cells per well in a six-well plate was plated in serum-free KGM (1% BSA and 1% penicillin-streptomycin) on fibronectin-coated glass coverslips (10 µg ml^{-1} fibronectin in PBS for 1 h at room temperature) or the indicated substrates for 3 h at 37 °C. Cells were imaged by a bright-field Axiovert 40 CFL microscope (20× objective; Carl Zeiss) and a CV640 camera (Prosilica) before fixation in 4% PFA-PBS and immunostaining with the indicated antibodies. The spreading area was quantified after staining with phalloidin–Alexa 488 (Invitrogen) with an AxioImager Z1 microscope (20× objective; Carl Zeiss) using the ImageJ software (Version 1.41n).

TGF-β stimulation assays. Keratinocytes were starved for several hours and stimulated with 5 ng ml^{-1} recombinant human TGF-β1 (PEROTech) in serum-free KGM for the indicated times, lysed and analyzed by western blotting. TGF-β–modulated proliferation was determined in 70% confluent keratinocytes that were cultured in six-well plates, incubated for 8 h with 10 µM 5-ethynyl-2′-deoxyuridine (EdU; Invitrogen) and the indicated concentrations of TGF-β1 and analyzed with the Click-iT EdU Alexa Fluor488 Flow Cytometry Assay kit (Invitrogen).

TGF-β release assay. TGF-β release was determined as described[34]. Briefly, CHO-LTBP1 cells were seeded (5.0×10^4 cells per well) for 48 h in a 96-well plate in triplicates to deposit an LTBP1–TGF-β–rich matrix. Cells were then detached with PBS and 15 mM EDTA, and the remaining LTBP1–TGF-β–rich matrix was washed twice with PBS and incubated with keratinocytes (2.0×10^4 cells per well) and tMLEC cells (1.5×10^4 cells per well) in a 100 µl final volume either in the absence or presence of $\alpha_v\beta_6$ integrin–blocking antibody (10D5; 20 µg ml^{-1}; Chemicon) or TGF-β neutralizing antibody (1D11; 15 µg ml^{-1}; BD Biosciences). The amount of released TGF-β was measured after 16–24 h using a Bright Glo luciferase kit (Promega).

Wnt and Notch reporter assay. Cells were plated on fibronectin- and collagen I–coated 12-well plates (6.0×10^5 cells per well) before transient transfection with 0.5 µg of pHes1-luc, SuperTOPFLASH or SuperFOPFLASH reporter, the indicated expression plasmid and 50 ng thymidine kinase–driven *Renilla* (Promega) for controlling the transfection efficiency. The total amount of transfected plasmid DNA was kept constant at 1.5 µg per well using the pEGFP-C1 expression vector as a transfection control (Clontech). After 24 h (Wnt reporter) or 48 h (Notch reporter), luciferase activity was analyzed with a Dual Luciferase reporter assay system (Promega). To determine the effect of Wnt or Notch signaling, cells were treated with the indicated inhibitor 18 h after transfection, and luciferase activity was measured 24 h later.

Statistical analyses. Analyses were performed with GraphPad Prism software (version 5.00, GraphPad Software). Experiments were routinely repeated at least three times, and the repeat number was increased according to effect size or sample variation. If not mentioned otherwise in the figure legend, statistical significance ($^*P < 0.05$; $^{**}P < 0.01$; $^{***}P < 0.001$; NS, not significant) was determined by unpaired *t* test (for biological effects with assumed normal distribution), Wilcoxon *t* test or Mann-Whitney *U* test. In the boxplots, the middle line represents the median, the box ends represent the 25th and 75th percentiles, the whisker ends show the minimum and maximum distribution or are at the 1.5-interquartile range, and outliers are shown as dots, as indicated in the figure legend. Unbiased and reproducible identification of cells with positive nuclear staining for β-catenin, Lef1 and NICD was ensured by quantification of nuclear staining intensities with ImageJ tool (version 1.41n).

57. Fässler, R. & Meyer, M. Consequences of lack of β1 integrin gene expression in mice. *Genes Dev.* **9**, 1896–1908 (1995).
58. Ramirez, A. *et al.* A keratin K5Cre transgenic line appropriate for tissue-specific or generalized Cre-mediated recombination. *Genesis* **39**, 52–57 (2004).
59. Abel, E.L., Angel, J.M., Kiguchi, K. & DiGiovanni, J. Multi-stage chemical carcinogenesis in mouse skin: fundamentals and applications. *Nat. Protoc.* **4**, 1350–1362 (2009).
60. Kasper, M. *et al.* Wounding enhances epidermal tumorigenesis by recruiting hair follicle keratinocytes. *Proc. Natl. Acad. Sci. USA* **108**, 4099–4104 (2011).
61. Sundberg, J.P., Sundberg, B.A. & Beamer, W.G. Comparison of chemical carcinogen skin tumor induction efficacy in inbred, mutant, and hybrid strains of mice: morphologic variations of induced tumors and absence of a papillomavirus cocarcinogen. *Mol. Carcinog.* **20**, 19–32 (1997).
62. Jensen, K.B., Driskell, R.R. & Watt, F.M. Assaying proliferation and differentiation capacity of stem cells using disaggregated adult mouse epidermis. *Nat. Protoc.* **5**, 898–911 (2010).
63. Lorenz, K. *et al.* Integrin-linked kinase is required for epidermal and hair follicle morphogenesis. *J. Cell Biol.* **177**, 501–513 (2007).
64. Kunder, C.A. *et al.* Mast cell–derived particles deliver peripheral signals to remote lymph nodes. *J. Exp. Med.* **206**, 2455–2467 (2009).
65. Montanez, E. *et al.* Analysis of integrin functions in peri-implantation embryos, hematopoietic system, and skin. *Methods Enzymol.* **426**, 239–289 (2007).
66. Mátés, L. *et al.* Molecular evolution of a novel hyperactive Sleeping Beauty transposase enables robust stable gene transfer in vertebrates. *Nat. Genet.* **41**, 753–761 (2009).
67. Brown, J.K. *et al.* Integrin-$\alpha_v\beta_6$, a putative receptor for foot-and-mouth disease virus, is constitutively expressed in ruminant airways. *J. Histochem. Cytochem.* **54**, 807–816 (2006).
68. Müller-Röver, S. *et al.* A comprehensive guide for the accurate classification of murine hair follicles in distinct hair cycle stages. *J. Invest. Dermatol.* **117**, 3–15 (2001).
69. Paus, R. *et al.* A comprehensive guide for the recognition and classification of distinct stages of hair follicle morphogenesis. *J. Invest. Dermatol.* **113**, 523–532 (1999).
70. Shi, Q. & Boettiger, D. A novel mode for integrin-mediated signaling: tethering is required for phosphorylation of FAK Y397. *Mol. Biol. Cell* **14**, 4306–4315 (2003).
71. Blümmel, J. *et al.* Protein repellent properties of covalently attached PEG coatings on nanostructured SiO_2-based interfaces. *Biomaterials* **28**, 4739–4747 (2007).
72. Morales-Avila, E. *et al.* Multimeric system of 99mTc-labeled gold nanoparticles conjugated to c[RGDfK(C)] for molecular imaging of tumor $\alpha_v\beta_3$ expression. *Bioconjug. Chem.* **22**, 913–922 (2011).

doi:10.1038/nm.3490

7.2 Paper II

Loss of Kindlin-1 causes skin atrophy and lethal neonatal intestinal epithelial dysfunction

Siegfried Ussar, Markus Moser, Moritz Widmaier, **Emanuel Rognoni**, Christian Harrer, Orsolya Genzel-Boroviczeny, Reinhard Fässler

Supplementary material

Tif files

Supplementary Figures 1-10

OPEN ACCESS Freely available online

PLoS GENETICS

Loss of Kindlin-1 Causes Skin Atrophy and Lethal Neonatal Intestinal Epithelial Dysfunction

Siegfried Ussar[1], Markus Moser[1], Moritz Widmaier[1], Emanuel Rognoni[1], Christian Harrer[1,2], Orsolya Genzel-Boroviczeny[2], Reinhard Fässler[1]*

1 Department of Molecular Medicine, Max-Planck Institute of Biochemistry, Martinsried, Germany, **2** Division of Neonatology, Perinatal Center, Children's Hospital, Ludwig-Maximilians University, Munich, Germany

Abstract

Kindler Syndrome (KS), characterized by transient skin blistering followed by abnormal pigmentation, skin atrophy, and skin cancer, is caused by mutations in the FERMT1 gene. Although a few KS patients have been reported to also develop ulcerative colitis (UC), a causal link to the FERMT1 gene mutation is unknown. The FERMT1 gene product belongs to a family of focal adhesion proteins (Kindlin-1, -2, -3) that bind several β integrin cytoplasmic domains. Here, we show that deleting Kindlin-1 in mice gives rise to skin atrophy and an intestinal epithelial dysfunction with similarities to human UC. This intestinal dysfunction results in perinatal lethality and is triggered by defective intestinal epithelial cell integrin activation, leading to detachment of this barrier followed by a destructive inflammatory response.

Citation: Ussar S, Moser M, Widmaier M, Rognoni E, Harrer C, et al. (2008) Loss of Kindlin-1 Causes Skin Atrophy and Lethal Neonatal Intestinal Epithelial Dysfunction. PLoS Genet 4(12): e1000289. doi:10.1371/journal.pgen.1000289

Editor: Veronica van Heyningen, Medical Research Council Human Genetics Unit, United Kingdom

Received May 16, 2008; **Accepted** November 3, 2008; **Published** December 5, 2008

Funding: This work was supported by the BMBF, the Austrian Science Foundation (SFB021) and the Max Planck Society.

Competing Interests: The authors have declared that no competing interests exist.

* E-mail: faessler@biochem.mpg.de

Introduction

Kindler Syndrome (KS; OMIM:173650) is a rare, recessive genodermatosis caused by mutations in the FERMT1 gene (C20ORF42/KIND1) [1,2]. KS patients suffer from varying skin abnormalities that occur at distinct phases of their life [3]. Skin blisters develop and disappear after birth, followed by skin atrophy, pigmentation defects and finally skin cancer. The severity of the individual symptoms varies extensively among individual patients. FERMT1 mutations are distributed along the entire gene and can give rise to different truncated Kindlin-1 proteins [4]. Interestingly, the different courses of the KS cannot be linked to mutations within specific regions of the FERMT1 gene [3] suggesting that additional environmental and/or genetic factors contribute to the disease course.

Kindlin-1 belongs to a novel family of cytoplasmic adaptor proteins consisting of three members (Kindlin-1-3) [5]. Kindlins are composed of a central FERM (band 4.1, ezrin, radixin, moesin) domain, which is disrupted by a pleckstrin homology (PH) domain. They localize to cell-matrix adhesion sites (also called focal adhesions, FAs) where they regulate integrin function. In line with the role of Kindlins in integrin function, keratinocytes from KS patients and Kindlin-1-depleted keratinocytes display impaired cell adhesion and delayed cell spreading [6,7]. The mechanism how Kindlin-1 regulates integrin function is not understood and controversial. Kindlin-2 (Fermt2) and Kindlin-3 (Fermt3) were shown to bind to the membrane distal NxxY motif of β1 (Itgb1) and β3 (Itgb3) integrin cytoplasmic domains. This binding, in concert with Talin (Tln1) recruitment to the membrane proximal NPxY motif, leads to the activation (inside-out signaling) of β1 and β3 class integrins enabling them to bind to their ligands. Following ligand binding, Kindlin-2 and Kindlin-3 stay in matrix adhesion sites where they link the ECM to the actin cytoskeleton by recruiting ILK and Migfilin (Fblim1) to FAs (outside-in signaling). Consistent with this adaptor function of Kindlins, keratinocytes from KS patients and keratinocytes depleted of Kindlin-1 display impaired cell adhesion and delayed cell spreading [6,7]. Importantly, however, Kindlin-1 was reported to have different properties than Kindlin-2 and -3, since it was shown to bind like Talin to the proximal NPxY motif of β1 integrin tails [6].

The Kindlins have a specific expression pattern. Kindlin-1 is expressed in epithelial cells, while Kindlin-2 is expressed almost ubiquitously. They are both found at integrin adhesion sites and/or cadherin-based cell-cell junctions. Kindlin-3 is exclusively expressed in hematopoietic cells, where it controls a variety of functions ranging from integrin signaling in platelets [8] to stabilizing the membrane cytoskeleton in mature erythrocytes [9].

Although the FERMT1 gene is expressed in epithelial cells of almost all tissues and organs [5], only abnormalities of the skin and the oral mucosa are associated with KS. Recently it has been reported, however, that some KS patients also develop ulcerative colitis (UC) [4,10,11], which together with Crohn's disease belongs to idiopathic inflammatory bowel disease.

UC usually occurs in the second or third decade of life, although the incidence in pediatric patients is steadily rising [12,13]. UC is restricted to the colon and is characterized by superficial ulcerations of the mucosa. It is currently believed that the mucosal ulcerations are triggered by the release of a complex mixture of inflammatory mediators leading to severe inflammation and subsequent epithelial cell destruction [12]. In line with this paradigm a large number of murine colitis models occur when the innate or adaptive immune response is altered [12]. Genetic linkage analysis in man led to the identification of several susceptibility loci [14,15].

Author Summary

Mutations in FERMT1, coding for the Kindlin-1 protein, cause Kindler Syndrome in humans, characterized by skin blistering, atrophy, and cancer. Recent reports showed that some Kindler Syndrome patients additionally suffer from ulcerative colitis. However, it is unknown whether this is caused by loss of Kindlin-1 or by unrelated abnormalities such as infections or additional mutations. We ablated the Fermt1 gene in mice to directly analyze the pathological consequences and the molecular mode of action of Kindlin-1. Kindlin-1–deficient mice develop a severe epidermal atrophy, but lack blisters. All mutant mice die shortly after birth from a dramatic, shear force-induced detachment of intestinal epithelial cells followed by a profound inflammation and organ destruction. The intestinal phenotype is very similar to, although more severe than, the one observed in Kindler Syndrome patients. In vitro studies revealed that impaired integrin activation, and thus impaired adhesion, to the extracellular matrix of the intestinal wall causes intestinal epithelial cell detachment. Therefore, we demonstrate that intestinal epithelial cells require adhesive function of integrins to resist the shear force applied by the stool. Furthermore, we provide evidence that the colitis associated with Kindler Syndrome is caused by a dysfunction of Kindlin-1 rather than by a Kindlin-1–independent event.

In line with the UC disease course most of the KS patients develop their first UC symptoms in adulthood. Interestingly, however, one of them suffered from a severe neonatal form of UC and was diagnosed with a null mutation in the FERMT1 gene after developing trauma-induced skin blistering [10]. Since only a few KS patients were reported to develop intestinal symptoms, it is currently debated whether UC development in these patients is directly linked to FERMT1 gene mutations or secondarily caused by a microbial infection or an abnormal inflammatory response.

In this study we directly investigated the role of Kindlin-1 in vivo by generating mice carrying a constitutive null mutation in the Kindlin-1 gene. We demonstrate that Kindlin-1 deficient mice develop skin atrophy and a lethal intestinal epithelial dysfunction, resembling the reported UC in KS patients. The intestinal epithelial dysfunction is caused by defective intestinal epithelial integrin activation leading to extensive epithelial detachment followed by a severe inflammatory reaction.

Results

Loss of Kindlin-1 Leads to a Lethal Intestinal Epithelial Dysfunction

To unravel the consequences of loss of Kindlin-1 in vivo, we established a mouse strain with a disrupted Fermt1 gene, leading to a complete loss of Kindlin-1 mRNA and protein (Figure 1A–C). Heterozygous Kindlin-1 mice (Kindlin-$1^{+/-}$) had no phenotype and were fertile. Kindlin-1-deficient mice (Kindlin-$1^{-/-}$) were born with a normal Mendelian ratio (29.6% +/+; 44.1% +/−; 26.3% −/−; n = 203 at P0) and appeared normal at birth. Two days postnatal (P2), all Kindlin-$1^{-/-}$ mice analyzed so far were dehydrated (Figure 1D), failed to thrive (Figure 1E) and died between P3-P5 (Figure 1E). Blood glucose and triglyceride levels of Kindlin-$1^{-/-}$ mice were normal suggesting a normal absorption of nutrients in the small intestine (Figure S1). Their urine showed an increased osmolarity and protein content further pointing to severe dehydration (Figure 1F, Figure S2A and B). Histology of Kindlin-$1^{-/-}$ kidneys at P3 revealed normal morphology of glomeruli and tubular systems (Figure S2C). Thus, these findings suggest that the peri-natal lethality is not caused by a renal dysfunction.

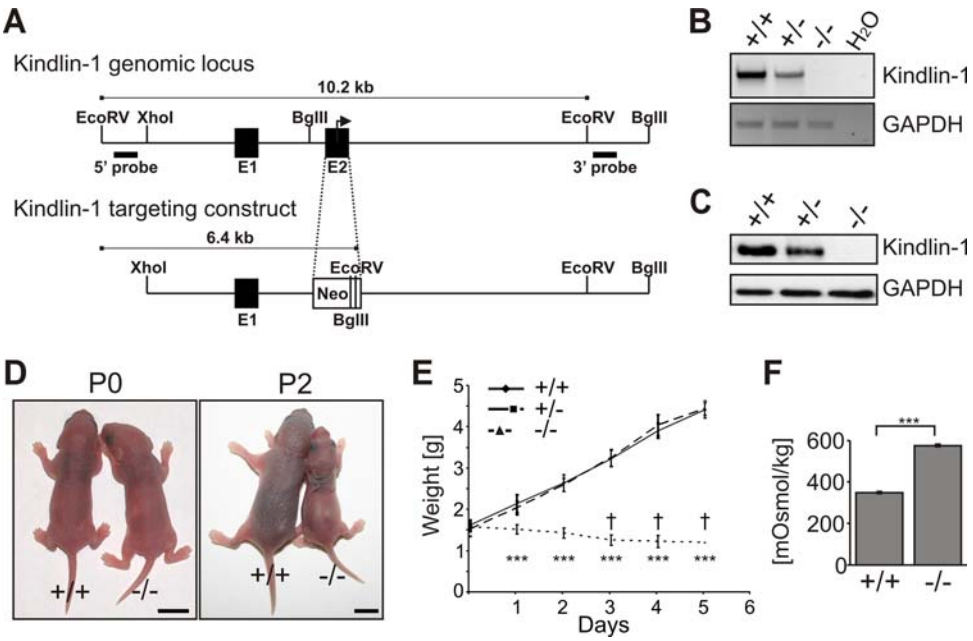

Figure 1. Loss of Kindlin-1 results in early postnatal lethality. (A) The Fermt1 gene was disrupted by replacing the ATG start codon containing exon 2 with a neomycin resistance cassette. (B) Kindlin-1 mRNA levels were determined by PCR from cDNAs derived from P3 kidneys. (C) Loss of Kindlin-1 protein was confirmed by western blotting in colonic IEC lysates. (D) Pictures from newborn (P0) and two day old mice (P2). Scale bars represent 5mm. (E) Weight curve of Kindlin-$1^{-/-}$ (n = 8) and control littermates (+/+; n = 8; +/−; n = 9) where a † indicates when mice died. *** indicates a P-value <0.0001. Error bars show standard deviations. (F) Osmolarity of P2 Kindlin-$1^{-/-}$ and control (+/+) urine (n = 3 per genotype). Error bars show standard deviations. *** indicates a P-value <0.0001.
doi:10.1371/journal.pgen.1000289.g001

Next we analyzed whether skin abnormalities caused the perinatal lethality. Although Kindlin-1$^{-/-}$ mice showed features of KS like skin atrophy and reduced keratinocyte proliferation (Figure 2A and B), adhesion of basal keratinocytes to the basement membrane (BM) was unaltered (Figure 2A and Figure S3). Histology of backskin sections from different developmental stages revealed normal keratinocyte differentiation (Figure S4), normal development of the epidermal barrier (Figure S5A and Figure 2C and D), and comparable epidermal thickness at E18.5 and P0 (Figure S5B). In line with the progressing proliferation defect quantified by the number of keratinocytes positive for the cell cycle marker Ki67 (Mki67), a reduction of the epidermal thickness was first observed at P1 (Figure S5B). Interestingly despite the mild in vivo phenotype, Kindlin-1$^{-/-}$ keratinocytes displayed severe adhesion and spreading defects in culture (Figure S6A and B) further indicating that Kindlin-1$^{-/-}$ keratinocytes from mouse and man display similar defects [7].

These results indicated that another defect is responsible for their perinatal lethality. When the stomach and the intestine of Kindlin-1$^{-/-}$ mice were examined, they were swollen and filled with milk and gas (Figure 3A) suggesting severe intestinal dysfunction might be the cause of death. The presence of milk in the stomach together with the normal histology of the oral and esophageal mucosa suggested that the lethality is not caused by impaired feeding (Figure S7). At P2, the terminal ileum and colon were shortened and swollen and strictures were evident in the distal colon, which are signs of acute inflammation (Figure 3B). By P3, when the majority of mutant mice were dying, more than 80% of the colonic epithelium was detached (Figure 3C and Figure S8A–C), became apoptotic (Figure S9) and infiltrated by macrophages, granulocytes (Mac-1; Itgam staining) and T cells (Thy staining) (Figure 3D). The shortened colon was neither a consequence of increased apoptosis, which was only seen in detached epithelium, nor a result of reduced intestinal epithelial cell (IEC) proliferation (Figure S9).

The epithelial detachment and severe inflammation extended into the ileum (Figure 3C). In contrast, the proximal small intestine (duodenum and jejunum) had no evidence of IEC detachment or inflammation (Figure 4). The phenotype of Kindlin-1$^{-/-}$ mice for the most part phenocopied the intestinal disease observed in the patient with a complete loss of Kindlin-1[10].

Kindlin-1 Is Required for Intestinal Epithelial Cell Adhesion

To define the cell type affected by loss of Kindlin-1 we localized Kindlin-1 in the normal intestine by immunostaining. Similar to the situation in man [4], Kindlin-1 is present throughout the cytoplasm of IECs of the colon and at the basolateral sites of both IECs of the colon (Figure 5A) and the small intestine (Figure 5B). The anti-Kindlin-1 polyclonal antibody produced some weak unspecific background signals in the intestinal mesenchyme of wild type and Kindlin-1$^{-/-}$ mice (Figure 5B). Kindlin-2 was exclusively found in cell-cell contacts and did not change its distribution in the absence of Kindlin-1 (Figure 5C and D). Focal adhesion (FA) components such as Talin and Migfilin as well as

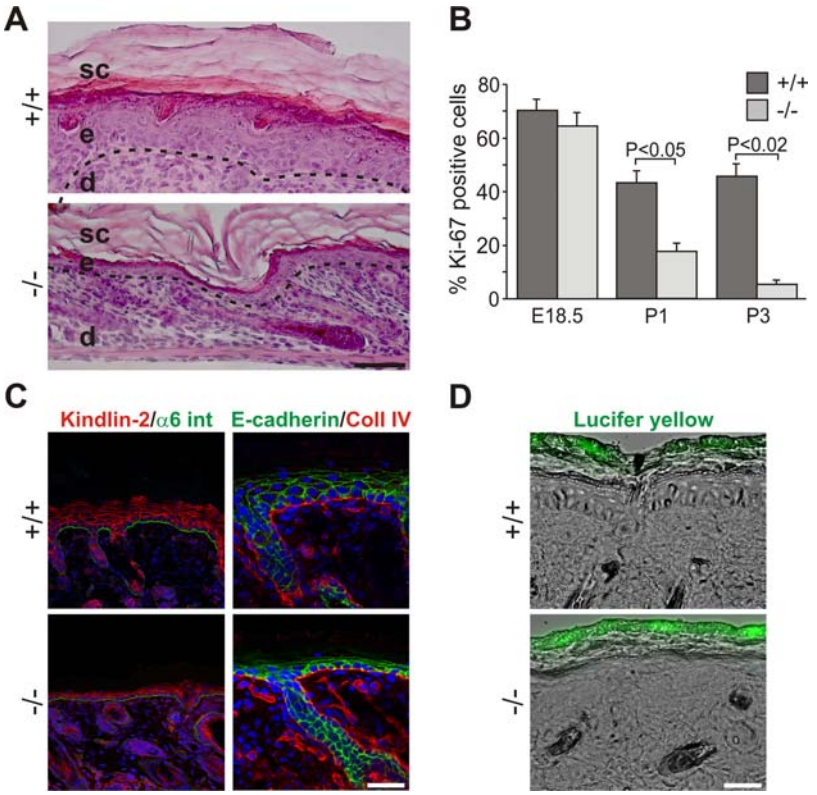

Figure 2. Atrophy and reduced proliferation in Kindlin-1$^{-/-}$ skin. (A) H&E stainings from P3 backskin show severe epidermal atrophy in Kindlin-1$^{-/-}$ mice. The BM is indicated by a dashed line and separates the epidermis (e) from the dermis (d). sc: stratum corneum. Scale bar indicates 50 μm. (B) Percentage of Ki67-positive interfollicular keratinocytes, indicating proliferating cells, at different ages (n = 7 per genotype). Error bars show standard errors of the mean. (C) Kindlin-2 (red; co-stained with α6 integrin (α6 int; in green) and E-cadherin (green, co-stained with Collagen IV (Coll IV) in red) staining of P3 backskin sections. Nuclei are shown in blue. Scale bar indicates 10 μm. (D) FITC-Lucifer yellow stain of P3 backskin overlaid with DIC. Lack of lucifer yellow dye penetration shows normal skin barrier in Kindlin-1$^{-/-}$ mice. Scale bar indicates 50 μm.
doi:10.1371/journal.pgen.1000289.g002

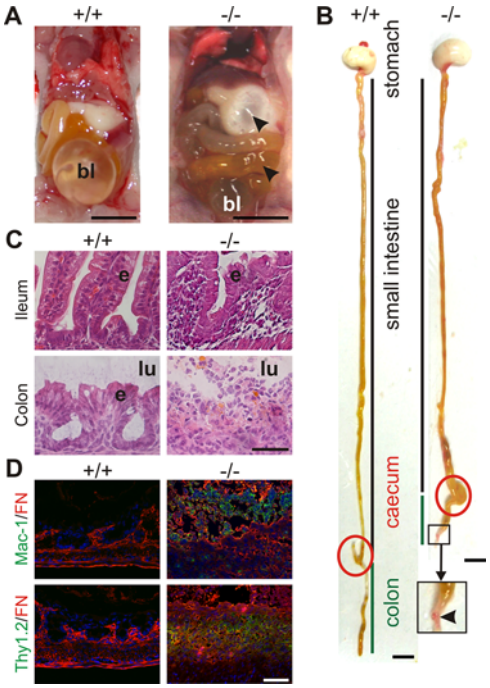

Figure 3. Severe inflammation and epithelial detachment in Kindlin-1$^{-/-}$ colon. (A) Opened abdomen with intestine from P2 mice. Arrowheads indicate air in the stomach and small intestine of Kindlin-1$^{-/-}$ mice. bl; bladder. Scale bar represents 5 mm. (B) Whole gut preparations from P2 mice. Scale bar represents 5 mm. Arrowhead indicates a stricture in the distal colon. The caecum is highlighted with a red circle and the colon is marked with a green line. (C) H&E staining of P3 colon and ileum. Kindlin-1$^{-/-}$ mice show complete absence of colonic epithelium (e), exposure of the submucosa to the intestinal lumen (lu) and severe inflammation in colon and ileum. Scale bar represents 50 µm. (D) Macrophage and granulocyte infiltrations in P3 colon shown with Mac-1 staining in green. T-cell infiltrates in P3 colon shown with Thy1.2 staining in green. Fibronectin (FN) is stained in red. Scale bar represents 50 µm.
doi:10.1371/journal.pgen.1000289.g003

filamentous actin (F-actin) were expressed normally in Kindlin-1$^{-/-}$ colonic epithelium that was still adhering to the BM (Figure 5C and data not shown).

Next we determined the time point when mutant mice began developing intestinal abnormalities. At E18.5 the ileum and colon of Kindlin-1$^{-/-}$ mice were histologically normal and electron microscopy revealed an intact epithelium and basement membrane (BM) (Figure 6A). Shortly after birth (P0), wild-type and Kindlin-1$^{-/-}$ mice began to suckle and accumulated milk in their stomachs. Within the first hours after birth nursed Kindlin-1$^{-/-}$ mice contained colostrum in the intestinal lumen and displayed extensive epithelial cell detachment (Figure 6B; see Colon P0) without infiltrating immune cells (Figure 6B and C) in the distal colon. No epithelial detachment occurred when Kindlin-1$^{-/-}$ mice were delivered by Caesarean section and incubated in a heated and humidified chamber for up to 7 hours (Figure 6B Colon CS) indicating that mechanical stress applied by stool caused IEC detachment. However, inflammatory infiltrates were clearly visible between the detached epithelial cells and the underlying mesenchyme at around 12 hours after birth in fed mice (Figure 6B; see Colon P0.5) and further increased during the following day (Figure 6D). The steady immune cell infiltrate was accompanied with increased expression of the proinflammatory cytokines TNF-α (Tnf) and IL-6 (Il6) and a reduction in goblet cell mucins (Figure 6D and E). The wide range of TNF-α and IL-6 expression levels in Kindlin-1$^{-/-}$ mice likely reflects the different severities of inflammation at the time tissues were prepared.

Although inflammation extended into the ileum at P2 and P3 (Figure 3B and C), the epithelial cells of the ileum were never detached suggesting that Kindlin-1$^{-/-}$ mice develop a so-called backwash ileitis caused by stool "washed back" from the colon into the ileum [13]. These analyses revealed that the epithelial detachment begins at P0 in the distal parts of the colon and subsequently expands proximally.

Kindlin-1 Controls Activation of Integrins

An important question is how Kindlin-1 deficiency leads to detachment of intestinal epithelial cells. One potential explanation could be loss of support by a disrupted BM as reported for skin of KS patients [1,2,3]. Moreover, it is known that BM digestion and epithelial detachment in inflammatory bowel disease (IBD) can be triggered via the secretion of MMPs by epithelial and/or infiltrating immune cells [17]. This possibility could be excluded, since Kindlin-1$^{-/-}$ mice at P1 showed a continuous BM with all major components present, both in areas of the colon where IECs were still adherent as well as in areas where IECs were detached (Figure 7A). Interestingly, also the skin of Kindlin-1$^{-/-}$ mice showed a normal BM distribution by immunostaining (Figure S3).

An alternative explanation for the IEC detachment could be a reduction of integrin levels, or a dysfunction of integrins, similar to that reported for Kindlin-3-deficient platelets [8] and Kindlin-2-deficient primitive endoderm [18]. The normal distribution of β1 integrin (Figure 7B) and the comparable levels of β1 and αv (Itgav)

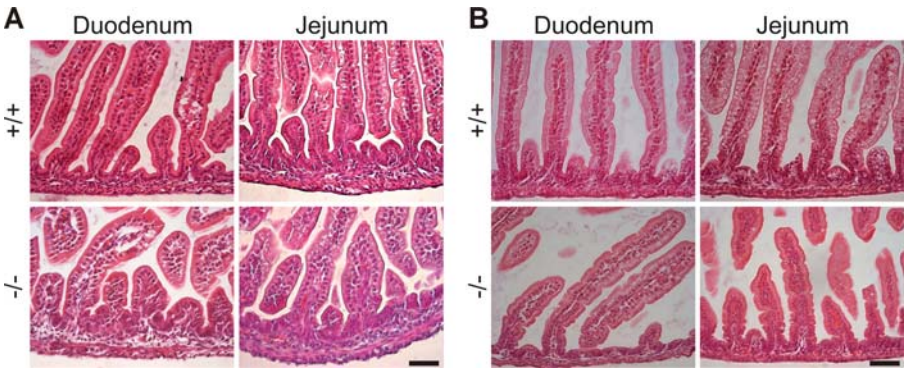

Figure 4. Normal duodenum and jejunum in Kindlin-1$^{-/-}$ mice. H&E stainings of (A) P1 and (B) P3 duodenal and jejunal sections reveal a normal histology of the Kindlin-1$^{-/-}$ small intestine. Scale bar represents 50 µm.
doi:10.1371/journal.pgen.1000289.g004

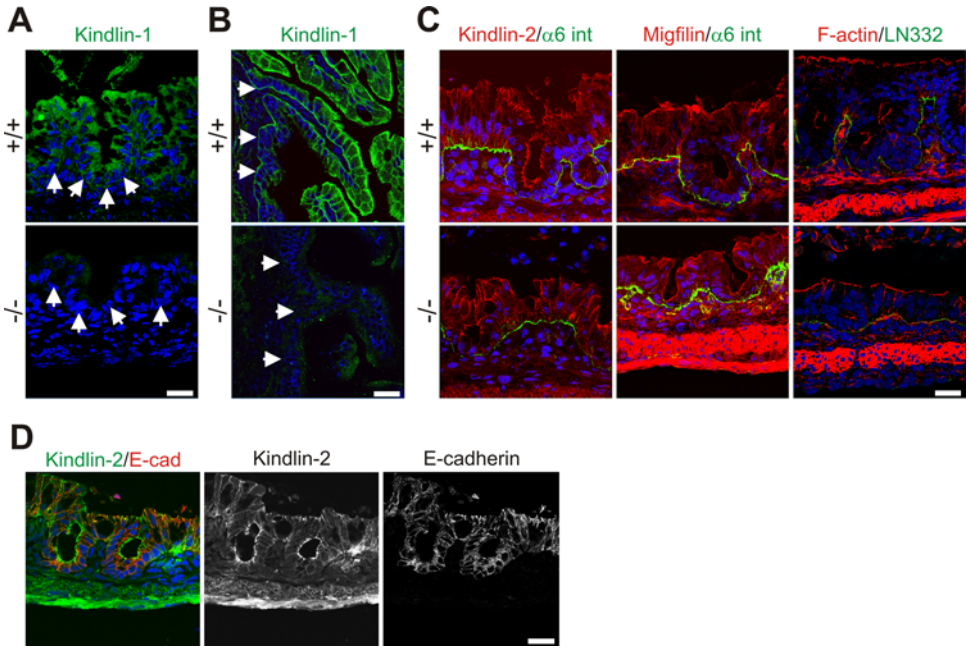

Figure 5. Kindlin-1 localization in mouse intestine. (A) Immunofluorescence staining of Kindlin-1 in neonatal colon. Arrows indicate BM. (B) Immunofluorescence staining of P1 ileum for Kindlin-1. Arrows indicate the BM. (C) Immunofluorescence staining of P1 colon for Kindlin-2, Migfilin, F-actin (red), α6 integrin (α6 int; green) and Laminin-332 (LN332; green). (D) Immunofluorescence staining of colon for Kindlin-2 (green) and E-cadherin (E-cad; red). All scale bars represent 10 μm.
doi:10.1371/journal.pgen.1000289.g005

integrins (Figure 7C and D and data not shown) excluded a defect in expression and/or translocation of integrins to the plasma membrane. Flow cytometry of primary IECs with the monoclonal antibody 9EG7, which recognizes an activation-associated epitope on the β1 integrin subunit, showed significantly reduced binding (Figure 8A) suggesting that loss of Kindlin-1 decreases activation (inside-out signaling) of β1 integrins. Primary keratinocytes from Kindlin-1$^{-/-}$ mice also showed normal localization (Figure S10A) and surface expression of β1 integrins (Figure S10B). Interestingly, 9EG7 staining revealed reduced, although not statistically significant, activation of β1 integrins in these cells (Figure S10C).

Since it is difficult to culture and maintain primary murine IECs, we depleted Kindlin-1 in a human colon carcinoma cell line (HT-29) using RNAi (HT-29siKind1; Figure 8B) to show that integrin-mediated cell adhesion and shear stress induced detachment were also perturbed in a colon cell line. HT-29siKind1 cells were unable to adhere to Fibronectin (FN; Fn1) and showed strongly reduced adhesion to Laminin-332 and Collagen IV (Figure 8C) and easily detached from FN upon exposure to low (0,5dyn/cm^2) as well as high shear stress (up to 4dyn/cm^2; Figure S11). The remaining adhesion to Laminin-332 and Collagen IV is likely mediated by other Laminin- and Collagen-binding receptors on colonic epithelial cells such as α6β4 integrins (Itga6,Itgb4) and discoidin domain receptors [19,20], which are both known to function independent of Laminin and Collagen binding β1 integrins [21].

These findings indicate that (i) loss of Kindlin-1 impairs integrin activation, which compromises adhesion of colonic epithelial cells, that (ii) Kindlin-2 cannot rescue Kindlin-1 loss in colonic epithelial cells, and that (iii) the residual IEC adhesion to Laminin and Collagen is suspended by shear forces exerted for example, by the feces.

It has been reported that Kindlin-1 associates with the membrane proximal NPxY motif of β1 and β3 integrins [6]. This observation, however, is in contrast with observations made with Kindlin-2 and -3, both of which bind the membrane distal NxxY motifs of β1 and β3 integrins to trigger their activation [8,18,22]. To explore the mechanism whereby Kindlin-1 induces integrin activation, we performed pull down experiments with recombinant GST-tagged cytoplasmic β integrin tails in IEC and keratinocyte lysates. The results confirmed that Kindlin-1 associated with the cytoplasmic domains of β1 and β3 (Figure 8D). Since substitutions of the tyrosine residues in the proximal NPxY motifs with alanine (β1Y788A; β3Y747A) allowed Kindlin-1 binding, while tyrosine to alanine substitutions in the distal NxxY motif of β1 and β3 integrin tails (β1Y800A; β3Y759A) abolished Kindlin-1 binding, we conclude that the binding and functional properties are conserved among all Kindlins. This was further confirmed with direct binding assays, which showed that the recombinant His-tagged C-terminal FERM domain of Kindlin-1 (aa 471–677) containing the phosphotyrosine binding (PTB) motif bound GST-tagged β1 but not the Y800A mutated β1 integrin cytoplasmic tail (Figure 8E).

It is well established that Talin can induce activation of integrins, and for a long time it was believed that it is sufficient for the execution of this task. This important function of Talin was discovered by overexpressing Talin or its FERM domain in CHO cells stably expressing the human platelet integrin αIIbβ3 (Itga2b, Itgb3) [23], which shifted the inactive conformation of αIIbβ3 integrin to a high affinity state, as demonstrated by increased binding of the PAC1 antibody recognizing activation associated epitopes on αIIbβ3 integrin (Figure 8F). In contrast to Talin, overexpression of Kindlin-1 failed to trigger activation of αIIbβ3 integrin in these cells (Figure 8F). Interestingly, as described for Kindlin-2 [18,22], overexpression of both the Talin FERM domain and Kindlin-1 doubled PAC1 binding when compared with cells expressing only the Talin FERM domain (Figure 8F). The synergism between Talin and Kindlin-1 depends on a Kindlin-1 and β integrin tail interaction, as a PTB mutant of

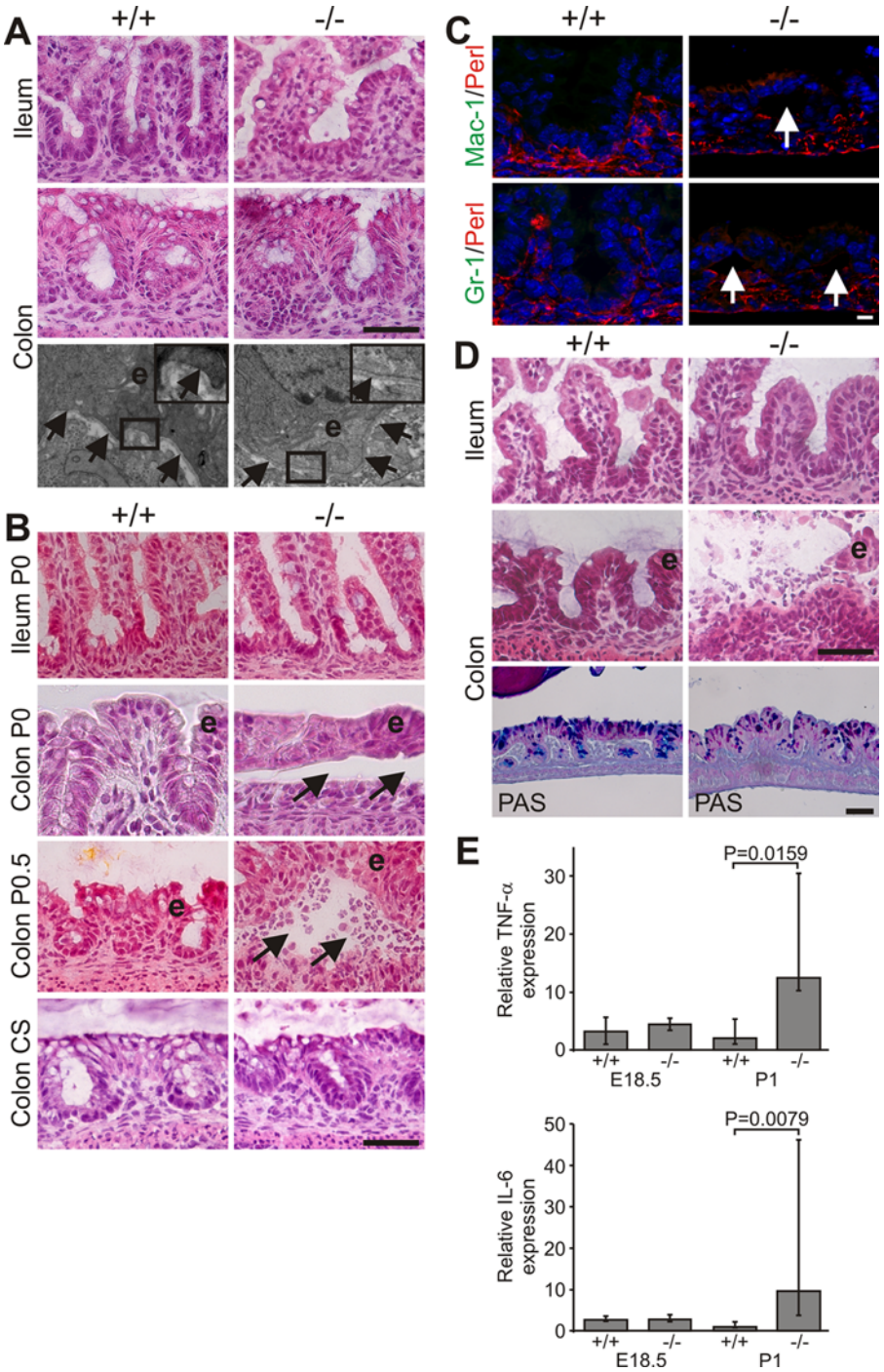

Figure 6. Progressive epithelial dysfunction in Kindlin-1$^{-/-}$ mice. (A) Normal morphology of IECs and BM at E18.5. Shown are H&E stainings of the ileum and colon and electron microscopy pictures at 12000× magnification from the colon. The boxed enlargement shows the BM, e: epithelium. Arrows point to the BM. (B) Colonic IEC (e) detachment at P0 (Colon P0, around 5–6 hours after birth) that becomes infiltrated by immune cells around 12 hours after birth (Colon P0.5). In mice delivered by Caesarean section (CS) and kept unfed for 7 hours no epithelial cell detachment can be observed. Arrows indicate blister. (C) IEC detachment but no macrophage (Mac-1) and granulocyte (GR-1) infiltrations at P0 (Mac-1 and GR-1 in green; Perlecan (Perl) indicating BM in red). Arrows indicate IEC detachment. (D) Immune cell infiltrations in the lumen of the colon and floating epithelial sheets (e) in the colonic lumen at P1. PAS staining shows reduced goblet cell mucins in Kindlin-1$^{-/-}$ colonic epithelium. Scale bars in A, B and D represent 50 μm and in C 10 μm. (E) Median of Real Time PCR results from whole colon mRNA at E18.5 (n = 2 per genotype) and P1 (n = 5 per genotype) for TNF-α and IL-6. Error bars show range. The P value was determined using a Mann-Whitney test.
doi:10.1371/journal.pgen.1000289.g006

Kindlin-1 (QW611/612AA) failed to bind β integrin tails (Figure 8G) and the synergistic effect with Talin was lost (Figure 8F). These findings suggest that Kindlin-1 is not sufficient for integrin activation but is required for inducing Talin-mediated integrin activation. This notion was confirmed with CHO cells, in which endogenous Kindlin-2 levels were depleted by RNAi

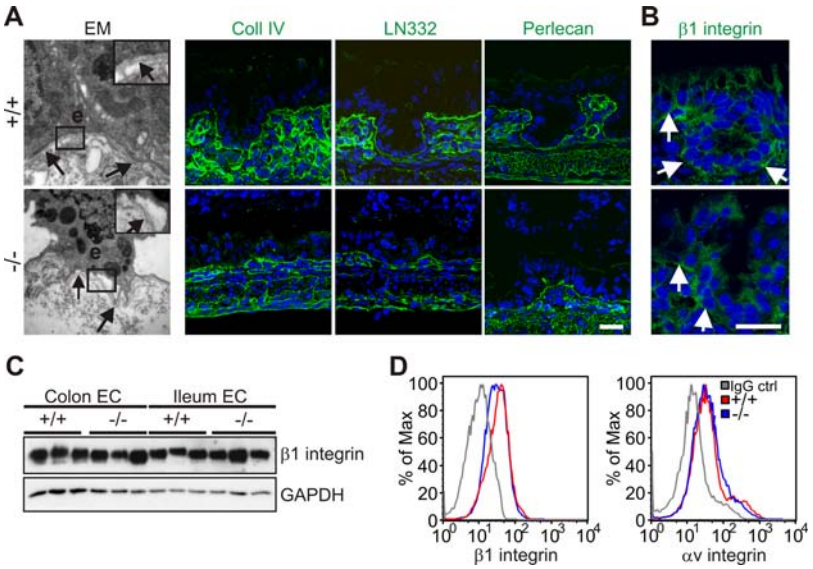

Figure 7. Normal BM composition and integrin localization in P1 colon. (A) Electron micrograph at 12000× magnification shows detachment of colonic IECs from the BM at P1. Arrows point to the BM. The boxed enlargement shows the BM, e: epithelium. Cryo-sections from the colon of P1 Kindlin-$1^{+/+}$ and Kindlin-$1^{-/-}$ mice stained for Collagen IV (Coll IV), Laminin-332 (LN332) and Perlecan. The staining of them shows a normal distribution and localization in Kindlin-$1^{-/-}$ colon. Scale bar represents 10 μm. (B) β1 integrin staining of P1 colon. Arrows indicate the BM. Scale bar represents 10 μm. (C) Western blot from IECs for β1 integrin. (D) β1 and αv integrin FACS profile on primary IECs.
doi:10.1371/journal.pgen.1000289.g007

(Figure 8H). Furthermore, overexpressing Talin failed to induce integrin activation in these cells, but expression of Kindlin-1 restored this function (Figure 8I).

These findings show (i) that Kindlin-1 and -2 require Talin for integrin activation, (ii) that Talin requires Kindlins for integrin activation, and (iii) that Kindlin-1 and Kindlin-2 have redundant functions in vitro *as* both Kindlin-1 and -2 are recruited to FAs where they exert similar functions on integrin cytoplasmic tails. However, in vivo this is not the case as Kindlin-2 is recruited to cell-cell contacts in IECs and apparently does not compensate Kindlin-1 loss.

Discussion

In the present study we show that a null mutation in the Fermt1 gene gives rise to skin atrophy and an acute and fulminant, neonatal intestinal epithelial dysfunction. We demonstrate that the primary defect is a loss of the intestinal epithelial barrier that secondarily leads to inflammatory cell infiltrates and the development of a severe colitis. Furthermore, we show that loss of the intestinal epithelial barrier is caused by a severe adhesion defect of intestinal epithelial cells to the underlying BM, which in turn is caused by the inability of integrins to become activated and to bind BM components. It is possible that in addition to defective integrin activation and epithelial detachment, Kindlin-1 exerts other yet unidentified functions that could contribute to the phenotype in Kindlin-$1^{-/-}$ mice.

Kindler syndrome (KS) is thought to be primarily a skin disease with a disease course that is characterized by epidermal atrophy and followed by epidermal blistering, pigmentation defects and skin cancer. The complex disease syndrome is difficult to diagnose at the disease onset due to similarities with other forms of skin blistering diseases (also called epidermolysis bullosa; EB) that are caused by mutations in keratin and BM genes [24]. Recent case reports showed that KS may involve more organs than only the skin, as several KS patients also suffer from intestinal symptoms. One patient with a severe form of KS developed a severe postnatal UC. Interestingly, this patient was diagnosed with a null mutation in the FERMT1 gene after developing trauma-induced skin blistering [10]. In line with this severe UC case of KS, we found that the null mutation of the Fermt1 gene in mice also leads to a dramatic and lethal intestinal epithelial dysfunction very shortly after birth. Lethality is usually not seen in KS patients, which is most likely due to the immaturity of the murine intestine at birth, making it more vulnerable to injury [25].

The intestinal epithelial dysfunction of Kindlin-1-deficient mice is characterized by flat and superficial ulcerations in the colon, as the epithelium detaches from an intact BM. The defects begin in the rectum and extend along the entire colon finally leading to a severe pancolitis. The ulcerations and epithelial cell detachments are restricted to the colon, although the ileum shows signs of a secondary inflammation at later stages of the disease. In vitro studies with primary IECs from Kindlin-$1^{-/-}$ mice and Kindlin-1-depleted HT-29 cells showed that the cell detachment is caused by impaired activation of integrins leading to weak adhesion of IECs to the underlying BM. Mechanistically Kindlin-1 requires direct binding to the β1 and β3 integrin cytoplasmic domains to promote the activation of the two integrin subfamilies. These biochemical and functional properties are conserved among the three members of the Kindlin family. Kindlin-2-mediated binding and activation of β1 and β3 integrins critically support the attachment of endoderm and epiblast cells to the underlying BM in peri-implantation embryos [18], while Kindlin-3 plays a central role for the activation of platelet integrins [8]. The findings of this report also demonstrate that Talin function crucially depends on the activity of Kindlin-1. Depletion of Kindlin-2 (the only Kindlin expressed in CHO cells) completely prevents overexpressed Talin from activating integrins. Re-expression of either Kindlin in Kindlin-2-depleted CHO cells, however, recovers the ability of Talin to trigger the activation of integrins. It will be important to next investigate how Kindlins become activated and why Kindlin-2 is unable to take over the function of Kindlin-1 in Kindler Syndrome and Kindlin-1-deficient mice.

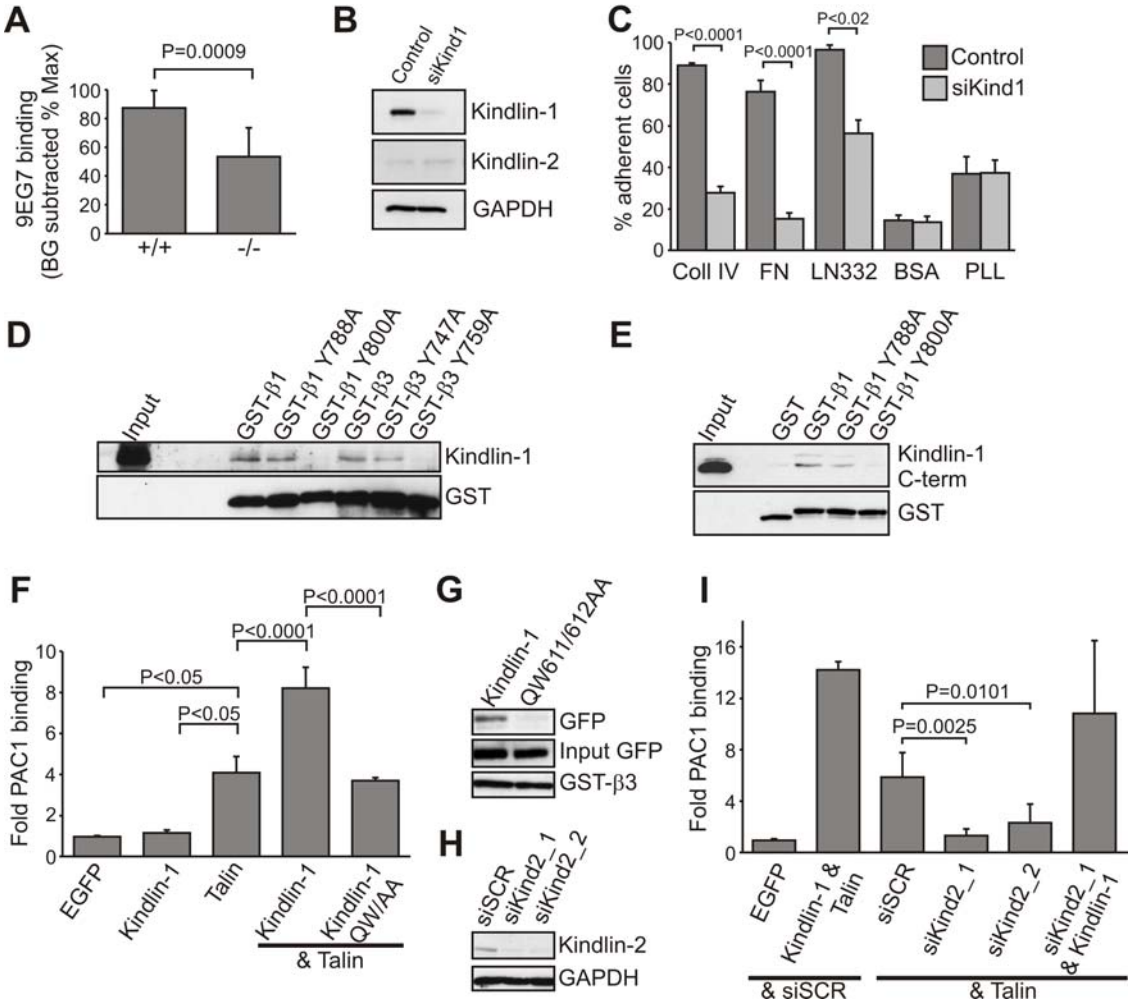

Figure 8. Kindlin-1 association with β integrins is required for Talin-mediated integrin activation. (A) Kindlin-1 IECs display significantly reduced 9EG7 binding (active β1 integrin). The 9EG7 binding was quantified by subtracting background (BG) values from mean fluorescence intensity (MFI) values and normalized to total β1 integrin expression (n = 8 mice per genotype). Error bars show standard deviations. (B) Western blot from HT-29 cells expressing a control siRNA or a siRNA directed against hKindlin-1 (siKind1) for Kindlin-1 and Kindlin-2. GAPDH was used to show equal loading. (C) Adhesion assay of control and Kindlin-1-depleted HT-29 cells on the indicated substrates (n = 5). Shown are mean values, error bars show standard errors of the mean. Coll IV, Collagen IV; FN, Fibronectin; LN332, Laminin-332; PLL, Poly-L lysine. (D) Kindlin-1 pull-down from IEC lysates using GST-tagged cytoplasmic β integrin tails. (E) Direct interaction of Kindlin-1 with β1 integrin cytoplasmic tails. His-tagged Kindlin-1 C-terminus was co-precipitated with GST-tagged β1 integrin cytoplasmic tails, but not with GST alone or an Y800A mutant form of β1 integrin. (F) Quantification of αIIbβ3 integrin activation, as measured by activation specific antibody PAC1 in CHO cells using flow cytometry (n = 9). Shown are mean values, error bars show standard deviations. (G) Pull-down with GST-tagged cytoplasmic β3 integrin tail from CHO cells transiently transfected with the indicated EGFP-constructs. (H) Western blot of CHO cells 24 hours after transfection with the indicated siRNAs. (siSCR: scrambled; siKind2_1 and siKind2_2: Kindlin-2 specific siRNAs) (I) Quantification of αIIbβ3 integrin activation in CHO cells transfected with the indicated cDNA constructs and/or siRNAs (n = 8). Shown are mean values, error bars show standard deviations.
doi:10.1371/journal.pgen.1000289.g008

The conclusion that the observed phenotype is triggered by IEC detachment rather than by a primary inflammatory defect in Kindlin-1 deficient mice is based on the observation that epithelial cell detachment always occurred prior to immune cell infiltration. We would therefore, argue that the detachment of IECs resembles an intestinal wound, which secondarily triggers a strong wound healing response leading to immune cell infiltrates and release of a cytokine storm. In line with this hypothesis, epithelial cell detachment and induction of inflammatory reactions can be completely prevented when Kindlin-1 pups are delivered by Caesarian section and subsequently incubated in a humidified and temperature controlled chamber. Mechanical stress applied by the colostrum is likely inducing the detachment of the weakly adhering epithelial cells in the colon. The vast majority of mouse models reported to develop colitis so far have an abnormal immune system [12,26]. This fact as well as the identification of several susceptibility loci in human patients [14,15] led to the conclusion that defects in the immune system are of central importance for UC development. Severe adhesion defects of IECs leading to a massive wound response may represent an alternative etiology for UC development.

Although adhesion is severely compromised in the colon of Kindlin-1-deficient mice, they are born without skin blisters. This is in line with KS patients, who are also born without skin blisters even when they are delivered by the vaginal route but develop blisters postnatally at trauma prone sites. Interestingly, Kindlin-1 deficient mice did not show defective adhesion of basal keratinocytes to the BM even after application of mechanical stress. The different severity of the adhesion defect in skin and

colon could be reflected by the functional properties of the distinct set of integrins expressed in the two organs and the absence of classical hemidesmosomes in intestinal epithelial cells [27].

Another pronounced skin defect in Kindlin-1-deficient mice as well as KS patients is skin atrophy, which seems to be due to reduced proliferation of interfollicular keratinocytes. This finding raises several questions; first, regarding the mechanism underlying the molecular control of cell proliferation by Kindlin-1. The mechanism is unknown and could result from a diminished cross talk between integrin and growth factor signaling. Second, it is also unclear how a molecular player that supports proliferation is giving rise to cancer at a later stage. It is possible that the localization of Kindlins in different cellular compartments, i.e. cell-matrix adhesion sites, cell-cell adhesion sites and in certain instances in the nucleus, equips them with different functions that become evident at different time points in life.

Kindlin-1 and -2 are co-expressed in epidermal cells as well as epithelial cells of the colon. Interestingly, we found that Kindlin-2 cannot compensate Kindlin-1 function in vivo, neither in the colon nor in skin. Since Kindlin-2 normally localizes to cell-cell adhesions in both cell types and does not translocate to integrin adhesion sites in mutant intestinal and epidermal epithelial cells, it is unable to compensate for the loss of Kindlin-1, although both Kindlins are capable of performing the same tasks at the integrin tails *ex vivo* and in vitro [27]. Hence, a therapeutic strategy to reroute some of the Kindlin-2 from cell-cell to the integrin adhesion sites may represent a promising approach to prevent ulceration in KS patients with severe UC.

Materials and Methods

Mouse Strains

The Kindlin-1$^{-/-}$ mice were obtained by replacing the ATG-containing exon 2 with a neomycin resistance cassette (detailed information on the cloning of the targeting construct can be obtained from Faessler@biochem.mpg.de). The construct was electroporated into R1 embryonic stem (ES) cells (passage 15) and homologous recombination was verified with southern blots. Genomic DNA was digested with EcoRV, blotted and then hybridized with a 5′ probe or digested with BglII, blotted and hybridized with a 3′ probe (Figure 1A). Targeted ES cells were injected into blastocysts and transferred into foster mice. Mice were housed in a special pathogen free mouse facility. All animal experiments have been approved by the local authorities.

Histology, Immunohistochemistry, and Immunfluorescence Stainings

For H&E stainings intestinal segments were either PFA fixed and embedded in paraffin, or frozen on dry-ice in cryo-matrix (Thermo). Immunhistochemistry of paraffin embedded sections was carried out as previously described [5]. Sections of 8 µm thickness were prepared and stained following routine protocols. Cryo sections were fixed in 4% PFA/PBS except for the Kindlin-1 staining where sections were fixed with 1:1 methanol/acetone at −20°C. Subsequently tissue sections were blocked with 3% BSA/PBS, incubated with primary antibodies in a humidity chamber over night at 4°C, with fluorescently labeled secondary antibodies for 1 h at RT and finally mounted in Elvanol. Pictures were taken with a Leica DMIRE2 confocal microscope with a 100× or 63× NA 1.4 oil objective.

GST-Pull Downs

Recombinant GST-β1, β1Y788A, β1Y800A, β3, β3Y747A, β3Y759A cytoplasmic tails were expressed and purified from *E.coli* under non denaturing conditions. 5 µg of recombinant tails were incubated with 500 µg IEC lysate (in 50 mM Tris pH 7.4, 150 mM NaCl, 1 mM EDTA, 1% Triton-X-100) overnight. GST-constructs were precipitated with glutathione beads (Novagen). Subsequent western blots were probed for Kindlin-1 and GST.

Antibodies

A polyclonal peptide antibody against Kindlin-1 was raised against the peptide YFKNKELEQGEPIEK as previously described [5].

The following antibodies were used at the given concentration indicated for western blot (W), immunoprecipitation (IP), immunfluorescence (IF), immunhistochemistry (IHC): Kindlin-1 (W: 1:5000, IF cells: 1:200, IF tissue: 1:1000), Kindlin-2 (W: 1:1000, IF cells 1:200, IF tissue: 1:200), E-cadherin (Cdh1; Zymed, W: 1:5000), Migfilin (W: 1:5000, IF cells 1:100, IF tissue: 1:100), GAPDH (Chemicon; W: 1:10000), phalloidin Tritc (Sigma; IF cells: 1:800, IF tissue: 1:800), Mac-1 (EuroBioscience; IF tissue: 1:100), GR-1 (Ly6g; eBioscience; IF tissue: 1:100), Thy1.2 (PharMingen; IF tissue: 1:100), GST (Novagen; W: 1:10000), His (CellSignaling; W: 1:1000), PAC1 (BD; FACS: 1:100), α6 integrin (Itga6; PharMingen; IF tissue: 1:100), CollagenIV (a gift from Dr. Rupert Timpl; IF tissue: 1:100), Laminin-332 (a gift from Dr. Monique Aumeilley; IF tissue: 1:200), Perlecan (Hspq2; a gift from Dr. Rupert Timpl; IF tissue: 1:100), β1 integrin (Chemicon; WB: 1:3000, IF tissue: 1:600), 9EG7 (PharMingen; FACS: 1:100), EGFP (Abcam; WB: 1:10000), β1 integrin (PharMingen; FACS: 1:200), αv integrin (PharMingen; FACS: 1:200). Keratin10 (Krt10; Covance; IHC: 1:600), Keratin14 (Krt14; Covance; IHC: 1:600), Loricrin (Lor; Covance; IHC: 1:500) Ki67 (Dianova; IHC: 1:50), cCaspase3 (CellSignaling, IHC: 1:100).

Caesarean Section

Pregnant mice were sacrificed by cervical dislocation when embryos were at E18.5–E19 of gestation. The uterus was removed and cut open. Embryos were taken out and the umbilical cord was cut. Mice were subsequently dried and kept in an incubator at 37°C and high humidity.

Real Time PCR

Total RNA from whole colons was extracted with a PureLink Micro to Midi RNA extraction kit (Invitrogen) following the manufacturers instructions. cDNA was prepared using the iScript cDNA Synthesis Kit (Biorad). Real Time PCR using a Sybr Green ready mix (Biorad) was performed in an iCycler (Biorad). Each sample was measured in triplicates and values were normalized to GAPDH. Following primers were used; TNFα fwd: AAAATTC-GAGTGACAAGCCTGTAGC, TNFα rev: GTGGGTGAG-GAGCACGTAG. IL-6 fwd: CTATACCACTTCACAAGTCG-GAGG IL-6 rev: TGCACAACTCTTTTCTCATTTCC. RT-PCR for Kindlin-1 and GAPDH was performed as previously described [5].

Isolation of IECs

Neonatal mouse intestine was removed and flushed with 1 ml PBS. The intestine was longitudinally cut open, rinsed with PBS and incubated for 40 min. in IEC isolation buffer (130 mM NaCl, 10 mM EDTA, 10 mM Hepes pH 7.4, 10% FCS and 1 mM DTT) at 37°C on a rotor. The epithelium was shaken off and pelleted by centrifugation at 2000rpm for 5 min. For WB analysis cells were washed once with PBS and subsequently lysed. For flow cytometry cells were washed once with PBS and trypsinized with

2× trypsin (GIBCO) for 10 min. at 37°C. Trypsin was inactivated with DMEM containing 10%FCS. A single cell suspension was prepared by passing cells through a cell strainer (BD).

Isolation of Keratinocytes

Primary keratinocytes were isolated from P3 mice as described previously [28]. Cells were cultured on a mixture of ColI (Cohesion) and 10 μg/ml FN (Invitrogen) coated plastic dishes in keratinocyte growth medium containing 8% chelated FCS (Invitrogen) and 45 μM Ca^{2+}.

Flow Cytometry

IEC's and keratinocytes were stained with 9EG7 antibody in Tris buffered saline [29]. For the PAC1 binding assay CHO cells were stained for 40 min. at RT as described previously [23]. Cells were gated for viability by excluding propidium iodide-positive cells. CHO cells transfected with EGFP-tagged constructs were additionally gated for highly EGFP-positive cells. Measurements were performed with a FACS Calibur (BD) and data evaluation was done with FlowJo software.

Constructs

The EGFP-Kindlin-1 expression plasmid was previously described [5]. The cDNA encoding His-Kindin-1 C-terminus (aa 471–677) was amplified by PCR and cloned into the pQE-70 vector (Qiagen). The Kindlin-1 PTB mutation QW611/612AA was introduced with a site directed mutagenesis kit (Stratagene) following the manufacturers recommendations. All EGFP constructs were cloned into the pEGFP-C1 vector (Clontech) and subsequently sequenced. EGFP-Talin head was previously described [8].

Cell Culture

CHO and HT-29 cells were maintained in DMEM containing penicillin/streptomycin, non-essential amino-acids and 10% or 20% FCS, respectively (GIBCO). Cells were transfected with 2 μg of each DNA in six well plates using Lipofectamine 2000 following the manufacturers' instructions (Invitrogen).

RNAi

To deplete Kindlin-1 constitutively from HT-29 cells, an shDNA corresponding to the cDNA sequence GTAAGT CCTGGTTTATACA of hKindlin-1 and a control cDNA with the sequence AGCAGTGCATGTATGCTTC were cloned into the pSuperRetro vector (OligoEngine). Viral particles were prepared as described previously [30]. HT-29 cells were infected and subsequently selected with 2mg/l puromycin. Transient knockdown of Kindlin-2 from CHO cells was achieved by transfection of the siRNAs; Kind2_1: GCCUCAAGCUCUU-CUUGAUdTdT and Kind2_2: CUCUGGACGGGAUAAG-GAUdTdT, and a control siRNA (purchased from Sigma) using Lipofectamine 2000 (Invitrogen), following the manufacturers instructions. Cells were harvested and assayed 24 hours after transfection.

Adhesion Assay

The adhesion assays were performed as previously described [29], using 40000 cells per well in serum free DMEM (HT-29) or MEM (primary keratinocytes).

Osmolarity

Osmolarity was measured from 50 μl urine using an Osmomat 030 from Gonotec.

X-Gal Barrier Assay

Embryonic skin barrier formation was determined as previously described [31].

Shear Stress Assay

Slides with a 1 μm diameter (ibidi BioDiagnostics) were coated overnight with 5 μg/ml FN and then blocked with 1% BSA. 100.000 cells were seeded onto the slides and incubated for 2.5 hours in a cell culture incubator. Cells were subsequently exposed to increasing amounts of shear force in two minute intervals (as indicated in the Figure S11) and pictures were taken every second.

Co-Immunoprecipitation

CHO cells were transiently transfected with the indicated EGFP constructs. Approximately 1mg of protein lysate was immunoprecipitated using the μMACS Epitope Tag Protein Isolation Kit for EGFP tags (Miltenyi Biotec) following the manufacturers instructions.

Electron Microscopy

Electron microscopy was performed as previously described [29].

Statistical Analysis

Analyses were performed with GraphPad Prism. If not mentioned otherwise in the figure legends, Gaussian distribution of datasets was determined by a D'Agostino & Pearson omnibus normality test. If samples were not Gaussian distributed a Mann-Whitney test was performed. Gaussian distributed samples were either compared with a one way ANOVA and a Tukey's multiple comparison post test or an unpaired two-tailed t-test.

Supporting Information

Figure S1 Normal triglyceride and glucose levels in the blood of P3 Kindlin-$1^{-/-}$ mice. Triglyceride (n = 7 per genotype) and glucose (n = 5 per genotype) levels from total blood at P3. The differences are statistically insignificant. Shown are mean values, error bars show standard deviations.
Found at: doi:10.1371/journal.pgen.1000289.s001 (0.5 MB TIF)

Figure S2 Normal kidney morphology in Kindlin-$1^{-/-}$ mice. (A) Coomassie stained gel of 10 μl urine from P2 and P3 control and Kindlin-$1^{-/-}$ mice. (B) Quantification of total protein in urine from Kindlin-$1^{+/+}$, Kindlin-$1^{+/-}$ and Kindlin-$1^{-/-}$ mice at P1 (n = 14/7/6) and P3 (n = 20/20/9). Error bars show standard deviation. (C) H&E staining of P3 Kindlin-$1^{+/+}$ and Kindlin-$1^{-/-}$ kidneys. Kindlin-$1^{-/-}$ kidneys do not show altered glomeruli and collecting duct morphology. Scale bar represents 200 μm. Enlargements show glomeruli (A1, A3) and collecting ducts (A2, A4). Scale bar represents 50 μm.
Found at: doi:10.1371/journal.pgen.1000289.s002 (8.6 MB TIF)

Figure S3 Normal BM composition and deposition in P3 Kindlin-$1^{-/-}$ backskin. P3 backskin of wild type and Kindlin-$1^{-/-}$ mice was stained for the BM components Laminin-332 (LN332; red), Collagen IV (Coll IV; red) and Fibronectin (FN; red) and co-stained with α6 or β4 integrin marking (green) the basal site of basal keratinocytes. The stainings reveal no differences in BM deposition and composition or α6 and or β4 integrin localization between control and Kindlin-$1^{-/-}$ littermates. Scale bar indicates 30 μm.
Found at: doi:10.1371/journal.pgen.1000289.s003 (9.8 MB TIF)

Figure S4 Normal skin differentiation. P3 backskin of control and Kindlin-1$^{-/-}$ mice was stained for epidermal differentiation markers Keratin14, Keratin10 and Loricrin (red) and co-stained with α6 integrin (green) to mark basal keratinocytes. The stainings show no difference in the differentiation pattern of Kindlin-1$^{-/-}$ keratinocytes. Scale bar indicates 10 μm.
Found at: doi:10.1371/journal.pgen.1000289.s004 (8.4 MB TIF)

Figure S5 Normal skin development. (A) Normal X-Gal staining in E17 Kindlin-1$^{-/-}$ embryos indicating normal barrier formation during development. Scale bar indicates 5 mm. (B) H&E staining of back skin from control and Kindlin-1$^{-/-}$ littermates of different age. In Kindlin-1$^{-/-}$ mice the epidermal (e) thickness at E18.5 and P0 is normal but clear epidermal atrophy is seen at P1. Scale bar indicates 50 μm. (d): dermis.
Found at: doi:10.1371/journal.pgen.1000289.s005 (8.5 MB TIF)

Figure S6 Altered adhesion and spreading of Kindlin-1$^{-/-}$ keratinocytes. (A) Adhesion assay of control and Kindlin-1$^{-/-}$ keratinocytes on LN332, Laminin-332; Coll IV, Collagen IV; FN, Fibronectin; PLL, Poly-L lysine (n = 3). Shown are mean values, error bars show standard error of the mean. (B) Cell area measured upon spreading on 5 μg/ml Fibronectin at the indicated time-points using MetaMorph software (n = 30 cells per genotype from 3 independent experiments). Shown are mean values, error bars show standard deviation (*** $p<0.0001$).
Found at: doi:10.1371/journal.pgen.1000289.s006 (0.8 MB TIF)

Figure S7 Oral and oesophageal mucosa in Kindlin-1$^{-/-}$ mice. Histology of the oral mucosa and the oesophagus of P3 Kindlin-1$^{+/+}$ and Kindlin-1$^{-/-}$ mice did not reveal an abnormal morphology. Scale bar represents 50 μm.
Found at: doi:10.1371/journal.pgen.1000289.s007 (8.1 MB TIF)

Figure S8 Progressive epithelial loss in Kindlin-1$^{-/-}$ colons. (A) Quantification of the extent of intact colonic epithelium at P1 and P3 (n = 3 per genotype and age). Error bars show range. (B) Overview of an H&E picture of a P3 control and Kindlin-1$^{-/-}$ colon. The Kindlin-1$^{-/-}$ colon shows a complete absence of colonic epithelium (black arrowheads), while the epithelium in the caecum is still present (white arrowheads). Scale bars show 500 μm. (C) Magnifications of the boxed areas shown in B.
Found at: doi:10.1371/journal.pgen.1000289.s008 (7.7 MB TIF)

Figure S9 Normal IEC proliferation but detachment induced apoptosis . P1 colons from wild type and Kindlin-1$^{-/-}$ mice were DAB stained for cleaved Caspase-3 to determine apoptosis and Ki67 stained to show proliferating IECs. Apoptosis occurs in detached epithelium of Kindlin-1$^{-/-}$ mice. In areas of still adhering epithelium the number of proliferating IECs is similar between wild type and Kindlin-1$^{-/-}$ mice. Scale bar indicates 50 μm.
Found at: doi:10.1371/journal.pgen.1000289.s009 (8.7 MB TIF)

Figure S10 β1 integrin activation in Kindlin-1$^{-/-}$ keratinocytes. (A) Immunofluorescence staining for β1 integrin (green) and Laminin-332 (LN332; red) from P3 backskin shows normal localization of β1 integrin in Kindlin-1$^{-/-}$ backskin. (B) FACS quantification of β1 integrin expression of freshly isolated control and Kindlin-1$^{-/-}$ keratinocytes at P2 shows unaltered β1 integrin expression on basal keratinocytes. Error bars show range (n = 4) (C) 9EG7 FACS quantification of these keratinocytes shows no significant reduction in β1 integrin activation. Error bars show range (n = 4).
Found at: doi:10.1371/journal.pgen.1000289.s010 (8.0 MB TIF)

Figure S11 Shear induced detachment of Kindlin-1 depleted HT-29 cells. Control and Kindlin-1 depleted HT-29 (siKind1) cells were plated on Fibronectin-coated flow chamber slides and exposed to increasing shear forces as indicated in the figure. Control cells did not detach from the matrix while Kindlin-1 depleted cells were unable to resist low or high shear forces (compare lane 1 (0dyn/cm^2) with lane 2 (0,5dyn/cm^2). Scale bar indicates 50 μm.
Found at: doi:10.1371/journal.pgen.1000289.s011 (9.0 MB TIF)

Acknowledgements

We would like to thank Wilhelm Bloch for electron microscopy, Reinhart Kluge for blood parameter measurements, Klaus-Peter Janssen for IL-6 and TNFα primers, Julia Schlehe, Sara Wickström, Mercedes Costell, Ralph Boettcher, Anika Lange, Ambra Pozzi, and Roy Zent for critical reading of the manuscript and Simone Bach and Melanie Ried for excellent technical assistance.

Author Contributions

Conceived and designed the experiments: SU MM RF. Performed the experiments: SU MW ER CH. Analyzed the data: SU RF. Contributed reagents/materials/analysis tools: OGB. Wrote the paper: SU RF.

References

1. Siegel DH, Ashton GH, Penagos HG, Lee JV, Feiler HS, et al. (2003) Loss of kindlin-1, a human homolog of the Caenorhabditis elegans actin-extracellular-matrix linker protein UNC-112, causes Kindler syndrome. Am J Hum Genet 73: 174–187.
2. Jobard F, Bouadjar B, Caux F, Hadj-Rabia S, Has C, et al. (2003) Identification of mutations in a new gene encoding a FERM family protein with a pleckstrin homology domain in Kindler syndrome. Hum Mol Genet 12: 925–935.
3. Lai-Cheong JE, Liu L, Sethuraman G, Kumar R, Sharma VK, et al. (2007) Five new homozygous mutations in the KIND1 gene in Kindler syndrome. J Invest Dermatol 127: 2268–2270.
4. Kern JS, Herz C, Haan E, Moore D, Nottelmann S, et al. (2007) Chronic colitis due to an epithelial barrier defect: the role of kindlin-1 isoforms. J Pathol 213: 462–470.
5. Ussar S, Wang HV, Linder S, Fassler R, Moser M (2006) The Kindlins: subcellular localization and expression during murine development. Exp Cell Res 312: 3142–3151.
6. Kloeker S, Major MB, Calderwood DA, Ginsberg MH, Jones DA, et al. (2004) The Kindler syndrome protein is regulated by transforming growth factor-beta and involved in integrin-mediated adhesion. J Biol Chem 279: 6824–6833.
7. Herz C, Aumailley M, Schulte C, Schlotzer-Schrehardt U, Bruckner-Tuderman L, et al. (2006) Kindlin-1 is a phosphoprotein involved in regulation of polarity, proliferation, and motility of epidermal keratinocytes. J Biol Chem 281: 36082–36090.
8. Moser M, Nieswandt B, Ussar S, Pozgajova M, Fassler R (2008) Kindlin-3 is essential for integrin activation and platelet aggregation. Nat Med 14: 325–330.
9. Kruger M, Moser M, Ussar S, Thievessen I, Luber CA, et al. (2008) SILAC mouse for quantitative proteomics uncovers kindlin-3 as an essential factor for red blood cell function. Cell 134: 353–364.
10. Sadler E, Klausegger A, Muss W, Deinsberger U, Pohla-Gubo G, et al. (2006) Novel KIND1 gene mutation in Kindler syndrome with severe gastrointestinal tract involvement. Arch Dermatol 142: 1619–1624.
11. Freeman EB, Koglmeier J, Martinez AE, Mellerio JE, Haynes L, et al. (2008) Gastrointestinal complications of epidermolysis bullosa in children. Br J Dermatol.
12. Xavier RJ, Podolsky DK (2007) Unravelling the pathogenesis of inflammatory bowel disease. Nature 448: 427–434.
13. Podolsky DK (2002) Inflammatory bowel disease. N Engl J Med 347: 417–429.
14. Fisher SA, Tremelling M, Anderson CA, Gwilliam R, Bumpstead S, et al. (2008) Genetic determinants of ulcerative colitis include the ECM1 locus and five loci implicated in Crohn's disease. Nat Genet 40: 710–712.
15. Franke A, Balschun T, Karlsen TH, Hedderich J, May S, et al. (2008) Replication of signals from recent studies of Crohn's disease identifies previously unknown disease loci for ulcerative colitis. Nat Genet 40: 713–715.
16. Mudter J, Neurath MF (2007) Il-6 signaling in inflammatory bowel disease: pathophysiological role and clinical relevance. Inflamm Bowel Dis 13: 1016–1023.

17. Medina C, Radomski MW (2006) Role of matrix metalloproteinases in intestinal inflammation. J Pharmacol Exp Ther 318: 933–938.
18. Montanez E, Ussar S, Schifferer M, Bosl M, Zent R, et al. (2008) Kindlin-2 controls bidirectional signaling of integrins. Genes Dev 22: 1325–1330.
19. Vogel W, Gish GD, Alves F, Pawson T (1997) The discoidin domain receptor tyrosine kinases are activated by collagen. Mol Cell 1: 13–23.
20. Alves F, Vogel W, Mossie K, Millauer B, Hofler H, et al. (1995) Distinct structural characteristics of discoidin I subfamily receptor tyrosine kinases and complementary expression in human cancer. Oncogene 10: 609–618.
21. Vogel W, Brakebusch C, Fassler R, Alves F, Ruggiero F, et al. (2000) Discoidin domain receptor 1 is activated independently of beta(1) integrin. J Biol Chem 275: 5779–5784.
22. Ma YQ, Qin J, Wu C, Plow EF (2008) Kindlin-2 (Mig-2): a co-activator of beta3 integrins. J Cell Biol 181: 439–446.
23. O'Toole TE, Katagiri Y, Faull RJ, Peter K, Tamura R, et al. (1994) Integrin cytoplasmic domains mediate inside-out signal transduction. J Cell Biol 124: 1047–1059.
24. Aumailley M, Has C, Tunggal L, Bruckner-Tuderman L (2006) Molecular basis of inherited skin-blistering disorders, and therapeutic implications. Expert Rev Mol Med 8: 1–21.
25. Hauck AL, Swanson KS, Kenis PJ, Leckband DE, Gaskins HR, et al. (2005) Twists and turns in the development and maintenance of the mammalian small intestine epithelium. Birth Defects Res C Embryo Today 75: 58–71.
26. Kang SS, Bloom SM, Norian LA, Geske MJ, Flavell RA, et al. (2008) An antibiotic-responsive mouse model of fulminant ulcerative colitis. PLoS Med 5: e41.
27. Fontao L, Stutzmann J, Gendry P, Launay JF (1999) Regulation of the type II hemidesmosomal plaque assembly in intestinal epithelial cells. Exp Cell Res 250: 298–312.
28. Romero MR, Carroll JM, Watt FM (1999) Analysis of cultured keratinocytes from a transgenic mouse model of psoriasis: effects of suprabasal integrin expression on keratinocyte adhesion, proliferation and terminal differentiation. Exp Dermatol 8: 53–67.
29. Czuchra A, Meyer H, Legate KR, Brakebusch C, Fassler R (2006) Genetic analysis of beta1 integrin "activation motifs" in mice. J Cell Biol 174: 889–899.
30. Massoumi R, Chmielarska K, Hennecke K, Pfeifer A, Fassler R (2006) Cyld inhibits tumor cell proliferation by blocking Bcl-3-dependent NF-kappaB signaling. Cell 125: 665–677.
31. Patel S, Xi ZF, Seo EY, McGaughey D, Segre JA (2006) Klf4 and corticosteroids activate an overlapping set of transcriptional targets to accelerate in utero epidermal barrier acquisition. Proc Natl Acad Sci U S A 103: 18668–18673.

7.3 Paper III

Kindlin-3 mediated integrin adhesion is dispensable for quiescent hematopoietic stem cells but required to maintain activated hematopoietic stem and precursor cells

Raphael Ruppert, Markus Moser, Markus Sperandio, **Emanuel Rognoni**, Martin Orban, Wen-Hsin Liu, Ansgar Schulz, Robert A. J. Oostendorp, Steffen Massberg, and Reinhard Fässler

(Manuscript under revision)

Supplementary material

PDF file

Supplementary Figures 1-6

Supplementary Table 1, Blood counts of $K3^{+/+}$ and $K3^{-/-}$ (moribund and healthy) chimeras

Supplementary Table 2, Blood counts of $K3^{+/+}$ and $K3^{-/-}$ mix-chimeras

Supplementary Table 3, Primer used for qPCR

Supplementary Table 4, Primer used for PCR genotyping of integrated K3 expression constructs

Extended Experimental Procedure

Supplemental References

Video files

Supplementary Movie 1, Intravital 2-photon microscopy of $K3^{+/+}$ LSK cells

Supplementary Movie 2, Intravital 2-photon microscopy of $K3^{-/-}$ LSK cells

Supplementary Movie 3, Intravital 2-photon microscopy of firm adherent $K3^{-/-}$ LSK cell

Kindlin-3 mediated integrin adhesion is dispensable for quiescent hematopoietic stem cells but required to maintain activated hematopoietic stem and precursor cells

Raphael Ruppert[1], Markus Moser[1], Markus Sperandio[2], Emanuel Rognoni[1], Martin Orban[3], Wen-Hsin Liu[1], Ansgar Schulz[4], Robert A. J. Oostendorp[5], Steffen Massberg[3], and Reinhard Fässler[1]*

[1]Department of Molecular Medicine, Max Planck Institute of Biochemistry, Martinsried, Germany; [2]Walter Brendel Center for Experimental Medicine, Ludwig Maximilian University, Munich, Germany; [3]Med. Clinic and Policlinic I, Klinikum der Universität, Munich, Germany; [4]Department of Pediatrics and Adolescent Medicine, University Medical Centre Ulm; [5]3rd Department of Internal Medicine, Klinikum rechts der Isar der Technischen Universität München, Munich, Germany.

*Correspondence should be addressed to R. F. (faessler@biochem.mpg.de)

SUMMARY

Blood cell lineages are formed by dividing hematopoietic precursor cells (HPCs). HPCs originate from hematopoietic stem cells (HSCs), which reside in a quiescent state and are only activated when the HPC pool is decreasing. Both, hematopoietic stem and precursor (HSPCs) express high levels of the essential integrin activating protein Kindlin-3, which is mutated in leukocyte adhesion deficiency type III (LAD-III) in man. Here we report that loss of Kindlin-3 in HSPCs impaired bone marrow (BM) homing due to reduced integrin-mediated adhesion to the microvascular endothelium. Using HSPC transplantations we also show that Kindlin-3 deficient HSCs were retained in the BM and became quiescent only when wild type HSCs were present. In their absence Kindlin-3 deficient HSCs lost quiescence and eventually became exhausted leading to reduced survival of transplanted recipient mice. This loss of HSC quiescence was caused by the continuous movement of activated HSPCs into the circulation because their retention in the BM niche requires Kindlin-3 dependent integrin adhesion. Since HSPCs also accumulate in the circulation of LAD-III patients we conclude that Kindlin-3 is dispensable for quiescent HSCs but essential for the maintenance of activated HSPCs in BM compartments of mouse and man.

INTRODUCTION

The entire hematopoietic system is derived from and maintained by a small number of hematopoietic stem cells (HSCs), which reside in the bone marrow (BM). HSCs are characterized by their low cycling rate and their ability to self-renew throughout the lifespan of an organism. After hematopoietic injury (e.g. bleeding) quiescent HSCs become activated, divide asymmetrically, replenish the pool of hematopoietic effector cells and then return to the quiescent state (Trumpp et al., 2010). To maintain HSCs throughout the lifespan of an animal, the oscillation of HSCs between quiescence, activation, self-renewal and differentiation is precisely regulated in a specific microenvironment referred to as the stem cell niche (Morrison and Spradling, 2008). The oscillation of HSCs is regulated through interactions with niche cells (Kiel and Morrison, 2008), extracellular matrix (ECM) proteins (van der Loo et al., 1998), the action of cytokines, chemokines and growth factors released by niche cells (Rizo, 2006), and calcium gradients established by osteoclasts during bone remodeling (Adams et al., 2006). Thus, an impairment of the HSC-niche interplay can result in loss of quiescence, uncontrolled activation and finally exhaustion of HSCs.

The interactions of HSCs with niche cells and ECM are mediated by adhesion molecules such as integrins (Wilson and Trumpp, 2006). Integrins are expressed on all cells including tissue stem cells, where they mediate binding to ECM and counter receptors (Hynes, 2002). The composition of niche cells and ECM components is unique in each organ and hence tissue stem cells express specific integrin profiles to interact with the niche microenvironment. The integrin profile of HSCs includes multiple members of the β1 class (α2β1, α4β1, α5β1, α6β1, α9β1), αLβ2 from the β2 class and αvβ3 from the αv-class (Grassinger et al., 2009). *In vivo* and *in vitro* studies using genetics or inhibitory antibodies demonstrated that integrins promote hematopoietic stem and precursor cell (HSPC) homing to the BM (Potocnik et al., 2000), their BM retention (Magnon and Frenette, 2008), proliferation and differentiation (Arroyo et al., 1999). Although these studies identified important roles for integrins in hematopoietic precursor cells (HPCs) it is not clear whether, similarly like other tissue stem cells, HSCs also require integrins to maintain quiescence.

Integrin ligand binding and signaling requires an activation step, which is induced following Talin and Kindlin binding to the cytoplasmic domains of integrin β subunits and associated with allosteric changes in the integrin ectodomain and transmembrane

domains (Moser et al., 2009a; Shattil et al., 2010). Kindlins are evolutionary conserved and consist of three members. Hematopoietic cells express Kindlin-3 (Ussar et al., 2006) whose deletion in mice abrogates integrin activation resulting in hemorrhages, leukocyte adhesion defects and osteopetrosis (Moser et al., 2009b; 2008; Schmidt et al., 2011). A human disease with similar abnormalities called leukocyte adhesion deficiency type III (LAD-III) is also caused by null mutations of the *KINDLIN-3* gene (Kuijpers et al., 2009; Malinin et al., 2009; Svensson et al., 2009).

Since Kindlin-3 activates all integrins analyzed so far, it is perfectly suited to broadly abrogate integrin-dependent functions in HSCs. We report that proliferating HSPCs require Kindlin-3 for their maintenance in the BM, while quiescent HSCs are retained independent of Kindlin-3 mediated integrin adhesion. In a situation of hematopoietic stress and high demand for HPCs, however, quiescent HSCs are activated to refill the decreasing pool of HPCs, become also dependent on Kindlin-3 and eventually exhaust.

RESULTS

Kindlin-3 is required for HSC engraftment

Kindlin-3, the sole Kindlin family member expressed in FACS-purified wt ($K3^{+/+}$) hematopoietic stem and precursor cells (HSPCs), was absent in Kindlin-3-null ($K3^{-/-}$) HSPCs (Figure S1A-B). Since FACS only enriches for HSCs, we will refer to the populations used in this study as HSPCs to account for potential progenitor cell contamination. To test whether Kindlin-3 is required for HSPC function we generated fetal liver (FL) chimeras by transplanting $5x10^6$ unfractionated FL cells (C57BL/6; $CD45.2^+$) from $K3^{+/+}$ or $K3^{-/-}$ E14.5 littermate embryos into lethally irradiated wt congenic B6.SJL ($CD45.1^+$) recipient mice (Figure S1C). Lifetime analysis revealed that the median survival of $K3^{+/+}$ FL cell recipients (termed $K3^{+/+}$ chimeras) and $K3^{-/-}$ FL cell recipients (termed $K3^{-/-}$ chimeras) was 48.7 and 24.6 weeks, respectively (Figure 1A).

To exclude that the diminished survival of $K3^{-/-}$ chimeras was due to transplantation of a reduced total number of HSPCs in $K3^{-/-}$ FLs we harvested mononuclear cells (MNCs) from FLs and determined the relative frequency of $lineage^-Mac\text{-}1^{med}AA4.1^+Sca\text{-}1^+c\text{-}kit^+$ (FL-LSK) cells (Figure S1D) (Jordan et al., 1990; Okada et al., 1992). The results revealed that the total number of MNCs was 2.75-fold decreased in E14.5 FLs of $K3^{-/-}$ mice (Figure S1E), while the relative FL-LSK cell number was significantly elevated compared to control FLs (Figure S1D, F) and the absolute number of LSK cells per FL was similar between $K3^{+/+}$ and $K3^{-/-}$ mice (Figure S1G). Further assessment of committed hematopoietic precursor cells with the colony-forming unit-culture (CFU-C) assay and more immature, long-term culture initiating cells (LTC-ICs) revealed that the frequencies of CFU-Cs as well as LTC-ICs were increased in FL-MNCs of $K3^{-/-}$ mice (Figure S1H, S1I). Interestingly, while the absolute numbers of CFU-Cs per FL were decreased (Figure S1J), the absolute numbers of LTC-ICs per FL were normal (Figure S1K). Immunohistochemistry demonstrated a normal vasculature and a similar distribution of hematopoietic effector cells in $K3^{+/+}$ and $K3^{-/-}$ FLs (Figure S1L). FACS analysis revealed changes in the relative numbers of non-hematopoietic ($CD45^-$) and hematopoietic cells ($CD45^+$ or $B220^+$ or $Mac\text{-}1^+$ or $Mac\text{-}1^+Gr\text{-}1^+$ or $CD71^+$and/or $Ter119^+$). While the absolute numbers of non-hematopoietic and all hematopoietic cell types were reduced in $K3^{-/-}$ FLs, the absolute numbers of vascular ($CD31^+$ and $EpCAM^+$) and hepatic cell numbers ($EpCAM^+$) were normal (Figure S1M-S). These data indicate that the transplantation of identical numbers of $K3^{+/+}$ and $K3^{-/-}$ FL MNCs together with

the increased frequency of HSPCs in K3$^{-/-}$ FL MNCs provides K3$^{-/-}$ chimeras with more donor HSPCs than K3$^{+/+}$chimeras and hence excludes a lack of HSPCs in K3$^{-/-}$ FLs as cause for the reduced survival of K3$^{-/-}$ chimeras.

Next, we tested whether defects in lineage differentiation caused the diminished survival of K3$^{-/-}$ chimeras by quantifying different hematopoietic lineages in BM, spleen (Spl) and peripheral blood (PB) of moribund and healthy chimeras 3 to 4 months after transplantation. Moribund K3$^{-/-}$ chimeras displayed a pronounced pancytopenia in the BM affecting B, T, erythroid cells, neutrophils and monocytes/macrophages, and in PB and Spl affecting B, T and erythroid cells (Figure 1B, 1C, S1T, S1U, Table S1). This was never observed in K3$^{+/+}$ chimeras. Healthy K3$^{-/-}$ chimeras had reduced T cells and erythroid cells and increased myeloid and B cells in the PB (Figure S1T, Table S1). The increase in myeloid cells is consistent with their inability to leave the vasculature (Moser et al 2008). In BM and Spl the numbers of MNCs in healthy K3$^{-/-}$ chimeras were not changed, while cell counts of lymphoid, erythroid and myeloid lineages were differentially affected (Figure 1B, 1C, S1U). However, they were still sufficiently high to exclude a severe differentiation defect as a cause for the increased lethality of K3$^{-/-}$ chimeras. Histology and immunohistochemistry of bone sections from K3$^{+/+}$ and K3$^{-/-}$ chimeras revealed similar morphologies also excluding a defective microenvironment as cause for the lethality (Figure S1V). To avoid secondary abnormalities due to imminent death, all further experiments were carried out with 'healthy' K3$^{-/-}$ chimeras that had a normal physical appearance and no anemia.

Kindlin-3 is required for BM homing of HSPCs

Homing of HSPCs to the BM requires β1 integrins (Magnon and Frenette, 2008; Potocnik et al., 2000) whose affinity is controlled by Kindlin-3 (Moser et al., 2009a). To assess the role of Kindlin-3 in homing, we analyzed short-term homing of FACS-isolated lineage^{-}Sca-1^{+}c-kit^{+} (LSK) cells from the BM of K3$^{+/+}$ and K3$^{-/-}$ chimeras. Injection of fluorescently labeled LSK cells into lethally irradiated wt recipient mice and their FACS quantification in the BM 18 h after transplantation revealed that K3$^{-/-}$ LSK cells homed about 5 times less efficient to the BM than K3$^{+/+}$ LSK cells (Figure 2A). These findings were confirmed by intravital 2-photon microscopy imaging of the central sinus and the surrounding BM cavity of the mouse calvaria, which also showed around 5 times less K3$^{-/-}$ LSK cells within the BM interstitium 18 h after transplantation (Figure 2B, C). Closer analysis revealed a significant reduction of K3$^{-/-}$ LSK cells firmly adhering to the

vessel surface (defined as adhesion to the same spot for at least 60 s) (Figure 2D). While most $K3^{-/-}$ LSK cells remained at the same spot for just a few seconds, the $K3^{+/+}$ LSK cells remained at the same spot up to 30 min (Figure 2E, F and Movie S1- S3).

The similar integrin expression profile of $K3^{+/+}$ and $K3^{-/-}$ LSK cells (Figure S2A, B) suggested that integrin function(s) rather than integrin levels were affected by the loss of Kindlin-3 expression. To test this hypothesis under flow conditions, we analyzed integrin-dependent adhesion of LSK cells in an *ex vivo* microflow chamber assay (Frommhold et al., 2008). Consistent with previous findings (Mazo et al., 2011), the numbers of adherent $K3^{+/+}$ LSK cells from the BM of chimeric mice (Figure 2G) or FL (Figure S2C) were highest on surfaces coated with recombinant murine (rm) VCAM-1, rmE-selectin and rmCXCL12. Adhesion of $K3^{+/+}$ LSK cell was efficiently blocked with antibodies against α4 integrin. In sharp contrast, $K3^{-/-}$ LSK cells from BM (Figure 2G) or FL (Figure S2C) adhered poorly to flow chambers coated with rmVCAM-1, rmE-selectin and rmCXCL12 or with rmVCAM-1 and rmE-selectin, suggesting that loss of Kindlin-3 dramatically impairs β1 integrin-dependent LSK cell adhesion. Importantly though, the low level adhesion of $K3^{-/-}$ LSK cells was still sufficient to enable residual homing to the BM compartment (Figure 2A-C). The inability of $K3^{+/+}$ and $K3^{-/-}$ LSK cells from the FL as well as BM to adhere to immobilized ICAM-1 under flow (Fig. S2D, E) suggests that α4β1 integrin is the predominant adhesion receptor that requires Kindlin-3 to firmly arrest LSK cells under flow conditions.

LT-HSCs are present in the BM of $K3^{-/-}$ chimeras

The data so far indicate that a reduced number of $K3^{-/-}$ HSPCs enters the BM but fails to accomplish a long-term reconstitution of the hematopoietic system. To test whether HSPCs were indeed present in the BM of $K3^{-/-}$ chimeras we performed CFU-C and LTC-IC assays with donor derived BM cells 4 months after transplantation and found similar numbers of CFU-Cs and a similar frequency of LTC-ICs in the $K3^{+/+}$ and $K3^{-/-}$ BM (Figure 3A, B). To further corroborate the presence of HSPCs in the $K3^{-/-}$ BM we phenotypically identified and quantified them with FACS using specific antibodies against CD34 and the signal lymphocyte activating molecule (SLAM) receptors (CD150 and CD48) (Kiel et al., 2005; Morita et al., 2010). In all $K3^{-/-}$ chimeras analyzed the total number of $K3^{-/-}$ LSK cells in the BM was normal, while LSK subpopulations were markedly altered (Figure 3C, D). The LSK $CD150^{+}CD48^{-}$ population containing the $CD34^{-}$ (enriched with quiescent LT-HSCs) and $CD34^{+}$ (enriched with more actively cycling

cells) subpopulations (Wilson et al., 2008) were significantly reduced in the BM of $K3^{-/-}$ chimeras. Instead, the LSK $CD150^{+}CD48^{+}$ and LSK $CD150^{-}CD48^{+}$ populations, containing HPCs, were increased (Figure 3C, D) suggesting a shift from the quiescent HSCs to the proliferating pool of HSPCs in $K3^{-/-}$ chimeras.

To determine whether populations enriched in LT-HSCs in the BM change over time, we analyzed the chimeras 1, 2, 4 and 9-13 months after transplantation. While the percentages of the $K3^{+/+}$ and $K3^{-/-}$ LSK subpopulations to total LSK cells was reduced already one month after BM transplantation, the total numbers of LSK $CD150^{+}CD48^{-}$ and LSK $CD150^{+}CD48^{-}CD34^{-}$ cells were comparable between $K3^{+/+}$ and $K3^{-/-}$ chimeras (Figure 3E-G). The numbers of LSK $CD150^{+}CD48^{-}$ and LSK $CD150^{+}CD48^{-}CD34^{-}$ cells steadily increased in the $K3^{+/+}$ BM, while they remained low in the $K3^{-/-}$ BM (Figure 3E-G). These results indicate that populations enriched in LT-HSCs are present in the BM of $K3^{-/-}$ chimeras but fail to expand with age.

Kindlin-3 maintains HSC quiescence and BM retention

The reduction of populations enriched in LT-HSCs in the BM of $K3^{-/-}$ chimeras could result from an increased proliferation, an enhanced differentiation into multipotent progenitors and/or an impaired BM retention, which would lead in all cases to their premature exhaustion. To test whether LT-HSCs are hyperactive we first determined the sensitivity of $K3^{+/+}$ and $K3^{-/-}$ chimeras to the cytostatic drug 5-Fluorouracil (5-FU), which eliminates cycling but not quiescent HSCs (Essers et al., 2009). In response to 5-FU treatment 2 out of 22 $K3^{+/+}$ chimeras and all $K3^{-/-}$ chimeras died suggesting that HSCs are actively cycling and quiescent LT-HSCs are absent or exist in extremely low numbers in $K3^{-/-}$ chimeras. Pre-treatment with polyI:C, which induces type I interferons (IFNα, IFNβ) expression and hence drives HSCs into the cell cycle (Essers et al., 2009), sensitized also $K3^{+/+}$ chimeras to 5-FU (Figure 4A, B).

The increased proliferative activity of $K3^{-/-}$ HSCs was confirmed with the BrdU uptake assay, which revealed that 3-4 months after BM transplantation the percentages of $BrdU^{+}$ LSK, LSK $CD150^{+}CD48^{-}$ and LSK $CD150^{+}CD34^{-}$ cells were increased in the $K3^{-/-}$ BM, while the percentage of $BrdU^{+}$ $lineage^{-}Sca\text{-}1^{-}c\text{-}kit^{+}$(LK) progenitor cells, which are highly proliferative, was similar in the BM of $K3^{+/+}$ and $K3^{-/-}$ chimeras (Figure 4C). Furthermore, DNA and Ki67 measurements in LSK cells also revealed increased numbers of cycling LSK cells in the BM of $K3^{-/-}$ chimeras (Figure 4D, E), and quantification of mRNA levels of the cyclin-dependent kinase inhibitors (CKIs) p21, p27,

and p57 in LSK CD150^{+} cells demonstrated that p57, which is required to maintain quiescence and stemness of HSCs (Matsumoto et al., 2011; Zou et al., 2011) ,were significantly decreased in K3$^{-/-}$ LSK CD150^{+} cells (Figure 4F).

Finally, label-retaining cell (LRC) assays (Wilson et al., 2008) also corroborated that the numbers of slowly dividing HSCs were reduced in the K3$^{-/-}$ BM. Administration of BrdU for 16 days labeled all HSPC populations in K3$^{+/+}$ and K3$^{-/-}$ BM (Figure 4G). After a BrdU-free chase of 45 days the percentage of BrdU label-retaining cells (LRCsBrdU) in the LSK, LSK CD150^{-}CD48^{+}, LSK CD150^{+}CD48^{+}, LSK CD150^{+}CD48^{-} and LSK CD150^{+}CD34^{-} cells were significantly diminished in the K3$^{-/-}$ BM (Figure 4H).

Despite the high proliferative activity of K3$^{-/-}$ HSPCs, the numbers of MNCs (Figure 1B) or LSK cells (Figure 3D) were not increased in the BM of healthy K3$^{-/-}$ chimeras suggesting that in addition to their proliferation defect, K3$^{-/-}$ HSPCs are not properly retained in the BM. In line with a retention defect, we observed increased frequencies and total numbers of LK in PB and LSK cells in Spl and PB (Figure 4I, J) and increased frequencies of CFU-Cs in Spl and PB of K3$^{-/-}$ chimeras (Figure S3A). Furthermore, transplantation of PB MNCs together with rescue Spl cells into lethally irradiated recipients demonstrated that K3$^{+/+}$ PB MNCs hardly contributed to total leukocytes, myeloid and lymphoid (i.e. B and T cells) lineages, while PB MNCs from K3$^{-/-}$ chimeras readily contributed to a multi-lineage hematopoietic chimerism in recipient mice up to 16 weeks after transplantation indicating that the PB of the K3$^{-/-}$ chimeras contains an increased number of circulating HSPCs (Figure 4K-N). The absence of T cells in K3$^{-/-}$ chimeras (Figure 4N) is due to an extravasation defect of preT cells into the thymus (manuscript in preparation).

To corroborate the BM retention defect of HSPCs we induced their mobilization with granulocyte colony-stimulating factor (G-CSF) (Figure 4O, S3B). G-CSF treatment increased LSK cells in the PB of K3$^{+/+}$ chimeras to the same extent as in PBS-treated K3$^{-/-}$ chimeras, while the LSK numbers rose even further in the PB of K3$^{-/-}$ chimeras (Figure 4O). The LSK cells were higher in the Spl of K3$^{+/+}$ compared to K3$^{-/-}$ chimeras (Figure S3B), which was probably due to the reduced extravasation potential of K3$^{-/-}$ HSPCs. Altogether these data demonstrate that HSCs in the K3$^{-/-}$ chimeras are constitutively cycling and that K3$^{-/-}$ HSPCs are less efficiently retained in the BM.

Loss of Kindlin-3 leads to a premature exhaustion of HSCs

Quiescent HSCs mediate multi-lineage long-term reconstitution (Trumpp et al., 2010; Wilson et al., 2008). Since most HSCs in the $K3^{-/-}$ chimeras were activated, we hypothesized that multi-lineage long-term reconstitution and thus survival of recipient mice exposed to an extreme hematopoietic stress such as serial BM transplantations or weekly 5-FU administration will be severely impaired without Kindlin-3. Although the 1^{st} generation $K3^{-/-}$ chimeras suffered from increased lethality (Figure 1A), approximately 50% of them maintained a multi-lineage long-term reconstitution for more than 5 months. We isolated $5x10^6$ whole BM (WBM) cells from these mice and transferred them intravenously (i.v.) into lethally irradiated secondary wt congenic B6.SJL recipients. As shown above (Figure 3C, D), $5x10^6$ $K3^{-/-}$ WBM cells contained sufficient numbers of HSCs to mediate long-term reconstitution. While all 42 recipients transplanted with $K3^{+/+}$ WBM cells were radio-protected for more than 10 weeks, only 4 out of the 55 recipients of $K3^{-/-}$ WBM cells were able to survive for 10 weeks. We next transferred $5x10^6$ WBM cells from 9 $K3^{+/+}$ and the 4 surviving $K3^{-/-}$ 2^{nd} generation donors to 5 tertiary recipients for each secondary donor and observed that within 10 weeks after transplantation 41 out of the 45 recipients of $K3^{+/+}$ WBM cells were protected against lethal irradiation, while all 20 recipients of $K3^{-/-}$ WBM cells succumbed. As expected, $K3^{+/+}$ WBM cells enabled long-term engraftment even in quaternary (Figure 5A) and quinary recipients (data not shown).

To ensure that the severe reconstitution defect of $K3^{-/-}$ WBM cells did not result from a reduced number of HSPCs in transplanted WBM cells but rather from HSPC dysfunctions described above, we performed transplantation experiments with $1x10^3$ LSK $CD150^+$ cells sorted by FACS from BM of $K3^{+/+}$ and $K3^{-/-}$ primary donor chimeras and supplemented the secondary recipients with $5x10^6$ congenic BL6.SJL unfractionated Spl cells. The experiments revealed that $K3^{+/+}$ LSK $CD150^+$ donor cells induced a high percentage of donor-derived myeloid, B and T cells in the PB 5 weeks after transplantation, which further increased at 11 weeks. In contrast, recipients of $K3^{-/-}$ LSK $CD150^+$ donor cells showed a significantly lower multi-lineage reconstitution in the PB 5 weeks after transplantation that further declined after 11 weeks (Figure 5B). Almost all differentiated cell lineages in BM and Spl in recipients of $K3^{+/+}$ LSK $CD150^+$ cells were donor-derived, while less than 5% were donor-derived cells in recipients of $K3^{-/-}$ LSK $CD150^+$ cells (Figure S4A, B). Furthermore, almost all cells in the different HSPC populations were donor-derived in $K3^{+/+}$ LSK $CD150^+$ cell recipients, while the

percentage of donor-derived HSPCs was around 10% in most $K3^{-/-}$ LSK $CD150^{+}$ cell recipients (Figure 5C).

To exclude that differences in transplanted LSK $CD150^{+}$ cell counts, defective homing, lodgment into the BM niche and engraftment properties of $K3^{-/-}$ HSPCs lead to their exhaustion, we disrupted the *Kindlin-3* allele in HSPCs 2-3 months after the transplantion of BM cells from mice carrying floxed *Kindlin-3* alleles and a $Rosa26^{Cre\text{-}ERT2}$ transgene into congenic B6.SJL recipients ($K3^{fl/fl}Rosa26^{Cre\text{-}ERT2}$ chimera). Tamoxifen-treated $K3^{fl/fl}Rosa26^{Cre\text{-}ERT2}$ chimeras developed defects (Figure S4C-L) resembling those of $K3^{-/-}$ FL chimeras (Figure 1, 4I). Furthermore, weekly 5–FU treatment 5 weeks after tamoxifen administration caused a 90% lethality of $K3^{fl/fl}Rosa26^{Cre\text{-}ERT2}$ chimeras within 20 days, whereas almost all control chimeras survived (Figure 5D) demonstrating that the impaired stress response of $K3^{-/-}$ HSCs operates independent of niche lodgment and number of transplanted HSCs. Altogether these findings demonstrate that the long-term BM reconstitution defect of $K3^{-/-}$ chimeras is due to an impaired stemness of $K3^{-/-}$ HSCs cells within the BM that is further aggravated by their homing defects.

$K3^{-/-}$ HSC defects are cell autonomous

Hematopoietic injury (e.g. blood loss) activates quiescent HSCs until all hematopoietic cells are replenished (Trumpp et al., 2010). Since $K3^{-/-}$ chimeras suffer from anemia, which could induce HSC activation, we performed several experiments to define whether $K3^{-/-}$ HSC quiescence is lost in a cell autonomous or non-autonomous manner.

First, we restored the anemia of $K3^{-/-}$ chimeras (Table S1) by generating mixed chimeric mice (mix-chimeras) with FL cells from E14.5 $K3^{+/+}$ or $K3^{-/-}$ embryos (C57BL/6; $CD45.2^{+}$) mixed with competitor FL cells from E14.5 wt congenic B6.SJL ($CD45.1^{+}$) embryos and transplanted both together into lethally irradiated F1 recipients ($CD45.2^{+}CD45.1^{+}$) (Figure S5A) in a 1:1 ratio for $K3^{+/+}$ and 1:1 or 20:1 for $K3^{-/-}$ mix-chimeras, respectively. Despite efficient reversal of the anemia (Table S2), $K3^{-/-}$ ($CD45.2^{+}$) LK and LSK cell numbers were still significantly increased in the PB compared to wt LK and LSK competitor cells ($CD45.1^{+}$) (Figure 6A), indicating that the elevation of $K3^{-/-}$ HSPCs in the PB occurs in a cell autonomous manner. Second, we compared G-CSF induced mobilization of LSK cells to the PB between $K3^{+/+}$ and $K3^{-/-}$ mix-chimeras (Figure 6B) and found that the high basal levels of $K3^{-/-}$ LSK cells in PBS-treated $K3^{-/-}$ mix-chimeras further increased after G-CSF treatment, while the $K3^{+/+}$ and the congenic

competitor derived LSK cells in $K3^{+/+}$ and $K3^{-/-}$ mix-chimeras increased after application of G-CSF to the basal $K3^{-/-}$ LSK cell level, demonstrating that the mobilization defect of $K3^{-/-}$ HSCs is also cell autonomous. Third, LRC assays revealed that a BrdU pulse of 18 days labeled almost all HSPCs in $K3^{+/+}$ or $K3^{-/-}$ mix-chimeras (Figure 6C), while a chase period of 45 to 50 days decreased the percentages of LRCsBrdU in the LSK, LSK $CD150^{-}CD48^{+}$ and LSK $CD150^{+}CD48^{-}$ populations significantly more in $K3^{-/-}$ than $K3^{+/+}$ mix-chimeras (Figure 6D), indicating that also the increased proliferation rate of HSPCs is cell autonomous. Interestingly, the reduction in LRCsBrdU in the LSK $CD150^{+}CD34^{-}$ population was not significant (Figure 6D), which may indicate that their activity is diminished in $K3^{-/-}$ mix-chimeras compared with 100% $K3^{-/-}$ chimeras. Fourth, we demonstrate that hematopoietic stress induced by 5-FU treatment of $K3^{+/+}$ or $K3^{-/-}$ mix-chimeras diminished the ratio between $K3^{-/-}$ to congenic competitor LSK cells by approximately 7-fold (Figure 6E), while the ratio between $K3^{+/+}$ and congenic competitor LSK cells remained unaffected indicating that also the 5-FU sensitivity is cell autonomous. Fifth, we investigated the long-term reconstitution potential of $K3^{+/+}$ and $K3^{-/-}$ HSPCs isolated from mix-chimeras in a competitive repopulation assay. Around 450 FACS-purified $K3^{+/+}$ or $K3^{-/-}$ LSK $CD150^{+}CD45.2^{+}$ cells were mixed with $5x10^{6}$ whole Spl cells from congenic B6.SJL mice and transplanted into lethally irradiated congenic B6.SJL recipients. While the average percentages of $K3^{+/+}$ and $K3^{-/-}$ donor-derived whole leukocytes were similar 4 weeks after transplantation, the average percentages of myeloid cells, B and T cells differed significantly in the respective recipient mice. The difference of $K3^{+/+}$ and $K3^{-/-}$ donor-derived cells further increased over the observation period of 8 and 12 weeks after transplantation (Figure 6F-I). Interestingly, the $CD45.1^{+}$ to $CD45.2^{+}$ ratio remained constant between HSPCs and mature effector cells in $K3^{+/+}$ mix-chimeras, while the ratio diminished in $K3^{-/-}$ mix-chimeras (Figure S5B, C) pointing to an additional differentiation defect of $K3^{-/-}$ HSPCs and/or a decreased production of effector cells due to impaired BM retention of $K3^{-/-}$ HSPCs in the BM. Since a decreased formation of $K3^{-/-}$ effector cells does not allow to correlate the percentage of donor-derived cells in the PB with the percentage of HSPCs in the BM, we assessed the percentage of donor-derived cells in different HSPC populations in the BM. Twelve months after transplantation, $K3^{+/+}$ LSK $CD150^{+}CD45.2^{+}$ donor cells produced nearly 100% of all HSPC populations analyzed, while in recipients of $K3^{-/-}$ LSK $CD150^{+}CD45.2^{+}$ cells the average engraftment capacity was reduced to around 50% (Figure 6J), indicating that the $K3^{-/-}$ HSCs reconstitution defect is also cell autonomous. Altogether

these findings demonstrate that abnormal mobilization, increased proliferation, enhanced 5-FU sensitivity and diminished engraftment of $K3^{-/-}$ HSPCs are cell autonomous defects.

Kindlin-3 is essential for activated HSPCs rather than quiescent HSCs

To address the question whether Kindlin-3 is required for quiescent, and/or activated HSCs and/or formation of HPCs, we first monitored donor-derived HSPC populations in the BM of mix-chimeras over time (Figure 7A-D). This analysis revealed that the average percentages of donor-derived LK and LSK $CD150^{-}CD48^{+}$ cells increased in $K3^{+/+}$ and decreased in $K3^{-/-}$ mix-chimeras during an observation period of 12 months after transplantation (Figure 7A, B), while the average percentages of donor-derived LSK $CD150^{+}CD48^{-}$ or LSK $CD150^{+}CD48^{-}CD34^{-}$ cells remained similar and stable, both in $K3^{+/+}$ and $K3^{-/-}$ mix-chimeras (Figure 7C, D) indicating that Kindlin-3 is required to maintain stable LSK $CD150^{-}CD48^{+}$ cell numbers but not for maintaining LSK $CD150^{+}CD48^{-}$ and LSK $CD150^{+}CD48^{-}CD34^{-}$ cells. This conclusion is further supported by the observation that 3-4 months post transplantation the percentage of donor-derived LSK $CD150^{-}CD48^{+}$ cells significantly dropped in comparison to LSK $CD150^{+}CD48^{-}$ or LSK $CD150^{+}CD48^{-}CD34^{-}$ cells in the BM of $K3^{-/-}$ mix-chimeras, while this cell population significantly increased in $K3^{+/+}$ mix-chimeras (Figure 7E).

To further confirm a differential role of Kindlin-3 for different HSPC populations and to exclude homing defects, we also monitored donor-derived HSPC populations in the BM of lethally irradiated mix-chimeras (F1 $CD45.2^{+}CD45.1^{+}$recipients) transplanted with wt BM cells from congenic B6.SJL ($CD45.1^{+}$) mice mixed in a 1:1 ratio with BM cells from either C57BL/6 ($CD45.2^{+}$) $K3^{fl/fl}Rosa26^{Cre\text{-}ERT2}$ or wt-$Rosa26^{Cre\text{-}ERT2}$ mice, supplied with tamoxifen three months after transplantation, and treated with either PBS or 5-FU five weeks later. Wt-$Rosa26^{Cre\text{-}ERT2}$ control and non-induced $K3^{fl/fl}Rosa26^{Cre\text{-}ERT2}$ mix-chimeras displayed similar average percentages of donor-derived LK, LSK $CD150^{+}CD48^{-}$ and LSK $CD150^{+}CD48^{-}CD34^{-}$ cells, while the percentage of LSK $CD150^{-}CD48^{+}$ cells was increased in the $K3^{fl/fl}Rosa26^{Cre\text{-}ERT2}$ mix-chimera compared control chimeras (Figure 7F-I). Tamoxifen-induced deletion of Kindlin-3 diminished the LK and LSK $CD150^{-}CD48^{+}$ populations in $K3^{fl/fl}Rosa26^{Cre\text{-}ERT2}$ mix-chimeras, while the percentages of donor-derived LSK $CD150^{+}CD48^{-}$ and LSK $CD150^{+}CD48^{-}CD34^{-}$ populations remained similar between $K3^{fl/fl}Rosa26^{Cre\text{-}ERT2}$ and control mix-chimeras, further confirming that Kindlin-3 is dispensable for these HSC populations under

homeostatic conditions (Figure 7F-I). Importantly, however, 5-FU-induced activation of HSCs further decreased the LK and LSK $CD150^{-}CD48^{+}$ populations and also induced a dramatic decrease of the average percentages of donor-derived LSK $CD150^{+}CD48^{-}$ and LSK $CD150^{+}CD48^{-}CD34^{-}$ populations in tamoxifen pretreated $K3^{fl/fl}Rosa26^{Cre\text{-}ERT2}$ mix-chimeras (Figure 7F-I).

Kindlin-3 maintains HSPCs in the BM by activating integrins

The results so far indicate that Kindlin-3 is essential to retain active/proliferating HSPCs in the BM. To test whether Kindlin-3 executes this function through integrin-mediated adhesion we compared the affinity state of β1 integrins on LSK $CD150^{-}CD48^{+}$ and LSK $CD150^{+}CD48^{-}$ cells from 100% $K3^{+/+}$ and $K3^{-/-}$ chimeras by determining the levels of the 9EG7 epitope, which is only found on active β1 integrins. The results show significantly decreased 9EG7 levels on $K3^{-/-}$ LSK $CD150^{-}CD48^{+}$ and LSK $CD150^{+}CD48^{-}$ cells compared to the $K3^{+/+}$ control populations (Figure 7J). To further confirm an important role for Kindlin-3 induced integrin activation on HSPCs, $K3^{+/+}$ and $K3^{-/-}$ LSK cells were isolated from the BM of 100% chimeras and lentivirally transduced with either a wt or an integrin-binding deficient Kindlin-3 expression construct, in which amino acid residues QW597/598 were substituted with alanines (thereby preventing Kindlin-3 binding to the NPxY motif of all β integrin tails). Approximately $1.5x10^{4}$ of the transduced LSK cells were transplanted together with $8.8x10^{5}$ $CD45.2^{+}$ WBM cells isolated from a $K3^{-/-}$ 100% chimera into lethally irradiated congenic B6.SJL recipients. The reconstitution potential of $K3^{+/+}$ LSK cells transduced with GFP ($K3^{+/+}$ LSK with GFP; positive control), $K3^{-/-}$ LSK cells transduced with either GFP ($K3^{-/-}$ LSK with GFP; negative control) or a K3-wt expression construct ($K3^{-/-}$ LSK with K3-wt) or a K3-QWAA expression construct ($K3^{-/-}$ LSK with K3-QWAA) was compared by monitoring the survival of recipients. As expected, recipients transplanted with $K3^{-/-}$ LSK cells with GFP died within 40 days (Figure 7K), while recipients transplanted with $K3^{+/+}$ LSK cells with GFP showed multi-lineage long-term rescue of all recipients (Figure 7K, S6A). Importantly, only one recipient transplanted with $K3^{-/-}$ LSK cells with K3-wt died and the remaining four survivors showed a multi-lineage long-term reconstitution, while 4 out of 5 recipients transplanted with $K3^{-/-}$ LSK cells with K3-QWAA died from severe pancytopenia (Figure 7K, S6A, and data not shown). The stable transduction of the different viral expression constructs in donor-derived blood cells of surviving recipients was confirmed by different PCRs (Figure S6B and Table S4).

The reduced 9EG7 epitope levels on K3$^{-/-}$ LSK CD150^{-}CD48^{+} and LSK CD150^{+}CD48^{-} cells together with the severely diminished reconstitution potential of LSK cells expressing an integrin-binding deficient Kindlin-3 indicates that Kindlin-3 regulates HSPC homeostasis in an integrin dependent manner.

Kindlin-3 in human HSPCs maintenance

To test whether the role of Kindlin-3 for regulating HSPCs is conserved in man, we quantified the number of CD45^{+}CD34^{+}, CD34^{+}CD38^{+} and CD34^{+}CD38^{-} HSPCs in PB of a patient suffering from LAD-III caused by a null mutation in the *KINDLIN-3* gene leading to a premature stop codon at the position coding for amino acid 529 and loss of protein expression (Schulz et al., manuscript in preparation). The experiment was controlled by determining the numbers of HSPCs in a blood sample from a healthy child of the same age as the LAD-III patient (Figure 7L). The results revealed that CD45^{+}CD34^{+} and CD34^{+}CD38^{+} cells were around 200 times and CD34^{+}CD38^{-} cells around 60 times higher in the blood of the LAD-III patient compared to the healthy subject. Importantly, the CFU assay revealed that blood samples from the healthy individual as well as from the LAD-III patient produced similar numbers of CFU-GM and BFU-E colonies when whole leucocytes with calculated 100 CD34^{+} cells were cultured (Figure 7M). These results indicate that the absence of Kindlin-3 in LAD-III patients impairs the homeostasis of HSPCs and hence is perfectly in line with the observations made in mice lacking Kindlin-3 in HSPCs (Figure 4I-N).

DISCUSSION

Kindlin-3 is expressed in all hematopoietic cells including HSPCs and is required for bidirectional integrin signaling (Moser et al., 2009a). HSPCs express several integrins (Grassinger et al., 2009) and therefore, one would predict that Kindlin-3 serves important roles for HSC homeostasis. To test this hypothesis, we designed a range of experiments, which assigned several important function(s) to Kindlin-3 in HSPCs. The results of our study demonstrate that Kindlin-3 is dispensable for the generation of HSCs, however it plays key roles for several important HSPC properties; first, Kindlin-3 supports the homing of HSPCs to the BM by facilitating integrin-mediated adhesion to the vessel wall. Second, it facilitates the retention of proliferating HSPCs in the BM microenvironment. Finally, the retention of proliferating HSPCs by Kindlin-3 prevents an excessive activation of quiescent HSCs under hematopoietic stress and thereby averts their premature exhaustion.

The homing of HSPCs to the BM is a multistep process that commences with their adhesion to the BM vessel wall and continues with their transendothelial migration finally leading to colonization of the stem cell niches (Magnon and Frenette, 2008). Our analysis showed that disruption of the *Kindlin-3* gene in HSPCs diminished short-term BM homing. A few $K3^{-/-}$ HSPCs assumed long lasting adhesions to endothelial cells and eventually crossed the vessel wall, which gave rise to significant numbers of $K3^{-/-}$ HSPCs in the BM of recipient mice 1 month after transplantation. Previous reports already demonstrated that β1 class integrins (mainly through α4β1, and most likely also through α9β1 binding to VCAM-1) are essential for BM homing of HSPCs (Magnon and Frenette, 2008; Potocnik et al., 2000; Taooka et al., 1999). Although activation of β1 and most likely all other integrin classes is impaired on $K3^{-/-}$ HSPCs there are still sufficient integrins functional to permit BM homing of $K3^{-/-}$ HSPCs, although at a much reduced efficiency. Hence, the ability of Kindlin-3 to shift the equilibrium of integrins toward high activity is not absolutely essential although tremendously instrumental in this process.

Our experiments also revealed that the numbers of $K3^{-/-}$ HSPCs were significantly elevated in the circulation and Spl, of both 100% chimeras and mix-chimeras. The accumulation of these cells in the periphery could be caused by a spontaneous mobilization of HSPCs and/or a diminished re-homing of circulating HSPCs to the BM (Massberg et al., 2007; Wright et al., 2001). The defects observed in $K3^{fl/fl}Rosa26^{Cre\text{-}ERT2}$ mix-chimeras, in which the *Kindlin-3* gene was deleted after transplantation, makes a

defective rehoming rather unlikely and argues for a defective retention of HSPCs. A defective retention is further supported by the increased sensitivity of K3$^{-/-}$ HSPCs to G-CSF and the observation that the K3$^{-/-}$ LSK CD150^{-}CD48^{-}CD34^{-} population fails to increase over time in the BM of 100% chimeras despite an elevated proliferation rate of these cells.

The hyperproliferative state of K3$^{-/-}$ HSCs in 100% chimeras results in HSC exhaustion characterized by the loss of LT-HSCs leading to pancytopenia in old K3$^{-/-}$ chimeras. The finding that K3$^{-/-}$ LSK CD150^{+}CD48^{-}CD34^{-} cell numbers remain quiescent in mix-chimeras reconstituted with wt and K3$^{-/-}$ HSPCs while the proliferative K3$^{-/-}$ LSK CD150^{-}CD48^{+} population diminishes points to a major task of Kindlin-3 for maintaining proliferating HSPCs rather than quiescent HSCs. In line with this conclusion, we found that the exposure of mix-chimeras to hematopoietic stress such as a weekly 5-FU treatment, which triggers HSC activation and proliferation, gradually diminishes the pool of K3$^{-/-}$ HSCs. Their reduction results from the loss of K3$^{-/-}$ HPCs and activated K3$^{-/-}$ HSCs into the circulation coupled with the demand to replenish their decreasing pools. In 5-FU treated mix-chimeras the presence of wt HSC compensates for the gradual decline of K3$^{-/-}$ HSC, while in 100% chimeras the loss of K3$^{-/-}$ HSPCs into the circulation is eventually leading to the exhaustion of the quiescent HSC pool and to the death of the animal. Since untreated K3$^{-/-}$ mix-chimeras are not exposed to hematopoietic stress, wt HSCs fill the HPC niches and only the few proliferating HSPCs derived from the K3$^{-/-}$ HSCs fail to retain in the BM and accumulate in the circulation.

Kindlin-3 maintains HSPCs in the BM in a cell autonomous manner, although factors such as anemia contribute to the defect in 100% chimeras. Mechanistically, this function is achieved through the ability of Kindlin-3 to activate integrins. In line with this conclusion, we observed that the 9EG7 epitope, which is only present on activated β1 integrins, is dramatically reduced in K3$^{-/-}$ HSPCs. Furthermore, the inability to reconstitute lethally irradiated recipients with K3$^{-/-}$ LSK cells expressing an integrin binding-deficient Kindlin-3 indicates that Kindlin-3 maintains HSPCs in the BM by activating integrins. Interestingly, Wnt/β-catenin and TGF-β signaling, which are essential in cutaneous stem cells, were unaffected in K3$^{-/-}$ HSPCs (data not shown). This is likely due to differences in the niche microenvironment, the different properties of the Kindlin isoforms and the different integrin subtypes expressed in different tissue stem cells. For example, cutaneous stem cells express high levels of the epithelial integrin

αvβ6, which is not expressed in HSPCs (Huang et al., 1996; Klimmeck et al., 2012), and hence is not employed to liberate TGF-β and regulate TGF-β signaling.

Why is Kindlin-3 only required in activated HSPCs and not in quiescent HSCs? It is possible that different classes of adhesion molecules such as CD44 or selectins compensate for each other on quiescent HSCs. These adhesion molecules have low affinities for their ligand, which is sufficient to retain quiescent HSCs in their BM compartments but insufficient to retain proliferating HSPCs that round up during mitosis and loosen their adhesion. Consequently, proliferating HSPCs (and most likely also active HSCs) detach and accumulate in the circulation. Finally, it is also conceivable that activated and quiescent HSCs reside in different niches. Although the presence of different niches for HSPCs is not entirely resolved, one could envisage that different niches differ in their niche components and hence require different adhesion molecules for cell retention. In line with these hypotheses, our findings indicate that Kindlin-3 mediated integrin adhesion is essential for proliferating HSPCs and to a lesser extent for quiescent HSCs. Live imaging microscopy of HSPCs in the BM should allow to see whether HSPCs move to a different BM compartments during cell division and/or whether they round up and detach during cell division and become lost when they lack Kindlin-3 expression.

In summary, our findings assign Kindlin-3 induced integrin adhesion an important role for maintaining actively proliferating HSPCs in the BM. This exquisite function is not required by quiescent HSCs, although stem cells in other tissues such as the hair bulge require integrin adhesion for their maintenance (Brakebusch et al., 2000; Raghavan et al., 2000). Furthermore, the important role of Kindlin-3 for integrin activation in HSPCs is conserved between mouse and man, as an individual suffering from LAD-III also demonstrates dramatically increased levels of circulating HSPCs.

EXPERIMENTAL PROCEDURES

Mice

$K3^{-/-}$ chimeras have been described (Moser et al., 2008). Kindlin-3 floxed mice carry lox P sites that flank exons 3-6 with loxP sites (manuscript in preparation). Mice were kept under specific pathogen-free conditions in the animal facility of the Max Planck Institute of Biochemistry. All mouse experiments were performed with approval by the District Government of Upper Bavaria.

LAD-III patient

LAD-III patient was a 6 months old female carrier of a homozygous nonsense mutation in exon 13 of the *KINDLIN-3* gene leading to a premature stop codon at the position coding for amino acid 529 and loss of protein expression (Schulz et al., manuscript in preparation). All tests were performed after obtaining a signed informed consent form from the parents.

Flow cytometry

For FACS analysis MNCs from BM (2x femur, 2x tibia, 2x pelvis, 2x humerus), PB or Spl were isolated, immunostained according to standard procedures and analyzed with a FACSCalibur or FACSCantoII or sorted for subpopulations with a FACSAriaII (BD Biosciences). HSPC subpopulations were gated as shown in Figure 3C. Antibodies are described in the extended experimental procedures.

Short-term homing assay

FACS-sorted LSK cells were stained with cell tracker CMTMR. Short-term homing was assessed directly after injection to the right external carotid artery or 18 h after tail vein injection using 2-photon intravital microscopy (LaVision BioTec) or flow cytometry.

In vitro flow chamber assay

Microflow chambers were prepared as previously described (Frommhold et al., 2008), see Extended Experimental Procedures. Cells were perfused through coated capillaries for 12 min under shear (shear stress 1 dyne/cm^2). After washing and fixation of adherent cells with Türks solution for 80 s, adherent cells were quantified using a ZEISS Axioskop40 microscope (Zeiss).

BM and PB transplantation

For noncompetitive serial transplantation, WBM cells were isolated from 1 mouse of the previous generation and $5x10^6$ cells were intravenously injected each into 5 lethally irradiated congenic B6.SJL wt recipients. After 10-12 weeks transplantation to the next generation recipients was performed using the same conditions. For competitive BM HSC transplantations 1000 FACS-sorted BM LSK $CD150^+$ cells from $K3^{+/+}$ or $K3^{-/-}$ chimeras or 450 FACS-sorted BM LSK $CD150^+$ cells from $K3^{+/+}$ or $K3^{-/-}$ mix-chimeras together with $5x10^6$ whole Spl competitor cells were injected to the tail vein of lethally irradiated F1 wt recipients. The percentage of donor-derived cells in the PB or BM and Spl of recipient mice was analyzed by FACS at time points after transplantation as indicated in the figures. For competitive PB transplantation, $3x10^6$ PB MNCs were mixed with $4x10^6$ host-type whole Spl cells and injected to the tail vein of lethally irradiated congenic B6.SJL wt recipients. Percentage of donor-derived lymphoid and myeloid cells in the PB of recipient mice was analyzed 5, 8, 12 and 16 weeks after transplantation. In all transplantation experiments recipient mice received a total body irradiation of 13.5 Gy (7.5 Gy and 6 Gy 4 h apart).

Administration of 5-FU

For the polyI:C (GE Healthcare) and 5-Fluorouracil (5-FU; Sigma-Aldrich) double treatment, polyI:C (10 mg/kg) and 5-FU (150 mg/kg) were injected intraperitoneally into BM chimeras (3-4 months after transplantation). For weekly 5-FU treatment, 5-FU was injected intraperitoneally at dose of 150 mg/kg for first two injections and 100 mg/kg for the following injections. In both experiments survival was monitored daily.

Statistical analysis

Unless otherwise noted, all values are reported as mean ±SD. Statistical tests used for each experiment are described in the figure legends. Statistical significance was assumed at $p < 0.05$. Statistical analyses were performed using Prism software (GraphPad Software) or MedCalc software (MedCalc Software).

ACKNOWLEDGEMENTS

We thank Karin Hirsch, Alexander Felber, Susanne Bierschenk and Sarah Longhi for expert technical assistance, Dr. Ernesto Bockamp for the R26creERT2 mouse and Dr. Roy Zent for critically reading the manuscript. The work was supported by the Deutsche Forschungsgemeinschaft (SFB 914, OO 8/2 and FOR 2033) and the Max Planck Society.

REFERENCES

Adams, G.B., Chabner, K.T., Alley, I.R., Olson, D.P., Szczepiorkowski, Z.M., Poznansky, M.C., Kos, C.H., Pollak, M.R., Brown, E.M., and Scadden, D.T. (2006). Stem cell engraftment at the endosteal niche is specified by the calcium-sensing receptor. Nature *439*, 599–603.

Arroyo, A.G., Yang, J.T., Rayburn, H., and Hynes, R.O. (1999). Alpha4 integrins regulate the proliferation/differentiation balance of multilineage hematopoietic progenitors in vivo. Immunity *11*, 555–566.

Brakebusch, C., Grose, R., Quondamatteo, F., Ramirez, A., Jorcano, J.L., Pirro, A., Svensson, M., Herken, R., Sasaki, T., Timpl, R., et al. (2000). Skin and hair follicle integrity is crucially dependent on beta 1 integrin expression on keratinocytes. Embo J *19*, 3990–4003.

Essers, M.A.G., Offner, S., Blanco-Bose, W.E., Waibler, Z., Kalinke, U., Duchosal, M.A., and Trumpp, A. (2009). IFNα activates dormant haematopoietic stem cells in vivo. Nature *458*, 904–908.

Frommhold, D., Ludwig, A., Bixel, M.G., Zarbock, A., Babushkina, I., Weissinger, M., Cauwenberghs, S., Ellies, L.G., Marth, J.D., Beck-Sickinger, A.G., et al. (2008). Sialyltransferase ST3Gal-IV controls CXCR2-mediated firm leukocyte arrest during inflammation. J Exp Med *205*, 1435–1446.

Grassinger, J., Haylock, D.N., Storan, M.J., Haines, G.O., Williams, B., Whitty, G.A., Vinson, A.R., Be, C.L., Li, S., Sørensen, E.S., et al. (2009). Thrombin-cleaved osteopontin regulates hemopoietic stem and progenitor cell functions through interactions with alpha9beta1 and alpha4beta1 integrins. Blood *114*, 49–59.

Huang, X.Z., Wu, J.F., Cass, D., Erle, D.J., Corry, D., Young, S.G., Farese, R.V., and Sheppard, D. (1996). Inactivation of the integrin beta 6 subunit gene reveals a role of epithelial integrins in regulating inflammation in the lung and skin. J. Cell Biol. *133*, 921–928.

Hynes, R.O. (2002). Integrins: bidirectional, allosteric signaling machines. Cell *110*, 673–687.

Jordan, C.T., McKearn, J.P., and Lemischka, I.R. (1990). Cellular and developmental properties of fetal hematopoietic stem cells. Cell *61*, 953–963.

Kiel, M.J., and Morrison, S.J. (2008). Uncertainty in the niches that maintain haematopoietic stem cells. Nature Reviews Immunology *8*, 290–301.

Kiel, M.J., Yilmaz, Ö.H., Iwashita, T., Yilmaz, O.H., Terhorst, C., and Morrison, S.J. (2005). SLAM Family Receptors Distinguish Hematopoietic Stem and Progenitor Cells and Reveal Endothelial Niches for Stem Cells. Cell *121*, 1109–1121.

Klimmeck, D., Hansson, J., Raffel, S., Vakhrushev, S.Y., Trumpp, A., and Krijgsveld, J. (2012). Proteomic cornerstones of hematopoietic stem cell differentiation: distinct signatures of multipotent progenitors and myeloid committed cells. Mol. Cell Proteomics *11*, 286–302.

Kuijpers, T.W., van de Vijver, E., Weterman, M.A.J., de Boer, M., Tool, A.T.J., van den Berg, T.K., Moser, M., Jakobs, M.E., Seeger, K., Sanal, O., et al. (2009). LAD-1/variant syndrome is caused by mutations in FERMT3. Blood *113*, 4740–4746.

Magnon, C., and Frenette, P.S. (2008). Hematopoietic stem cell trafficking (Cambridge (MA): Harvard Stem Cell Institute).

Malinin, N.L., Zhang, L., Choi, J., Ciocea, A., Razorenova, O., Ma, Y.-Q., Podrez, E.A., Tosi, M., Lennon, D.P., Caplan, A.I., et al. (2009). A point mutation in KINDLIN3 ablates activation of three integrin subfamilies in humans. Nat. Med. *15*, 313–318.

Massberg, S., Schaerli, P., Knezevic-Maramica, I., Köllnberger, M., Tubo, N., Moseman, E.A., Huff, I.V., Junt, T., Wagers, A.J., Mazo, I.B., et al. (2007). Immunosurveillance by Hematopoietic Progenitor Cells Trafficking through Blood, Lymph, and Peripheral Tissues. Cell *131*, 994–1008.

Matsumoto, A., Takeishi, S., Kanie, T., Susaki, E., Onoyama, I., Tateishi, Y., Nakayama, K., and Nakayama, K.I. (2011). p57 Is Required for Quiescence and Maintenance of Adult Hematopoietic Stem Cells. Cell Stem Cell *9*, 262–271.

Mazo, I.B., Massberg, S., and Andrian, von, U.H. (2011). Hematopoietic stem and progenitor cell trafficking. Trends in Immunology *32*, 493–503.

Morita, Y., Ema, H., and Nakauchi, H. (2010). Heterogeneity and hierarchy within the most primitive hematopoietic stem cell compartment. J Exp Med *207*, 1173–1182.

Morrison, S.J., and Spradling, A.C. (2008). Stem cells and niches: mechanisms that promote stem cell maintenance throughout life. Cell *132*, 598–611.

Moser, M., Legate, K.R., Zent, R., and Fassler, R. (2009a). The Tail of Integrins, Talin, and Kindlins. Science *324*, 895–899.

Moser, M., Bauer, M., Schmid, S., Ruppert, R., Schmidt, S., Sixt, M., Wang, H.-V., Sperandio, M., and Fässler, R. (2009b). Kindlin-3 is required for beta2 integrin-mediated leukocyte adhesion to endothelial cells. Nat. Med. *15*, 300–305.

Moser, M., Nieswandt, B., Ussar, S., Pozgajova, M., and Fässler, R. (2008). Kindlin-3 is essential for integrin activation and platelet aggregation. Nat. Med. *14*, 325–330.

Okada, S., Nakauchi, H., Nagayoshi, K., Nishikawa, S., Miura, Y., and Suda, T. (1992). In vivo and in vitro stem cell function of c-kit- and Sca-1-positive murine hematopoietic cells. Blood *80*, 3044–3050.

Potocnik, A.J., Brakebusch, C., and Fassler, R. (2000). Fetal and adult hematopoietic stem cells require beta1 integrin function for colonizing fetal liver, spleen, and bone marrow. Immunity *12*, 653–663.

Raghavan, S., Bauer, C., Mundschau, G., Li, Q., and Fuchs, E. (2000). Conditional ablation of beta1 integrin in skin. Severe defects in epidermal proliferation, basement membrane formation, and hair follicle invagination. J. Cell Biol. *150*, 1149–1160.

Rizo, A. (2006). Signaling pathways in self-renewing hematopoietic and leukemic stem

cells: do all stem cells need a niche? Human Molecular Genetics *15*, R210–R219.

Schmidt, S., Nakchbandi, I., Ruppert, R., Kawelke, N., Hess, M.W., Pfaller, K., Jurdic, P., Fassler, R., and Moser, M. (2011). Kindlin-3-mediated signaling from multiple integrin classes is required for osteoclast-mediated bone resorption. J. Cell Biol. *192*, 883–897.

Shattil, S.J., Kim, C., and Ginsberg, M.H. (2010). The final steps of integrin activation: the end game. Nat Rev Mol Cell Biol *11*, 288–300.

Svensson, L., Howarth, K., McDowall, A., Patzak, I., Evans, R., Ussar, S., Moser, M., Metin, A., Fried, M., Tomlinson, I., et al. (2009). Leukocyte adhesion deficiency-III is caused by mutations in KINDLIN3 affecting integrin activation. Nat. Med. *15*, 306–312.

Taooka, Y., Chen, J., Yednock, T., and Sheppard, D. (1999). The integrin alpha9beta1 mediates adhesion to activated endothelial cells and transendothelial neutrophil migration through interaction with vascular cell adhesion molecule-1. J. Cell Biol. *145*, 413–420.

Trumpp, A., Essers, M., and Wilson, A. (2010). Awakening dormant haematopoietic stem cells. Nature Reviews Immunology *10*, 201–209.

Ussar, S., Wang, H.-V., Linder, S., Fässler, R., and Moser, M. (2006). The Kindlins: subcellular localization and expression during murine development. Exp. Cell Res. *312*, 3142–3151.

van der Loo, J.C., Xiao, X., McMillin, D., Hashino, K., Kato, I., and Williams, D.A. (1998). VLA-5 is expressed by mouse and human long-term repopulating hematopoietic cells and mediates adhesion to extracellular matrix protein fibronectin. Journal of Clinical Investigation *102*, 1051–1061.

Wilson, A., and Trumpp, A. (2006). Bone-marrow haematopoietic-stem-cell niches. Nature Reviews Immunology *6*, 93–106.

Wilson, A., Laurenti, E., Oser, G., van der Wath, R.C., Blanco-Bose, W., Jaworski, M., Offner, S., Dunant, C.F., Eshkind, L., Bockamp, E., et al. (2008). Hematopoietic Stem Cells Reversibly Switch from Dormancy to Self-Renewal during Homeostasis and Repair. Cell *135*, 1118–1129.

Wright, D.E., Wagers, A.J., Gulati, A.P., Johnson, F.L., and Weissman, I.L. (2001). Physiological migration of hematopoietic stem and progenitor cells. Science *294*, 1933–1936.

Zou, P., Yoshihara, H., Hosokawa, K., Tai, I., Shinmyozu, K., Tsukahara, F., Maru, Y., Nakayama, K., Nakayama, K.I., and Suda, T. (2011). p57Kip2 and p27Kip1 Cooperate to Maintain Hematopoietic Stem Cell Quiescence through Interactions with Hsc70. Cell Stem Cell *9*, 247–261.

FIGURE LEGENDS

Figure 1: Survival of K3$^{-/-}$ chimeras and distribution of K3$^{-/-}$ HSPCs

(A) Kaplan-Meier survival curve of 1st generation K3$^{+/+}$ and K3$^{-/-}$ FL chimeras (***p<0.0001 by log-rank test), n=41-47 per genotype.

(B) Total number of MNCs from BM (2x femur, 2x tibia, 2x pelvis, 2x humerus) and whole Spl. K3$^{+/+}$ chimeras are compared with healthy and moribund K3$^{-/-}$ chimeras (***p< 0.0001 by Kruskal-Wallis test and Dunn's multiple comparison post-test), n=10-15 per group. Data are mean cell counts ±SD.

(C) Total number of B cells (B220^{+}), T cells (CD3e^{+}), erythroid cells (Erythro; Ter119^{+}), neutrophils (Neutro; Gr-1^{hi}Mac-1^{+}) and monocyets/macrophages (Mono/Macro; Gr-1^{int}Mac-1^{+}) in the BM of K3$^{+/+}$, healthy and moribund K3$^{-/-}$ chimeras. Data are presented as box-and-whisker plots. The horizontal lines inside the boxes represent the median, the box edges show the lower and upper quartiles, and the whiskers indicate the minimum and maximum (*p<0.05, **p<0.01, ***p<0001 by Kruskal–Wallis test and Dunn's multiple comparison post-test). n=10-15 per genotype.

Figure 2: BM homing of K3$^{-/-}$ LSK cells

(A) Short-term homing assay with labeled BM LSK cells from K3$^{+/+}$ and K3$^{-/-}$ chimeras quantified by FACS. Shown are mean percentages of injected cells in BM after 18 h ±SD (**p=0.0046 by unpaired t-test), n=5-6 per genotype.

(B) Quantification of extravasated K3$^{+/+}$ and K3$^{-/-}$ LSK cells in BM by intravital 2-photon microscopy 18 h after transplantation, given as mean value ±SD of the absolute number of transmigrated cells per 1x10^{5} injected LSK cells (*p=0.0159 by Mann-Whitney test), n=4-5 per genotype.

(C) Representative images illustrating transmigration of K3$^{+/+}$ (upper panels) and K3$^{-/-}$ LSK cells (lower panels) up to 6 h after injection in Col2.3-GFP recipients. LSK cells, white (CMTMR); bone, blue (second harmonic signal); blood, red (Q-Tracker 695 nm). Arrowheads indicate LSK cells transmigrating across endothelium (white dashed lines), left colum before and right colum after transmigration. Scale bars are 100 µm.

(D) LSK cells of either genotype were visualized in BM microvessels for up to 6 h after injection. The numbers of adherent LSK cells are shown as percentage (mean ±SD) of all LSK cells visualized. (***p=0.0006 by unpaired t-test), n=5 per genotype.

(E) Firm adherent cells shown in (D) grouped according to their residence time on the BM endothelium shown as frequencies ±SEM of the absolute number of visualized cells

(***p<0.0001 for < 1 min, **p=0.0037 for >1 min, ***p=0.0008 for >10 min, by Fisher´s test).

(F) Representative images of adherent $K3^{+/+}$ (upper panels) and $K3^{-/-}$ (lower panels) LSK cells at indicated time points after transfer (upper right corner). LSK cells, red (CMTMR); bone, blue (second harmonic signal); blood, green (FITC-dextran). Arrows, arrowheads and asterisk indicate different single LSK cells; white dashed line outlines endothelium; Scale bars indicate 100 μm.

(G) Adhesion analysis of sorted $K3^{+/+}$, $K3^{-/-}$ and $K3^{+/+}$ BM LSK cells under shear in microflow chambers and preincubated with an anti-α4 integrin blocking mAb. Microflow chambers were precoated with: rmE-selectin 'E' alone; rmE-selectin and VCAM-1 or rmE-selectin, CXCL12 and VCAM-1. Scale bars represent mean percentage of adherent cells to total LSK cells ±SEM (*p<0.05, **p<0.01 by Kruskal–Wallis test and Dunn's multiple comparison post-test), n≥4 per group.

Figure 3: Kindlin-3 deficient HSCs home to the BM

(A) Frequency of CFU-Cs in sorted $CD45.2^{+}$ BM cells isolated from chimeras 4 months after transplantation (p=0.8857 by Mann-Whitney test). n=4 per genotype. Scale bars show average cell counts ±SD.

(B) LTC-IC assay performed by limiting dilutions of donor derived BM MNCs from $K3^{+/+}$ and $K3^{-/-}$ FL chimeras 4 months after transplantation. The percentage of wells in each experimental group that failed to generate colony-forming units is plotted against the number of test MNCs cells. The frequency of LTC-ICs is shown at the bottom. (p=0.0965 by Person chi-squared test), n= 4 per genotype.

(C) Representative FACS plots of BM cells derived from chimeras 1-13 months after transplantation gated for HSPCs using SLAM markers. The left column shows c-kit and Sca-1 expression on lin^{-} cells. Gating from left to right on LSK cells, LSK $CD150^{+}CD48^{-}$ cells and the $CD34^{-}$ or $CD34^{+}$ subsets of this population, respectively. Numbers above each boxed gate refer to the frequencies in BM (percentages of live leukocytes ±SD), n=24-27 per genotype.

(D) Quantification of (C). LSK $CD150^{-}CD48^{+}$ (*p=0.0121 by unpaired t-test); LSK $CD150^{+}CD48^{+}$ (***p<0.0001 by unpaired t-test); LSK $CD150^{+}CD48^{-}$ (***p<0.0001 by Mann-Whitney test); LSK $CD150^{+}CD48^{-}CD34^{+}$ (***p=0.0003 by unpaired t-test) and LSK $CD150^{+}CD48^{-}CD34^{-}$ (***p<0.0001 by Mann-Whitney test) cells. Mean cell numbers ±SD are given. n=24-27 per genotype.

(E) Representative FACS plots of BM LSK cells from $K3^{+/+}$ and $K3^{-/-}$ chimeras, gated for CD150 against CD48. FACS plots show the distribution of 3 populations, $CD150^{+}CD48^{-}$ cells (upper left gate); $CD150^{-}CD48^{+}$ cells (upper right gate); $CD150^{+}CD48^{-}$ cells (lower gate) 1, 2, 4 and 9-13 months after transplantation. Numbers next to each gate represent mean percentage ±SD of events within the LSK population, n=3-11 per genotype and time point.

(F) Quantification of BM LSK $CD150^{+}CD48^{-}$ cells from $K3^{+/+}$ and $K3^{-/-}$ chimeras. Compared are the $K3^{+/+}$ and $K3^{-/-}$ mean cell counts ±SD 1, 4 and 9-13 months after transplantation (1 month: p=0.4 by Mann-Whitney test; 4 months: ***p<0.0001; by unpaired t-test; 9-13 months: ***p=0.0001 by unpaired t-test). n=3-8 per genotype.

(G) Quantification of BM $CD150^{+}CD48^{-}CD34^{-}$ cells from $K3^{+/+}$ and $K3^{-/-}$ FL chimeras. Compared are the $K3^{+/+}$ and $K3^{-/-}$ mean cell counts ±SD 1, 4 and 9-13 months after transplantation (1 month: p=0.2 by Mann-Whitney test; 4 months: ***p=0.0005 by unpaired t-test; 9-13 months: **p=0.002 by unpaired t-test). n=3-9 per genotype.

Figure 4: $K3^{-/-}$ HSC remain hyperactive and accumulate in the PB

(A-B) Poly(I:C) and 5-FU double treatment of $K3^{+/+}$ and $K3^{-/-}$ chimeras. (A) Diagram of tested drug combinations and timing. (B) Kaplan-Meier survival curves of experimental groups indicated in (A) (***p<0.0001 by log-rank test), n=16-22 per treatment group. Data are combined from 5 independent experiments.

(C) *In vivo* BrdU uptake assay. Mean percentage ±SD of $BrdU^{+}$ cells determined by FACS in LK cells (p=0.4078 by unpaired t-test), LSK cells (***p=0.0009 by unpaired t-test), LSK $CD150^{+}CD48^{-}$ (**p=0.0014 by Mann-Whitney test) and LSK $CD150^{+}CD34^{-}$ (***p=0.0004 by Mann-Whitney test) cells.

(D) Representative FACS plots of a cell cycle analysis of BM LSK cells. Cells were stained with DAPI and intracellular (ic) Ki67 and analyzed by FACS. The different cell cycle phases are indicated in the scheme above.

(E) Quantification of (D). Percentage of $icKi67^{+}$ BM LSK cells (G1 + S + G2/M phase cells), obtained by FACS. Horizontal bars indicate mean values ±SD (**p=0.0022 by paired t-test). n=18 per genotype.

(F) Relative expression of *p21*, *p27* and *p57* mRNA in sorted $CD150^{+}$ LSK cells, analyzed by qPCR. Data are normalized for *gapdh* expression and presented as mean ±SD from individual mice. n=6-7 per genotype (***p=0.0007 by unpaired t-test).

(G-H) LRC-assay. (G) Percentage of $BrdU^{+}$ cells (LRCsBrdU) present in the indicated

populations after 16 days of labeling, obtained by FACS. (H) Mean percentage ±SD of LRCsBrdU in the indicated populations after 45 days of chase phase. Total LSK cells (***p<0.0001); LSK CD150^{-}CD48^{+} (***p<0.0001); LSK CD150^{+}CD48^{+} (***p=0.0006); LSK CD150^{+}CD48^{-} (**p=0.0014); LSK CD150^{+}CD34^{-} (*p=0.0350) LSK cells were analyzed by unpaired t-test, n=7-8 per genotype.

(I) Representative FACS plots showing the expression of c-kit and Sca-1 on lin^{-} cells from Spl and PB. The frequencies of LK (orange box) and LSK cells (green box) are marked above plots (percentages of live leukocytes ±SD). n=24-26 per genotype.

(J) Quantification of LK and LSK cells in Spl and in PB analyzed by FACS. Scale bars show mean cell counts ±SD (***p<0.0001; **p=0.0031 by Mann-Whitney test). n=25-26 per genotype.

(K-N) Multi-lineage engraftment potential of PB cells isolated from K3$^{+/+}$ and K3$^{-/-}$ chimeras. Percentage donor-derived whole leukocytes (CD45^{+}) (K), myeloid cells (Gr-1^{+}, Mac-1^{+}, and Gr-1^{+}Mac-1^{+}) (L), B cells (B220^{+}) (M), or T cells (CD3e^{+}) (N) are shown from PB 5, 8, 12 and 16 weeks after transplantation. Data are plotted for individual recipients n=5 for K3$^{+/+}$ (blue lines) and n=19 for K3$^{-/-}$ (red lines) from 3 independent transplantation experiments. Significant differences in average lineage engraftment 16 weeks post transplantation are indicated (leukocytes: *p=0.0157, myeloid cells: **p=0.0085, B cells: **p=0.0028, T cells: **p=0.0008 by Mann-Whitney test).

(O) Mobilization of LSK cells from K3$^{+/+}$ and K3$^{-/-}$ chimeras to the PB, shown as LSK cells per ml blood after G-CSF or PBS treatment. Significance at day 6 is indicated (K3$^{+/+}$ vs. K3$^{-/-}$ with G-CSF: ***p<0.0001, K3$^{+/+}$ vs. K3$^{-/-}$ with PBS: **p=0.0049 by unpaired t-test). n=3-5 per genotype.

Figure 5: Premature exhaustion of K3$^{-/-}$ HSCs under hematopoietic stress

(A) Analysis of radioprotection by donor K3$^{+/+}$ und K3$^{-/-}$ WBM cells in 3 rounds of serial BM transplantations. Kaplan-Meier survival curve of the 2nd generation, 3rd generation and 4th generation recipients are shown. Results are combined from 9 independent transplantation experiments. n=42-55 recipients per genotype (***p<0.0001 by log-rank test).

(B) Blood cell counts of the 2nd generation recipients transplanted with 1000 BM LSK CD150^{+} cells sorted from K3$^{+/+}$ or K3$^{-/-}$ chimeras with 5x10^{6} host-type whole Spl cells. Percentages of donor-derived whole leukocytes (CD45^{+}), myeloid cells (Gr-1^{+},

Mac-1$^+$, and Gr-1$^+$Mac-1$^+$), B cells (B220$^+$), or T cells (CD3e$^+$) in PB 5 and 11 weeks post transplantation are shown. Scale bars show the mean percent ±SD (***p<0.0001 by Mann-Whitney test). n=23-28 from 4-5 independent experiments.

(C) Percentage of donor-derived HSPCs in BM of 2nd generation recipients after 11 weeks, obtained by FACS. Horizontal bars indicate mean values ±SD (***p<0.0001 by Mann-Whitney test). n=23-28 from 4-5 independent experiments.

(D) Kaplan-Meier survival curve showing response of K3$^{fl/fl}$Rosa26$^{Cre-ERT2}$ (n=10) and control mice to a sequential 5-FU treatment. Mice were treated with 5-FU weekly, and survival was monitored daily. Kindlin-3 gene deletion was induced by administration of tamoxifen (TAM) 3 months after transplantation and 5 weeks before 5-FU treatment. The control group contained K3$^{fl/fl}$Rosa26$^{Cre-ERT2}$ (w/o TAM n=7), wtRosa26$^{Cre-ERT2}$ (with TAM n=6 or w/o TAM n=5) and K3$^{fl/fl}$ (with TAM n=2 or w/o TAM n=2) mice, (***p<0.0001 by log-rank test).

Figure 6: Defects in K3$^{-/-}$ HSCs are cell autonomous

(A) Representative FACS plots of PB from K3$^{+/+}$ and K3$^{-/-}$ mix-chimeras 4 months after transplantation. Upper row shows whole leukocytes gated for CD45.2 against CD45.1. In lower row lin$^-$ cells of CD45.2$^+$ and CD45.1$^+$ populations are gated for c-kit against Sca-1. Gates for LK (right) and LSK cells (left) are shown. Numbers next to the gates represent the overall frequencies (percent of live PB leukocytes) ±SD from events in each gate, n=6-8 per genotype.

(B) G-CSF induced mobilization of BM LSK cells from K3$^{+/+}$ and K3$^{-/-}$ mix-chimeras. MNCs from PB were analyzed by FACS for LSK cells. Histogram shows the mean number of LSK cells per ml PB ±SD. (**p<0.01 and ***p<0.001 by one-way ANOVA followed by Tukey's multiple comparison test).

(C-D) LRC assay in K3$^{+/+}$ and K3$^{-/-}$ mix-chimeras. (C) Percentage of LRCsBrdU in indicated populations after 18 days of labeling determined by FACS. (D) Percentage of LRCsBrdU in indicated populations after 45-50 days of chase phase. Total LSK (**p=0.0073); LSK CD150$^-$CD48$^+$ (*p=0.0309); LSK CD150$^+$CD48$^-$ (**p=0.0017); LSK CD150$^+$CD34$^-$ (ns: p=0.0583) cells by paired t-test. Scale bars show mean percentage ±SD, n= 4 per genotype.

(E) 5-FU treatment (day 0 and 7) of K3$^{+/+}$ and K3$^{-/-}$ mix-chimeras. LSK cells from BM analyzed by FACS for percentage of CD45.1$^+$ and CD45.2$^+$ cells before and 45 days after first 5-FU injection. Histogram shows the mean percentage ±SD (***p<0.0001 by

unpaired t-test). n=9 per genotype in 2 independent experiments.

(F-I) Results of a competitive repopulation assay with BM LSK CD150^{+}CD45.2^{+} cells FACS-sorted from K3$^{+/+}$ and K3$^{-/-}$ mix-chimeras. Each recipient received 450 LSK CD150^{+}CD45.2^{+} cells together with 5x10^{6} host-type whole Spl cells. Percent donor-derived whole leukocytes (CD45^{+}) (F), myeloid cells (Gr-1^{+}, Mac-1^{+}, and Gr-1^{+}Mac-1^{+}) (G), B cells (B220^{+}) (H), or T cells (CD3e^{+}) (I) from PB 4, 8 and 12 weeks post transplantation are shown. Data are plotted for individual recipients K3$^{+/+}$ (blue solid lines) and K3$^{-/-}$ (red lines). Significant differences in average lineage engraftment are indicated (4 weeks post transplantation: leukocytes (ns, p=0.8707) by unpaired t-test; myeloid cells (**p=0.0093), B cells (*p=0.0337), T cells (**p=0.0074) by Mann-Whitney test; 8 and 12 weeks post transplantation: leukocytes: ***p<0.0001 by unpaired t-test; myeloid, B and T cells: ***p<0.0001 (or p=0.0006 for myeloid cells after 8 weeks) by Mann-Whitney test). n=14-17 from 4 independent experiments.

(J) Percentage of donor-derived HSPCs in BM of 2nd generation recipients after 12 weeks obtained by FACS. Horizontal bars indicate mean values ±SD (***p<0.0001 by Mann-Whitney test). n=14-17 from 4 independent experiments.

Figure 7: Kindlin-3 mediated activation of integrins is essential for activated rather than quiescent HSCs

(A-D) Comparisons of the percentage of donor-derived cells in the LK (A), LSK CD150^{-}CD48^{+} (B), LSK CD150^{+}CD48^{-} (C) and LSK CD150^{+}CD48^{-}CD34^{-} (D) populations in the BM from K3$^{+/+}$ and K3$^{-/-}$ fetal liver mix-chimeras 1, 3-4 and 12 months post transplantation. Significances between K3$^{+/+}$ and K$^{-/-}$ mix-chimeras are indicated. Dots show the mean percentage ±SD (***p<0.001; ns, p>0,05 by either unpaired t-test or Mann-Whitney test). n=4-11 per genotype and time point.

(E) Comparisons of the percentage of donor-derived cells in the indicated populations in the BM from K3$^{+/+}$ and K3$^{-/-}$ fetal liver mix-chimeras 3-4 months post transplantation. Histogram shows the mean percentage ±SD. (ns, p<0,05, **p<0.01 and ***p<0.001 by Repeated Measures ANOVA followed by Tukey's multiple comparison test). n=5-11 per genotype.

(F-I) Comparisons of the percentage of donor-derived cells in the LK (F), LSK CD150^{-}CD48^{+} (G), LSK CD150^{+}CD48^{-} (H) and LSK CD150^{+}CD48^{-}CD34^{-} (I) populations in the BM from wt-Rosa26$^{Cre\text{-}ERT2}$ (blue) and K3$^{fl/fl}$Rosa26$^{Cre\text{-}ERT2}$ (red) mix-chimeras untreated (Ctrl.) or after treatments with tamoxifen (TAM PBS) or

tamoxifen and 5-FU (TAM 5-FU). Recipients were treated with tamoxifen 3 months after transplantation and 5 weeks before weekly 5-FU treatment. Histogram shows the mean percentage ±SD. (ns $p>0,05$, $^{**}p<0.01$ and $^{***}p<0.001$ by either unpaired t-test or Mann-Whitney test). n=4-6 per genotype and treatment.

(J) 9EG7 binding on BM LSK $CD150^{-}CD48^{+}$ and LSK $CD150^{+}CD48^{-}$ cells from 100% $K3^{+/+}$ and $K3^{-/-}$ chimeras. Shown is the relative 9EG7 MFI (Geom mean FI). Error bars indicate +SD. ($^{**}p<0.01$ by paired t-test). n=3 per genotype.

(K) Kaplan-Meier survival curve of lethally irradiated recipients transplanted with $1.5x10^{4}$ $K3^{+/+}$ or $K3^{-/-}$ LSK cells transduced with lentiviral expression constructs as indicated together with $8.8x10^{5}$ WBM cells from a $K3^{-/-}$ 100% chimera. n=5 recipients per group.

(L) FACS plots of PB from an LAD-III patient (lower row) and a healthy child with the same age as control (upper row). Shown are MNC gated for CD34 against CD45 (left) and CD38 against CD34 (right).

(M) CFU assay with blood MNC containing 100 $CD34^{+}$ cells (calculated according to the FACS frequencies) from an LAD-III patient and healthy child. Shown are the numbers of colonies per blood MNC containing 100 $CD34^{+}$ cells. Two types of colonies were distinguished. BFU-E (burst forming unit-erythroid); CFU-GM (colony forming unit-granulocyte/macrophage).

Figure

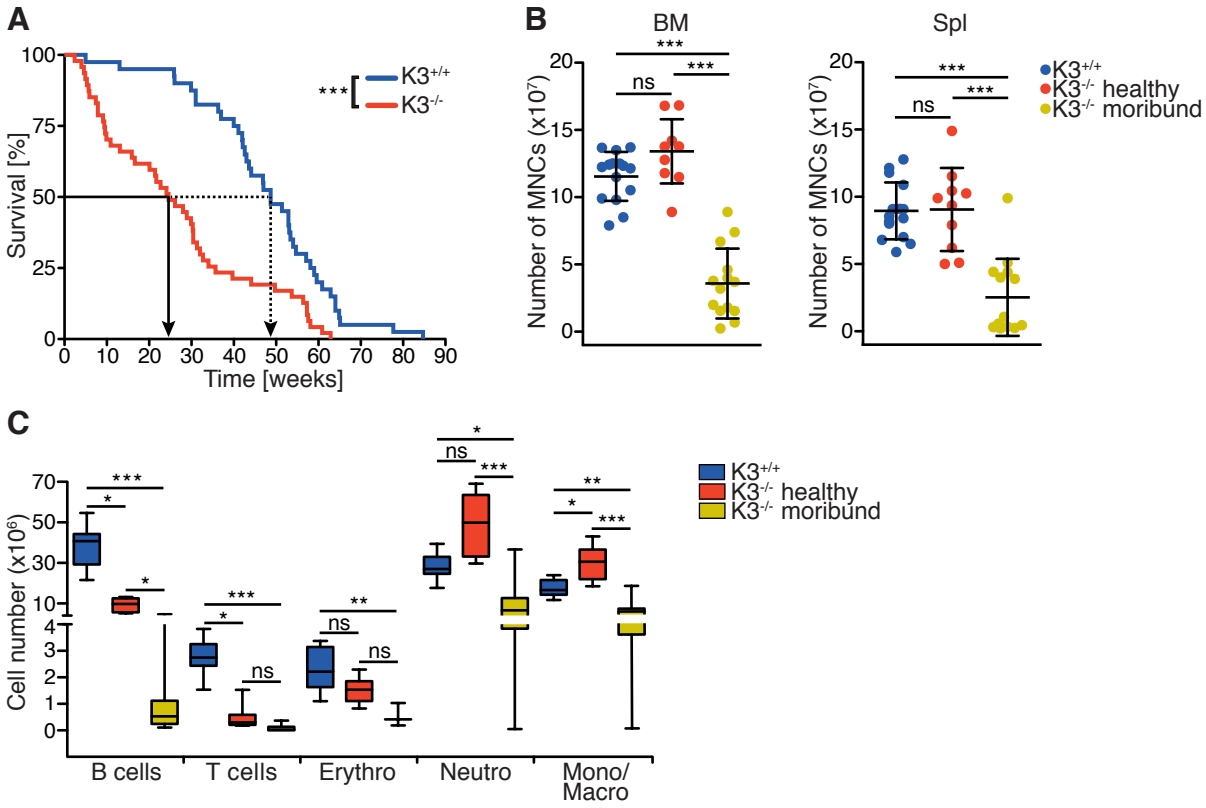

Figure 1
Ruppert et al.

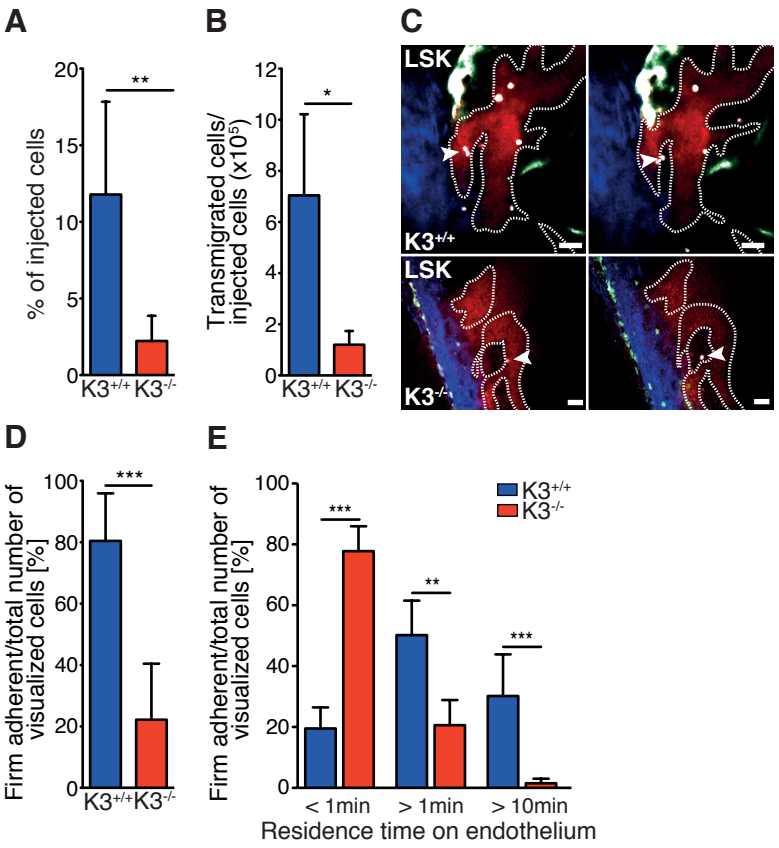

Figure 2
Ruppert et al.

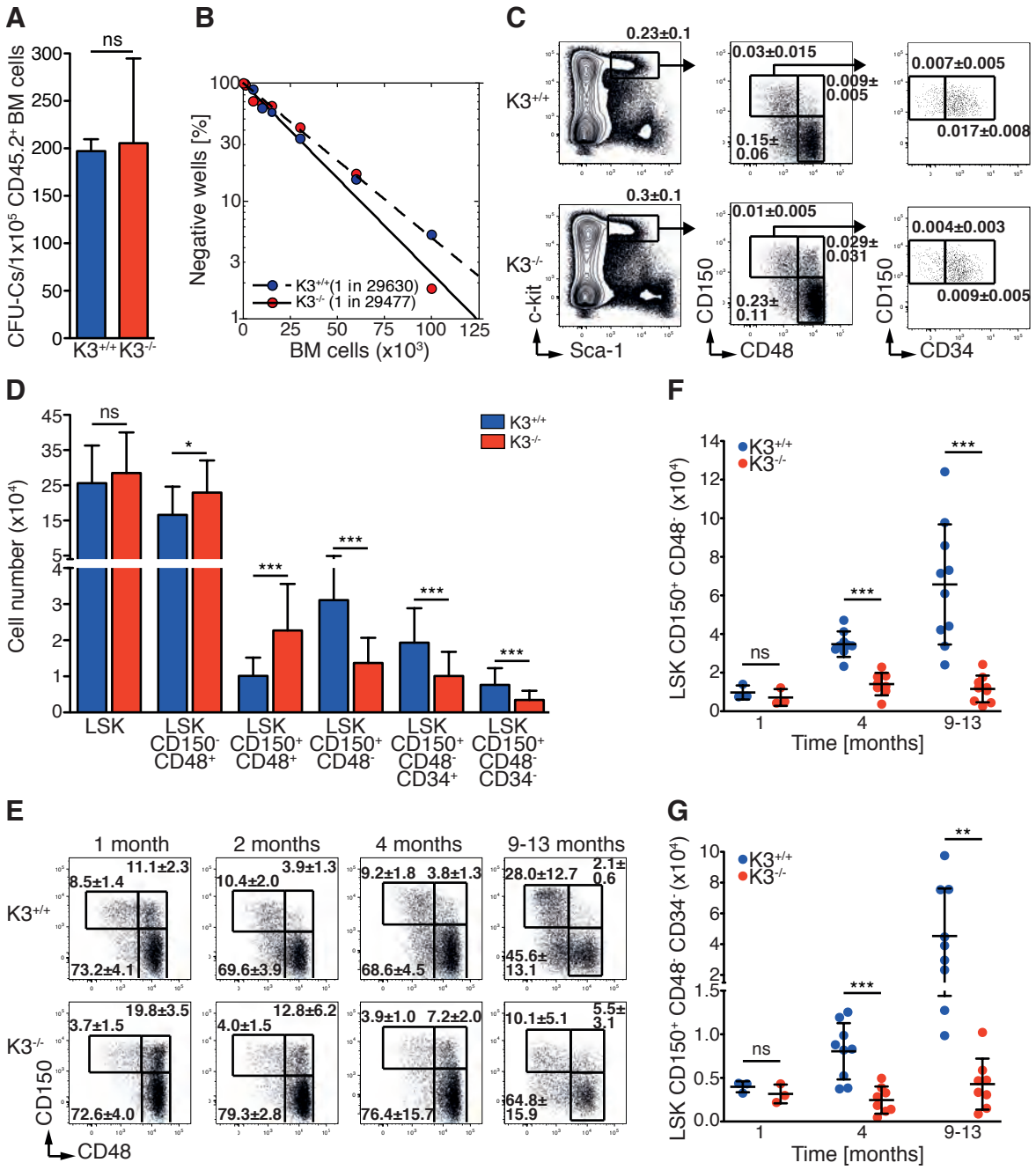

Figure 3
Ruppert et al.

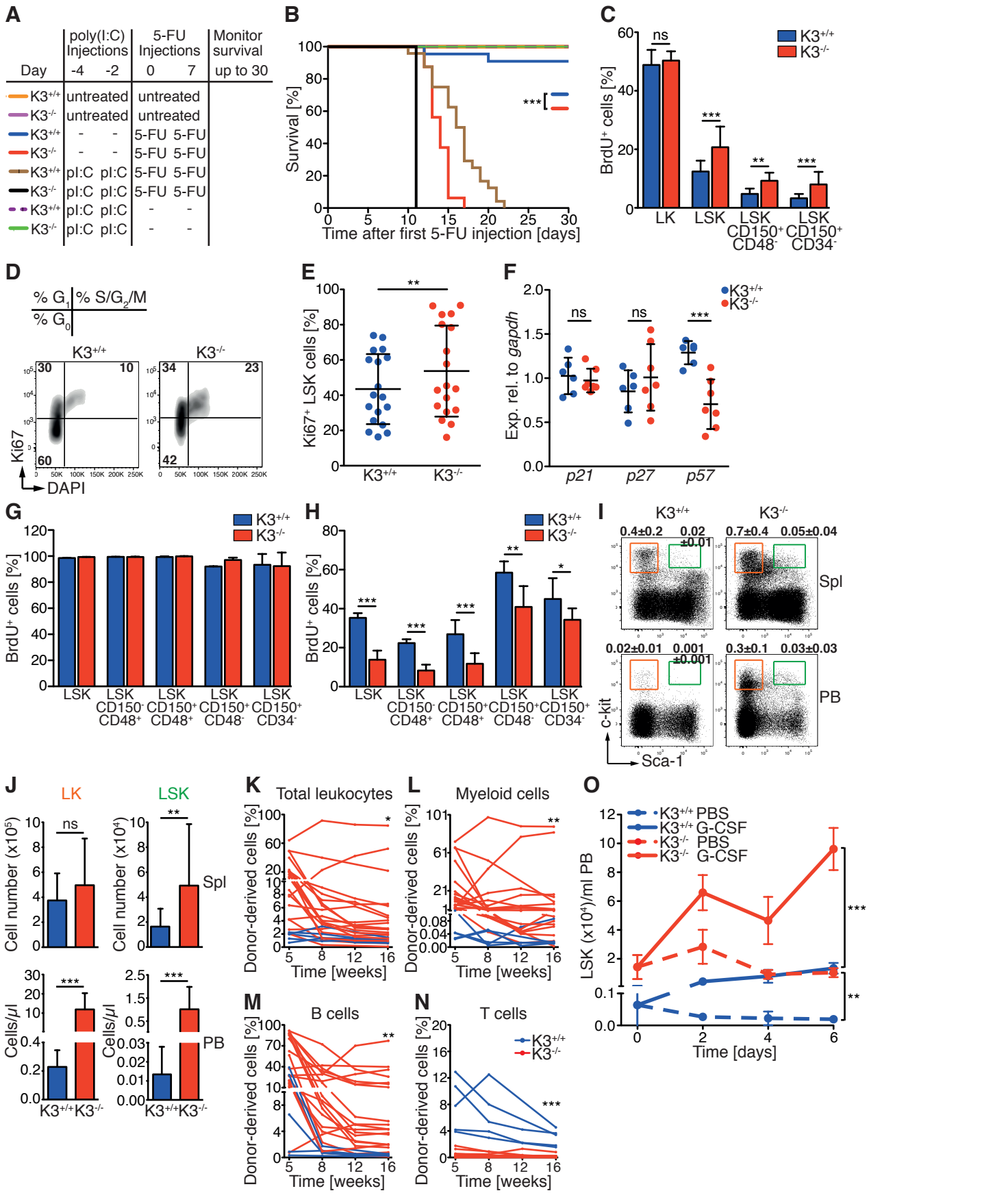

Figure 4
Ruppert et al.

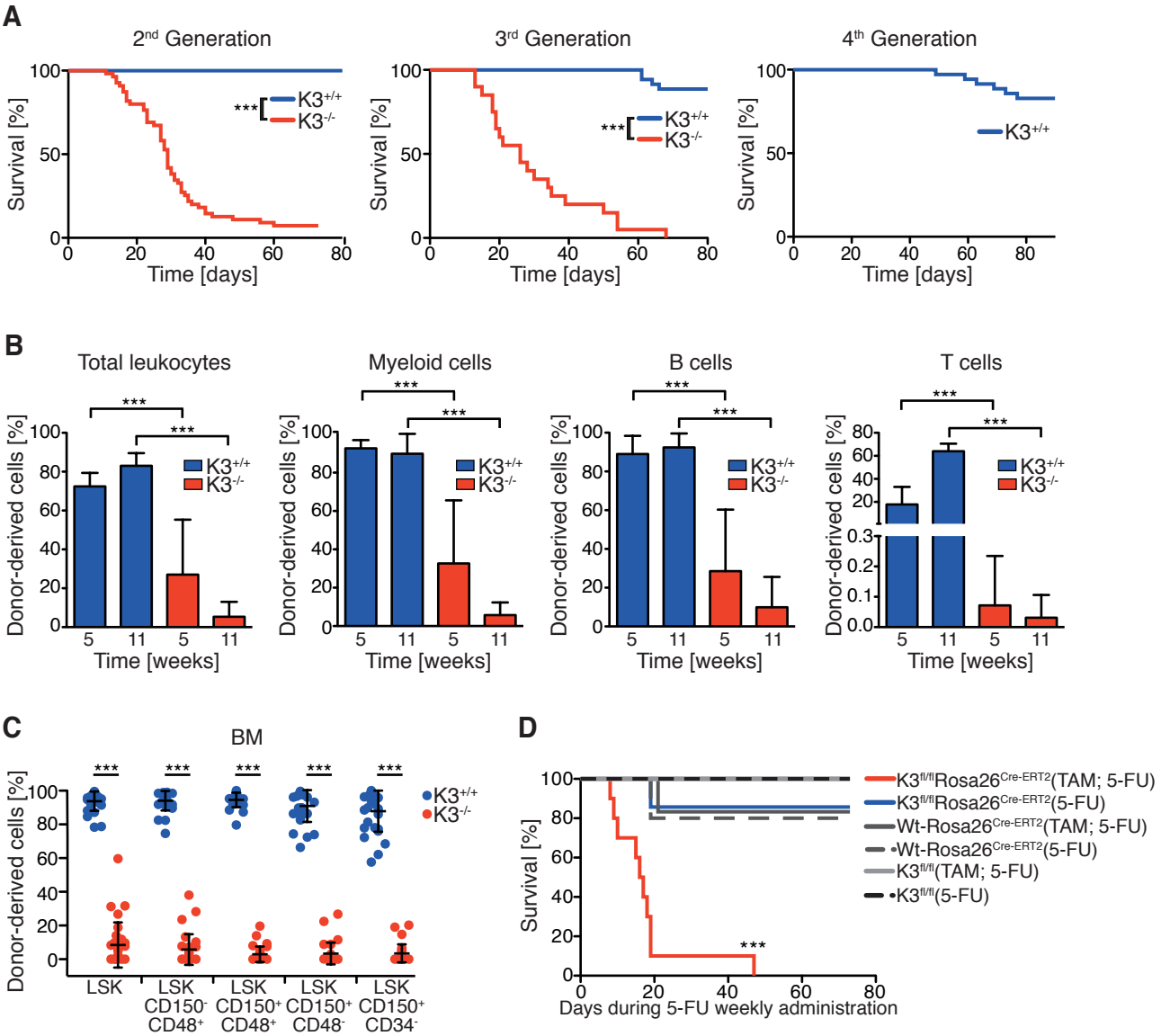

Figure 5
Ruppert et al.

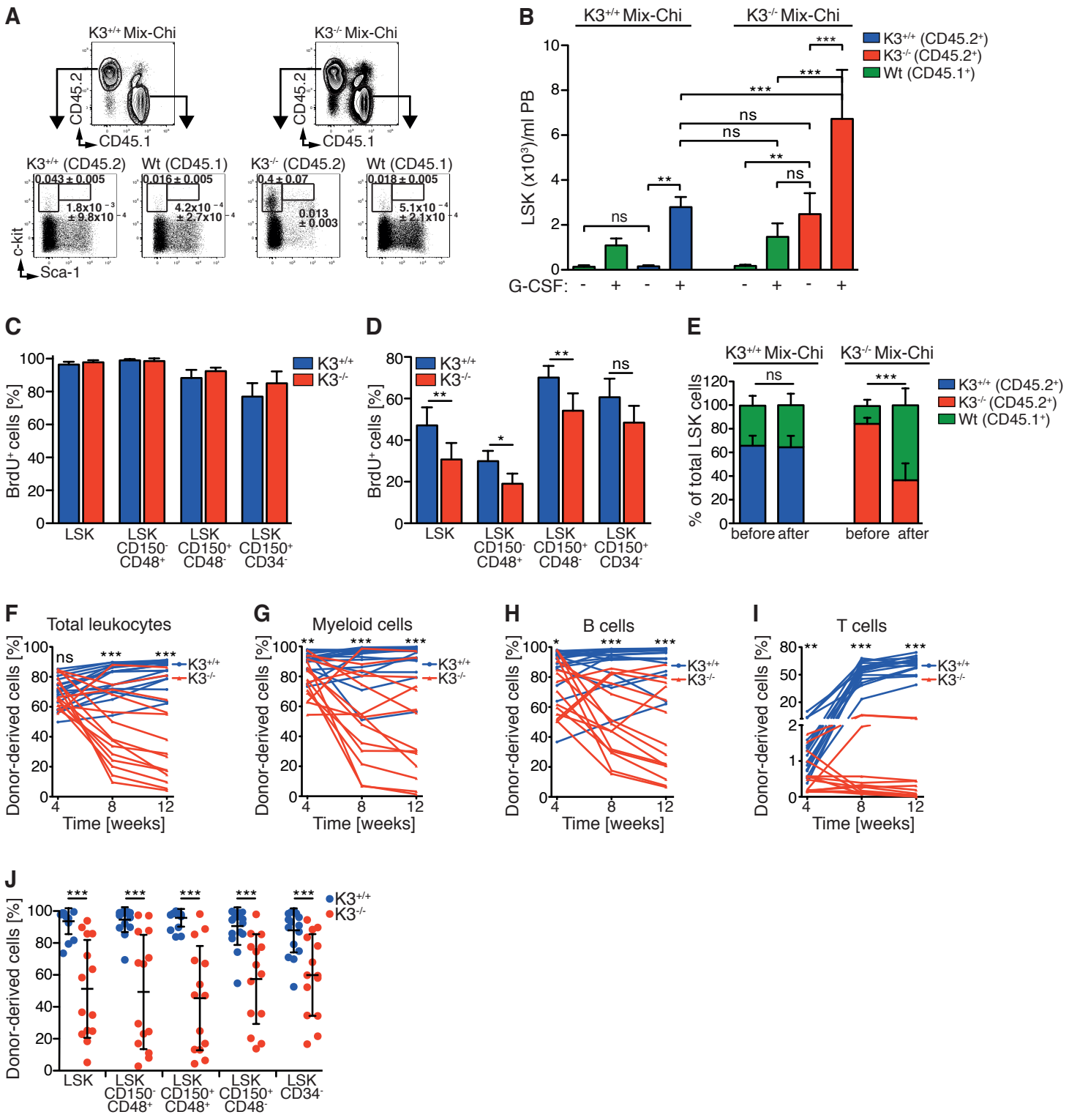

Figure 6
Ruppert et al.

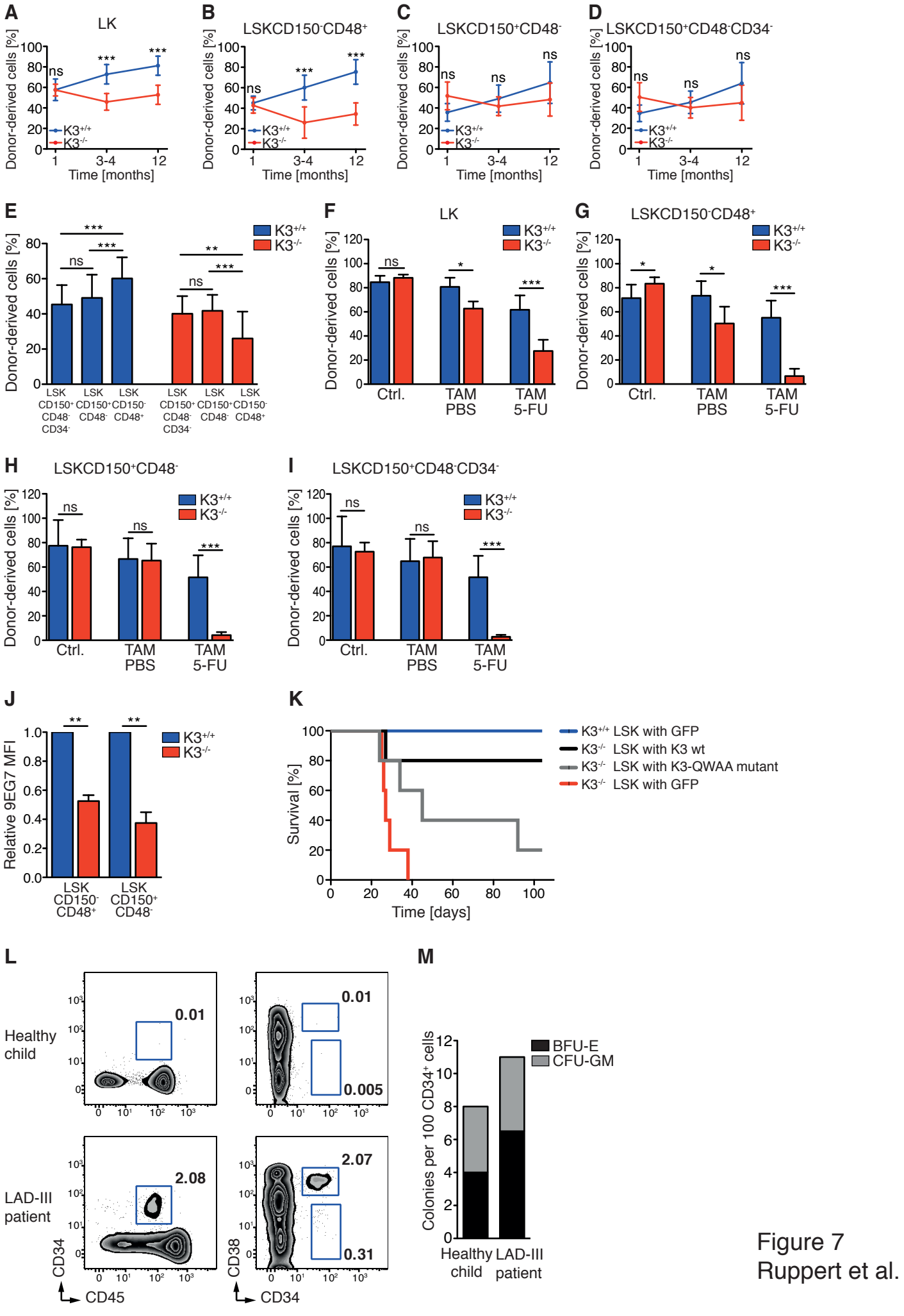

Figure 7
Ruppert et al.

7.4 Paper IV

Integrins synergistically induce the MAL/SRF target gene ISG15 to ISGylate cytoskeletal and focal adhesion proteins necessary for cancer cell invasion

Michaela-Rosemarie Hermann, **Emanuel Rognoni**, Madis Jakobson, Moritz Widmaier, Assa Yeroslaviz, Roy Zent, Guido Posern, Ferdinand Hofstädter and Reinhard Fässler

(Manuscript in preparation)

Supplementary material

PDF file

Supplementary Figures 1-4

Excel files

Supplementary Table 1, ISG15 pull-down mass spectrometry analysis

Supplementary Table 2, List of primer sequences

Supplementary Table 3, List of antibodies

Integrins synergistically induce the MAL/SRF target gene ISG15 to ISGylate cytoskeletal and focal adhesion proteins necessary for cancer cell invasion

Michaela-Rosemarie Hermann[1], Emanuel Rognoni[1], Madis Jakobson[1], Moritz Widmaier[1], Assa Yeroslaviz[2], Roy Zent[3], Guido Posern[4], Ferdinand Hofstädter[5] and Reinhard Fässler[1]

[1]Department of Molecular Medicine and [2]Bioinformatics Group, Max Planck Institute of Biochemistry, 82152 Martinsried, Germany; [3]Division of Nephrology, Department of Medicine, Vanderbilt Medical Center, Nashville, TN, 37232, USA; [4]Institute of Physiological Chemistry, 06114 Halle, Germany; [5]Institute of Pathology, 93053 Regensburg, Germany

Keywords: Integrin, Focal Adhesion, Adhesome, SRF, MAL, ISG15

Corresponding author: Reinhard Fässler (faessler@biochem.mpg.de)

ABSTRACT

Integrin-mediated activation of small GTPases polymerizes g-Actin into different Actin structures. Here we report that the g-Actin pools correlated with low nuclear MAL levels and MAL/SRF activities in αV single, intermediate in β1 single and high in αV,β1 double expressing cells. Integrin-mediated activation of MAL/SRF induced expression of the ubiquitin-like modifier interferon-stimulated gene 15 (ISG15) resulting in the ISGylation of integrins, Actin, Focal Adhesion and Actin binding proteins. The increased stability and/or activity of these proteins enhanced kidney fibroblast but also human breast cancer cell invasion and correlated with poor patient survival. Our findings show that integrin adhesions, MAL/SRF and ISG15 constitute a new autoregulatory feed-forward loop that precisely adjusts actin- and adhesion-based functions required for cell spreading, migration and invasion.

INTRODUCTION

Integrin-mediated cell adhesion and signalling control numerous cellular processes, which are crucial for development, postnatal homeostasis and pathology. Integrin signalling is a multistep process that is initiated with integrin activation and ligand binding, followed by integrin clustering and the progressive assembly of signalling platforms consisting of adaptor, signalling/catalytic and cytoskeletal proteins. The first integrin-induced signalling platforms are small and unstable nascent adhesions (NAs), which eventually mature into large focal adhesions (FAs) that are connected to filamentous (f-) Actin.

Integrin signalling induces both short- and long-term effects. The short-term effects consist of cytoskeletal rearrangements that allow cells to adopt their characteristic shape and initiate migration, and are caused by the activation of Rho family GTPases and actin-binding proteins (Danen et al., 2002). Long-term effects of integrin signalling result from changes in gene expression, which regulate cell proliferation and differentiation. Integrin-dependent regulation of gene expression is primarily thought to arise from cross talk with growth factor receptors (GFR) that increase the activity of mitogen activating protein (MAP) kinase pathways. A recent study, however, reported that β1-class integrins can change gene programs of mesenchymal stem cells involved in lineage commitment to bone, fat or cartilage by activating Rho GTPase signalling cascades, which result in the nuclear localization of the transcriptional co-activators Yes-associated protein (YAP) and transcriptional co-activator with PDZ-binding motif (TAZ) (Tang et al., 2013). In addition to the control of YAP/TAZ, Rho family GTPases can also control gene transcription by releasing the association of the transcriptional co-activator Megakaryocyte Acute Leukemia protein (MAL; also known as MRTF-A or MKL1) from monomeric or

globular (g-) Actin. Once g-Actin is assembled into Actin networks, free MAL translocates into the nucleus, where it associates with and activates the transcription factor Serum Response Factor (SRF), which regulates the expression of cytoskeletal proteins including Actin and Focal Adhesion proteins. Thus it is possible that integrin-mediated activation of Rho GTPases regulates cytoskeletal dynamics but also adhesion through effector proteins and the control of MAL`s nucleo-cytoplasmic shuttling in order to initiate target gene transcription.

To test this hypothesis we investigated whether and which integrins regulate MAL/SRF-mediated gene expression. To achieve this goal, we used recently engineered cell lines that express Fibronectin (FN)-binding integrins of the αV- (αVβ3, αVβ5) and/or β1-class (α5β1) that allowed us to assign stress fibre formation to αV-class integrins and myosin II activation and lamellipodia formation to α5β1 integrin (Schiller et al., 2013). We report that αV- and β1-class integrins synergize to regulate expression of MAL/SRF target genes. One new MAL/SRF target is the ubiquitn-like modifier Interferon-specific gene 15 (ISG15), which becomes covalently attached to specific lysine residues of numerous known MAL/SRF target gene products including Vinculin, Talin and Eplin. ISG15 modifications are known and thought to negatively impact ubiquitination by a) inhibition of ubiquititin-specific E2 enzymes (Malakhova and Zhang, 2008; Okumura et al., 2008; Zou et al., 2005) and b) possible occupation of lysine residues also used by Ubiquitin through ISGylation . Thus it is possible that ISG15-linked proteins could be protected from proteasomal targeting (Liu et al., 2003). Our findings identify a new synergistic activity of fibronectin-binding integrins that controls cell invasion by regulating transcription and subsequent ISGylation.

RESULTS

FN bound α5β1 and αV-class integrins control f-Actin and nuclear MAL levels

We generated immortalized fibroblast cell lines lacking the expression of all integrins (pan-knockouts, pKO) and re-expression of β1 and/or αV integrin cDNAs produced cells expressing αV- (pKO-αV), β1- (pKO-β1) or αV- and β1-class integrins (pKO-αV,β1) ((Schiller et al., 2013) Fig.S1A). When the three cell lines were seeded on FN-coated, circular micropatterns separated by non-adhesive polyethylene glycol, pKO-αV cells expressing the FN-binding αVβ3 and αVβ5 integrins preferentially formed large focal adhesions (FAs) that were shown with labelled phalloidin to be connected by thick radial stress fibres. In contrast, pKO-β1 cells expressing the FN-binding α5β1 integrin preferentially formed small, nascent adhesions (NAs), thin stress fibres and a dense subcortical actin network, and pKO-αV,β1 cells developed both large FAs and small NAs with thick and thin stress fibres and a dense subcortical actin meshwork (Fig.1A, B; Fig.S1A). To visualize non-polymerized Actin in the cytoplasm of the three cell lines, we stained the cells with fluorescently labelled DNaseI (Gabbiani et al., 1984; Heacock and Bamburg, 1983; Hitchcock, 1980). Surprisingly, we observed that also the cytoplasmic g-Actin pool was highest in pKO-αV, intermediate in pKO-β1 and lowest in pKO-αV,β1 cells (Fig.1A, 1C). This finding was further confirmed by separating the cells into soluble (S, validated with GAPDH), nuclear (N) and cytoskeletal (C, validated with Vimentin) fractions and determining their β-Actin contents (Fig.1D). The experiment demonstrated that Actin contents in the soluble (representing g-Actin), cytoskeletal (representing f-Actin) and nuclear fraction as well as the calculated g-/f-Actin ratios were significantly higher in pKO-αV cells compared to pKO-β1 and pKO-αV,β1 cells (Fig.1D-F). The increased Actin contents in all fractions of pKO-αV cells indicated that the total Actin levels are higher in pKO-αV cells compared to pKO-β1 and pKO-αV,β1 cells, which was indeed confirmed by western blotting and immunostaining of cells with anti-β-Actin antibodies (Fig.S1B). To precisely determine the g-Actin levels in cytoplasm and nucleus, we performed precipitation assays with soluble and nuclear fractions using DNaseI coupled to beads and found significantly higher g-Actin contents in the cytoplasm and nucleus of pKO-αV compared to pKO-β1 and pKO-αV,β1 cells (Fig.1G, H). FACS analysis excluded differences in nuclear size in our cell lines as cause for the different actin contents (Fig.S1C).

Next we consulted our published whole cell proteome and phospho-proteome of pKO-αV, pKO-β1 and pKO-αV,β1 cells (Schiller et al., 2013) to evaluate whether a differential expression and activity of Actin sequestering, polymerizing and depolymerizing proteins either further aggravates or compensates for the different amounts of free g-Actin. Our analysis revealed significantly increased levels of Thymosin β4 (Tβ4) and phosphoSer3-Cofilin in pKO-β1 cells (Fig. S1D-F) indicating that g-Actin is significantly more

sequestered and f-Actin significantly less severed in pKO-β1 and pKO-αV,β1 cells compared to pKO-αV cells.

The pool of g-Actin regulates nuclear translocation and activity of the transcriptional transactivator MAL, whose binding to the transcription factor SRF induces the expression of genes encoding "immediate-early", cytoskeletal and focal adhesion proteins. Therefore, the different free g-Actin levels in pKO-αV, pKO-β1 and pKO-αV,β1 cells suggested that their nuclear MAL levels should also be different. To test this hypothesis, we seeded the three cell lines on FN and immunostained them with specific rabbit polyclonal anti-MAL antibodies. The results revealed lowest nuclear MAL levels in pKO-αV, intermediate in pKO-β1 and highest in pKO-αV,β1 cells (Fig.1I, S1G). Importantly, treatment with Jasplankinolide, which diminishes free g-Actin by stabilizing Actin filaments, increased nuclear MAL in the three cell lines (Fig.1I, S1G). Conversely, treatment with Latrunculin A, which increases free g-Actin by disassembling f-Actin, decreased nuclear MAL in the three cell lines (Fig.1I, S1G). Altogether these results show that FN-binding integrin classes differentially regulate cellular g-/f-Actin content, which significantly influences nuclear levels of MAL.

αV- and β1-class integrins cooperate to control SRF/MAL activity

To test functional consequences of the different nuclear MAL contents in the three cell lines, we first measured SRF/MAL activity with SRF luciferase reporter assays. Whereas pKO-αV cells showed low SRF reporter activity, pKO-β1 cells displayed 4-fold higher and pKO-αV,β1 cells ~10 fold higher SRF reporter activities. Importantly, Jasplankinolide treatment increased SRF activities to a similar extent in all three cell lines, while Latrunculin A (which had to be short due to cell lethality) showed as light opposite effect (Fig.2A). Treatment with serum (to induce nuclear translocation of MAL) or Leptomycine B (to inhibit nuclear export of MAL) increased SRF reporter activities in pKO-β1 and pKO-αV,β1 cells to a much higher extent as compared to pKO-αV cells (Fig.S2A, S2B). Expression of a dominant-negative MAL reduced SRF reporter activity to basal levels in the three cell lines (Fig.S2C), while overexpression of a g-Actin binding-deficient MAL (ΔN MAL, lacking the N-terminal G-actin binding motif) and a constitutive active mDia increased SRF/MAL induced luciferase activities to similar extents in the three cells (Fig.2B).

To exclude that cell spreading defects (Connelly et al., 2010) caused the reduced nuclear MAL levels and SRF/MAL reporter activities in pKO-αV cells, we seeded the three cell lines on FN-coated circular micropatterns with 28μm and 40μm diameters, respectively, and performed SRF reporter assays and immunostainings. The results of these experiments revealed that pKO-αV cells displayed similar SRF reporter activities and nuclear MAL levels on small and large FN-coated circular micropatterns, while

pKO-β1 and pKO-αV,β1 cells increased SRF activities and nuclear MAL levels on 40µm sized micropatterns compared to 28µm sized micropatterns (Fig.2C-E) indicating that the reduced cell spreading of pKO-αV cells is not responsible for the reduced MAL/SRF activity.

Next we performed experiments aimed at testing whether changes in the expression levels and/or activities of FN-binding integrin classes affect SRF reporter activity. First, Mn^{2+} treatment, which increases integrin activities, significantly elevated SRF reporter activity in all three cell lines, most prominently in pKO-β1 cells, intermediate in pKO-αV,β1 and lowest in pKO-αV cells (Fig.2F). Second, overexpression of αV- or β1-class integrins revealed that elevation of αV in pKO-αV did not change SRF activity, whereas elevation of β1 in pKO-β1 cells induced a small, significant increase of SRF activity and elevation of β1 in pKO-αV and αV in pKO-β1 cells induced a more prominent increase of SRF activity (Fig.2G). Similarly, overexpression of either αV or β1 in pKO-αV,β1 cells also significantly increased SRF/MAL activity. Third, pKO-αV,β1 cells were seeded on FN (bound by αV- and β1-class integrins), Vitronectin (VN) and Gelatin (both ligands bound by αV-class integrins only), treated with either anti-α5β1 blocking antibodies or the αV-class specific small molecule inhibitor cilengitide and immunostained for MAL and assayed for SRF reporter activity (Fig.2H, 2I). The experiments showed that inhibition of α5β1 or αVβ3 Integrins on FN adherent pKO-αV,β1 cells significantly reduced nuclear MAL levels and SRF activities and hence phenocopied the pKO-αV cells indicating efficient activation of SRF requires the cooperation of both FN-binding integrin classes. Similarly, when pKO-αV,β1 cells were seeded on VN and Gelatin, respectively, they showed low nuclear MAL activity, which was not further decreased with the inhibition of α5β1 integrin. As expected, treatment of VN- or Gelatin-seeded pKO-αV,β1 cells with cilengitide blocked adhesion (Fig.2H). Finally, loss of the integrin activator proteins in FN-adherent fibroblasts double deficient for either Kindlin-1 and -2 or Talin-1 and -2 abolished SRF reporter activities (Fig.S2D). Altogether these results show that FN-binding integrin classes cooperate to activate SRF/MAL.

αV- and β1-class integrins induce transcription of SRF/MAL target genes

The high nuclear MAL content and SRF activity in pKO-αV,β1 cells suggest that MAL/SRF-induced gene transcription is controlled, at least in part, by integrins. To test this hypothesis, we compared published MAL/SRF transcriptomes (Balza and Misra, 2006; Cooper et al., 2007; Descot et al., 2009; Philippar et al., 2004; Selvaraj and Prywes, 2004; Sun et al., 2006; Zhang et al., 2005) with the whole cell proteome of pKO-αV, pKO-β1 and pKO-αV,β1 cells (Schiller et al., 2013) and found a large number of MAL/SRF target genes including SRF and FA proteins such as Filamins, Vinculin, Talin, Eplin and integrins enriched in pKO-β1 and pKO-αV,β1 cells (Table 1). The increased levels of SRF, Talin, Vinculin and Eplin (Lima1) mRNA

and protein in pKO-β1 and pKO-αV,β1 cells were confirmed by qRT-PCR and western blotting (Fig.3A, 3B).

We also noted that ISG15 mRNA, dramatically down-regulated in SRF-deficient ES cells (Philippar et al., 2004), was significantly elevated in pKO-αV,β1, intermediate in pKO-β1 cells and low in pKO-αV cells (Fig.3A; Table 1). Western blotting confirmed high ISG15 levels in pKO-αV,β1, intermediate levels in pKO-β1 and low levels in pKO-αV cells but no secretion of ISG15 (Fig.3C, S3F). Similar results were obtained with immunostainings, which revealed ISG15 co-localisation with f-Actin fibres and the Actin cortex beneath membrane protrusions (Fig.3D) and with Paxillin in FAs of unroofed cells (Fig.3E). ISG15 is an ubiquitin-like modifier, whose expression is induced by type I (α and β) interferons (Farrell et al., 1979; Haas et al., 1987). ELISA and qRT-PCR excluded endogenous interferon α and β expression in pKO-αV,β1 cells as cause for the high ISG15 levels. Importantly, however, poly I:C treatment, which triggers endogenous interferon α and β expression, induced a strong ISG15 expression (Fig.S3A-E). To directly show that ISG15 and the FA protein Talin are new SRF/MAL target genes, we performed SRF and MAL chromatin-immunoprecipitation (CHIP) assays. SRF CHIPseq experiments performed in murine HL-1 cells (http://deepbase.sysu.edu.cn/index.php) identified potential SRF consensus binding sites (CArG box), which allowed designing primers to PCR amply the immunoprecipitaed DNA fragments (Fig.3F). The *vinculin* gene, as a known MAL/SRF target, and the *gapdh* gene not regulated by MAL/SRF were used as controls (Vartiainen et al., 2007) (Fig.3G, 3H). Immunoprecipitations of chromatin using either MAL or SRF antibodies resulted in a positive CHIP. In contrast, neither precipitation control rabbit IgG nor the *gapdh* gene resulted in a positive signal (Fig.3G, 3H).

ISG15 is an ubiquitin-like modifier, which might compete with Ubiquitin at specific lysine residues and hence stabilize target proteins, modify the Ubiquitin E2 enzyme Ubc13 and Nedd4 leading to its inhibition, and alter the function of proteins by inducing or preventing the recruitment of binding partners (Jeon et al., 2009; Malakhova and Zhang, 2008; Takeuchi et al., 2005; Zou et al., 2005). Since protein levels of Talin and Eplin are higher in pKO-αV,β1 cells than predicted from their mRNA levels (Fig. 3A, 3B), we hypothesized that they might be modified with ISG15 and protected from degradation. To test this hypothesis we precipitated ISGylated proteins in pKO-αV,β1 cells with an ISG15-specific antibody and subsequently analysed them by mass spectrometry (Table S1). This analysis revealed a large number of focal adhesion and cytoskeletal proteins including Talin and Vinculin. These findings indicate that αV-class and α5β1 integrin-mediated SRF/MAL activation triggers the expression of SRF/MAL targets that include cytoskeletal proteins, integrins, focal adhesion proteins and ISG15, which modifies SRF/MAL targets to stabilize them and/or change their activity.

αV- and β1-class integrin induced SRF/MAL activity and ISG15 levels to promote cell invasion

MAL/SRF and ISG15 promote tumour cell invasion and are up-regulated in cancer (Desai et al., 2012; Kressner et al., 2013). To test whether the invasive properties of MAL and ISG15 are associated and triggered by β1 integrin-mediated adhesion we analysed integrin, nuclear MAL and ISG15 levels of the non-invasive MCF-7 and invasive MDA-MB-231 breast cancer cell lines. FACS analysis revealed significantly higher α5 and β1 levels and higher Integrin β1 activity (by probing 9EG7 antibody) on MDA-MB-231 cells compared to MCF-7 cells (Fig.4A). The levels of αV integrin were significantly elevated in MCF-7 cells compared to MDA-MB-231 cells (Fig.4A). To test whether the high β1 integrin levels and activity are associated with high nuclear MAL activity in MDA-MB-231 cells we immunostained for f-Actin and MAL, and investigated MAL/SRF activities. We observed that MCF7 cells formed tight cell-cell contacts with f-Actin accumulating at these sites and contained MAL in the cytoplasm and nucleus. In contrast, MDA-MB-231 were not adhering to each other, contained numerous stress fibres and almost the entire pool of MAL protein in the nucleus (Fig.4B, 4C). In line with high nuclear MAL levels, MDA-MB-231 cells also displayed significantly higher SRF/MAL reporter activity (Fig.4D) expressed significantly higher levels of SRF/MAL target gene transcript levels (Fig.4E). The high levels of ISG15 resulted in an elevated ISGylation of target proteins in MDA-MB-231 compared to MCF-7 cells (Fig.4F).

The invasive properties of MDA-MB-231 cells depend on the expression of MAL (Hu et al., 2011; Medjkane et al., 2009). To test whether ISG15 is required for SRF/MAL-induced cell invasion, we depleted ISG15 or overexpressed the de-ISGylase UBP43 in MCF-7 and MDA-MB-231 cells and performed invasion assays with a basement membrane model (Fig.4G, H). While MCF-7 cells were unable to invade through the basement membrane model, MDA-MB-231 cells efficiently moved through the membrane. siRNA-mediated depletion of ISG15 or overexpression of the de-ISGylase UBP43 almost completely prevented the invasion of MDA-MB-231 cells (Fig.4G, H).

Next we tested whether high β1 integrin and ISG15 levels are prognostic markers for breast cancer patients. To this end, we consulted microarray data of breast cancer samples and correlated αV, β1 integrins and ISG15 transcript levels with patient survival. The analyses revealed that patients with high expression of αV, β1 integrin or ISG15 displayed a significant increase in the hazardous ratio (HR) and p-value compared to patients with low levels of either transcript (Fig.5A, 5B). Interestingly, patients with high levels of αV, β1 integrin and ISG15 transcripts in their cancer specimen show a significantly reduced survival rate compared to patients with low ISG15 levels (Fig.5C). To corroborate these *in silico* findings, we performed MAL and β1 integrin immunostainings of human breast cancer samples classified according to the Bloom-Richardson scale and modified by Elston and Ellis (1991) as grade 1 (G1), grade 2

(G2), and grade 3 (G3). Hereby the grading system involves a semi-quantitative evaluation of three morphological features a) the percentage of tubule formation, b) the degree of nuclear pleomorphism and c) an accurate mitotic count using a defined field area. By the usage of a numerical scoring system, the overall grade is derived from a summation of individual scores for the three grades (Elston and Ellis, 1991). (Fig.5D, 5E). Importantly to note, these patient biopsies also include normal healthy tissue next to pathologic malformations. In line with our findings, the overall expression of β1 integrin and nuclear MAL levels increased concomitantly from G1 to G2 and to G3 stage (Fig.5D, 5E, S5). Altogether our data show that integrin-mediated MAL/SRF/ISG15 signaling is elevated in cancer cell invasion *in vitro* and *in vivo.*

DISCUSSION

Tumour metastasis is initiated with the detachment of an individual tumour cell from a tumour cell aggregate followed by invasion into the surrounding tissue, entry into the circulation and finally settlement in a distant organ. The process of tumour cell invasion is critically dependent on the selection of tumour cells that are able to survive without tumour stroma, on the release of proteases that degrade and remodel the tumour- and tissue-derived ECM, and on cell adhesion molecules such as integrins (Hood and Cheresh, 2002). Integrins constitute the core components of the invasive machinery of tumour cells. They regulate the activity of small GTPases, Actin binding, bundling and modifying proteins to allow for cytoskeletal dynamics, membrane protrusions and invadopodia formation (Bishop and Hall, 2000; Hall, 2012; Hoshino et al., 2013; Murphy and Courtneidge, 2011). Since tumour cells express different types of integrins, it is unclear whether, and if yes, how they co-operate to achieve maximal efficiency in tissue invasion. The task of the present study was to define the integrin subfamily and the signalling pathways involved in tumour cell invasion.

We have recently engineered a fibroblast-like cell line that allows expressing the FN-binding integrin αVβ3 and/or α5β1. These cell lines were used to demonstrate that αVβ3 and α5β1 integrins control actomyosin-based cell contractility in a cooperative manner. In the present study we also observed that cells expressing αVβ3 and α5β1 integrins (pKO-αV,β1 cells) most pronouncedly decrease their g-Actin pool, which results in the nuclear translocation of the g-Actin binding transcriptional transactivator MAL (also referred as MRTF-A). The consequences of the nuclear accumulation of MAL include binding to the transcription factor SRF and the transcription of MAL/SRF target genes, which comprise known genes such as Actin, Vinculin, Filamin, etc, as well as novel genes such as Talin, EPLIN and ISG15, which all contain functional CArG boxes that bind SRF and are required for responding to the active MAL/SRF complex.

Our findings show that ISG15 is particularly highly elevated when αVβ3 and α5β1 bind FN. ISG15 is a ubiquitin like modifier protein and thought to be induced exquisitely by type I interferons (Farrell et al., 1979; Haas et al., 1987). ISG15 is highly expressed in all tumours investigated so far (www.oncomine.org). Since the tumour stroma is infiltrated by immune cells it is believed that they are the source of interferon α/β production and hence the trigger for the high expression of ISG15 in cancer cells (van der Veen and Ploegh, 2012). While immune cell-derived interferon α/β strongly promotes expression of ISG15 in tumours it is unknown why ISG15 remains upregulated in tumour cells isolated and cultured *ex vivo* in the absence of immune cells and interferon α/β (Han et al., 2002; Hermeking et

al., 1997; Lock et al., 2002). Based on our findings we propose that αVβ3/α5β1-induced nuclear translocation of MAL and activation of SRF are responsible for the high ISG15 transcription *ex vivo*.

ISG15 is conjugated to proteins (ISGylation) in a multistep process that requires E1, E2 and E3 enzymes comparable to the protein-ubiquitination pathway (Haas et al., 1987; Lenschow et al., 2005; Loeb and Haas, 1992; Morales and Lenschow, 2013; Okumura et al., 2008; Yuan and Krug, 2001). Furthermore, a protease called Ubp43 removes ISG15 resulting in deISGylation of proteins (Malakhov et al., 2002). Protein ISG15lyation can alter protein function. Rac1 and MAPK, for example, dissociate from ISG15-modified Filamin-B. This dissociation can terminate JNK signalling and inhibit apoptosis (Jeon et al., 2009). It has also been shown that ISG15 modification can stabilize proteins either by ISGylation and inhibition of ubiquititn-specific E2 enzymes (Desai et al., 2006; Malakhova and Zhang, 2008; Okumura et al., 2008) or by competing with free ubiquitin for lysine residues on target proteins (Liu et al., 2003). Finally, ISGylation was shown to inhibit protein translation by either increasing the cap structure-binding activity of the ISGylated translational suppressor 4EHP (Okumura et al., 2007) or by down-regulating eIF2α through ISGylation of dsRNA-dependent protein kinase (PKR) (Okumura et al., 2013).

The expression of ISG15 is high in tumour cells *in vivo* and *ex vivo* indicating that ISG15 modification represents a tumour promoting and oncogenic function in primary tumours where interferon α/β levels are high as well as during and after invasion when interferon levels decrease. Hence, it is conceivable that αVβ3/α5β1 signalling kicks in to compensate low interferon levels and to sustain high ISG15 expression. Our mass-spectrometry analysis of ISG15 modified protein (ISGylome) in pKO-αV,β1 cells revealed that numerous proteins including integrins, FA proteins (Talin, Vinculin, EPLIN, etc.) and Actin become ISGylated upon FN binding. We therefore, propose that αVβ3/α5β1 integrin-mediated signalling has two major consequences for tumour cell invasion; αVβ3/α5β1 integrins activate GTPases leading to polymerization of f-Actin networks and stress fibers, which are essential for membrane protrusions, cell contractility and adhesion reinforcement. In addition, the consumption of g-Actin for the f-Actin network formation results in liberation and nuclear translocation of MAL, binding to SRF and transcription of cytoskeletal, FA proteins and ISG15. ISG15 modifies integrins, FA proteins and Actin to increase their stability and/or improve their function (Fig. 6). This novel feed forward loop operates in fibroblasts as well as in invading cancer cells. The highly metastatic breast cancer cell line MDA-MB-231 expressed significantly more α5β1, contained higher levels of nuclear MAL and ISG15 modified proteins, and performed significantly better in invasion assays than the non-metastatic MCF7 cell line. Most importantly, transcriptome analyses of breast cancer samples from large cohorts of patients revealed a

statistically highly significant association between patient survival and high β1 integrin, MAL and ISG15 levels. These findings indicate that the selection of tumour cells for high integrin levels in a tumour aggregate renders them independent of decreasing interferon and growth factor levels. This independence is facilitated with an increased strength of integrin signalling, which has the principal task in a metastasizing tumour cells to establish and maintain an efficient invasive machinery that compensates essential cues from the tumour stroma and eventually allows a long and harshly journey to distant and extraneous organ to succeed.

EXPERIMENTAL PROCEDURES

Isolation, immortalization, viral reconstitution and transfection of cell lines

Mouse pKO fibroblasts and reconstituted pKO-αV, pKO- β1 and pKO-αV,β1 cell lines were generated from fibroblasts (floxed parental) derived from the kidney of 21-day-old male mice carrying floxed αV and β1 alleles (αV flox/flox, β1flox/flox), and constitutive β2 and β7 null alleles (β2−/−, β7−/−). Individual kidney fibroblast clones were immortalized by retroviral delivery of the SV40 large T. The immortalized floxed fibroblast clones were then retrovirally transduced with mouse αV and/or β1 integrin cDNAs and the endogenous floxed β1 and αV integrin loci were simultaneously deleted by adenoviral transduction of the Cre recombinase. Reconstituted cell lines were FACS sorted to obtain cell populations with comparable integrin surface levels to the parental cell clones(Schiller et al., 2013) or to have high or low integrin expression levels. Fibroblasts homozygous for floxed kindlin-1 and -2 or talin-1 or -2 genes were isolated from kidneys of 21-day-old double-floxed mice (whose generation will be described elsewhere), immortalized as described above and cloned. To obtain Kindlin-1 and -2 double-null or Talin-1 and -2 double-null cells, the floxed kindlin alleles were removed by adenoviral Cre transduction. The breast cancer cell lines MDA-MB-231 and MCF-7 were purchased from ATCC (http://www.lgcstandards-atcc.org/Products/Cells_and_Microorganisms/Cell_Lines.aspx?geo_country=de).

Patient samples/biopsies

For histological and immunostaining analysis, staged human breast cancer samples were kindly provided by Prof. Ferdinand Hofstädter, Institute of Pathology, 93053 Regensburg, Germany.

Immunostainings and surface coating

For immunofluorescence microscopy, cells were seeded on micropatterns or coated glass surfaces (Coating: 5 µg/ml Fibronectin (Calbiochem) or 1% Gelatin (Sigma) or 1% Collagen (Advanced BioMatrix) or 10 µg/ml Laminin (Roche) or 10 µg/ml Vitronectin (STEMCELL technologies) in PBS or 0.01% Poly-L-lysine (Sigma)) in DMEM (GIBCO by Life Technologies) containing 10 % FCS at 37 °C, 5% CO_2. For micropatterns the cell culture medium contained 0.5% FCS. After indicated time points the medium was soaked off, and cells were fixed with 3% PFA in PBS for 10 min at room temperature, washed with PBS, blocked with 1% BSA in PBS for 1 h at room temperature and then incubated with antibodies in a solution of 0.1% Triton X-100, 3% BSA in PBS. The fluorescent images were collected with a laser scanning confocal microscope (Leica SP5). For visualization g- and f-Actin structures, we followed a

protocol published earlier (Small et al., 1999). H&E staining was performed according to standard procedures.

Antibodies

All antibodies are listed in Supplementary Information Table S3.

Crosslinking

Enrichment for focal-adhesion-associated proteins was achieved by shortly fixing the ventral cell cortex using DSP crosslinker (DTSP; Dithiobis[succinimidyl propionate]), followed by removal of non-crosslinked proteins and big organelles by stringent cell lysis and hydrodynamic sheer flow washing.

Cell fractionation

For cell fractionation a kit (ProteoExtract® Cytoskeleton Enrichment and Isolation Kit purchased from Millipore) was used according to the manufacturer´s instructions or a centrifugation-based method. For the centrifugation-based method to isolate the nuclei, cells were washed with PBS and harvest in a buffer containing 250 mM Sucrose, 10 mM HEPES and 1.5 mM EDTA. With the help of a syringe and a 26Ga needle (Terumo) cells were opened further. After centrifugation the pellet (nuclei fraction) was washed 5 times with a buffer containing 20 mM Tris, 0.1 mM EDTA and 2 mM $MgCl_2$. The pellet was resuspended in FACS buffer or staining solution for immunostaining.

G-Actin-DNaseI pulldown

DNaseI (Sigma-Aldrich) was covalently linked to CNBr-activated Sepharose beads (Sigma-Aldrich) at a concentration of 1 mg/ml according to the manufacturer´s protocol. BSA-Sepharose beads, which served as control, were prepared in the same way. For g-Actin pulldown 15µg protein lysate in RIPA buffer was incubated with 35µl of DNaseI- or BSA-coupled Sepharose beads in a volume of 300 µl over night at 4°C in an end-over-end-mixer. Next day, the beads were washed five times with cold wash buffer (1% NP-40, 0.1 % SDS, 1mM DTT, 1mM PMSF in PBS). Beads were dried with a syringe and needle and SDS-sample buffer was added for subsequent western blot analysis.

Constructs and transfections

Constitutive active MAL (ΔNMAL), dominant negative MAL (DN MAL: ΔN1B1 and ΔNΔC), SRF:MAL reporter constructs were provided by Prof. Guido Posern, Institute of Physiological Chemistry, 06114

Halle, Germany. Constitutive active myc-mDia1 construct (myc-mDia1 FH1FH2) expression construct was amplified from an existing plasmid with forward primer 5'-gcc aag aat gaa atg gct tc-3' and reverse 5'-tgc aga gct tct aga aga ct and the PCR product was cloned into the pCRII-TOPO vector and sequenced. The integrin αV-mCherry and integrin β1-mCherry were provided by Ralph Böttcher. The knockdown constructs for stable knockdown of murine ISG15 were purchased from Origene and the UBP43 overexpression construct was purchased from Addgene. All transfections were carried out with Lipofectamine 2000 (Invitrogen through Life Technologies) according to the manufacturer's instructions.

SRF/MAL reporter assay

Cells were plated on FN coated 12-well plates (6.0 x 105 cells per well) before transient transfection with 0.5 µg of MAL/SRF reporter (p3DA.luc) reporter (Sotiropoulos et al., 1999), indicated expression plasmid and 25 ng thymidine kinase-driven renilla (Promega) for controlling transfection efficiency. The total amount of transfected plasmid DNA was kept constant at 1.5 µg per well by using pEGFP-C1 expression vector (Clontech). After 24h luciferase activity was analyzed with a Dual Luciferase reporter assay system (Promega). Jasplankinolide (100 nM, #420107-50UG from Merck Millipore) and Latrunculin A (500 nM, L5163 from Sigma) treatment was performed 3h prior to reporter read-out.

Micropatterning

Micropatterns were generated on PEG-coated glass coverslips with deep-ultraviolet lithography(Azioune et al., 2010). Glass coverslips were incubated in a 1 mM solution of a linear PEG, CH3–(O–CH2–CH2)43–NH–CO–NH–CH2–CH2–CH2–Si(OEt)3 in dry toluene for 20 h at 80 °C under a nitrogen atmosphere. The substrates were removed, rinsed intensively with ethyl acetate, methanol and water, and dried with nitrogen. A pegylated glass coverslip and a chromium-coated quartz photomask (ML&C, Jena) were immobilized with vacuum onto a mask holder, which was immediately exposed to deep ultraviolet light using a low-pressure mercury lamp (NIQ 60/35 XL longlife lamp, quartz tube, 60 W from Heraeus Noblelight) at 5 cm distance for 7 min. The patterned substrates were subsequently incubated overnight with 100 µl of fibronectin (20 µg ml−1 in PBS) at 4 °C and washed once with PBS.

FACS analysis

For FACS analysis s suspension of fibroblasts was incubated for 1 h with primary antibodies on ice and then washed twice with FACS-PBS (3 mM EDTA, 2% FCS in PBS). Cell viability was assessed by propidium iodide staining. FACS analysis was carried out using a FACSCalibur Cytometer (BD Biosciences) and cell

sorting with an AriaFACSII high-speed sorter (BD Biosciences), both equipped with FACS DiVa software (BD Biosciences). Purity of sorted cells was determined by post sort FACS analysis and typically exceeded 95%. Data analysis was conducted using the FlowJo program (Version 9.4.10).

Real-time PCR

Total RNA from cells was extracted with RNeasy Mini extraction kit (Qiagen) following manufacturer's instructions. cDNA was prepared with a iScript cDNA Synthesis Kit (Biorad). Real Time PCR was performed with an iCycler (Biorad). Each sample was measured in triplicates and values were normalized to *gapdh.* PCR primers are listed in Supplementary Information Table S2.

Mass spectrometry

The mass spectrometry was performed and analyzed as previously described (Schiller et al., 2013). For the investigation of ISG15 target proteins, a Flag-murineISG15 construct was used for overexpression followed by a FLAG pulldown by using ANTI-FLAG® M2 Affinity Gel according to manufacturer´s instructions (Sigma, product #A2220), SDS PAGE gel electrophoresis and subsequent treatment for mass spectrometry analysis.

Interferon ELISA

Cells were plated on FN-coated tissue culture dishes for three days and the cells` supernatant was analyzed. To induce interferon production cells were transfected with 100 µg/ml Poly(I:C). ELISA for interferon α and interferon β secretion was performed with the VeriKine™ Mouse IFN-α and Mouse IFN-β ELISA kit (PBL Interferon Source, product #42120 and #42400) according to manufacturer´s instructions.

Invasion assay

Invasion assay was purchased (Merck Millipore's QCM™ Boyden chamber, 8 µm pore size) and performed according to manufacturer´s instructions 24 hours post-transfection with either shScr control, shISG15 or UBP43 constructs.

CHIP

For each immunoprecipitation, pKO-αV,β1 cells were used. Cross-linking, nuclei preparation and nuclease digestion of chromatin was performed according to manufacturer`s advice (SimpleCHIP

Enzymatic Chromatin IP Kit (Magnetic Beads, #9003, Cell Signaling Technology). Then, 500 ml of chromatin was incubated overnight at 4°C with 1 to 50 dilution of anti-SRF (#5147; Cell Signaling Technology) or 30 µl home-made anti-MAL rabbit serum (#79). After washing of the Immunoprecipitated chromatin, the DNA– protein complexes were eluted with supplied CHIP elution buffer. Crosslinks were reversed overnight at 65°C, and DNA purified via columns also provided in the kit. Quantification was done by quantitative real-time PCR and is shown as the percentage of input chromatin. Gene-specific primers for amplification of immunoprecipitated DNA are listed in supplementary material Table S3. Primers for *Gapdh* and *Srf* were published previously (Vartiainen et al., 2007).

RNA interference

Cells were infected with retroviral 29mer shISG15 expression constructs purchased from Origene (#TG502956). The pGFP-V-RS plasmid vector was created with an integrated turboGFP element to readily verify transfection efficiency and with a puromycine selection cassette to select for cells carrying integrations.

Kaplan Meier analysis of gene expression microarray

To analyze the prognostic value of integrin αV, integrin β1 and ISG15 gene the Kaplan-Meier plotter was used (http://kmplot.com/analysis/). The patient samples were split into two groups according to various quantile expressions of the proposed biomarker (low and high expression). The two patient cohorts were compared by a Kaplan-Meier survival plot, and the hazard ratio with 95% confidence intervals and logrank P value were calculated.

ACKNOWLEDGEMENTS

We thank the ERC, DFG and the Max Planck Society for financial support and Dr. Julien Polleux (our group) for material and excellent discussions. MRH was a fellow of the Boehringer Ingelheim Fonds.

AUTHOR CONTRIBUTIONS

RF and MRH designed the experiments and wrote the paper; MRH, ER, MJ, MW performed experiments; MRH, ER, MJ, MW, AY analyzed data; GP, FH, and BH provided important reagents and/or analytical tools. All authors read and approved the manuscript.

REFERENCES

Andersen, J. B., Aaboe, M., Borden, E. C., Goloubeva, O. G., Hassel, B. A., and Orntoft, T. F. (2006). Stage-associated overexpression of the ubiquitin-like protein, ISG15, in bladder cancer. British journal of cancer *94*, 1465-1471.

Azioune, A., Carpi, N., Tseng, Q., Thery, M., and Piel, M. (2010). Protein micropatterns: A direct printing protocol using deep UVs. Methods in cell biology *97*, 133-146.

Balza, R. O., Jr., and Misra, R. P. (2006). Role of the serum response factor in regulating contractile apparatus gene expression and sarcomeric integrity in cardiomyocytes. The Journal of biological chemistry *281*, 6498-6510.

Bektas, N., Noetzel, E., Veeck, J., Press, M. F., Kristiansen, G., Naami, A., Hartmann, A., Dimmler, A., Beckmann, M. W., Knuchel, R*., et al.* (2008). The ubiquitin-like molecule interferon-stimulated gene 15 (ISG15) is a potential prognostic marker in human breast cancer. Breast cancer research : BCR *10*, R58.

Brandt, D. T., Baarlink, C., Kitzing, T. M., Kremmer, E., Ivaska, J., Nollau, P., and Grosse, R. (2009). SCAI acts as a suppressor of cancer cell invasion through the transcriptional control of beta1-integrin. Nat Cell Biol *11*, 557-568.

Brooks, P. C., Clark, R. A., and Cheresh, D. A. (1994). Requirement of vascular integrin alpha v beta 3 for angiogenesis. Science *264*, 569-571.

Connelly, J. T., Gautrot, J. E., Trappmann, B., Tan, D. W., Donati, G., Huck, W. T., and Watt, F. M. (2010). Actin and serum response factor transduce physical cues from the microenvironment to regulate epidermal stem cell fate decisions. Nat Cell Biol *12*, 711-718.

Cooper, S. J., Trinklein, N. D., Nguyen, L., and Myers, R. M. (2007). Serum response factor binding sites differ in three human cell types. Genome research *17*, 136-144.

Danen, E. H., Sonneveld, P., Brakebusch, C., Fassler, R., and Sonnenberg, A. (2002). The fibronectin-binding integrins alpha5beta1 and alphavbeta3 differentially modulate RhoA-GTP loading, organization of cell matrix adhesions, and fibronectin fibrillogenesis. Journal of Cell Biology *159*, 1071-1086.

Desai, S. D., Haas, A. L., Wood, L. M., Tsai, Y. C., Pestka, S., Rubin, E. H., Saleem, A., Nur, E. K. A., and Liu, L. F. (2006). Elevated expression of ISG15 in tumor cells interferes with the ubiquitin/26S proteasome pathway. Cancer research *66*, 921-928.

Desai, S. D., Reed, R. E., Burks, J., Wood, L. M., Pullikuth, A. K., Haas, A. L., Liu, L. F., Breslin, J. W., Meiners, S., and Sankar, S. (2012). ISG15 disrupts cytoskeletal architecture and promotes motility in human breast cancer cells. Experimental biology and medicine *237*, 38-49.

Desai, S. D., Wood, L. M., Tsai, Y. C., Hsieh, T. S., Marks, J. R., Scott, G. L., Giovanella, B. C., and Liu, L. F. (2008). ISG15 as a novel tumor biomarker for drug sensitivity. Molecular cancer therapeutics *7*, 1430-1439.

Descot, A., Hoffmann, R., Shaposhnikov, D., Reschke, M., Ullrich, A., and Posern, G. (2009). Negative regulation of the EGFR-MAPK cascade by actin-MAL-mediated Mig6/Errfi-1 induction. Molecular cell *35*, 291-304.

Eduardo-Correia, B., Martinez-Romero, C., Garcia-Sastre, A., and Guerra, S. (2014). ISG15 is counteracted by vaccinia virus E3 protein and controls the proinflammatory response against viral infection. Journal of virology *88*, 2312-2318.

Elston, C. W., and Ellis, I. O. (1991). Pathological prognostic factors in breast cancer. I. The value of histological grade in breast cancer: experience from a large study with long-term follow-up. Histopathology *19*, 403-410.

Farrell, P. J., Broeze, R. J., and Lengyel, P. (1979). Accumulation of an mRNA and protein in interferon-treated Ehrlich ascites tumour cells. Nature *279*, 523-525.

Frisch, S. M., Vuori, K., Ruoslahti, E., and Chan-Hui, P. Y. (1996). Control of adhesion-dependent cell survival by focal adhesion kinase. The Journal of cell biology *134*, 793-799.

Gabbiani, G., Gabbiani, F., Heimark, R. L., and Schwartz, S. M. (1984). Organization of actin cytoskeleton during early endothelial regeneration in vitro. Journal of cell science *66*, 39-50.
Haas, A. L., Ahrens, P., Bright, P. M., and Ankel, H. (1987). Interferon induces a 15-kilodalton protein exhibiting marked homology to ubiquitin. The Journal of biological chemistry *262*, 11315-11323.
Han, S. Y., Kim, S. H., and Heasley, L. E. (2002). Differential gene regulation by specific gain-of-function JNK1 proteins expressed in Swiss 3T3 fibroblasts. The Journal of biological chemistry *277*, 47167-47174.
Heacock, C. S., and Bamburg, J. R. (1983). The quantitation of G- and F-actin in cultured cells. Analytical biochemistry *135*, 22-36.
Hermeking, H., Lengauer, C., Polyak, K., He, T. C., Zhang, L., Thiagalingam, S., Kinzler, K. W., and Vogelstein, B. (1997). 14-3-3 sigma is a p53-regulated inhibitor of G2/M progression. Molecular cell *1*, 3-11.
Hitchcock, S. E. (1980). Actin deoxyroboncuclease I interaction. Depolymerization and nucleotide exchange. The Journal of biological chemistry *255*, 5668-5673.
Hood, J. D., and Cheresh, D. A. (2002). Role of integrins in cell invasion and migration. Nature reviews Cancer *2*, 91-100.
Hu, Q., Guo, C., Li, Y., Aronow, B. J., and Zhang, J. (2011). LMO7 mediates cell-specific activation of the Rho-myocardin-related transcription factor-serum response factor pathway and plays an important role in breast cancer cell migration. Mol Cell Biol *31*, 3223-3240.
Jeon, Y. J., Choi, J. S., Lee, J. Y., Yu, K. R., Kim, S. M., Ka, S. H., Oh, K. H., Kim, K. I., Zhang, D. E., Bang, O. S., and Chung, C. H. (2009). ISG15 modification of filamin B negatively regulates the type I interferon-induced JNK signalling pathway. EMBO Rep *10*, 374-380.
Kressner, C., Nollau, P., Grosse, R., and Brandt, D. T. (2013). Functional interaction of SCAI with the SWI/SNF complex for transcription and tumor cell invasion. PloS one *8*, e69947.
Lenschow, D. J., Giannakopoulos, N. V., Gunn, L. J., Johnston, C., O'Guin, A. K., Schmidt, R. E., Levine, B., and Virgin, H. W. t. (2005). Identification of interferon-stimulated gene 15 as an antiviral molecule during Sindbis virus infection in vivo. Journal of virology *79*, 13974-13983.
Liu, M., Li, X. L., and Hassel, B. A. (2003). Proteasomes modulate conjugation to the ubiquitin-like protein, ISG15. The Journal of biological chemistry *278*, 1594-1602.
Lock, C., Hermans, G., Pedotti, R., Brendolan, A., Schadt, E., Garren, H., Langer-Gould, A., Strober, S., Cannella, B., Allard, J*., et al.* (2002). Gene-microarray analysis of multiple sclerosis lesions yields new targets validated in autoimmune encephalomyelitis. Nature medicine *8*, 500-508.
Loeb, K. R., and Haas, A. L. (1992). The interferon-inducible 15-kDa ubiquitin homolog conjugates to intracellular proteins. The Journal of biological chemistry *267*, 7806-7813.
Luo, X. G., Zhang, C. L., Zhao, W. W., Liu, Z. P., Liu, L., Mu, A., Guo, S., Wang, N., Zhou, H., and Zhang, T. C. (2014). Histone methyltransferase SMYD3 promotes MRTF-A-mediated transactivation of MYL9 and migration of MCF-7 breast cancer cells. Cancer letters *344*, 129-137.
Ma, Z., Morris, S. W., Valentine, V., Li, M., Herbrick, J. A., Cui, X., Bouman, D., Li, Y., Mehta, P. K., Nizetic, D*., et al.* (2001). Fusion of two novel genes, RBM15 and MKL1, in the t(1;22)(p13;q13) of acute megakaryoblastic leukemia. Nature genetics *28*, 220-221.
Malakhova, O. A., and Zhang, D. E. (2008). ISG15 inhibits Nedd4 ubiquitin E3 activity and enhances the innate antiviral response. The Journal of biological chemistry *283*, 8783-8787.
Matter, M. L., and Ruoslahti, E. (2001). A signaling pathway from the alpha5beta1 and alpha(v)beta3 integrins that elevates bcl-2 transcription. The Journal of biological chemistry *276*, 27757-27763.
Medjkane, S., Perez-Sanchez, C., Gaggioli, C., Sahai, E., and Treisman, R. (2009). Myocardin-related transcription factors and SRF are required for cytoskeletal dynamics and experimental metastasis. Nat Cell Biol *11*, 257-268.
Mercher, T., Coniat, M. B., Monni, R., Mauchauffe, M., Nguyen Khac, F., Gressin, L., Mugneret, F., Leblanc, T., Dastugue, N., Berger, R., and Bernard, O. A. (2001). Involvement of a human gene related to

the Drosophila spen gene in the recurrent t(1;22) translocation of acute megakaryocytic leukemia. Proceedings of the National Academy of Sciences of the United States of America *98*, 5776-5779.
Mizejewski, G. J. (1999). Role of integrins in cancer: survey of expression patterns. Proceedings of the Society for Experimental Biology and Medicine *222*, 124-138.
Morales, D. J., and Lenschow, D. J. (2013). The Antiviral Activities of ISG15. Journal of molecular biology *425*, 4995-5008.
Okumura, A., Pitha, P. M., and Harty, R. N. (2008). ISG15 inhibits Ebola VP40 VLP budding in an L-domain-dependent manner by blocking Nedd4 ligase activity. Proceedings of the National Academy of Sciences of the United States of America *105*, 3974-3979.
Okumura, F., Okumura, A. J., Uematsu, K., Hatakeyama, S., Zhang, D. E., and Kamura, T. (2013). Activation of double-stranded RNA-activated protein kinase (PKR) by interferon-stimulated gene 15 (ISG15) modification down-regulates protein translation. The Journal of biological chemistry *288*, 2839-2847.
Okumura, F., Zou, W., and Zhang, D. E. (2007). ISG15 modification of the eIF4E cognate 4EHP enhances cap structure-binding activity of 4EHP. Genes Dev *21*, 255-260.
Philippar, U., Schratt, G., Dieterich, C., Muller, J. M., Galgoczy, P., Engel, F. B., Keating, M. T., Gertler, F., Schule, R., Vingron, M., and Nordheim, A. (2004). The SRF target gene Fhl2 antagonizes RhoA/MAL-dependent activation of SRF. Molecular cell *16*, 867-880.
Raff, M. C. (1992). Social controls on cell survival and cell death. Nature *356*, 397-400.
Schiller, H. B., Hermann, M. R., Polleux, J., Vignaud, T., Zanivan, S., Friedel, C. C., Sun, Z., Raducanu, A., Gottschalk, K. E., Thery, M*., et al.* (2013). beta1- and alphav-class integrins cooperate to regulate myosin II during rigidity sensing of fibronectin-based microenvironments. Nat Cell Biol *15*, 625-636.
Selvaraj, A., and Prywes, R. (2004). Expression profiling of serum inducible genes identifies a subset of SRF target genes that are MKL dependent. BMC molecular biology *5*, 13.
Small, J., Rottner, K., Hahne, P., and Anderson, K. I. (1999). Visualising the actin cytoskeleton. Microscopy research and technique *47*, 3-17.
Sotiropoulos, A., Gineitis, D., Copeland, J., and Treisman, R. (1999). Signal-regulated activation of serum response factor is mediated by changes in actin dynamics. Cell *98*, 159-169.
Stupack, D. G., Puente, X. S., Boutsaboualoy, S., Storgard, C. M., and Cheresh, D. A. (2001). Apoptosis of adherent cells by recruitment of caspase-8 to unligated integrins. The Journal of cell biology *155*, 459-470.
Sun, Q., Chen, G., Streb, J. W., Long, X., Yang, Y., Stoeckert, C. J., Jr., and Miano, J. M. (2006). Defining the mammalian CArGome. Genome research *16*, 197-207.
Takeuchi, T., Iwahara, S., Saeki, Y., Sasajima, H., and Yokosawa, H. (2005). Link between the ubiquitin conjugation system and the ISG15 conjugation system: ISG15 conjugation to the UbcH6 ubiquitin E2 enzyme. Journal of biochemistry *138*, 711-719.
Tang, Y., Rowe, R. G., Botvinick, E. L., Kurup, A., Putnam, A. J., Seiki, M., Weaver, V. M., Keller, E. T., Goldstein, S., Dai, J*., et al.* (2013). MT1-MMP-dependent control of skeletal stem cell commitment via a beta1-integrin/YAP/TAZ signaling axis. Dev Cell *25*, 402-416.
van der Veen, A. G., and Ploegh, H. L. (2012). Ubiquitin-like proteins. Annual review of biochemistry *81*, 323-357.
Vartiainen, M. K., Guettler, S., Larijani, B., and Treisman, R. (2007). Nuclear actin regulates dynamic subcellular localization and activity of the SRF cofactor MAL. Science *316*, 1749-1752.
Yuan, W., and Krug, R. M. (2001). Influenza B virus NS1 protein inhibits conjugation of the interferon (IFN)-induced ubiquitin-like ISG15 protein. The EMBO journal *20*, 362-371.
Zhang, C., Luo, X., Liu, L., Guo, S., Zhao, W., Mu, A., Liu, Z., Wang, N., Zhou, H., and Zhang, T. (2013). Myocardin-related transcription factor A is up-regulated by 17beta-estradiol and promotes migration of

MCF-7 breast cancer cells via transactivation of MYL9 and CYR61. Acta biochimica et biophysica Sinica *45*, 921-927.
Zhang, S. X., Garcia-Gras, E., Wycuff, D. R., Marriot, S. J., Kadeer, N., Yu, W., Olson, E. N., Garry, D. J., Parmacek, M. S., and Schwartz, R. J. (2005). Identification of direct serum-response factor gene targets during Me2SO-induced P19 cardiac cell differentiation. The Journal of biological chemistry *280*, 19115-19126.
Zou, W., Papov, V., Malakhova, O., Kim, K. I., Dao, C., Li, J., and Zhang, D. E. (2005). ISG15 modification of ubiquitin E2 Ubc13 disrupts its ability to form thioester bond with ubiquitin. Biochemical and biophysical research communications *336*, 61-68.

FIGURE AND TABLE LEGENDS

Figure 1. FN bound α5β1 and αV-class integrins control f-Actin and nuclear MAL levels. (**A**) Superimposed picture (confocal stack) of indicated cell types immunostained for f-Actin (Phalloidin), g-Actin (DNaseI) and DAPI plated on FN-coated glass surfaces. The intensity map shows the cytoplasmic distribution of g-Actin. Scale bar, 20 µm. (**B**, **C**) Quantification of cytoplasmic g-Actin by DNaseI (B) and f-Actin fibres by Phalloidin (C) relative fluorescence intensities (n>20; 3 independent experiments). (**D**) Cell fractionation into soluble (S), nuclear (N) and cytoskeletal (C) components followed by western blot analysis with a β-Actin antibody. Antibodies against Vimentin and GAPDH confirm efficiency of subcellular protein fractionation (representative western blot of four independent experiments is shown). (**E, F**) Ratio of g-Actin versus GAPDH (E) and g-Actin versus f-Actin (F) of the indicated cell types is shown (n=4; 4 independent experiments). (**G**) Western blot analysis by Profilin and β-Actin antibody of g-Actin pulldown experiment with DNAseI- or BSA-coupled Sepharose beads (representative western blot of three independent experiments in technical duplicates is shown). (**H**) DNaseI-bound g-Actin in nuclear (N) and soluble (S) cell fraction was analysed (n=3; 3 independent experiments). (**I**) Immunostaining of indicated cell types plated on FN-coated glass coverslips and treated with DMSO (control), 100 nM Jasplankinolide (Jasp) and 500 nM Latrunculin A (LatA), respectively. The merged images display an overlay of Paxilin, MAL, f-Actin and nuclear staining (DAPI). Scale bar, 10 µm. All p-values were calculated using a paired Students-*t*-test.

Figure 2. αV-class integrins cooperate with α5β1 to induce SRF/MAL activity. (**A**) SRF-driven luciferase reporter activity in cells plated on FN and treated with DMSO, 100 nM Jasplankinolide (Jasp) or 500 nM Latrunculin A (LatA) (3 independent experiments). (**B**) SRF-driven luciferase reporter activity in cells plated on FN transfected with EGFP, a constitutive active (ca) MAL (ΔN-MAL) or a ca mDia construct (4 independent experiments). (**C**) SRF-driven luciferase reporter activity in cells plated on circular FN-coated micropatterns with either 40 µm or 28 µm diameter (3 independent experiments). (**D**) Z-stacks of immunostained cells seeded on circular FN-coated micropatterns with indicated diameters. The cartoon on the left illustrates the position of the indicated stack. The merged picture displays an overlay of MAL (yellow), f-Actin (white) and nuclear staining (DAPI). Scale bar, 10 µm. (**E**) Quantification of nuclear fluorescence intensity for MAL from superimposed images shown in (D) (n=5). (**F, G**) SRF-driven luciferase reporter activity in indicated cells treated with Mn^{++} (n=5) (F) or transfected with the αV or β1 Integrin (G) (n=4). (**H**) Immunostaining of pKO-αV,β1 cells plated on Fibronectin (FN), Vitronectin (VN) and Gelatin and untreated or treated with anti-α5β1 blocking antibodies or Cilengitide for MAL (red), f-

Actin (white) and nucleus (DAPI; green). The inserts show MAL in the different settings. Scale bar, 25 µm. (**I**) SRF/MAL luciferase reporter activity (n=3) in pKO-αV,β1 cells plated on FN and untreated (n=15) or treated with anti-α5β1 blocking antibodies (n=22) or Cilengitide (n=27). All error bars represent ±SEM. All p-values were calculated using a paired Students-*t*-test. pKO-αV (green); pKO-β1 (orange); pKO-αV,β1 (blue).

Figure 3. αV- and β1-class integrins induce transcription of SRF/MAL target genes.

(**A**) Quantitative realtime-PCR of the SRF/MAL target genes *srf, talin, flnb, vcl, lima1* but also *mrtf-a* and *isg15*. mRNA levels are shown relative to GAPDH transcript levels (n>3; minimum of 3 independent RNA isolations, double blind). (**B**) Western blot analysis of SRF, Talin, Filamin B (FLN B), Vinculin (VCL), Lima1 but also MAL (or MRTF-A). GAPDH was used to control protein loading. (**C**) Densitometric analysis of free ISG15 protein in the indicated cell lines (5 independent experiments). (**D**) Immunostaining for Paxillin (Pxn), ISG15, f-Actin and DAPI. Arrowheads indicate co-localization of f-Actin and ISG15. Scale bar, 10 µm. (**E**) Immunostaining of ISG15, Paxillin, f-Actin and nucleus (DAPI) in FAs of cross-linked and unroofed indicated cells. The merged images display an overlay of ISG15, Paxillin, f-Actin and DAPI. Scale bar, 10 µm. (**F**) Scheme to illustrate location of CArG boxes (SRF binding sites; Blue boxes) in *isg15, vcl* as control and *tln-1* gene along Exons (Black boxes;). (**G, H**) Chromatin immunopreciptiation was performed with MAL, SRF or rabbit IgG antibody as control. *Isg15, vcl, tln* and *gapdh* as control CArG boxes were amplified by conventional PCR and visualized by agarose gel electrophoresis (G). Real-time PCR was performed from three independent chromatin preparations and IPs. Shown is the relative quantitation of *isg15, vcl* and *tln* relative to input chromatin (H). All error bars represent ±SEM. All p-values were calculated using a paired Students-*t*-test. pKO-αV (green); pKO-β1 (orange); pKO-αV,β1 (blue).

Figure 4. αV- and β1-class Integrin induced SRF/MAL activity and ISG15 levels to promote 3D cell invasion. (**A**) FACS analysis of integrin α5, αV and β1 surface levels and β1 activity by 9EG7 staining MCF-7 and MB231. (**B, C**) Immunostaining of non-invasive MCF-7 and highly invasive MB231 breast cancer cell lines seeded on FN (B). A representative example for threshold used for nuclear MAL quantification(C) is shown (In two independent experiment a minimum of 129 cells per cell line were analysed). The merged images display an overlay of MAL, f-Actin and nuclear staining (DAPI). Scale bar, 10 µm. (**D**) SRF/MAL luciferase reporter assay of MCF-7 and MDA-MB-231 cells (n=3; three independent experiments). (**E**) Quantitative real-time PCR was performed for *itgaV* and SRF/MAL targets *itgb1, isg15*, *srf,* and *lima1* but also for *mrtf-a*. Shown is the quantitation relative to *gapdh* (n=3, from 3 independent isolations, double blind). (**F**) Western blot of MDA-MB-231 and MCF-7 with ISG15 specific antibody.

GAPDH was used to control loading. (**G-H**) FN-coated transwell cell invasion assay with MDA-MB-231 and MCF-7 cells upon ISG15 knockdown, UBP43 overexpression or scrambled shRNA control (n=3; 3 independent experiments). Immunostaining of transmigrated cell by Phalloidin and DAPI (G). Quantification of transmigrated cells compared to scrambled control (H). Scale bar, 100 µm. All error bars represent ±SEM. All p-values were calculated using a paired Students-*t*-test. ■ pKO-αV (green); ■ pKO-β1 (orange); and ■ pKO-αV,β1 (blue); □ MCF-7 (white); ■ MB231 (black).

Figure 5. αV- and β1-class integrin induced ISGylation of SRF/MAL targets results in bad breast cancer patient prognosis. (**A, B**) Kaplan Meier analysis indicates that breast cancer patients with high integrin β1 (A), or high ISG15 levels (B) die earlier. (**C**) Kaplan Meier analysis indicate bad patient outcome at high compared to low ISG15 transcript amounts by constant high α5 and β1 Integrin levels. (**D**) H/E staining of indicated breast cancer samples. Approximate area used for immunostaining (IF) is indicated. (**E**) Immunostaining of indicated patient samples for MAL, integrin β1 and f-Actin. The merged images display an overlay of MAL, integrin β1 and f-Actin and nuclear staining (DAPI). Scale bar, 50 µm.

Figure 6. Model of how α5β1/αV-class integrins synergistically induce MAL/SRF, leading to multi-layered protein ISGylation and enhanced 3D migration and invasion of tumour cells. Both, αV-class integrin induced RhoA/mDia and β1-class integrin induced Rac/WAVE/Arp2/3 activities are combined in FN-adherent pKO-αV,β1 cells leading to low g-Actin levels, the release and nuclear translocation of MAL, binding to SRF and transcription of target genes such as ISG15 and FA proteins. Production of ISG15 and its coupling machinery results in multi-layered protein ISGylation and subsequent stabilization of FA- and cytoskeletal-related proteins. Advanced cell migration properties leads to improved 3D migration and invasion of tumour cells.

Table 1. Qualitative Comparison of SRF/MAL target genes to the proteome data of pKO-αV, pKO-β1 and pKO-αV,β1 cells published in Schiller and Hermann et al., NCB, 2013. Data mining and comparison of seven different SRF/MAL target gene screening approaches were manually filtered for association with FA and actin functions and co-localization. A qualitative comparison with the pKO-cell proteome was performed. Data sources were cited by numbers: (**1**) Balza R. O. et al., JBC, 2006; (**2**) Philippar et al., MolCell, 2004; (**3**) Selvaraj A. et al., BMC, 2004; (**4**) Sun Q. et al., Genome Res, 2006; (**5**) Zhang S. X. et al., JBC, 2005; (**6**) Descot A. et al., MolCell, 2009; and (**7**) Cooper S. J. et al., Genome Res, 2007; ■ enrichment in pKO-αV cells (green); ■ enrichment in pKO-β1 cells (orange); and ■ enrichment in pKO-αV,β1 cells (blue); ■ not found in pKO-cell proteome list; □ not enriched in the indicated cell type.

SUPPLEMENTARY INFORMATION

Figure S1. Different total Actin levels and distribution in pKO-αV, pKO-β1 and pKO-αV,β1 cells. (**A**) Immunostaining of indicated cell types for Paxillin and f-Actin plated for 90 minutes on circular FN-coated micropatterns. The merged images display an overlay of Paxillin, f-Actin and nuclear (DAPI) staining. Scale bar, 25 µm. (**B**) Cell lysates were immunoblotted for total Actin. GAPDH was used as a loading control. Densitometric quantification of western blots (n=3) is depicted as fold changes below the corresponding blot with +/- SEM values. (**C**) FACS analysis of indicated cell types by propidium iodide staining to measure nuclear size. (**D**) Box plot of all actin modifying proteins (Schiller et al., 2013) in indicated cell lines classified into their effect on g-Actin pool: Neutral (black), decrease (blue), increase (yellow). Protein abundance is presented by Log2 ratios. Thymosin beta 4 (Tmsb4), Cofilin-1 (Cfl-1) and Advillin (Advil) were highlighted. (**E**) Log2 ratio of Tmsb4 expression in indicated cell lines (n=3; 3 independent experiments). (**F**) Western blot of Cofilin and phospho-Cofilin (Ser3) (representative western blot of 4 independent experiments is shown). (**G**) Microscopy of indicated cells upon Latrunculin A (LatA) or Jasplankinolide (Jasp) treatment. DMSO was used as control. Dashed lines highlight lamellipodia and long protrusions caused by Jasp treatment. Scale bar, 20µm.

Figure S2. αV-class integrins cooperate with α5β1 to induce SRF/MAL activity. (**A-C**) Reporter activity measurements of a SRF-driven firefly normalized to a thymidine kinase-driven renilla luciferase of cells plated on FN-coated culture dishes. Cells were starved and serum boosted with 40% FCS (A) and in (B) treated with Methanol (MeOH) as a control and Leptomycin B (LeptoB) to inhibit the nuclear export of MAL or (C) transfected with EGFP only or a dominant negative MAL (DN MAL) construct. (**D**) Reporter activity measurements of a SRF-driven firefly normalized to a thymidine kinase-driven renilla luciferase of Kindlin-1 and -2 or Talin-1 and -2 wild type (WT) and knockout cells (KO) seeded on FN. All error bars represent SEM and p-values were calculated using a paired Students-*t*-test. ■ pKO-αV (green); ■ pKO-β1 (orange); ■ pKO-αV,β1 (blue);

Figure S3. Type I interferon response independent but SRF/MAL dependent ISG15 transcription in pKO-αV, pKO-β1 and pKO-αV,β1 cells. (**A-C**) Quantitative real-time PCR of Interferon α (IFNα; A), Interferon β (IFNβ; B) and ISG15 upon 100µg/ml poly I:C stimulation (C) (n=3; 3 independent isolations). (**D, E**) ELISA-based quantification of IFNα (D) or IFNβ (E) levels in supernatants of indicated cells treated with Poly I:C. Error bars represent ±SEM. p-values were calculated using a paired Students-*t*-test. (**F**) Western blot of free ISG15 in total cell lysate or supernatant of 72h cultured indicated cells. GAPDH was used to control protein loading. FN was used as a secreted protein control. Densitometric quantification

of western blots (n>3; >3 independent experiments) is depicted as fold changes below the corresponding blot with +/- SEM values.

Figure S5. αV- and β1-class integrin induced ISGylation of SRF/MAL targets results in bad breast cancer patient prognosis. Quantification of nuclear MAL in grade (G) 1 to G3 breast cancer sections (G1: n=10, G2: n=12, G3: n=20).

SUPPLEMENTARY TABLES

Table S1. ISG15 pull-down mass spectrometry analysis

Table S2. List of primer sequences

Table S3. List of antibodies

Hermann et al., Fig.1

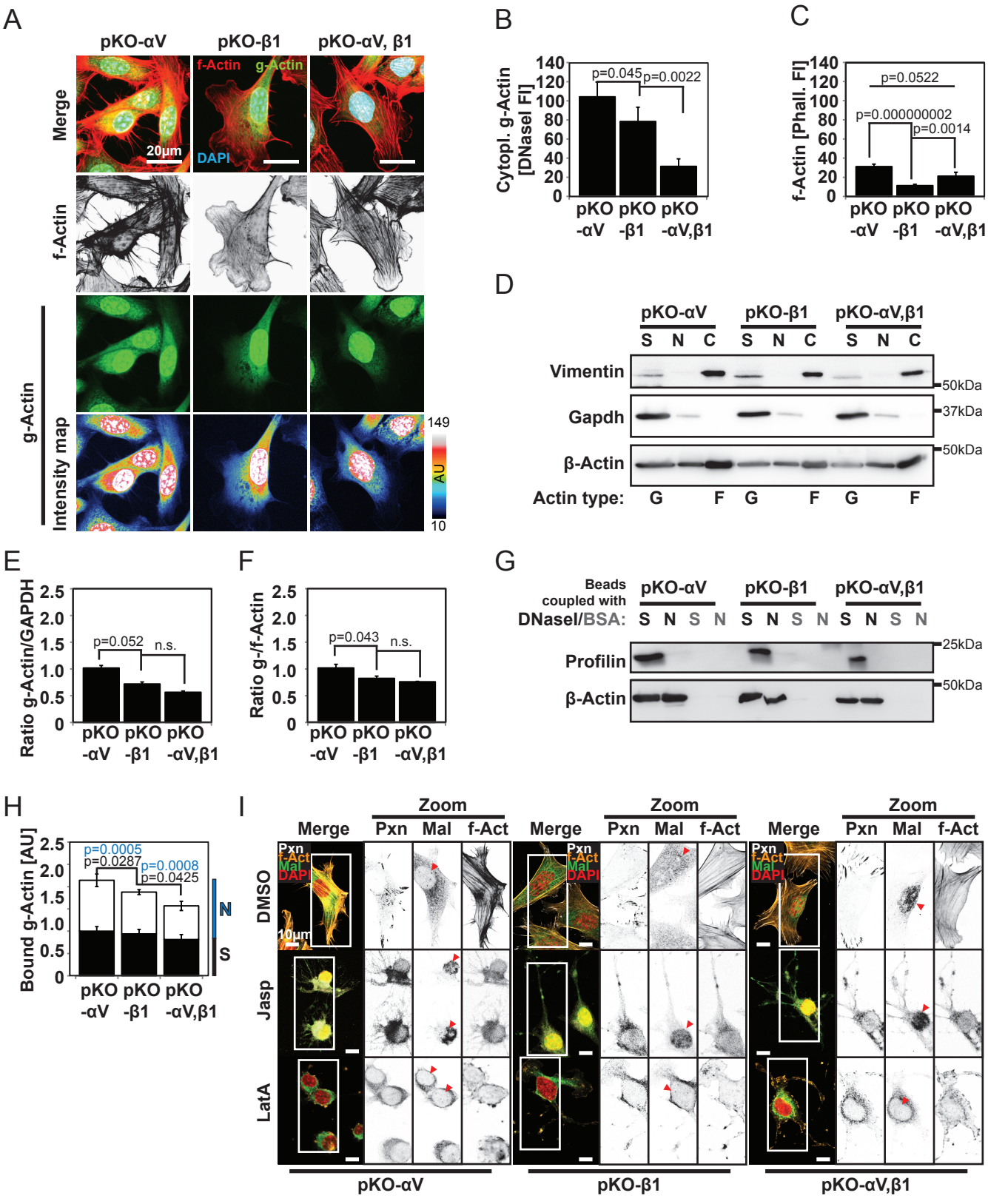

Hermann et al., Fig.2

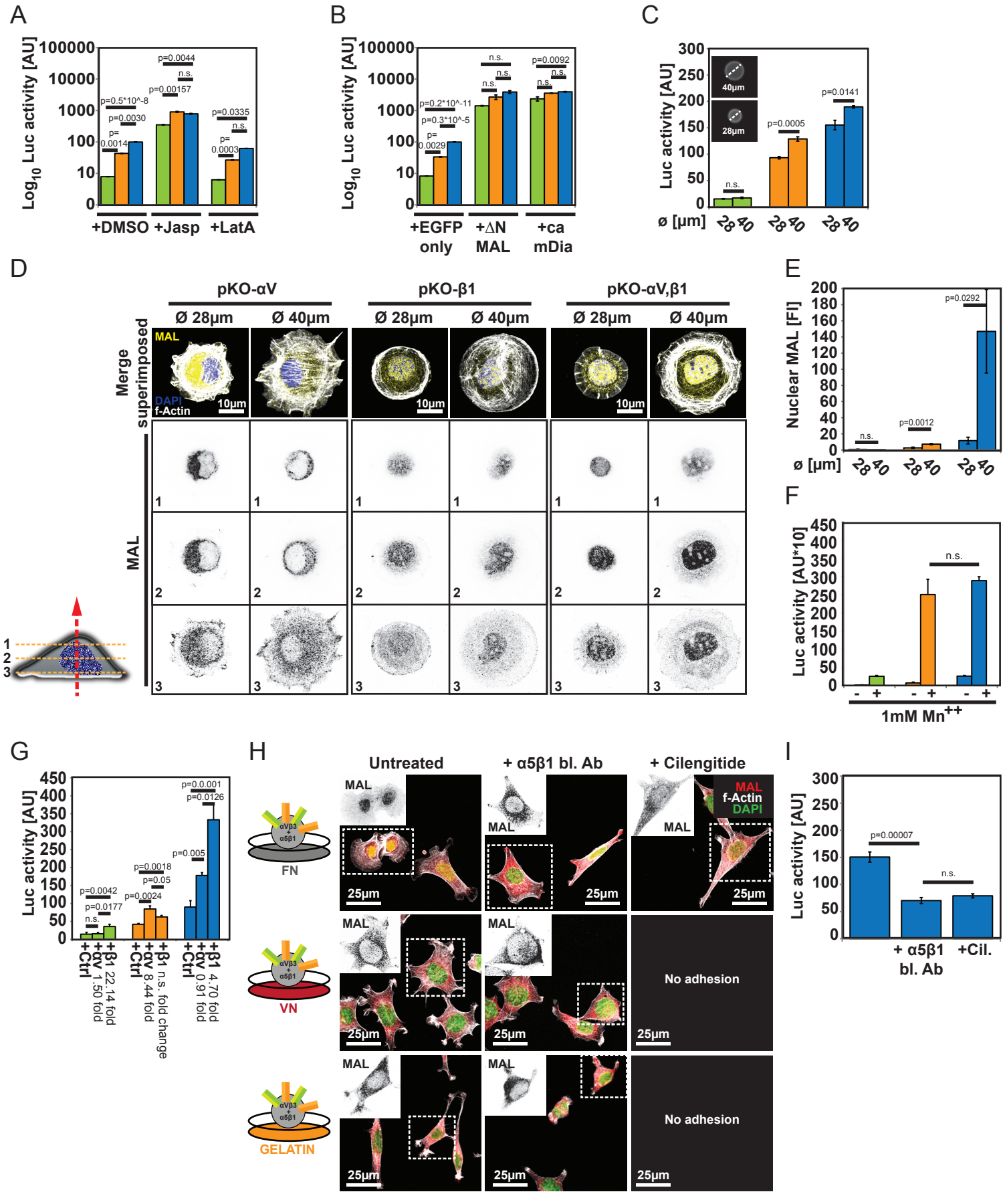

Hermann et al., Fig.3

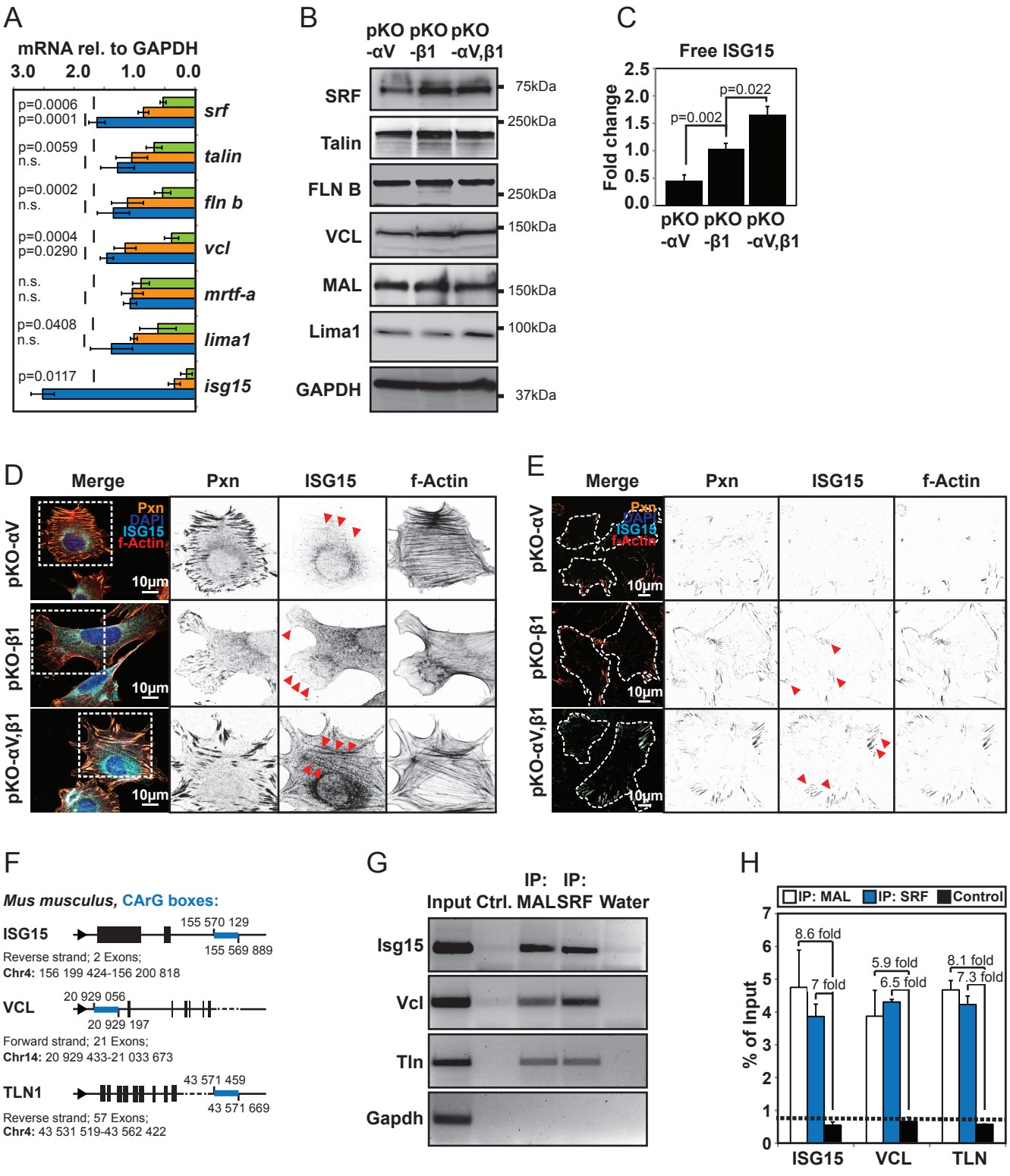

Hermann et al., Fig.4

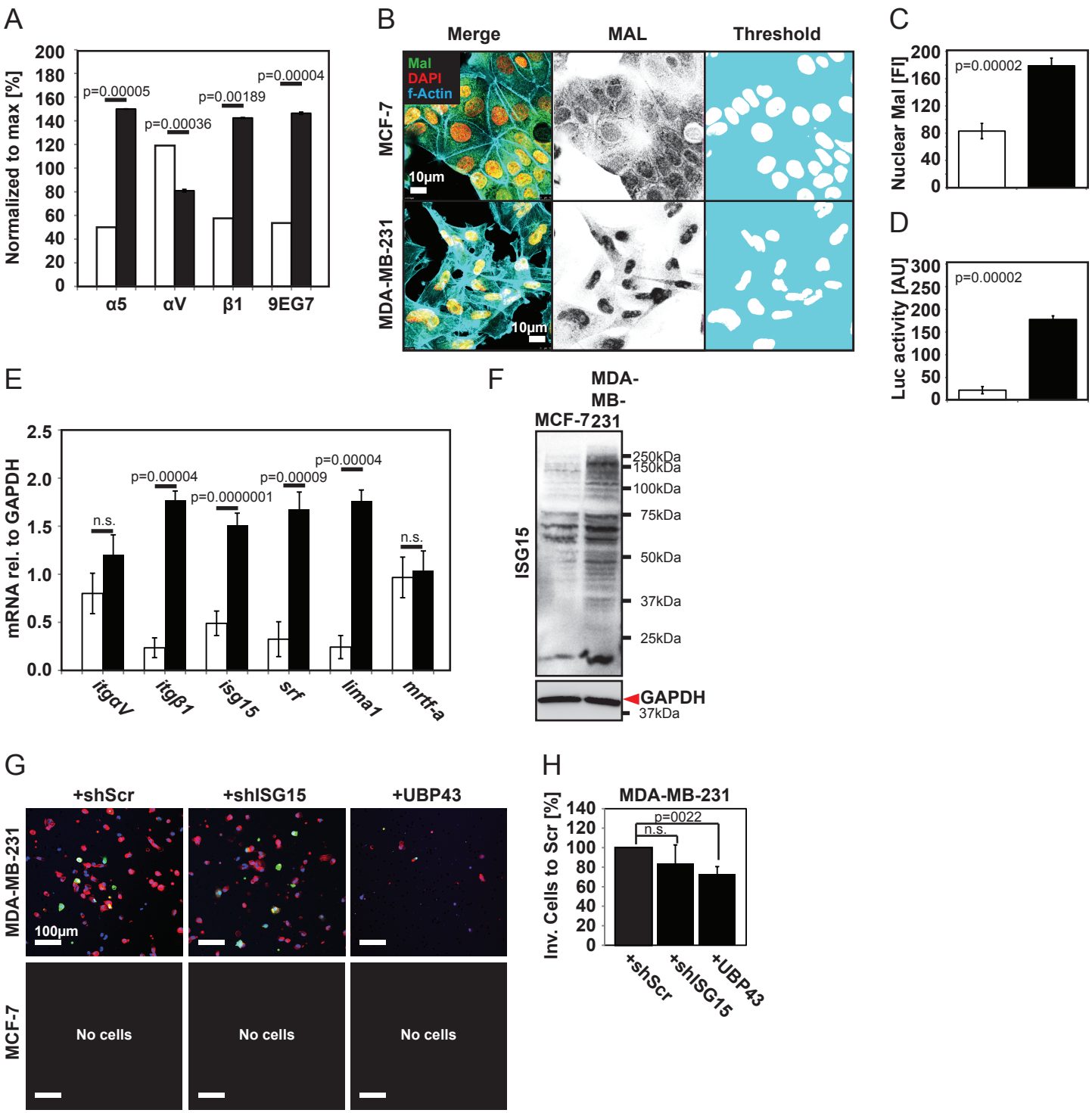

Hermann et al., Fig.5

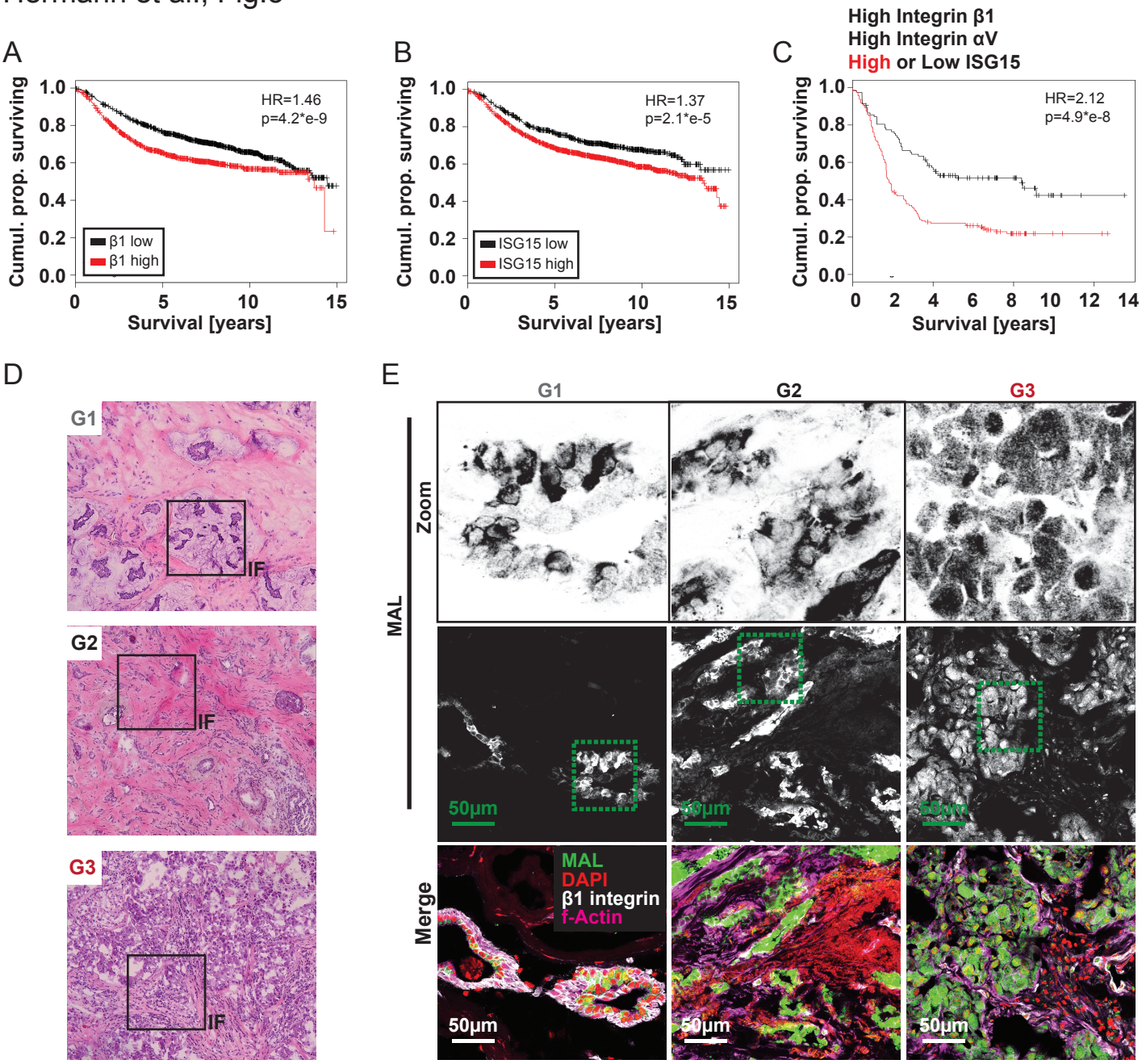

Hermann et al., Fig.6

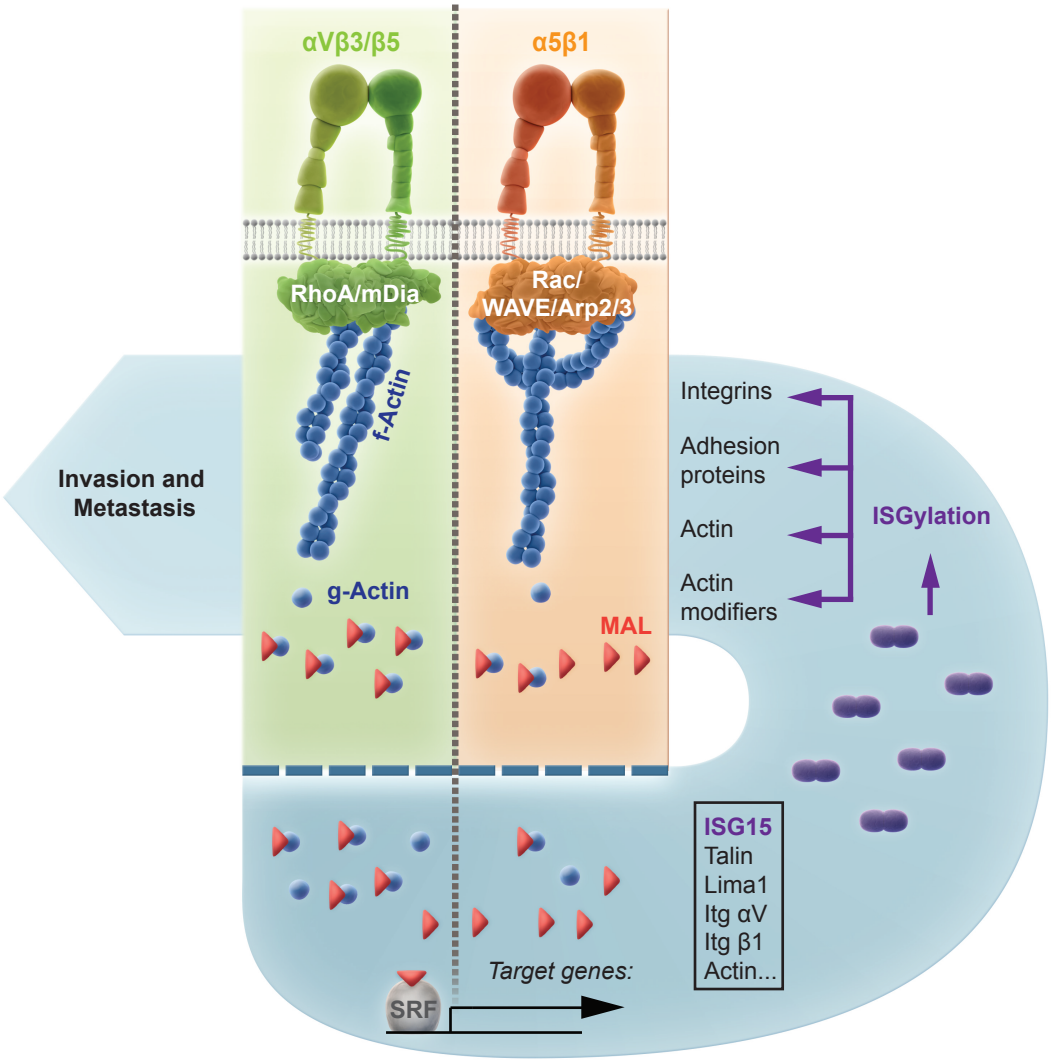

Hermann et al., Table 1

SRF target genes			Proteome		
Gene Name	**Annotation**	**Source**	**Enriched**		
ACTA1	Skeletal alpha actin	1,2,6			
ACTA2	Smooth muscle alpha actin	1,2,6			
ACTC	Alpha-cardiac actin	2			
ACTC1	Actin, alpha cardiac muscle 1	1,5,6			
ACTG	Actin, cytoplasmic 2	2			
ACTN1	Alpha-actinin-1	4			
CAPZA3	F-actin-capping protein subunit alpha-3	4			
CFL1	Cofilin, non-muscle isoform	4			
CFL2	Cofilin2, muscle	1,4			
DSTN	Destrin, Actin-depolymerizing factor, ADF	4,6,7			
ENAH, MENA	Protein enabled homolog	1			
EPLIN	LIM domain and actin-binding protein 1	6			
FBLN5	Fibulin-5	4			
FHL1	Four and a half LIM domains protein 1	4,6			
FHL2	Four and a half LIM domains protein 2	2,4			
FLNA	Filamin A	4			
FLNC	Filamin C	4			
FNBP1	Formin-binding protein 1	1			
IQGAP	Ras GTPase-activating-like protein IQGAP1				
ISG15	Interferon-induced 15kDa protein	2			
ITGA1	Integrin alpha 1	7			
ITGA5	Integrin alpha5	4,6			
ITGA9	Integrin alpha 9	1,5			
ITGB1	Integrin beta 1	1			
ITGB1BP2	Integrin beta 1 binding protein 2 (melusin)	1,4,7			
LPP	LIM domain-containing preferred translocation partner in lipoma	2,6			
MAP3K14	Mitogen-activated protein kinase kinase kinase 14	5,6			
MAP3K4	Mitogen-activated protein kinase kinase kinase 4	5			
MAPK10	Mitogen-activated protein kinase 10, JNK3	5			
MYH11	Myosin heavy chain, smooth muscle isoform, SMMHC	7			
MYH6	Myosin heavy chain, cardiac muscle alpha isoform, MyHC-alpha	1			
MYH7	Myosin heavy chain, cardiac muscle beta isoform, MyHC-beta	1			
MYH9	Non-muscle myosin heavy chain A, NMMHC-A, NMMHC-lia	6,7			
MYL3	Myosin light chain 1, slow-twitch muscle B/ventricular isoform, MLC1SB	1,5			
MYL4	Myosin light chain 1, atrial/fetal isoform, MLC1A	1			
MYL9	Myosin light chain 9, smooth muscle	1,5			
PDLIM5	Enh, Enigma homolog	4			
PDLIM7	Enigma	1,6			
PFN1	Profilin-1	4			
SRF	Serum response factor	1,3			
SVIL	Supervillin	1,7			
TLN	Talin	4			
TRIP6	Zyxin-related protein 1	4			
VCL	Vinculin	2,3,6,7			
VIL1	Villin-1	6			
ZYX	Zyxin	3			
			pKO-αV	**pKO-β1**	**pKO-αV,β1**

7.5 Paper V

Integrin-linked kinase at a glance

Moritz Widmaier, **Emanuel Rognoni**, Korana Radovanac, S. Babak Azimifar, Reinhard Fässler

Integrin-linked kinase at a glance

Moritz Widmaier, Emanuel Rognoni, Korana Radovanac, S. Babak Azimifar and Reinhard Fässler*

Max Planck Institute of Biochemistry, Department of Molecular Medicine, Am Klopferspitz 18, D-82152 Martinsried, Germany

*Author for correspondence (faessler@biochem.mpg.de)

Journal of Cell Science 125, 1839–1843

doi: 10.1242/jcs.093864

Integrins are a large family of cell–extracellular matrix (ECM) and cell–cell adhesion molecules that regulate development and tissue homeostasis by controlling cell migration, survival, proliferation and differentiation (Hynes, 2002). They are non-covalently associated heterodimers consisting of α- and β-subunits. On the cell surface, integrins exist in a conformation with either high (active) or low (inactive) ligand affinity. Upon activation (inside-out signalling) (Moser et al., 2009), integrins cluster and form nascent focal adhesions, which eventually mature into focal adhesions (FAs) (outside-in signalling) (Legate et al., 2009; Geiger and Yamada, 2011). Major functions of integrins in FAs include their ability to link the ECM to the actin cytoskeleton and to fine tune growth factor receptor signalling (Legate et al., 2009).

Given that integrins lack intrinsic enzymatic activity, their signalling crucially depends on recruiting adaptor and signalling proteins (Schiller et al., 2011). One of the best described of these proteins is integrin-linked kinase (ILK), which is directly recruited to β1 and β3 integrin cytoplasmic domains. Since its discovery 15 years ago (Hannigan et al., 1996), ILK has been shown to play crucial roles in actin rearrangement, cell polarisation, spreading, migration, proliferation and survival (Legate et al., 2006). Despite its predominant localisation in FAs, ILK has also been shown to reside in cell–cell adhesion sites, in centrosomes and in the nucleus. Here, we summarise the functional properties of ILK and highlight the recent evidence demonstrating that ILK serves as a scaffold protein rather than a kinase.

ILK and the Pinch–parvin complex

In vivo studies have revealed that ILK is a ubiquitously expressed protein, whose predominant function is to organise the actin cytoskeleton during invertebrate and vertebrate development and homeostasis. In

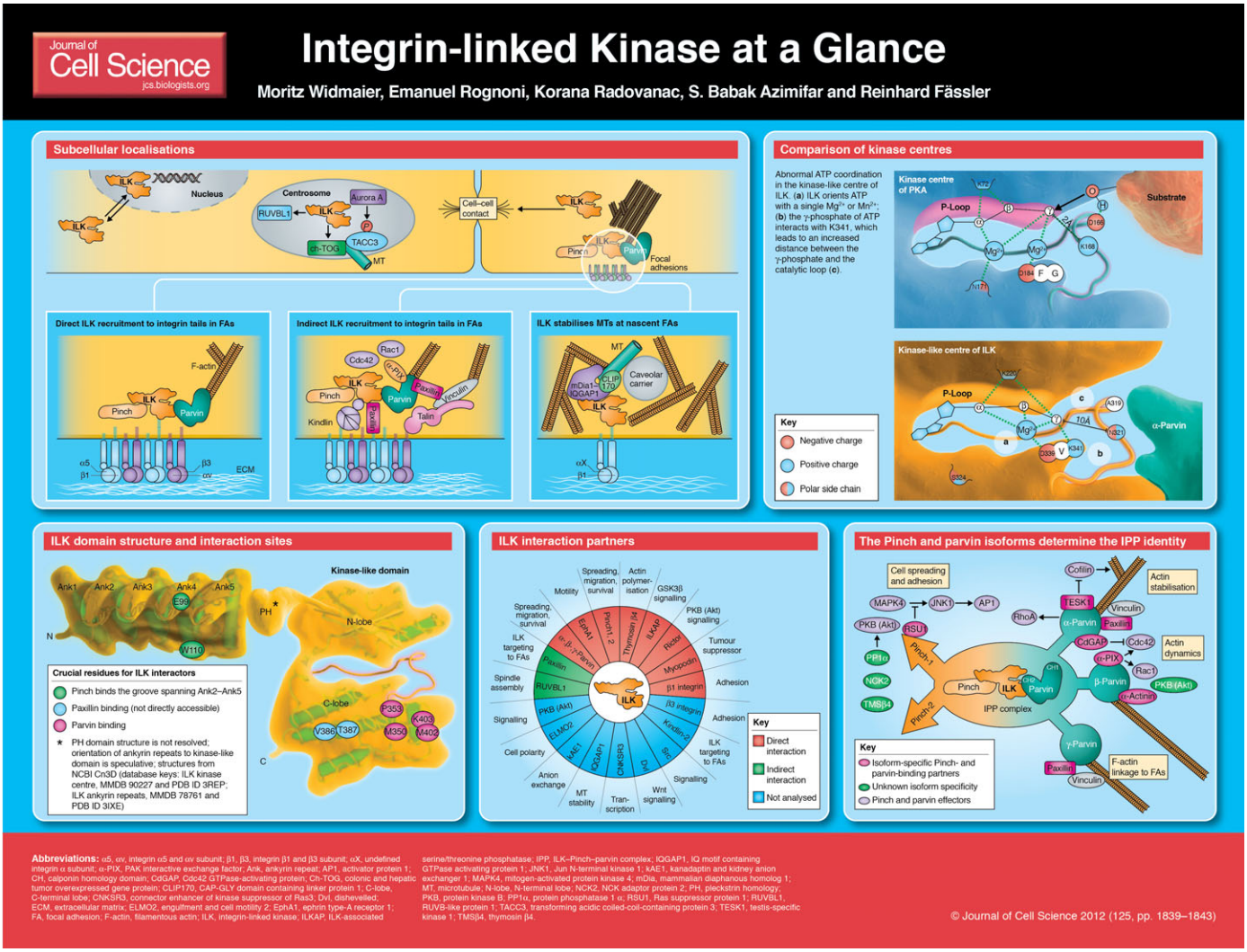

(See poster insert)

Caenorhabditis elegans, the ILK orthologue PAT-4 localises to integrins at muscle attachment sites. Deletion of the *pat-4* gene causes a 'paralysed at two-fold-stage' (PAT) phenotype that is characterised by muscle detachment through defective integrin–actin linkage and early lethality (Mackinnon et al., 2002). In *Drosophila melanogaster*, a germline deletion of ILK leads to muscle detachment and lethality (Zervas et al., 2001). Mice lacking ILK die during the peri-implantation stage owing to a failure to organise the F-actin cytoskeleton in epiblast cells (Sakai et al., 2003). In addition to the constitutive deletion, the mouse ILK-encoding gene has been deleted in several organs and cell types using the *Cre*/*loxP* recombination system. The outcome of these studies has been extensively reviewed elsewhere (Rooney and Streuli, 2011; Ho and Bendeck, 2009; Hannigan et al., 2007; Wickström et al., 2010b).

Structurally, ILK has three different domains: five ankyrin repeats at the N-terminus, followed by a pleckstrin homology (PH)-like domain and a kinase-like domain at the C-terminus (Chiswell et al., 2008; Yang et al., 2009) (see poster). Although ILK was shown to directly interact with integrin cytoplasmic tails, it appears that the recruitment of ILK to integrins depends, at least in some cells, on kindlin-2 (also known as Fermt2 and Plekhc1) (Montanez et al., 2008; Chen et al., 2008), α-parvin (Fukuda et al., 2009) or paxillin (Nikolopoulos and Turner, 2001). Structural studies of ILK have revealed, however, that the proposed paxillin-interacting residues are buried within a polypeptide fold and thus are not directly accessible (Fukuda et al., 2009), suggesting that these residues indirectly contribute to paxillin binding. Before the recruitment of ILK to FAs, ILK forms a ternary complex with the two adaptor proteins Pinch and parvin (termed the IPP complex). Although it is not understood how the IPP complex forms, its formation ensures the stability of the individual components and their faithful targeting to the adhesion site (Zhang et al., 2002; Fukuda et al., 2003a). Mammals have two Pinch genes (Pinch-1 and Pinch-2; also known as *LIMS1* and *LIMS2*, respectively), which encode proteins consisting of five cysteine-rich, zinc-binding LIM domains followed by a nuclear export signal. The first LIM domain of Pinch-1 and -2 binds to a concave surface that extends from the second to the fifth ankyrin repeat of ILK (Chiswell et al., 2008; Yang et al., 2009) (see poster). The three mammalian parvin isoforms (α-, β- and γ-parvin) are composed of an N-terminal polypeptide followed by two calponin homology (CH) domains, the second of which binds to the kinase-like domain of ILK (Tu et al., 2001; Fukuda et al., 2009) (see poster). As ILK can only bind one Pinch and one parvin isoform at the same time (Chiswell et al., 2008; Montanez et al., 2009), ILK is capable of being part of several distinct IPP complexes, each resulting in different signalling outputs (see poster and below).

The parvin proteins can interact directly with F-actin (Legate et al., 2006) or they can recruit actin-binding proteins, such as α-actinin – shown for β-parvin (Yamaji et al., 2004) – or vinculin, an interaction mediated through paxillin (Turner, 2000), which has been shown for α- and γ-parvin (Yoshimi et al., 2006). In addition, they control actin regulatory proteins such as testicular protein kinase 1 (TESK1), which can bind α-parvin and promote F-actin polymerisation through phosphorylation of cofilin (LaLonde et al., 2005). By contrast, β-parvin regulates actin dynamics through PAK-interactive exchange factor alpha (α-PIX, encoded by *ARHGEF6*), a guanidine exchange factor (GEF) for Rac1 and Cdc42 (Mishima et al., 2004). Finally, α-parvin has been shown to inhibit G-proteins by recruiting Cdc42 GTPase-activating protein (CdGAP, also known as RHG31 and Kiaa1204, and encoded by *ARHGAP31*) to FAs (LaLonde et al., 2006), and to negatively regulate Rho-associated protein kinase (ROCK)-driven contractility in vascular smooth muscle cells (Montanez et al., 2009).

Pinch-1 binds the Ras suppressor protein 1 (RSU1), which is important for integrin-mediated cell adhesion and spreading (Kadrmas et al., 2004; Ito et al., 2010). RSU1 is a negative regulator of growth-factor-induced Jun N-terminal kinase 1 (JNK1, also known as MAPK8) (Kadrmas et al., 2004). Taken together these findings suggest that the assembly of distinct IPP complexes in a given cell, together with the differential expression patterns of Pinch and parvin isoforms, provides a means for multiple alternative signalling outputs (see poster).

Emerging functions of ILK

The most prominent subcellular localisation of ILK is in integrin adhesion sites. In recent years it has been reported that ILK is also present in additional subcellular regions and compartments where it might exert integrin-independent functions.

Functions in microtubule trafficking networks

Keratinocytes, and probably other cells, employ ILK to capture microtubule (MT) tips to connect them to the cortical actin network (see poster). ILK-mediated MT capture occurs exclusively in nascent FAs and is mediated by recruitment of the large scaffold protein IQ-motif-containing GTPase-activating protein 1 (IQGAP1) (Wickström et al., 2010a). The capture of MT tips can be achieved either directly through binding of IQGAP1 to the MT tip protein CLIP170 (cytoplasmic linker protein 170; also known as CLIP1), or indirectly through IQGAP1-mediated recruitment of mammalian diaphanous homolog 1 (mDia1; also known as DRF1), which is also able to stabilise MTs. As both IQGAP1 and mDia1 are also able to bind F-actin, the ILK–IQGAP1–mDia1 complex connects MTs with actin tracks at β1-integrin-containing nascent adhesion sites (Wickström et al., 2010a) (see poster). Exocytotic carriers that are transported on MT tracks require a switch from MT-based to actin-based motility at the plasma membrane to pass through the cortical F-actin network and finally fuse with the plasma membrane. Thus, the connection of both networks by the ILK–IQGAP1–mDia1 complex at nascent adhesion sites is essential for the exocytosis of caveolar carriers (Wickström et al., 2010a). Consequently, ILK not only contributes to epithelial cell polarisation through actin remodelling, but also through vesicular trafficking and MT organisation.

Nuclear functions

Despite its prominent localisation in different integrin adhesion sites, ILK has also been observed in the nucleus of several cell lines, including COS-1 cells (Chun et al., 2005), MCF-7 cells (Acconcia et al., 2007), HeLa cells and keratinocytes (Nakrieko et al., 2008a) (see poster). The nuclear function of ILK, however, is still not well understood. In keratinocytes, nuclear ILK has been shown to induce DNA synthesis (Nakrieko et al., 2008a) and, in MCF-7 cells, it has been found to control the expression of the connector enhancer of kinase suppressor of Ras3 (*CNKSR3*) gene (Acconcia et al., 2007). It is known that CNKSR3 regulates the

epithelial Na^+ channel (ENaC) through inhibition of the MAPK kinase MEK1 (Ziera et al., 2009). However, the significance of ILK-regulated *CNSKR3* expression is not understood.

It is also not well understood how ILK translocates into the nucleus. For example, it is not known whether the nuclear import of ILK depends on its N-terminus (Acconcia et al., 2007) or on a C-terminal nuclear localisation signal (Chun et al., 2005). The nuclear export of ILK requires the kinase-like domain (Acconcia et al., 2007; Nakrieko et al., 2008a) and is apparently controlled by the nuclear export factor CRM1, integrin-linked kinase-associated serine and threonine phosphatase 2C (ILKAP) and p21-activated kinase 1 (PAK1) (Acconcia et al., 2007; Nakrieko et al., 2008a).

Organisation of cell–cell contacts

ILK has been shown to serve as a scaffold for promoting the formation of cell–cell contacts (see poster) and the recruitment of tight junction proteins (Vespa et al., 2003; Vespa et al., 2005). Following treatment of cultured keratinocytes with Ca^{2+}, they undergo differentiation. This process is accompanied by the translocation of ILK from FAs to cell–cell adhesion sites (Vespa et al., 2003). This translocation is known to require the N-terminal ankyrin repeats (Vespa et al., 2003); however, it is unclear whether Pinch-1 or -2 translocate together with ILK. In contrast to these in vitro findings, deletion of the *Ilk* gene in mouse keratinocytes neither affects cell–cell adhesion nor barrier function in the epidermis, but severely impairs keratinocyte migration on and adhesion to the epidermal-dermal basal membrane (BM), resulting in skin blistering, epidermal hyperthickening and hair loss (Lorenz et al., 2007; Nakrieko et al., 2008b).

Centrosome functions

A proteomic search for new ILK-interacting proteins identified a number of proteins, including several centrosome- and mitotic-spindle-associated proteins, such as α- and β-tubulin, the tubulin-binding proteins RUVBL1 and colonic and hepatic tumor overexpressed gene protein (ch-TOG, also known as CKAP5) (Dobreva et al., 2008) (see poster). Although ILK probably binds these proteins in an indirect manner (Fielding et al., 2008), it colocalises with them in centrosomes from interphase and mitotic cells where it has an essential role in controlling centrosome function during mitotic spindle organisation and centrosome clustering (Fielding et al., 2008; Fielding et al., 2011). The organisation of the mitotic spindle requires the kinase Aurora A and the association of ch-TOG with the centrosomal transforming acidic coiled-coil-containing protein 3 (TACC3), which in turn promotes the polymerisation and stabilisation of centrosomal MTs (Barr and Gergely, 2007). In ILK-depleted cells, Aurora A kinase, although active, is unable to phosphorylate and thus activate TACC3, resulting in disruption of mitotic spindles. Similarly, the clustering of supernumerary centrosomes in cancer cells is also achieved by the TACC3–ch-TOG complex in an ILK- and Aurora-A-dependent manner (Fielding et al., 2011). ILK associates with ch-TOG, but not with TACC3 or Aurora A. Therefore, it is not clear how ILK supports the phosphorylation of TACC3 by Aurora A. Similarly, it is also unclear how ILK is recruited to centrosomes. The centrosomal localisation of ILK requires RUVBL1 expression and occurs without the known ILK-binding partners, α-parvin and Pinch (Fielding et al., 2008). Finally, it is also not known why the treatment of cells with QLT-0267, a small chemical compound that binds to the ATP-binding site of ILK, is as effective as siRNA-mediated depletion of ILK in blocking the association of TACC3 with Aurora A (Fielding et al., 2008). The mechanistic interpretation of this work is based on the assumption that ILK acts as a kinase, which has been disproved by genetic and structural studies (see below). A potential explanation for the inhibitory effect of QLT-0267 could be an impairment of the stability of ILK (see the next section).

The kinase controversy

The experimental evidence that the kinase-like domain of ILK lacks catalytic activity is overwhelming (Wickström et al., 2010b). Although ILK was initially identified by Dedhar and colleagues as a serine/threonine kinase (Hannigan et al., 1996), it lacks several important motifs that are conserved in most kinases (Hanks et al., 1988) (see poster). Furthermore, genetic studies in flies, worms and mice have demonstrated that the putative kinase activity is not required for development and homeostasis (Zervas et al., 2001; Mackinnon et al., 2002; Lange et al., 2009). Despite this compelling evidence, many papers have been and are still published claiming that ILK is a bona fide kinase, with only marginal evidence at best.

The crystallisation of kinase-like domain of ILK in complex with the CH domain of α-parvin and its comparison to the kinase domain of protein kinase A (PKA) has provided a mechanistic explanation for why the kinase function of ILK is not executed (Fukuda et al., 2009). The catalytic activity of a kinase depends on a coordinated interplay of the N- and C-lobes and the catalytic loop of the kinase domain with the substrate and ATP. The N- and C-lobes and the catalytic loop of ILK show major differences to those of bona fide kinases that render the 'kinase' of ILK non functional: (1) The catalytic loop lacks important acidic and positively charged residues. The acidic residue (D166 in PKA), which polarises the hydroxyl group of the substrate and accepts its proton, is replaced in ILK with the uncharged alanine residue (A319) (Fukuda et al., 2009). (2) The positively charged residue in the catalytic loop (K168 in PKA), which stabilises the intermediate state of the phosphoryl transfer reaction by neutralizing the negative charge of the γ-ATP phosphoryl group, is replaced in ILK by N321 resulting in a misrouting of ATP to the C-lobe. (3) In the N-lobe, the ATP-binding p-loop captures ATP at a too great distance from the active centre (10 Å), which precludes its movement towards the catalytic loop, and the lysine residue K220 contacts the α- and γ-ATP phosphoryl groups instead of the α- and β-phosphoryl groups resulting in an aberrant ATP orientation. (4) Furthermore, the C-lobe of ILK chelates ATP with only one instead of the expected two metal ions. The metal ion is bound by the aspartate residue (D339) of the DVK motif of ILK (a DFG motif in PKA), whereas the second potential metal-binding residue (S324) remains unoccupied. Another divergence from bona fide kinases is the coordination of the γ-ATP phosphoryl-group by the lysine residue (K341) of the DVK motif of the N-lobe, which usually is mediated by the catalytic loop (Fukuda et al., 2009). Nevertheless, despite this structural evidence, dissenting views are still expressed and the controversy rages on (Hannigan et al., 2011).

Thermodynamic and structural analysis of ILK mutants has revealed that the K220A and K220M mutations, previously described as affecting kinase function, destabilise the global ILK structure

(Fukuda et al., 2011), thus reducing ILK stability and the binding of interaction partners such as α-parvin. This observation provides an explanation for the severe kidney defects observed in mice which either lack α-parvin expression or carry K220A or K220M mutations in ILK (Lange et al., 2009).

Redefining the role of ILK in cancer

ILK is overexpressed in many types of cancer, and it has been reported that its depletion or inhibition with the small molecule inhibitor QLT-0267 inhibits anchorage-independent growth, cell cycle progression and invasion (Hannigan et al., 2005). The oncogenic effects of ILK have been attributed for the most part to the catalytic activity of the kinase domain resulting in the activation of protein kinase B (PKB, also known as Akt) and glycogen synthase kinase-3 beta (GSK3β), which in turn regulates the stability of proto-oncogenic β-catenin (Hannigan et al., 2005). The recent findings showing that mammalian ILK lacks catalytic activity and serves as a scaffold protein in FAs of mammalian cells (Lange et al., 2009; Fukuda et al., 2009) raise the question of how ILK mediates its oncogenic potential despite this functional twist.

One possibility is that ILK controls the activity of oncogenes, such as PKB by controlling their subcellular localisation. For example, the ILK-binding partners α- and β-parvin induce the recruitment of PKB to the plasma membrane where PKB mediates its oncogenic activity (Fukuda et al., 2003b; Kimura et al., 2010). An alternative possibility is that ILK and ILK-interacting protein(s) regulate oncogenic kinases by controlling the activity of phosphatases. This has been shown for Pinch-1, which binds to and inhibits protein phosphatase 1α (PP1α) resulting in sustained PKB phosphorylation and activity (Eke et al., 2010). Consequently, reducing the amounts of the IPP complex in FAs will concomitantly result in an increased PP1α activity and decreased PKB function. It is also conceivable that ILK exerts its oncogenic function through its ability to cluster supernumerary centrosomes in cancer cells, thereby preventing their genomic instability and death (Fielding et al., 2011). Finally, ILK might also promote oncogenesis by regulating gene expression in the nucleus or by modulating the assembly of ECM proteins, as shown for fibronectin (Wu et al., 1998), which has been reported to affect cancer development and invasion (Akiyama et al., 1995).

Outlook and perspectives

ILK research has been significantly advanced in the past years by the resolution the long-lasting debate regarding the catalytic activity of ILK and by identifying novel functions for ILK, many of which occur outside of FAs. However, most of the emerging functions of ILK (e.g. in the nucleus, at cell–cell adhesion sites and in the centrosome) have only been studied in cultured cells thus far and still await confirmation in vivo.

In addition, several basic functions of ILK in FAs are still unresolved, including the mechanism(s) of the recruitment of ILK to FAs, the role of ILK in FA maturation and as a potential stretch sensor (Bendig et al., 2006), and the turnover and modifications of ILK, to name a few. Whether the recruitment of ILK to FAs occurs through a direct association with the integrin cytoplasmic domains or indirectly, e.g. through binding to kindlins (Montanez et al., 2008) or paxillin (Nikolopoulos and Turner, 2001) is currently unclear. In this regard, it is also not known whether ILK binds or associates with all β-integrin tails or whether this association is more selective. A co-crystallisation of the kinase-like domain of ILK with β-integrin tails should help to answer some of these questions. Similarly, a structural analysis of the predicted PH domain of ILK would clarify whether it adopts a classical PH fold, as predicted in the original publication (Hannigan et al., 1996), or a different motif, whose function would then have to be determined. Zebrafish studies point to a stretch-sensing function for ILK in cardiomyocytes (Bendig et al., 2006). This observation raises the question of whether mechanical stress sensing by ILK is restricted to cardiomyocytes or whether it also occurs in other cells, and of how ILK is executing this function at the molecular level. Finally, it will be important to re-evaluate the role of ILK in cancer. Ideally, these experiments should be performed in an unbiased manner with tumour models in mice (e.g. colon cancer and mammary cancer models) that lack ILK expression, and are complemented by sophisticated in vitro studies with cells derived from the tumours.

It is obvious that despite the rapid progress in ILK research, many questions are still unanswered. Recent advances in imaging and proteomics combined with genetics, cell biology and biochemistry will make the years to come exciting for all ILK aficionados.

Acknowledgements

We thank Kyle Legate and Roy Zent for careful reading of the manuscript and Max Iglesias for help with preparation of the art work.

Funding

The ILK work in the Fässler laboratory is supported by the Tiroler Zukunftsstiftung and the Max Planck Society.

A high-resolution version of the poster is available for downloading in the online version of this article at jcs.biologists.org. Individual poster panels are available as JPEG files at http://jcs.biologists.org/lookup/suppl/doi:10.1242/jcs.093864/-/DC1

References

Acconcia, F., Barnes, C. J., Singh, R. R., Talukder, A. H. and Kumar, R. (2007). Phosphorylation-dependent regulation of nuclear localization and functions of integrin-linked kinase. *Proc. Natl. Acad. Sci. USA* **104**, 6782-6787.

Akiyama, S. K., Olden, K. and Yamada, K. M. (1995). Fibronectin and integrins in invasion and metastasis. *Cancer Metastasis Rev.* **14**, 173-189.

Barr, A. R. and Gergely, F. (2007). Aurora-A: the maker and breaker of spindle poles. *J. Cell Sci.* **120**, 2987-2996.

Bendig, G., Grimmler, M., Huttner, I. G., Wessels, G., Dahme, T., Just, S., Trano, N., Katus, H. A., Fishman, M. C. and Rottbauer, W. (2006). Integrin-linked kinase, a novel component of the cardiac mechanical stretch sensor, controls contractility in the zebrafish heart. *Genes Dev.* **20**, 2361-2372.

Chen, K., Tu, Y., Zhang, Y., Blair, H. C., Zhang, L. and Wu, C. (2008). PINCH-1 regulates the ERK-Bim pathway and contributes to apoptosis resistance in cancer cells. *J. Biol. Chem.* **283**, 2508-2517.

Chiswell, B. P., Zhang, R., Murphy, J. W., Boggon, T. J. and Calderwood, D. A. (2008). The structural basis of integrin-linked kinase-PINCH interactions. *Proc. Natl. Acad. Sci. USA* **105**, 20677-20682.

Chun, J., Hyun, S., Kwon, T., Lee, E. J., Hong, S. K. and Kang, S. S. (2005). The subcellular localization control of integrin linked kinase 1 through its protein-protein interaction with caveolin-1. *Cell. Signal.* **17**, 751-760.

Dobreva, I., Fielding, A., Foster, L. J. and Dedhar, S. (2008). Mapping the integrin-linked kinase interactome using SILAC. *J. Proteome Res.* **7**, 1740-1749.

Eke, I., Koch, U., Hehlgans, S., Sandfort, V., Stanchi, F., Zips, D., Baumann, M., Shevchenko, A., Pilarsky, C., Haase, M. et al. (2010). PINCH1 regulates Akt1 activation and enhances radioresistance by inhibiting PP1alpha. *J. Clin. Invest.* **120**, 2516-2527.

Fielding, A. B., Dobreva, I., McDonald, P. C., Foster, L. J. and Dedhar, S. (2008). Integrin-linked kinase localizes to the centrosome and regulates mitotic spindle organization. *J. Cell Biol.* **180**, 681-689.

Fielding, A. B., Lim, S., Montgomery, K., Dobreva, I. and Dedhar, S. (2011). A critical role of integrin-linked kinase, ch-TOG and TACC3 in centrosome clustering in cancer cells. *Oncogene* **30**, 521-534.

Fukuda, K., Gupta, S., Chen, K., Wu, C. and Qin, J. (2009). The pseudoactive site of ILK is essential for its binding to α-Parvin and localization to focal adhesions. *Mol. Cell* **36**, 819-830.

Fukuda, K., Knight, J. D. R., Piszczek, G., Kothary, R. and Qin, J. (2011). Biochemical, proteomic, structural, and thermodynamic characterizations of integrin-linked kinase (ILK): cross-validation of the pseudokinase. *J. Biol. Chem.* **286**, 21886-21895.

Fukuda, T., Chen, K., Shi, X. and Wu, C. (2003a). PINCH-1 is an obligate partner of integrin-linked kinase (ILK) functioning in cell shape modulation, motility, and survival. *J. Biol. Chem.* **278**, 51324-51333.
Fukuda, T., Guo, L., Shi, X. and Wu, C. (2003b). CH-ILKBP regulates cell survival by facilitating the membrane translocation of protein kinase B/Akt. *J. Cell Biol.* **160**, 1001-1008.
Geiger, B. and Yamada, K. M. (2011). Molecular architecture and function of matrix adhesions. *Cold Spring Harb. Perspect. Biol.* **3**, a005033.
Hanks, S. K., Quinn, A. M. and Hunter, T. (1988). The protein kinase family: conserved features and deduced phylogeny of the catalytic domains. *Science* **241**, 42-52.
Hannigan, G., Troussard, A. A. and Dedhar, S. (2005). Integrin-linked kinase: a cancer therapeutic target unique among its ILK. *Nat. Rev. Cancer* **5**, 51-63.
Hannigan, G. E., Leung-Hagesteijn, C., Fitz-Gibbon, L., Coppolino, M. G., Radeva, G., Filmus, J., Bell, J. C. and Dedhar, S. (1996). Regulation of cell adhesion and anchorage-dependent growth by a new beta 1-integrin-linked protein kinase. *Nature* **379**, 91-96.
Hannigan, G. E., Coles, J. G. and Dedhar, S. (2007). Integrin-linked kinase at the heart of cardiac contractility, repair, and disease. *Circ. Res.* **100**, 1408-1414.
Hannigan, G. E., McDonald, P. C., Walsh, M. P. and Dedhar, S. (2011). Integrin-linked kinase: not so 'pseudo' after all. *Oncogene* **30**, 4375-4385.
Ho, B. and Bendeck, M. P. (2009). Integrin linked kinase (ILK) expression and function in vascular smooth muscle cells. *Cell Adhes. Migr.* **3**, 174-176.
Hynes, R. O. (2002). Integrins: bidirectional, allosteric signaling machines. *Cell* **110**, 673-687.
Ito, S., Takahara, Y., Hyodo, T., Hasegawa, H., Asano, E., Hamaguchi, M. and Senga, T. (2010). The roles of two distinct regions of PINCH-1 in the regulation of cell attachment and spreading. *Mol. Biol. Cell* **21**, 4120-4129.
Kadrmas, J. L., Smith, M. A., Clark, K. A., Pronovost, S. M., Muster, N., Yates, J. R., 3rd and Beckerle, M. C. (2004). The integrin effector PINCH regulates JNK activity and epithelial migration in concert with Ras suppressor 1. *J. Cell Biol.* **167**, 1019-1024.
Kimura, M., Murakami, T., Kizaka-Kondoh, S., Itoh, M., Yamamoto, K., Hojo, Y., Takano, M., Kario, K., Shimada, K. and Kobayashi, E. (2010). Functional molecular imaging of ILK-mediated Akt/PKB signaling cascades and the associated role of beta-parvin. *J. Cell Sci.* **123**, 747-755.
LaLonde, D. P., Brown, M. C., Bouverat, B. P. and Turner, C. E. (2005). Actopaxin interacts with TESK1 to regulate cell spreading on fibronectin. *J. Biol. Chem.* **280**, 21680-21688.
LaLonde, D. P., Grubinger, M., Lamarche-Vane, N. and Turner, C. E. (2006). CdGAP associates with actopaxin to regulate integrin-dependent changes in cell morphology and motility. *Curr. Biol.* **16**, 1375-1385.
Lange, A., Wickström, S. A., Jakobson, M., Zent, R., Sainio, K. and Fässler, R. (2009). Integrin-linked kinase is an adaptor with essential functions during mouse development. *Nature* **461**, 1002-1006.
Legate, K. R., Montañez, E., Kudlacek, O. and Fässler, R. (2006). ILK, PINCH and parvin: the tIPP of integrin signalling. *Nat. Rev. Mol. Cell Biol.* **7**, 20-31.
Legate, K. R., Wickström, S. A. and Fässler, R. (2009). Genetic and cell biological analysis of integrin outside-in signaling. *Genes Dev.* **23**, 397-418.
Lorenz, K., Grashoff, C., Torka, R., Sakai, T., Langbein, L., Bloch, W., Aumailley, M. and Fässler, R. (2007). Integrin-linked kinase is required for epidermal and hair follicle morphogenesis. *J. Cell Biol.* **177**, 501-513.
Mackinnon, A. C., Qadota, H., Norman, K. R., Moerman, D. G. and Williams, B. D. (2002). C. elegans PAT-4/ILK functions as an adaptor protein within integrin adhesion complexes. *Curr. Biol.* **12**, 787-797.
Mishima, W., Suzuki, A., Yamaji, S., Yoshimi, R., Ueda, A., Kaneko, T., Tanaka, J., Miwa, Y., Ohno, S. and Ishigatsubo, Y. (2004). The first CH domain of affixin activates Cdc42 and Rac1 through alphaPIX, a Cdc42/Rac1-specific guanine nucleotide exchanging factor. *Genes Cells* **9**, 193-204.
Montanez, E., Ussar, S., Schifferer, M., Bösl, M., Zent, R., Moser, M. and Fässler, R. (2008). Kindlin-2 controls bidirectional signaling of integrins. *Genes Dev.* **22**, 1325-1330.
Montanez, E., Wickström, S. A., Altstätter, J., Chu, H. and Fässler, R. (2009). Alpha-parvin controls vascular mural cell recruitment to vessel wall by regulating RhoA/ROCK signalling. *EMBO J.* **28**, 3132-3144.
Moser, M., Legate, K. R., Zent, R. and Fässler, R. (2009). The tail of integrins, talin, and kindlins. *Science* **324**, 895-899.
Nakrieko, K. A., Vespa, A., Mason, D., Irvine, T. S., D'Souza, S. J. and Dagnino, L. (2008a). Modulation of integrin-linked kinase nucleo-cytoplasmic shuttling by ILKAP and CRM1. *Cell Cycle* **7**, 2157-2166.
Nakrieko, K. A., Welch, I., Dupuis, H., Bryce, D., Pajak, A., St Arnaud, R., Dedhar, S., D'Souza, S. J. and Dagnino, L. (2008b). Impaired hair follicle morphogenesis and polarized keratinocyte movement upon conditional inactivation of integrin-linked kinase in the epidermis. *Mol. Biol. Cell* **19**, 1462-1473.
Nikolopoulos, S. N. and Turner, C. E. (2001). Integrin-linked kinase (ILK) binding to paxillin LD1 motif regulates ILK localization to focal adhesions. *J. Biol. Chem.* **276**, 23499-23505.
Rooney, N. and Streuli, C. H. (2011). How integrins control mammary epithelial differentiation: a possible role for the ILK-PINCH-Parvin complex. *FEBS Lett.* **585**, 1663-1672.
Sakai, T., Li, S., Docheva, D., Grashoff, C., Sakai, K., Kostka, G., Braun, A., Pfeifer, A., Yurchenco, P. D. and Fässler, R. (2003). Integrin-linked kinase (ILK) is required for polarizing the epiblast, cell adhesion, and controlling actin accumulation. *Genes Dev.* **17**, 926-940.
Schiller, H. B., Friedel, C. C., Boulegue, C. and Fässler, R. (2011). Quantitative proteomics of the integrin adhesome show a myosin II-dependent recruitment of LIM domain proteins. *EMBO Rep.* **12**, 259-266.
Tu, Y., Huang, Y., Zhang, Y., Hua, Y. and Wu, C. (2001). A new focal adhesion protein that interacts with integrin-linked kinase and regulates cell adhesion and spreading. *J. Cell Biol.* **153**, 585-598.
Turner, C. E. (2000). Paxillin interactions. *J. Cell Sci.* **113**, 4139-4140.
Vespa, A., Darmon, A. J., Turner, C. E., D'Souza, S. J. and Dagnino, L. (2003). Ca2+-dependent localization of integrin-linked kinase to cell junctions in differentiating keratinocytes. *J. Biol. Chem.* **278**, 11528-11535.
Vespa, A., D'Souza, S. J. and Dagnino, L. (2005). A novel role for integrin-linked kinase in epithelial sheet morphogenesis. *Mol. Biol. Cell* **16**, 4084-4095.
Wickström, S. A., Lange, A., Hess, M. W., Polleux, J., Spatz, J. P., Krüger, M., Pfaller, K., Lambacher, A., Bloch, W., Mann, M. et al. (2010a). Integrin-linked kinase controls microtubule dynamics required for plasma membrane targeting of caveolae. *Dev. Cell* **19**, 574-588.
Wickström, S. A., Lange, A., Montanez, E. and Fässler, R. (2010b). The ILK/PINCH/parvin complex: the kinase is dead, long live the pseudokinase! *EMBO J.* **29**, 281-291.
Wu, C., Keightley, S. Y., Leung-Hagesteijn, C., Radeva, G., Coppolino, M., Goicoechea, S., McDonald, J. A. and Dedhar, S. (1998). Integrin-linked protein kinase regulates fibronectin matrix assembly, E-cadherin expression, and tumorigenicity. *J. Biol. Chem.* **273**, 528-536.
Yamaji, S., Suzuki, A., Kanamori, H., Mishima, W., Yoshimi, R., Takasaki, H., Takabayashi, M., Fujimaki, K., Fujisawa, S., Ohno, S. et al. (2004). Affixin interacts with alpha-actinin and mediates integrin signaling for reorganization of F-actin induced by initial cell-substrate interaction. *J. Cell Biol.* **165**, 539-551.
Yang, Y., Wang, X., Hawkins, C. A., Chen, K., Vaynberg, J., Mao, X., Tu, Y., Zuo, X., Wang, J., Wang, Y. X. et al. (2009). Structural basis of focal adhesion localization of LIM-only adaptor PINCH by integrin-linked kinase. *J. Biol. Chem.* **284**, 5836-5844.
Yoshimi, R., Yamaji, S., Suzuki, A., Mishima, W., Okamura, M., Obana, T., Matsuda, C., Miwa, Y., Ohno, S. and Ishigatsubo, Y. (2006). The gamma-parvin-integrin-linked kinase complex is critically involved in leukocyte-substrate interaction. *J. Immunol.* **176**, 3611-3624.
Zervas, C. G., Gregory, S. L. and Brown, N. H. (2001). Drosophila integrin-linked kinase is required at sites of integrin adhesion to link the cytoskeleton to the plasma membrane. *J. Cell Biol.* **152**, 1007-1018.
Ziera, T., Irlbacher, H., Fromm, A., Latouche, C., Krug, S. M., Fromm, M., Jaisser, F. and Borden, S. A. (2009). Cnksr3 is a direct mineralocorticoid receptor target gene and plays a key role in the regulation of the epithelial sodium channel. *FASEB J.* **23**, 3936-3946.
Zhang, Y., Chen, K., Tu, Y., Velyvis, A., Yang, Y., Qin, J. and Wu, C. (2002). Assembly of the PINCH-ILK-CH-ILKBP complex precedes and is essential for localization of each component to cell-matrix adhesion sites. *J. Cell Sci.* **115**, 4777-4786.